Comparative study of catalase-peroxidases (KatGs)

by

Rahul Singh

A thesis

submitted to the Faculty of Graduate Studies

in partial fulfillment of the requirements for the degree of

DOCTOR OF PHILOSOPHY

Department of Microbiology

University of Manitoba

Winnipeg, Manitoba

THE UNIVERSITY OF MANITOBA

FACULTY OF GRADUATE STUDIES

*****

COPYRIGHT PERMISSION

Comparative study of catalase-peroxidases (KatGs)

BY

Rahul Singh

A Thesis/Practicum submitted to the Faculty of Graduate Studies of The University of Manitoba in partial fulfillment of the requirement of the degree

OF

DOCTOR OF PHILOSOPHY

Dedicated to my mother

Banmala Singh (1951-2005)

ABSTRACT

Catalase-peroxidases (KatGs) act as a protective enzyme against oxidative stress during the exponential phase of growth. KatG from *M. tuberculosis* is better known for its role in the activation of isoniazid (INH), a front line anti-tuberculosis prodrug, through it's conversion to isonicotinoyl-NAD adduct, which inhibits the mycolic acid synthesis. Biochemical characterization of KatGs from *Burkholderia pseudomallei*, *Mycobacterium tuberculosis*, *Escherichia coli*, *Bacillus stearothermophilus*, *Archaeoglobus fulgidus*, *Synechosystis* PCC 6803, and *Rhodobacter capsulatus*, was carried out to compare their enzyme kinetics in view of the recent success in crystallization of the KatGs. Catalase-peroxidases show substantial catalase specific activity with significant variation among the seven KatGs studied. A large variation was also evident in the peroxidase activity of the seven KatGs. Differences in the K_m values for both catalase and peroxidase reactions are indicative of the subtle differences in the protein structure, particularly in the vicinity of active site heme and the access channel for the substrate. The role of catalase-peroxidases in the activation of INH was also characterized and compared using NADH and some other pyridine derivatives as substrate. KatGs catalyze the oxidation of NADH to form NAD^+ and either H_2O_2 or superoxide radical depending on pH. The NADH oxidase reaction requires molecular oxygen, does not require hydrogen peroxide, is not inhibited by superoxide dismutase or catalase, and has a pH optimum of 8.75, clearly differentiating it from the peroxidase and catalase reactions with pH optima of 5.5 and 6.5, respectively, and from the NADH peroxidase-oxidase reaction of horseradish peroxidase. *B. pseudomallei* KatG has a relatively high affinity for NADH (K_m=12 μM), but the oxidase reaction is slow (k_{cat}=0.54 min^{-1}) compared with the peroxidase and

catalase reactions. The catalase-peroxidases also catalyze the hydrazinolysis of isonicotinic acid hydrazide (INH) in an oxygen- and H_2O_2-independent reaction, and KatG-dependent radical generation from a mixture of NADH and INH is two to three times faster than the combined rates of separate reactions with NADH and INH alone. The major products from the coupled reaction, identified by HPLC fractionation and mass spectrometry, are NAD^+ and isonicotinoyl-NAD. Isonicotinoyl-NAD synthesis from a mixture of NAD^+ and INH is KatG-dependent and is activated by manganese ion. *M. tuberculosis* KatG catalyzes isonicotinoyl-NAD formation from NAD^+ and INH more efficiently than *B. pseudomallei* KatG. A similar comparison of Ser315Thr and Ser315Asn variants of MtKatG, the two most common mutations occurring in the *katG* gene among drug resistant strains of *M. tuberculosis*, demonstrates that variants have lower rates of hydrazinolysis and isonicotinoyl-NAD synthase activity and undetectable NADH oxidase activity while maintaining substantial catalase and peroxidase activities. These properties are consistent with the enzyme being required for the maintenance of virulence while developing resistance against INH.

ACKNOWLEDGEMENTS

I am deeply indebted to my advisor, Dr. Peter Loewen, for his expert guidance and faith in my abilities throughout this project. His financial and personal support during my studies is very much appreciated. His thoughtfulness and dedication towards his research always remained a source of inspiration. I am also thankful for the guidance and encouragement I received from my advisory committee members, Dr. E. Worobec, Dr. J. O'Neil and especially Dr. I. J. Oresnik for his critical analysis of my progress. I am also very grateful to Mr. Jacek Switala for his help and cooperation with his excellent technical expertise. I would also like to thank Dr. Lynda Donald, Dr. Maureen Spearman, Dr. Linda Cameron, and Mr. Norm Huzel for their assistance. I greatly appreciate Ms. Sharon Berg for the unreserved support I have received countless time from her. Our collaborators in Spain (Prof Ignacio Fita's lab) and France (Dr. Anabella Ivancich's Lab) are greatly appreciated. A special thank goes to the Loewen lab members; Taweewat, Ben, Amarbeer and Vikas and the past members Prashen and Sherif. I would also thank to the faculty members and support staff in the department of microbiology for their cooperation and support. My fellow graduate students are greatly appreciated for their friendship and encouragement with special mention of Ayush, Patrick, Matt, Taylor, and many more. Finally I owe a great deal to my father, my sister Priyanka, her husband Avnish, my friends, Gurusharan and Ajay, for always been there for me, and my wife Tejomayee who deserves a very special appreciation for the patience, understanding and tremendous support she has continually provided while I was writing this thesis.

TABLE OF CONTENTS

LIST OF FIGURES

Figure **Page**

LIST OF TABLES

Table **Page**

List of Abbreviations

A	Absorbance
ABTS	2,2'-azinobis(3-ethylbenzothiazolinesulfonic acid)
Amp^R	Ampicillin resistance
APX	Ascorbate peroxidase
AfKatG	KatG from *Archeoglobus fulgidus*
bp	Base pairs (s)
BpKatG	KatG from *Burkholderia pseudomallei*
BLC	Bovine liver catalase
BsKatG	KatG from *Bacillus stearotthermophilus*
CcP	Cytochrome *c* peroxidase
Ci	Curie
CIP	calf intestinal alkaline phosphatase
Da	Daltons(s)
DEAE	Diethylaminoethyl
DMSO	DImethylsulfoxide
DNA	Deoxyribonucleic acid
dNTP	Deoxyribonucleoside triphosphate
e^-	Electron
EcKatG	KatG from *Escherichia coli*
EDTA	Ethylenediaminetetraacetic acid
H^+	Proton
HmKatG	KatG from *Haloarcula marismortui*
H_2O	Water
H_2O_2	Hydrogen peroxide
HPI	Hydroperoxidase I from *Escherichia coli*
HPII	Hydroperoxidae II from *Escherichia coli*
HRP	Horseradish peroxidase
INH	Isonicotinic acid hydrazide (isoniazid)
KatG	Catalase-peroxidase
Kbp	Kilo base pairs(s)
k_{cat}	Turnover number
kDa	Kilo Daltons
K_m	Michealis-Menten constant
LB	Lauria-Bertani
µM	Micromolar
M	Molarity/molar
mg	Milligrams
mL	Milliliter
mM	Millimolar
MtKatG	KatG from *Mycobacterium tuberculosis*
NADH	Nicotinamide adenine dinucleotide (reduced)
NADPH	Nicotinamide adenine dinucleotide phosphate
NAD^+	Nicotinamide adenine dinucleotide (oxidized)
NBT	Nitroblue Tetrazolium

nm	Nanometers(s)
RcKatG	KatG from *Rhodobacter capsulatis*
SyKatG	KatG from *Synechocystis*
OD	Optical density
PAGE	Polyacrylamide gel electrophoresis
PEG	Polyethylene glycol
PMSF	Phenylmethylsulfonyl fluoride
RNAse	Ribonuclease
ROS	Reactive oxygen species
SDS	Sodium dodecyl sulfate
Tris	Tris (hydroxymethyl) aminomethane
V	volts
V_{max}	Maximum velocity
w/v	Weight per volume
w/w	Weight per weight

1. General Introduction

1.1. Oxygen: Elixir of life — and death

Although the story of oxygen (O_2) began with the discoveries of the British theologian J. B. Priestley, the French chemist A. L. Lavoisier, and the Swedish pharmacist C.W. Scheele in the eighteenth century, the concept of O_2 as a requirement for aerobic life existed even in ancient civilization and history is full of such examples referring to the significance of oxygen; for example, the Sanskrit word "prana vayu" which means "the gas of life" appears frequently in the Vedas, the sacred writings of ancient Indian civilization. Another example came from 1604, when the Polish alchemist Michael Sendivogius wrote that "Man was created of the earth, and lives by virtue of the air; for there is in the air a secret food of life…whose invisible congealed spirit is better than the whole Earth" and proposes that this 'aerial food of life' circulated between the air and earth by way of an unusual salt — nitre, or saltpeter. He evidently believed that he had discovered the Elixir of life, "without which no mortal can live, and without which nothing grows or is generated in the world" (Lane, 2002). Thus, for centuries considered critical to life itself, O_2 remains, and will always remain one of our essential elements. However, by the end of twentieth century, O_2 had become the focus of controversy, resulting from observations that it can be dangerous, toxic and deleterious to biological systems (Doroshow, 1989).

During the past 30 years, the fields of free radical chemistry and biology have risen from relative obscurity to become mainstream elements of biomedical investigation

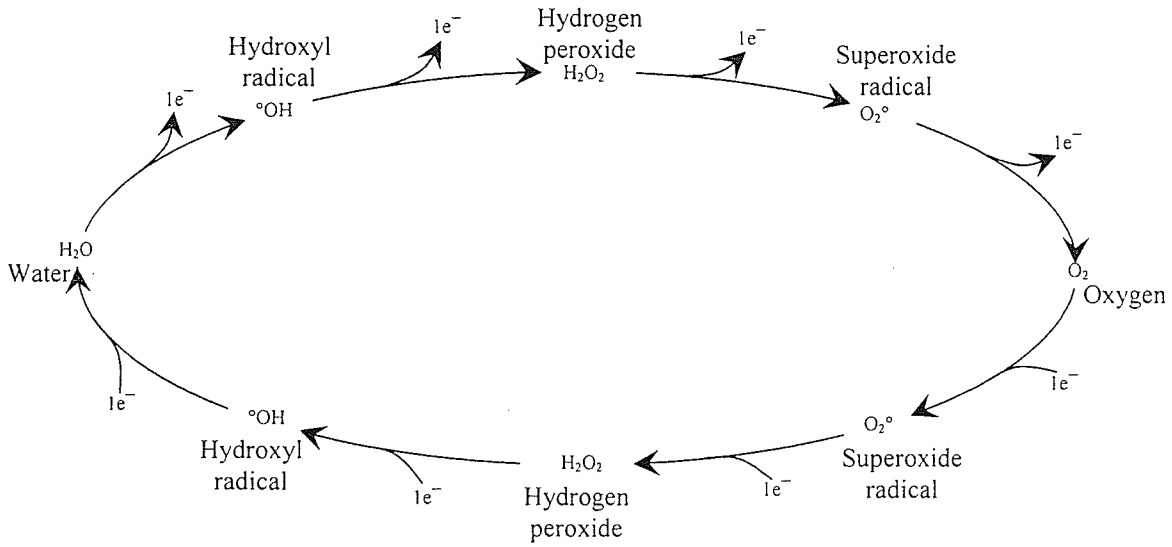

Figure 1.1. Schematic representation of intermediates between water and oxygen. Only changes in number of electron (e^-) is shown in each direction.

and pharmaceutical development. There is increasing evidence that oxidative stress, defined as an imbalance between oxidants and antioxidants in favor of the former, leads to detrimental biochemical reactions between O_2 and other molecules within both the human body and the environment, which generate reactive species of oxygen better known as reactive oxygen species (ROS). During evolution nature selected O_2 as the primary electron acceptor in the most efficient mechanisms for producing usable biological energy. With the use of O_2 as a terminal oxidant came the formation of the partially reduced oxygen species: the superoxide anion, hydrogen peroxide, and the hydroxyl radical which are too reactive to be tolerated within living systems. These reactive oxygen species are an important contributing factor in several chronic human diseases, including atherosclerosis and related vascular diseases, mutagenesis and cancer, neurodegeneration, immunologic disorders, and the aging process (Doroshow, 1989, Harman, 1986, Rice-Evans, 1988). The first direct proof in our understanding that oxygen free radicals mediated oxygen toxicity appeared in 1954, when Rebeca Gerschman, Daniel Gilbert, and colleagues noted that the pattern of X-radiation damage to lung tissue was similar to that induced by high oxygen concentrations (Greshman *et al.*, 1954). Apart from showing the cumulative effects of hyperoxia and x-irradiation, they also reported that many chemical agents affording protection against the toxic effect of radiation also protected against oxygen poisoning. The essential feature of their theory was that both oxygen poisoning and the biological effects of x-irradiation share a common mechanism of action, specifically the reactions of free radicals, which is mediated by exactly the same fleeting intermediates which can be produced either from oxygen or water (Figure 1.1). In radiation poisoning they are produced from water, and in oxygen poisoning from

oxygen. As stated by Irwin Fridovich, a Professor of Biochemistry at Duke University: "This was a remarkably prescient theory, considering the paucity of information concerning the generation and scavenging of specific free radicals available at that time" (Fridovich, 1975). In 1969, Joe McCord and Irwin Fridovich went on to solidify the concept of free radical mediation of oxygen toxicity by identifying a catalytic function for the enzyme superoxide dismutase (SOD) (Fredovich and McCord, 1969) providing direct analytical evidence of the *in vivo* generation of the superoxide radical. Thus, aerobic life is a high wire act supported by O_2 chemistry and balanced precariously between the biosynthetic powers provided by the rich energy supplies of respiration and the destructive effects of O_2 radicals formed during O_2 metabolism.

Microorganisms have a limited tolerance for oxygen. This property is most evident in the cases of obligate anaerobes and microaerophiles, which cannot grow in air saturated media, but it applies as well to committed aerobes, which grow poorly, or even die, when they are exposed to hyperoxia. Yet the basis of this universal phenomenon is not intuitive; after all, the structural molecules from which cells are made, amino acids, lipids, and nucleic acids, are reasonably stable in aerobic buffers (Imlay, 2003).

The chemistry of oxygen plays a major role in its unique behavior. It explains not only why oxygen free radicals are formed, but also why we do not spontaneously combust (despite a favorable energetics).

1.2. The oxygen molecule

Oxygen is a paradox. The secret of the behavior of molecular oxygen and its partially reduced species lies in their reduction potentials and molecular orbital structures.

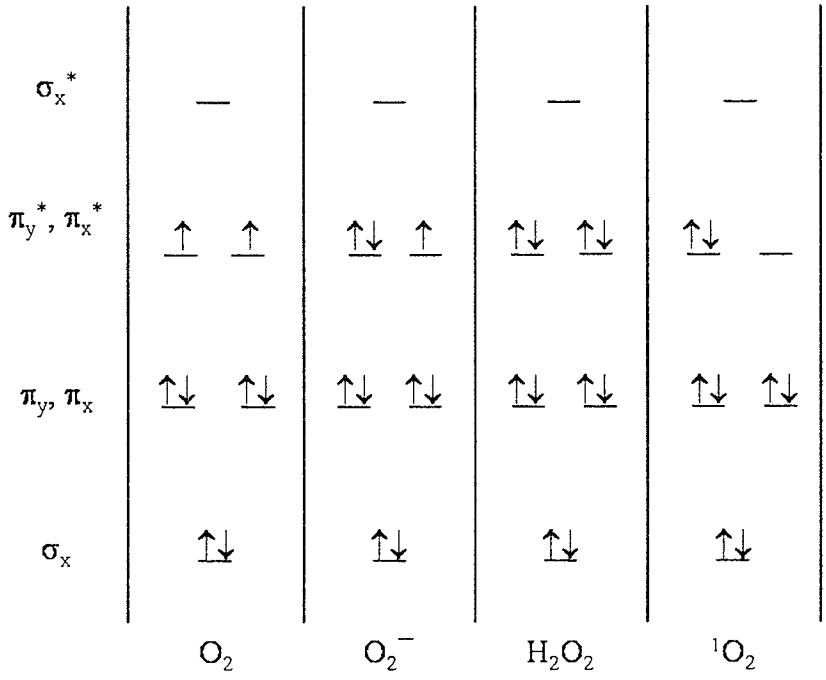

Figure1.2. Molecular orbital diagrams of molecular oxygen (O_2), superoxide (O_2^-), hydrogen peroxide (H_2O_2), and singlet oxygen ($^1O_2$).

Molecular oxygen itself is a rarity, a stable diradical, with two spin-aligned, unpaired electrons in its π antibonding orbital (Figure 1.2).

An important consequence of this structure is that organic molecules with spin paired electrons cannot transfer more than one electron at a time to oxygen. Because oxygen is a weak electron acceptor (and most organic molecules are poor electron donors), this restriction ensures that oxygen cannot efficiently oxidize amino acids and nucleic acids. However, the unpaired electrons of dioxygen readily interact with the unpaired electrons of transition metals and organic radicals.

In contrast, the reduction potentials of $O_2^{\circ-}$, H_2O_2 and the hydroxyl radical dictate that in thermodynamic terms they are much stronger univalent oxidants than dioxygen. However, the anionic charge of $O_2^{\circ-}$ inhibits its effectiveness as an oxidant of electron rich molecules, while the reactivity of H_2O_2 is diminished by the stability of its oxygen-oxygen bond. Neither of these features applies to the hydroxyl radical, and indeed HO° reacts at virtually diffusion rates with most biomolecules.

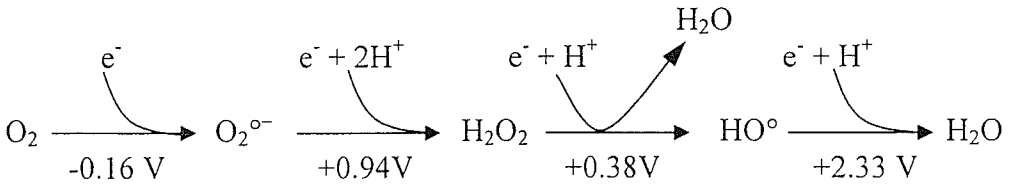

1.3. Antioxidant Systems

During the course of evolution, while life adapted to an aerobic atmosphere, all living organisms, both aerobes and anaerobes, evolved mechanisms to protect themselves specifically from oxidative stress and its toxic effects (Sies, 1993; Gutteridge *et al.*,

1999). During the last 30 years, biochemists and biologists working in this field have thus focused their attention mainly on the following three objects. The first is the identification of the toxic species, the biological targets and the molecular mechanism by which an oxidative stress is expressed within an organism. The second is the role played by oxidative stress in ageing and a number of diseases (neurological disorders, some types of cancers and inflammations, etc.) with the object of developing suitable therapeutic strategies. The third is an understanding of the nature and mechanism of the complex antioxidant machinery which control the balance between the generation and the scavenging of reactive oxygen species, continuously (aerobes) or transiently (anaerobes). These antioxidants include both non-enzymatic and enzymatic species. Historically, the term antioxidants referred to any substance that hindered the reaction of a substance with oxygen. Since every such reaction usually involves radicals, the term "antioxidants" has taken a more mechanistic flavor and now generally refers to any substance which inhibits a free radical reaction (Feldman *et al.*, 1997).

1.3.1. Non-Enzymatic Defenses

The non-enzymatic antioxidants include various low molecular weight scavengers such as L-ascorbic acid (Vitamin C), β-carotene, α-tocopherol (Vitamin E), glutathione, phenolic compounds and ubiquinones (coenzyme Q). There are also certain reductants and some iron binding proteins.

1.3.2. Enzymatic Defenses

Enzymatic antioxidants, comprising the primary tier of defense include superoxide dismutases (SODs), catalases, peroxidases, catalase-peroxidases (KatG), and in mammalian cells, glutathione peroxidases (GPx). In addition there is a second tier of defense that includes methionine sulfoxide reductase, proteases, endonucleases and phospholipases (Fridovich, 1999). The major advantage of having specific antioxidant enzymes is that the steady-state concentrations of peroxide or superoxide can be adapted to cellular requirements. Several of these enzymes can be induced, activated or inhibited. The best example of a well studied protein induced in *E.coli* when grown at high levels of oxygen or exposed to redox-cycling agents is superoxide dismutase (Fridovich, 1995). These agents also induce glucose-6-phosphate dehydrogenase to replenish the NADPH consumed in the antioxidant reactions (such as GSH reductase) (Kao and Hassan, 1985). GSH levels have been known to increase upon exposure to H_2O_2 in *E. coli* and *S. typhimurum* (Christman *et al.*, 1985).

SODs and catalases form a defensive team that prevents the less reactive species $O_2^{\circ -}$ and H_2O_2 from being converted into the highly reactive hydroxyl radical (OH°) (Liochev & Fridovich, 1992). Superoxide dismutase, first discovered in 1969 (McCord *et al.*, 1969) catalyzes the dismutation of $O_2^{\circ -}$ to H_2O_2 and O_2 at diffusion limiting rates:

$$O_2^{\circ -} + O_2^{\circ -} + 2H^+ \longrightarrow H_2O_2 + O_2$$

These supremely efficient catalysts are abundant in aerobic cells and keep the steady state level of $O_2^{\circ -}$ in the 10^{-10} mol l^{-1} range (Imlay and Fridovich, 1991). In *E. coli*, SODs provide approximately 95% protection to all targets susceptible to $O_2^{\circ -}$ attack (Linochev and Fridovich, 1997).

There are three classes of SODs that differ in utilizing Cu and Zn, Mn, or Fe and Ni. SODs can be cytosolic, localized to specific sub-cellular organelles or secreted (Fridovich, 1997). The presence of SOD enzymes in strictly anaerobic bacteria further supported the notion that $O_2^{\circ-}$ is a key and general component of oxidative stress (Hatchikian *et al.*, 1977; Dos Santos *et al.*, 2000). These organisms may be transiently exposed to oxygen and the availability of the antioxidant mechanism may be an advantage (Cypionka, 2000). Some microaerophilic and anaerobic bacteria use not only SOD but also a relatively new class of superoxide-scavenging enzymes, the superoxide reductase (SOR) (Jenney *et al.*, 1999; Lombard *et al.*, 2000; Lombard *et al.*, 2000b., Jovanovic *et al.*, 2000), that catalyze the reduction of superoxide radical anion to H_2O_2 :

$$O_2^{\circ-} + e^- + 2H^+ \longrightarrow H_2O_2$$

SOD dismutates toxic superoxide anion radical but, in so doing produces hydrogen peroxide, another toxic product, which is degraded by catalases and peroxidases, the latter using organic electron donors (Fridovich, 1978):

$$H_2O_2 + H_2O_2 \longrightarrow 2H_2O + O_2 \quad \text{(Catalases)}$$

$$H_2O_2 + 2RH \longrightarrow 2H_2O + 2R^{\circ} \quad \text{(Peroxidases)}$$

Catalases, or more correctly hydroperoxidases, are one of the most studied enzymes. The name catalase was first used in 1900 (Loew O, 1900) and the protein has been the object of study in many organisms ever since. Three classes of catalase, unrelated on the basis of sequence and structure exhibit significant catalase activity. The class that is most widespread in nature and which has been most extensively characterized is composed of mono-functional, heme-containing enzymes subdivided based on having large (> 75 kDa) or small (< 60 kDa) subunits. Phylogenetic analysis has

demonstrated the existence of two clades of small subunit enzymes and one clade of large subunit enzymes among monofunctional catalases (Klotz *et al.*, 1997). The second less widespread class of catalase is composed of bifunctional, heme containing catalase-peroxidases that are closely related in sequence and structure to plant peroxidases. The third class includes the nonheme or Mn-containing catalases. In addition, a diverse group of proteins, all heme-containing such as chloroperoxidases, plant peroxidases and myoglobins, exhibit very low levels of catalase activity, attributable to the heme, which alone exhibits catalase activity (Nicholls *et al.*, 2001).

Most bacteria produce one or more catalases that usually respond to oxidative stress, either directly to H_2O_2 levels or to the presence of other active oxygen species. In *E. coli,* the catalase-peroxidase HPI (Hydroperoxidase I), or EcKatG, is controlled as part of the OxyR regulon, which senses active oxygen species, and the monofunctional catalase HPII is controlled as part of the σ^S regulon in the stationary phase. Recently, polyamines, including putrescine, spermidine and spermine, were reported to upregulate both the *oxy*R and *rpo*S regulons in *E.coli* (Jung *et al.*, 2003), but the mechanism remains unclear. There is a commonality of a reactive oxygen sensor or growth phase or σ-transcription factor control mechanism in controlling catalase gene expression, although there is no consistency in the pairing of the type of catalase and the type of regulator.

Like the catalases, peroxidases are predominantly heme-containing enzymes which catalyze the dismutation of hydrogen peroxide using an electron donor other than H_2O_2 (AH):

$$H_2O_2 + 2\ AH\ (\text{reduced}) \longrightarrow 2H_2O + 2A\ (\text{oxidized})$$

There is a significant variability in peroxidases compared to catalases in regard to their structural properties. This is probably a consequence of the many different roles that individual peroxidases play. While the majority of known peroxidases are hemoproteins, such as horseradish peroxidase (HRP), cytochrome *c* peroxidase (CCP), and other mammalian, plant and fungal peroxidases, there are also non-heme peroxidases, such as the vanadium containing chloroperoxidase enzyme from thr fungus *Cuvularia inaequalis* (Messerschmidt and Wever, 1996), the FAD cysteine redox center NADH peroxidase from *Streptococcus faecalis* (Stehle *et al.*, 1991), and the human peroxiredoxin (peroxidase) (Choi *et al.*, 1998). Peroxidases are discussed in detail in the later sections.

Glutathione peroxidases (GPx) or ascorbate peroxidases are reductases which receive reducing equivalents or are regenerated by electrons from NADPH in metabolic pathways. GPxs are absent in *E.coli*, but in animal cells these are selenoenzymes, which catalyze the reduction of hydroperoxidases at the expense of GSH (Flohe, 1988; Ursini *et al.*, 1995). The GPx active site contains selenium in the form of the selenocysteine residue (Flohe *et al.*, 1973; Stadtman, 1991). There has been no report of a selenium dependent glutathione peroxidase activity in plants and H_2O_2 is degraded by ascorbate peroxidase (Bunkelmann and Trelease, 1996; Smirnoff, 1996).

1.4. The monofuctional, heme containing catalases

1.4.1. Introduction

All heme-containing catalases have a common two stage mechanism for the degradation of H_2O_2. In the first step, one hydrogen peroxide molecule oxidizes the heme

to an oxyferryl species, the so called compound I, in which one oxidation equivalent is removed from the iron and one from the porpyrin ring to generate a porphyrin cation radical [reaction 1]:

$$\text{Enz (Por-Fe}^{III}\text{)} + H_2O_2 \longrightarrow \text{CpdI (Por}^{\circ+}\text{-Fe}^{IV}\text{=O)} + H_2O \qquad (1)$$

Compound I is a short lived catalytic intermediate with a distinct absorption spectrum characterized by a reduction of absorption intensity of the Sorêt band (at approximately 406 nm; a band diagnostic of hemoprotein). Compound I formation is believed to be initiated by a histidine side-chain in the active site above the plane of the heme. The distal histidine act as a general acid-base catalyst forming a hydrogen bond with the hydrogen peroxide also coordinated to the heme iron. This facilitates the formation of the transition state, which is stabilized by an additional hydrogen bond with an asparagine, leading to scission of the peroxide O-O bond with one oxygen transferred to the iron forming compound I and the second oxygen being connected to water (Fita and Rossman, 1985). A second molecule of hydrogen peroxide is utilized as a reductant of compound I to regenerate the resting enzyme, water and oxygen [reaction 2]:

$$\text{CpdI (Por}^{\circ+}\text{-Fe}^{IV}\text{=O)} + H_2O_2 \longrightarrow \text{Enz (Por-Fe}^{III}\text{)} + H_2O + O_2 \qquad (2)$$

Despite this common reaction, there are significant differences in reactive capability among the members of this very large family of enzymes (Switala and Loewen, 2002).

Approximately 256 sequences of mono-functional catalase have been divided into three clades arising from a minimum of two gene duplication events (Klotz and Loewen, 2003). Recent induction of catalase-peroxidase and non-heme catalases into the universal tree of life created a larger picture. Clade 1 catalases are predominantly of plant origin, but with one algal representative and a sub group of bacterial origin. Clade 2 enzymes are

all large subunit enzymes of bacterial and fungal origin. The one archaebacterial clade 2 enzyme is postulated to have arisen in a horizontal transfer event from a bacillus species. The clad 3 enzymes are all small subunit enzymes from bacteria, archaebacteria, fungi and other eukaryotes (Koltz and Loewen, 2003).

Catalases do not follow Michaelis-Menton kinetics except at low substrate concentration; rather, they show pseudo first order saturation kinetics. A comparative study of 16 catalases has shown the great divergence in properties within the catalase family (Switala and Loewen, 2002). Different enzymes are affected differently at higher substrate concentration. Most small subunit enzymes suffer inactivation by H_2O_2 at concentrations above 300-500 mM and never reach the Michaelis-Menten V_{max} predicted by extrapolation from rates at lower substrate concentrations. Large subunit enzymes show inhibition to H_2O_2 only at concentrations above 3 M, if at all, and exceed the predicted Michaelis-Menten V_{max}. Consequently the presentation of observed data in terms of the typical constants K_m and V_{max} is misleading because true Michaelis-Menten kinetics are not applicable. Sequence differences among catalases are considered to be responsible for the widely differing reactions rates and substrate affinities, but a rationale for how has not been proposed (Chelikani *et al.*, 2004).

1.4.2. Structural properties of catalases

All monofunctional catalases so far characterized are tetrameric, but there are reports of hexamers and an unusual heterotrimer from *Pseudomonas aeruginosa* which have not yet been substantiated by structural analysis. To date the crystal structures of eleven monofunctional catalases have been reported. These include catalases from:

bovine liver (BLC) (Murthy *el al.*, 1981, Melik-Adamyan *et al.*, 1986), *Penicillium vitale* (PVC) (Vanishtein *et al.*, 1981 and 1986), *Micrococcus lysodeikticus* (MLC) (Murshudov *et al.*, 1982), *Proteus mirabilis* (PMC) (Gouet *et al.*, 1995), *Escherichia coli* (HPII) (Bravo *et al.*, 1995 and 1999), human erythrocytes (HEC) (Ko *et al.*, 1999; Puntam *et al.*, 1999), *Pseudomonas syrengae* (CatF) (Carpena *et al.*, 2001 and 2003), *Helicobactor pylori* (HPC) (Loewen *et al.*, 2004), *Neurospora crasa* (Cat 1) (Diaz *et al.*, 2004) and *Enterococcus faecalis* (Håkansson *et al.*, 2004). The characteristic feature of a catalase structure is a core beta barrel inside which is the deeply buried heme active site accessed by two or three channels (Loewen *et al.*, 2004). In BLC, CATA, HEC, PMC and MLC, there is a common orientation of the active site His imidazole ring over ring III of the heme (His-III orientation) which was concluded to be the normal heme orientation in catalase. In PVC and HPII, the heme orientation is flipped with the active site His located above ring IV of the heme (His-IV) (Murshodov *et al.*, 1996; Chelikani *et al.*, 2004). This flipped orientation in large subunit enzymes is accompanied by oxidation of the heme to heme d to form a cis-hydroxyspirolactone group on ring III (Murshudov *et al.*, 1996) and suggested that large subunit enzymes are unique. Demonstration of the His-IV orientation in CatF, a clade I catalase, suggested a more general distribution. Recent structure-function studies on variants of HPII (Chelikani *et al.*, 2003) and CatF (Carpena *et al.*, 2003) have revealed significant information about the channel architecture in catalases. The deeply buried heme is connected to the surface by three channels. The main channel gives the most obvious access route to the heme as it approaches the heme perpendicular to its plane and has long been considered the primary access route for substrate H_2O_2 (Mate et al., 1999; Sevenic *et al.*, 1999; Melic-Adamayan *et al.*, 2001; Chelikani *et al.*,

2003). The second channel approaches the heme laterally, almost in the plane of the heme, and has been referred as the minor or lateral channel. The third channel has been proposed to connect the heme to the central cavity but the role of this channel has not been proposed (Chelikani *et al.*, 2003).

1.4.3. An electrical potential field in the channel of mono-functional catalases

In 2003, Chelikani *et al,* demonstrated the striking influence of the negatively charged side chain of a conserved Asp (181 in HPII) on catalase activity. When replaced with any uncharged residue, polar or non-polar, including Asn, Ala, Ser, and Ile, enzymatic activity was lost accompanied by a reduction in solvent occupancy in the channel including the sixth ligand water in all subunits of Asp181Ala, Asp181Ser, and Asp181Gln. However, variant Asp181Glu exhibited normal levels of activity and contained the sixth ligand water in all subunits as part of an unbroken water matrix extending the full length of the channel. The existence of an electrical potential field in the hydrophobic portion of the channel between the negatively charged carboxylate and positively charged heme iron was proposed as an explanation for the phenomenon. The potential field influences the orientation of any molecule with an electrical dipole including both H_2O and H_2O_2. In both cases, the preferred orientation will be with oxygen atoms pointed toward the positively charged heme iron and the hydrogens toward the negatively charged side chain of Asp or Glu. The uniform orientation of waters favours hydrogen bond formation and explains the high water occupancy with both Asp181 and the variant Asp181Gln. A second result of the induced orientation of hydrogen peroxide is that it will enter the active site with the a-oxygen oriented toward

the heme iron and the a-hydrogen on this oxygen located within the hydrogen bonding distance of the NH_2 of the active-site Asn, thereby explaining conclusion from molecular dynamic studies that the substrate hydrogen peroxide enters the active site in a preferred orientation (Kalko *et al.*, 2001).

1.5. Non-heme or manganese containing catalases

There is another group of catalases that, instead of heme, contains a manganese complex at the reaction center. This group was initially referred to as pseudo-catalases because the enzyme lacked a heme prosthetic group (Kono and Fridovich, 1983), but now are more commonly called Mn-containing catalases (Allgood and Perry, 1986), with the terms non-heme (Nicholls, 2001) and dimanganase catalase (Antonyuk *et al.*, 2000) also being used. These are not as widespread as the heme-containing catalases, being found only in eubacteria with the exception of *Pyrobaculum calidifontis* (a facultative aerobic respiratory, hypertherophylic Chrenarcheabacterium). They show lower enzymatic activity than heme-containing catalases with the exception of *P. calidifontis* catalase (Koltz *et al.*, 1997).

1.6. Monofunctional peroxidases

Peroxidases are predominantly heme containing and catalyze the hydrogen peroxide mediated oxidation of various organic and inorganic substrates generating in some cases, free radial species (Hillar *et al.*, 1999). The overall reaction can be summarized as:

$$H_2O_2 + 2AH \text{ (reduced)} \longrightarrow 2H_2O + 2A \text{ (oxidized)} \qquad (1)$$

Typical reducing substrates include aromatic phenols, phenolic acids, indoles, amines and sulfonates although inorganic ions are used by a few enzymes (Preston *et al.*, 1987). The reaction proceeds in three steps, with the first step involving formation of Compound I, a high oxidation state intermediate comprising an Fe(IV) oxoferryl centre and a porphyrin-based cation radical [reaction 2], common to both catalases and pereoxidases:

$$\text{Enz (Por-Fe}^{III}\text{)} + H_2O_2 \longrightarrow \text{CpdI (Por}^{\bullet+}\text{-Fe}^{IV}\text{=O)} + H_2O \quad (2)$$

$$\text{CpdI (Por}^{\bullet+}\text{-Fe}^{IV}\text{=O)} + AH_{red} \longrightarrow \text{CpdII (Por-Fe}^{IV}\text{-OH)} + A_{ox} \quad (3)$$

$$\text{CpdII (Por-Fe}^{IV}\text{-OH)} + AH_{red} \longrightarrow \text{Enz (Por-Fe}^{III}\text{)} + A_{ox} \quad (4)$$

A transient intermediate (compound 0) formed prior to compound I has been detected in reactions between HRP C and H_2O_2 at low temperatures and described as an Fe(III)-hydroperoxy complex (Filizola and Loew, 2000). In formal terms, compound I is two oxidizing equivalents above the resting state. The first one-electron reduction step requires the participation of a reducing substrate and leads to the generation of compound II, an Fe(IV) hydroxoferryl species that is one-oxidising equivalent above the resting state [reaction 3]. Both compound I and compound II are powerful oxidants, with redox potentials estimated to be close to +1 V. The second one-electron reduction step returns compound II to the resting state of the enzyme. Reaction of excess hydrogen peroxide with the resting state enzyme gives compound III, which can also be prepared by several other routes (Dunford, 1991). This intermediate is best described as a resonance hybrid of iron (III)-superoxide and iron (II)-dioxygen complexes. A high-resolution crystal structure of 95% compound III shows dioxygen bound to heme iron in a bent conformation (Berglund *et al.*, 2002), . A similar but irreversibly inactivated compound

IV formation has also been reported (Baynton *et al.*, 1994). A covalently modified heme iron, possibly with a perhydroxy or dioxygen group in a compound III like structure, has been reported in the crystal structure of *Helicobacter pylori* catalase (HPC), with and without formic acid bound, (Loewen *et al.*, 2004). In the HPC structure, the elongated electron density associated with the iron in subunit B resembles the maps of oxymyoglobin (Vojtechovsky *et al.*, 1999) and compound III of horseradish peroxidase (Berglund *et al.*, 2002). High resolution crystal structures of the oxidised intermediates of HRP C has shown that distal heme pocket residues Arg38 and His42 (conserved in all members of the plant peroxidase superfamily) play a significant role in the formation of compound I (Berglund *et al.*, 2002).

In 1992, Welinder performed multiple sequence alignment of number of peroxidases and classified them into three distinct structural families or classes. Class I enzymes are identified as bacterial peroxidases, and include the sequence of *E. coli* catalase-peroxidase and yeast cytochrome *c* peroxidase. Class II enzymes include the plant peroxidases such as horseradish peroxidase isoenzyme C while class III contains the classical secretory plant peroxidases for example horseradish peroxidase. It should be noted that the structural classes identified do not imply degrees of evolutionary relatedness, simply structural variation (Hillar, 2000). Among class I enzymes, for example, the yeast cytochrome c peroxidase has been shown to be evolutionarily distinct from bacterial peroxidases (KatGs) by phylogenetic analysis (Klotz, 1997).

1.7. Catalase-peroxidases

Catalase-peroxidases, also called KatGs after the encoding gene *katG* (Loewen *et al*, 1985), are found in bacteria, archaebacteria and a few fungi. In 1992, catalase-peroxidases gained significant notoriety with the reports confirming that mutations in the *katG* gene encoding the *Mycobacterium tuberculosis* catalase-peroxidase (MtKatG) were responsible for resistance against isoniazid (Zhang *et al.*, 1992), the front line anti-tuberculosis drug, and were the leading cause of the world-wide resurgence of tuberculosis (Deretic *et al.*, 1996). This gave rise to significant interest among researchers, worldwide. These fascinatingly complex enzymes show strong catalatic activity, although with turnover rates only 1-20 % of mono-functional catalases and a broad spectrum peroxidatic activity. They have recently been associated with a slow NADH oxidase, hydrazinolysis and isonicotinyl NAD synthase activities (Singh *et al.*, 2004). The catalase-peroxidase HPI of *E. coli* was first purified and characterized in 1979 (Claiborn and Fridovich, 1979), and its encoding gene *katG,* was sequenced in 1988 (Triggs-Raine *et al.*, 1988), providing the first catalase-peroxidase sequence and demonstrating the sequence similarity to plant peroxidases. Since then a wide variety of KatGs have been purified, characterized and sequenced.

1.7.1. Phylogeney of catalase-peroxidases

Catalase-peroxidases bear significant sequence similarity to eukaryotic class I heme peroxidases of the plant, fungal and bacterial peroxidase superfamily (Welinder *et al.*, 1992). This superfamily includes three independent evolutionary lineages depending upon the cellular location and function of the enzyme. Class I (peroxidases of prokaryotic

origin) contains the large family of ascorbate peroxidases from higher plants and green algae, cytochrome *c* peroxidase (CcP) from *Saccharomayces cerevisiae*, and catalase-peroxidases. Class II comprises extracellular fungal peroxidases (e.g lignin peroxidase, manganese peroxidase), while class III contains the classical secretory plant peroxidases (e.g horseradish peroxidase) (Zàmocký *et al.*, 2000). All representatives possess the same heme prosthetic group containing high spin ferric heme. Catalase peroxidases are the only member of this superfamily that possesses notable catalase activity (i.e. they can reduce and oxidize hydrogen peroxide). All other members of the superfamily are restricted to reducing hydrogen peroxide with subsequent oxidation of a secondary substrate. These 'noncatalase' members of class I exhibit strong specificity for electron donors: the preferred substrate is ascorbate in the case of ascorbate peroxidase and cytochrome *c* in case of cytochrome *c* peroxidase. The *in vivo* substrate for the peroxidatic reaction of catalase-peroxidases remains unidentified. Sequence analysis has revealed that catalase-peroxidases have evolved from a common ancestor, shared with class I, II and III peroxidases (Zàmocký *et al.*, 2000). The core of the enzyme is a non-bundled α-helical fold consisting of ten helices with bound ferric protoporphyrin IX (Zàmocký *et al.*, 2000), but KatGs arose from a gene duplication event, giving rise to a two domain structure in which the N-terminal domain is active and the C-terminal domain is inactive (Welinder, 1992). The first review on KatG phylogeny included 19 sequences (Faguy *et al.*, 2000) while the most recent has 60 sequences (Zàmocký *et al.*, 2004). With the large number of sequences in the data set, the tree is less robust than previous trees that were based on a much smaller set of selected sequences (Klotz *et al.*, 1997; Faguy and Doolittle, 2000; Loewen *et al.*, 2000) leading to several possible

interpretations of relationships. Upon integration into a conceptual tree of life, it is apparent that KatGs evolved much later than the heme-containing mono-functional catalases, and a significant frequency of lateral gene transfer is evident (Klotz and Loewen, 2003). A recent report has also supported this by analyzing sixty representative sequences covering all known subgroups of class I of the super-family of bacteria, fungal and plant heme peroxidases, showing that the duplication event in *katG* occurred at a later phase of evolution (Zàmocký *et al.*, 2004).

1.7.2. Regulation of catalase-peroxidase gene (*katG*) expression.

Regulation of KatG normally occurs through the OxyR regulator belonging to the LysR family. OxyR is an H_2O_2 sensing transcriptional regulator and transducer of oxygen stress. It is activated by disulfide bond formation between two cysteine residues and induces the expression of *oxyS* (which encodes a small, nontranslated regulatory RNA), *katG* (which encodes hydrogen peroxidase I), *ahpC* (which encodes alkyl hydroperoxide reductase), *gorA* (which encodes glutathione reductase), *dps* (which encodes DNA binding protein), and *grxA* (which encodes glutaredoxin 1). Glutaredoxin 1 deactivates OxyR by reducing the disulfide bond, forming an autoregulatory feedback loop (Zheng *et al.*, 1998). Only the oxidized form of the protein is able to activate the expression of downstream genes and negatively autoregulate its expression by binding to specific regions in promoters (Christman *et al.*, 1989). Irrespective of its redox state, OxyR also acts as a repressor of its own expression like other LysR transcriptional regulators. Several *oxyR* genes have been identified in other organisms, such as *Burkholderia pseudomallei* (Loprasert *et al.*, 2002), *Haemophilus influenzae* (Maciver and Hensen,

1998), various *Mycobacterium* species (Dertci *et al.*, 1995, Dhandayuthapani *et al.*, 1997), *Xanthomonas* species (Loprasert *et al.*, 1997), and even the anaerobic bacterium *Bacteroides fragilis* (Rocha *et al.*, 2000). In *E. coli*, *katG* is transcriptionally induced during the logarithmic phase in response to low concentrations of H_2O_2, and requires the transcriptional regulator, OxyR (Visick *et al.*, 1997). Conversely, monofunctional HPII is induced during the transition from the exponential phase to stationary phase by RpoS, an alternative sigma factor, which is neither regulated by OxyR nor induced by H_2O_2 (Loewen *et al.*, 1985; Mukhopadhyay *et al.*, 1994; Mulvey *et al.*, 1990; Schellhorn *et al.*, 1992). *M. tuberculosis* has a non functional OxyR gene with several mutations making it a natural mutant of OxyR (Deretic *et al.*, 1995; Sherman *et al.*, 1995). In all the mycobacterial species studied, the DNA region immediately upstream of the *katG* genes is highly conserved and encodes the *furA* gene, suggesting a putative involvement of the FurA protein in *katG* regulation (Anna *et al.*, 2001). In *M. smegmatis*, a knockout *furA* mutant over expressed the catalase-peroxidase KatG and was complemented by expression of FurA suggesting that FurA is a negative regulator of *katG*. Fur-like proteins are transcriptional repressors that exhibit a Fe^{2+}-dependent DNA binding activity and regulate several genes involved in iron metabolism (Escolar *et al.*, 1999). There is an intimate relationship between iron metabolism and oxidative stress as the cytotoxic effects of reactive oxygen species are largely mediated by iron, and regulators of *E coli* involved in oxidative stress response, OxyR and SoxRS, activate the expression of Fur (Zheng and Storz, 2000). *E. coli* Δ*fur* mutants are more sensitive to hydrogen peroxide than are Fur-proficient strains (Touati *et al.*, 1995). In *M. smegmatis*, hydrogen peroxide sensitivity is increased by iron starvation (Lundrigan *et al.*, 1997); in *Staphylococcus*

aureus, Fur is necessary for oxidative stress resistance (Horsburgh *et al.*, 2001); and in *Streptomyces* spp., Fur-like proteins regulate catalase-peroxidase genes in an iron-dependent manner (Zou *et al.*, 1999).

1.7.3. Structure and Mechanism of catalase-peroxidases

Catalase-peroxidases are unique in modulating substantial catalase and peroxidase activity from a single enzyme. Despite the lack of similarity in the sequence and structure between catalase-peroxidases and mono-functional catalases, they share a common catalatic reaction for the compound I formation [reaction 1]. Biochemical and structural characterization of KatGs suggested this common reaction could be attributed to the active sites of both enzymes, which contain heme and have similar roles for the active site residues, though in catalase-peroxidases asparagine is replaced by the arginine or tyrosine (Carpena *et al.*, 2003; Jakopitsch et al., 2003). In catalases, the compound I is reduced to the ground state in a single two-electron reduction step using a second molecule of hydrogen peroxide while the peroxidatic reaction requires an electron doner to reduce the compound I to the ground state in two one-electron reduction steps [reactions 2 and 3]. A variety of organic substances, such as *o*-dianisidine, ABTS and pyragallol, act as the electron donating substrate, *in vitro*, for the peroxidatic reaction, but *in vivo*, the peroxidatic substrate remains unknown.

Attempts to crystallize KatGs were unsuccessful until 2001 when the first report describing the crystal structure of the halophilic archaebacterium *Haloarcula marismortui* (HmKatG; Yamada *et.al.*, 2001, 2001) appeared. This was followed by the

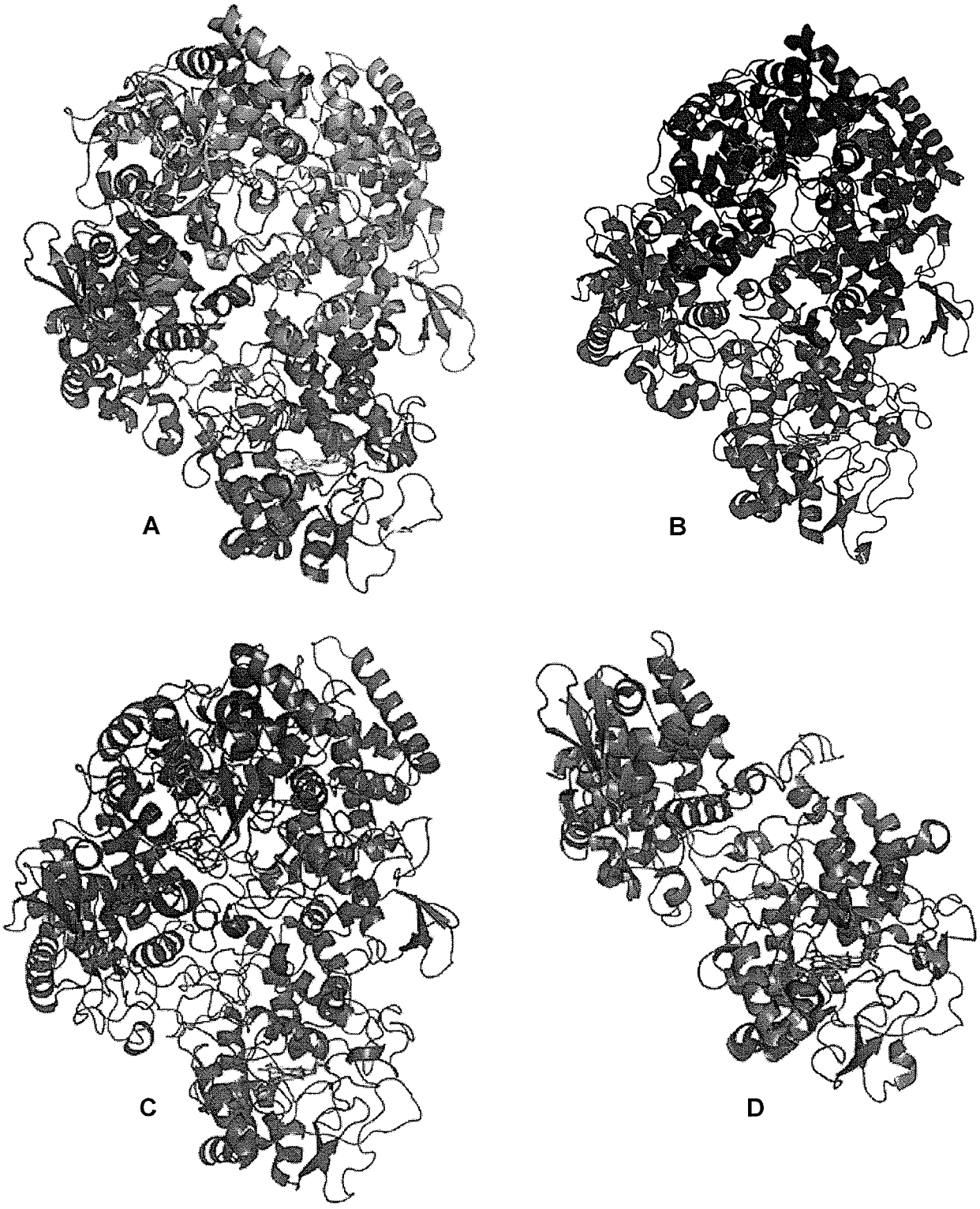

Figure 1.3. Structures of catalase-peroxidase (KatG) from *Burkholderia pseudomallei* (A), *Mycobacterium tuberculosis* (B), *Haloarcula marismortui* (C), and *Synechocystis* PCC 7942 (D). Each subunit is shown with different colour and the heme is shown in green. Ribbon representations are prepared using Pymol (Deleno, 2002)) and the coordinates submitted to the protein data bank.

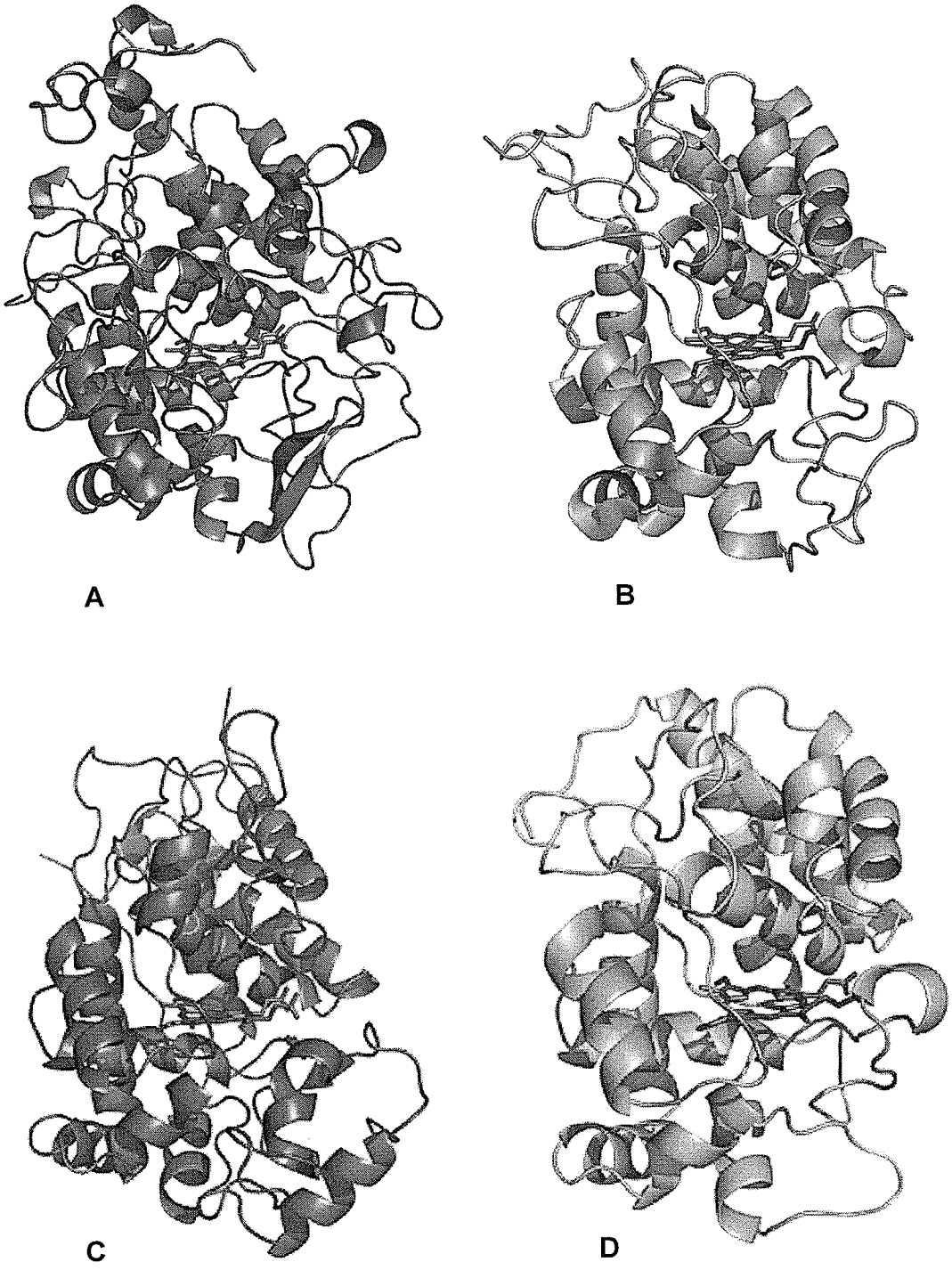

Figure 1.4. Structures of the N-terminal of BpKatG (A), cytochrome *c* Peroxidase (B), Horseradish peroxidase (C), and ascorbate peroxidase (D). The heme is shown in green.Ribbon representations are prepared using Pymol (Deleno, 2002) and the coordinates submitted to the protein data bank.

crystal structure reports of KatGs from *Burkholderia pseudomallei* (BpKatG; Carpena *et al.*, 2002, 2003), *Synechococcus* (SyKatG; Wada *et al.*, 2002) and *Mycobacterium tuberculosis* [Figure1.3] (Bertrand *et al.*, 2004). In addition, the crystal structure of the C-terminal domain of *E. coli* HPI has been reported (Carpena *et al.*, 2004).

Crystal structure analysis confirms that KatGs are normally active as homodimers, although homotetrameric associations do occur, as in EcKatG or HPI. The individual subunits are relatively large at approximately 80,000 Da and have two distinct but sequence related domains, possibly fused during a gene duplication event (Welinder, 1991). During subsequent evolution, the N-terminal domain retained (or acquired) the ability to bind heme and the C-terminal domain lost (or never acquired) this ability. Despite this functional divergence, considerable structural homology has been conserved, with a root mean square deviation (r.m.s.d) of 2.19 Å for the Cα atoms of 133 residues in the ten α helical sections that are topologically equivalent in the two domains of BpKatG. The two subunits in the molecule are associated mainly through interactions between the N- and C-terminal domains, with few N-terminal to N-terminal and no C-terminal to C-terminal domain interactions.

A role for the C-terminal domain, other than as an agent for dimer formation and stabilization, has not been determined (Carpena *et al.*, 2004). The heme is located in the N-terminal region (Figure 1.3) and the heme environment in KatG has been shown to be similar to that of plant peroxidases [Figure1.4] (Yamada *et al.*, 2002; Carpena *et al.*, 2003; Wada *et al.*, 2002; Bertrand *et al.*, 2004). On the distal side of heme, the active site triad of Arg108, Trp111, and His112 (BpKatG numbering) is typical of all

catalase-peroxidases and of class I peroxidases. On the proximal side, His279 is the fifth ligand to the heme iron atom also as in the peroxidases, and it is in close association with the fully conserved Asp389, which interacts with the indole N atom from the proximal Trp330 (Carpena *et al.*, 2003) as shown in Figure 1.5.

Crystal structures from four KatGs and one variant from BpKatG (Ser324Thr, Deemagaran *et al.*, 2005) and MtKatG (Ser315Thr Zhao *et al.*, 2006) has provided better insight into the structural properties but there is no consensus on the structural basis for the high catalase activity of KatGs. It is not clear whether the role of KatG compound I is the same as in monofunctional catalases or it follows a different path. KatG's thermodynamics present no barrier to the two electron oxidation of hydrogen peroxide to dioxygen. The standard reduction potential of the redox couple E'^{o} (O_2/H_2O_2) is 280 mV (Wood, 1988), and normally the oxidizing intermediates of heme peroxidases are strong oxidants (Dunford, 1999).

It has previously been shown that KatG compound I, like that of monofunctional catalases, does not accumulate during H_2O_2 degradation but can be trapped by using organic peroxides (Jakopitsch *et al.*, 1999). However, this intermediate shows a low reactivity towards H_2O_2 (Jakopitsch *et al.*, 1999). Also, both in the absence and in the presence of one electron donors, accumulation of a hydroxo ferryl like compound II was never observed in wild type KatGs, suggesting that the spectral signature of KatG compound II could be similar to that of the ferric protein (Jakopitsch *et al.*, 1999; Reglesberger *et al.*, 2000). Unlike plant peroxidases, in KatGs the formation of compound III has not be confirmed even at higher concentration of H_2O_2 (Chauchane *et al.*, 2000). Besides these mechanistic peculiarities, KatG's structural analysis has

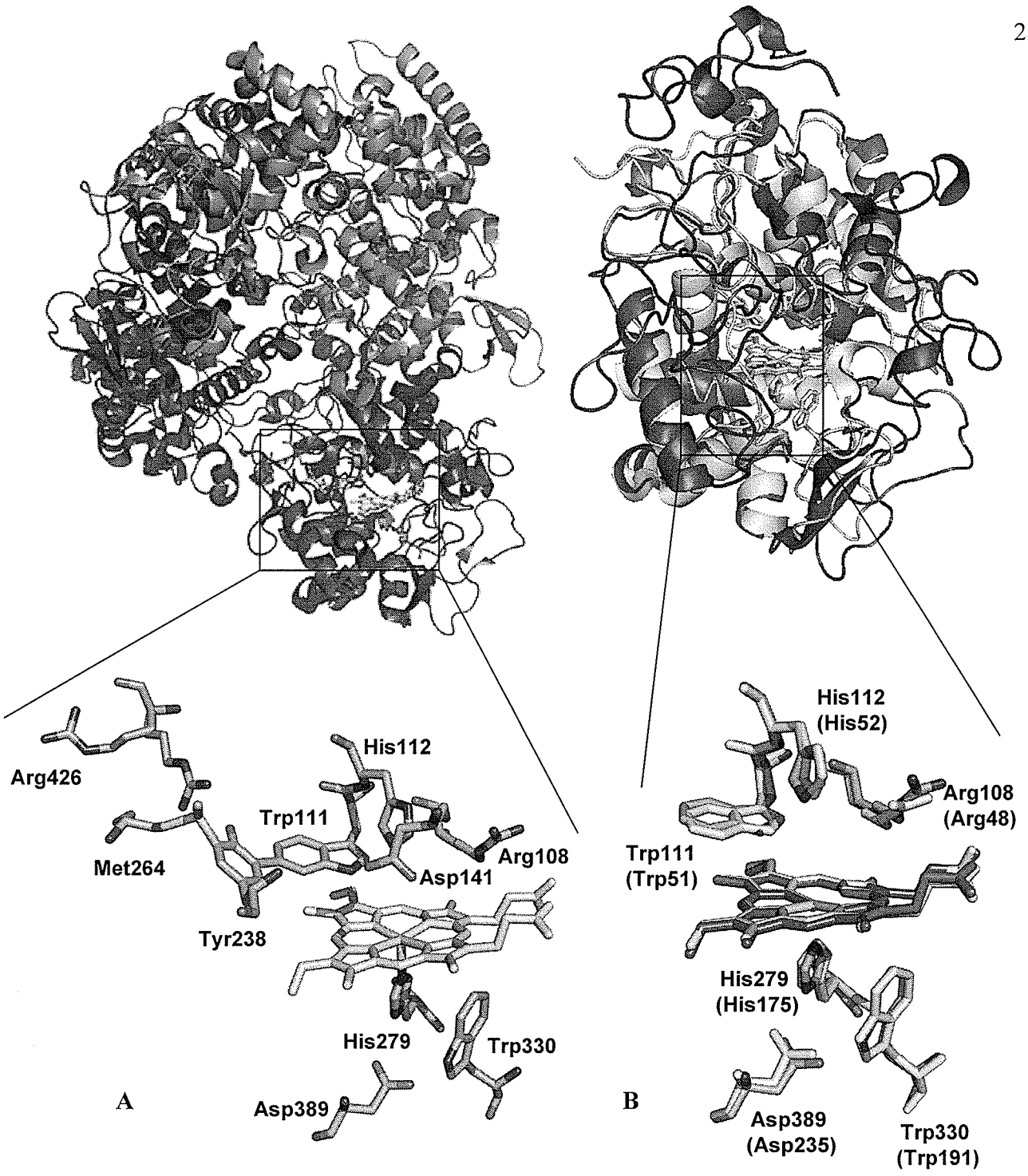

Figure 1.5. Panel A shows the active site residues in the proximal and distal side of BpKatG. In the panel B, an overlay of cytochrome *c* peroxidase with the N-terminal of BpKatG has been shown. KatG's subunits are shown with different colours and CcP is shown in yellow and parenthesis indicates residues numbering in CcP. Figures are prepared using Pymol (Deleno, 2002) and the coordinates submitted to the protein data.

revealed some striking difference from heme peroxidases as discussed in the following sections.

1.7.3.1. The unusual covalent modifications

In a wide range of metalloenzymes, active site residues undergo covalent modification such as in cytochrome *c* oxidase (His240-Tyr244; $heme_{a3}$-Cu_B) (Ostermeier *et al.*, 1997; Yoshikawa *et al.*, 1998; Buse *et al.*, 1999), catalase HPII (His392-Tyr415; heme) (Bravo *et al.*, 1997), galactose oxidase (Tyr272-Cys228; copper) (Ito, *et al.*, 1994; Ito, *et al.*, 1994), catalase 1 (Cys-356-Tyr379; heme) (Diaz *et al.*, 2004), and amine oxidases (2,4,5 trihydroxyphenylalanine quinine; copper) (Parsons *et al.*, 1995). In KatGs three unusal covalent modifications has been reported. The most prominent modification is the cross linking of three amino acid side chains, Trp111, Tyr238 and Met264 (BpKatG numbering) located on the distal side of the heme [Figure 1.6a] and has been reported in the crystal structure reports of all four KatGs and the variant Ser324Thr of BpkatG (Yamada *et al.*, 2002; Carpena *et al.*, 2003; Wada *et al.*, 2002; Bertrand *et al.*, 2004; Deemagaran *et al.*, 2005).

This modification has also been confirmed by mass spectrometric analysis of BpKatG (Donald *et al.*, 2003) and MtKatG (Ghiladi *et al.*, 2005; Ghiladi *et al.*, 2005a). Met–Tyr–Trp crosslink appears to be a characteristic common to all KatGs and has been shown to be essential for catalase activity (Donald *et al.*, 2003; Jakopitsch *et al.*, 2003; Ghiladi *et al.*, 2005; Santoni *et al.*, 2004; Jakopitsch *et al.*, 2003a; Jakopitsch *et al.*, 2004; Ghiladi *et al.*, 2005a). Similar cross-link has not been reported in heme peroxidases and these distal tyrosine and methionine are not conserved. Other modifications include a perhydroxy group added to the vinyl group on the ring I of the heme of BpKatG [Figure

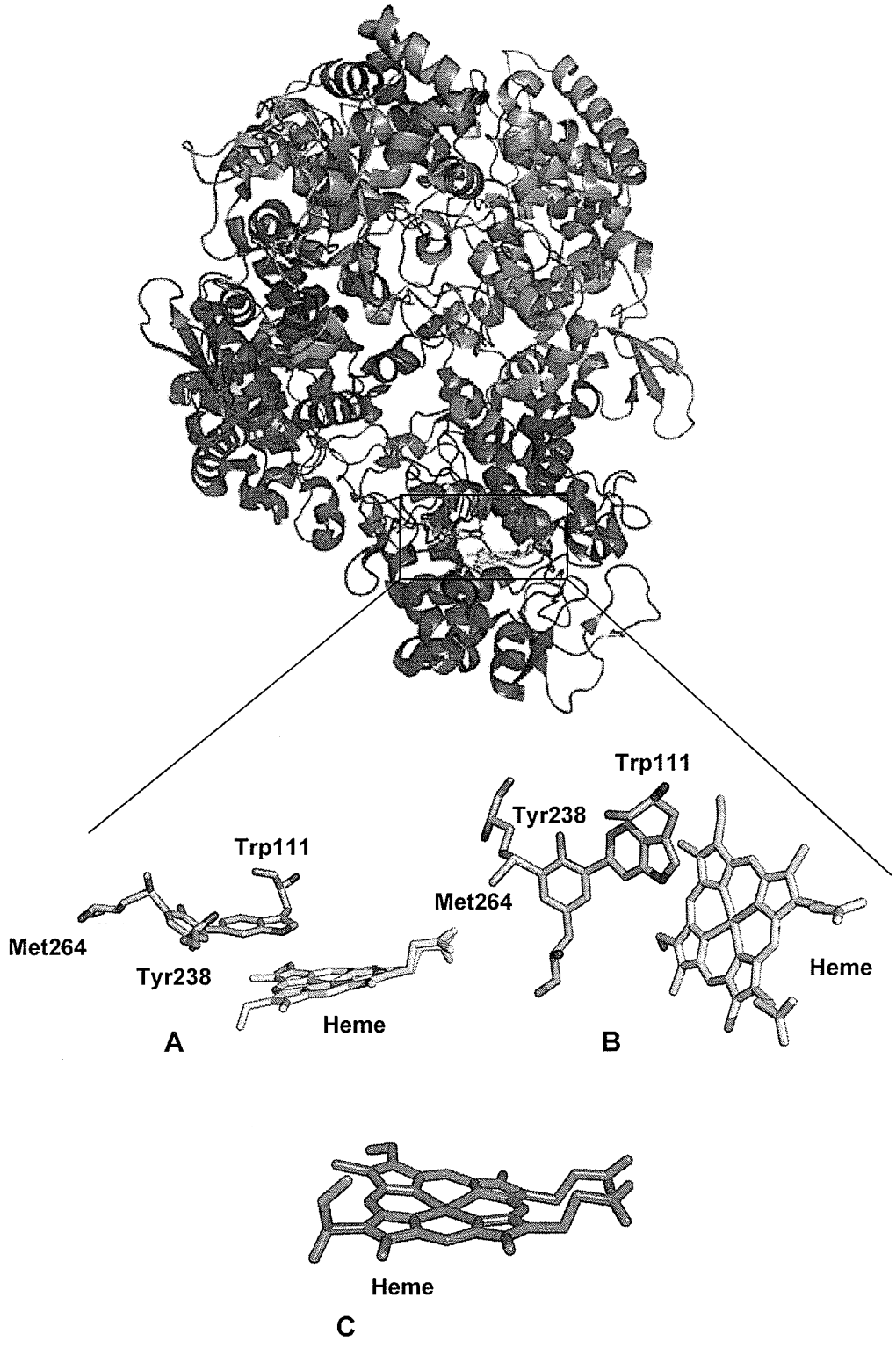

Figure 1.6. Structural representation of covalent modifications in BpKatG: Trp111-Tyr238-Met264 cross link has been shown in two views; A is rotated almost 90° to B. Panel C shows the peroxy modification (shown in red) on heme. Figures are prepared using Pymol (DElono, 2002) the coordinates submitted to the protein data bank.

1.6b] (Carpena *et al.*, 2003) and a perhydroxy group on the indole N of Trp111 of BpKatG (Deemagarn *et al.*, 2005; Carpena *et al.*, 2006).

1.7.3.1.1. The covalent Trp111-Tyr238-Met264 cross link

The crossed linked peptide (Trp-Tyr-Met) in KatGs has been subjected to extensive study using structural, mass spectrometric and HPLC analysis. Studies on BpKatG demonstrated that the covalent adduct involves the indole ring of the active site Trp111 and the sulfur of Met264 joined to the two ortho positions of Tyr238, and is found in close proximity to the heme [Figure1.6a] (Donald *et al.*, 2003). Trp111 is a catalytic residue required for compound I reduction in the catalatic reaction (Hillar *et al.*, 2000 and Jakopitsch *et al.*, 2003). Possible roles suggested for the covalent adduct include stabilizing the indole ring in the active site and providing a route for electron transfer. Mass spectrometric analysis of BpKatG, EcKatG (Donald *et al.*, 2003), *Synechocystis* KatG (Jakospitch *et al.*, 2003) and MtKatG (Ghiladi *et al.*, 2005; Ghiladi *et al.*, 2005a) have confirmed the presence of the Trp-Tyr-Met adduct in the five catalase-peroxidases and supports the conjecture that the structure may be common to all catalase-peroxidases (Smulevich *et al.*, 2006).

Recently, De Montelleno demonstrated that formation of the Met–Tyr–Trp crosslink is autocatalytic and requires compound I as the two electron oxidizing species rather than compound II (Ghiladi *et al.*, 2005). A comparison of apoMtKatG with holoMtKatG demonstrated the lack of cross link in holoenzyme and its reconstitution with heme alone did not generate the cross link rather a 33% cross link formation was

observed after incubating the reconstituted enzyme with PAA (peroxy acetic acid) (thus generating compound I) but generation of compound II by incubating the enzyme with even an higher concentration of MMMP (2-methyl-1-phenyl-2-propyl hydroperoxide), leads to a negligible increase in the cross link present. Auther attributed higher efficiency (as compared to 33%) *in vivo* to the presence of bound substrate.

The cross link formation has been proposed to be a sequential process with both Trp107 and Tyr229 (MtKatG numbering) necessary for complete Met–Tyr–Trp crosslink. Variants of Met255 still produced a Tyr–Trp linkage despite the lack of a Met–Tyr linkage, suggesting that the cross link forms first between the Cη2 of Trp107 and Cε1 of Tyr229, followed by bond formation between the Cε2 of Tyr229 and Sδ of Met264 (Jakopitsch *et al.*, 2003; Ghiladi *et al.*, 2005). Thus, the over all reaction starts with compound I formation either by a peracid (*in vitro*) or hydrogen peroxide (*in vivo*) leading to oxidation of both Tyr229 and Trp107 which, being in close proximity to the heme periphery (~3.7 Å and 5.9 Å), remains within the threshold for long range electron transfer (Gray and Winkler, 1996; Gray and Winkler, 2003) and are capable of being oxidized by compound I with concomitant formation of Trp107$^{\circ+}$ and Tyr229$^{\circ+}$ radicals. Simultaneous formation of these protein radicals from a single turnover event makes possible their coupling to the Tyr-Trp bond. Formation of a second compound I intermediate results in further oxidation of the Tyr-Trp cross link leading to nucleophilic attack of the sulfur atom of Met255 on the quinine-like intermediate, ultimately forming the Met-Tyr-Trp cross link (Ghiladi *et al.*, 2005). A similar process for Tyr-Trp cross link formation has been proposed for Met255 variant of MtKatG but in this variant further reaction with oxidized Tyr-Trp was not possible (Ghiladi *et al.*, 2005a). Mutating

equivalent Trp to Ala in SyKatG did not yield any Met-Tyr-Trp cross link (Jakotipsch *et al.*, 2003) which supported a sequential formation of bond between Tyr229 and Trp108, followed by Tyr229 and Met255.

The studies of Obinger and coworkers on the ferric, ferrous and fluoride complexes of Tyr249Phe, Met275Ile and Trp122Ala and Trp122Phe (SyKatG numbering) variants of SyKatG showed no significant effect on the protein structure on the proximal side of heme and attributed this to no change in frequency for the Fe-imidazole stretching modes as compared to the wild type SyKatG (Heering *et al.*, 2002; Santoni *et al.*, 2004; Santoni *el al.*, 2004a). Tyr249Phe and Met275Ile variants showed similar ferric spectra as that of wild type with a tendency to loose heme which was attributed to the presence of a shoulder at 368 nm in conjugation with an increase of a 6-coordinated (c) low spin (LS) heme at the expense of a native 5-coordinated high spin (HS) heme (Heering *et al.*, 2002). The Trp122Phe and Trp122Ala variants exhibit increased *pK*a of the alkaline transition and showed the presence of aquo 6-coordinated HS heme and hydroxyl 6-coordinated HS heme (Santoni *et al.*, 2004a). These authers demonstrated weakened heme binding with a destabilized protein when the crosslink was only partially formed, but the absence of the cross-link did not alter the disposition of the distal the Trp because the binding of fluoride was unaffected compared to native protein. On the other hand the variants Trp122Phe and Trp122Ala affected the protein to bind fluoride (Smulevich *et al.*, 2006).

A similar characterization of the equivalent variants (Tyr229Phe and Met255Ile) of MtKatG by Magliozzo and coworkers demonstrated spectroscopic features slightly different from those reported for SyKatG. The Met255Ile variant of MtKatG showed

greater relative population of 6-coordinated HS heme than either native KatG or Tyr229Phe variant and all three (native MtKatG and the variants Tyr229Phe and Met255Ile) lacking a detectable LS heme component (Chouchane *et al.*, 2003).

Jakopitsch *et al* demonstrated that KatGs can be converted into monofunctional peroxidases by mutating Tyr249Phe (in case of SyKatG). The variant Tyr249Phe also demonstrated the formation of an oxoferryl-porphyrin radical compound I upon addition of equimolar H_2O_2 to the ferric enzyme (a phenomenon difficult to observe in native enzyme due to its high catalase activity), followed by rapid formation of an intermediate with a oxoferryl type compound II spectrum similar to HRP (Jakopitsch *et al.*, 2003). Auther attributed this spectrum to the result of an endogenous electron transfer similar to a kinetic coupling demonstrated between the generation of a tyrosyl radical and the formation of the intermediate with the compound II like spectrum in Tyr229Phe variant of MtKatG (Yu *et al.*, 2003). This was also confirmed by sequential mixing-stopped flow analysis which directly produced oxoferryl type compound II by one electron reduction of the ferryl-porphyrin radical compound I (Jakopitsch *et al.*, 2003). In the presence of micromolar concentration of H_2O_2 and in the absence of one-electron donors, a compound III like spectrum has also been reported in Tyr249Phe variant of SyKatG (Regelsberger *et al.*, 2001; Jakopitsch *et al.*, 2003). These reports support the conjecture that covalent cross linking of distal Met-Tyr-Trp plays a significant role in maintaining the catalase and peroxidase activities of KatGs.

1.7.3.1.2. Perhydroxy modification of Heme

The second unusual modification is evident only in the BpKatG but not in the other three KatG structures. This is a perhydroxy modification on the ring I vinyl group of the heme (Carpena *et al.*, 2003). A simple hydration like addition of hydrogen peroxide across the double bond of the vinyl group has been suggested as the reason for this modified heme (Carpena *et al.*, 2003) [Figure 1.6b]. This modification on heme is shown to be removed easily by treatment of the enzyme with INH (X. Carpena, personal communication). The function of the perhydroxy group could be to serve as a reservoir of H_2O_2 in the active site, available for the immediate reaction when a peroxidatic substrate is contacted (Carpena *et al.*, 2003).

1.7.3.1.3. Perhydroxy modification on the Indole of Trp111

A perhydroxy modification on the indole nitrogen atom of Trp111 was reported in the crystal structure of the Ser324Thr variant of BpKatG (Carpena *et al.*, 2005). Interestingly, the modified Trp111 was not observed in the first crystal structure report of the wild-type BpKatG (Carpena *et al.*, 2003) but was present in a recent report and has been shown to be associuated the change in pH (Carpena *et al.*, 2006). The crystals of BpKatG soaked at different pH values showed almost no extraneous electron density in the vicinity of the indole nitrogen at pH 4.5 and almost 100% occupancy when pH was raised to 8.5, suggesting the gradual appearance of modification from 0% occupancy to almost 100% occupancy (Carpena *et al.*, 2006). EPR spectra were also correlated with the presence of the Trp 111 modification at pH above 7. The rapidity of perhydroxy-indole formation, 100% yield after just 1 min soaking of the crystal at pH 8.5, suggests a very

facile reaction with molecular oxygen in the buffer at higher pH, which correlates with the higher pH of NADH oxidase reaction (Singh *et al.*, 2004). The explanation for the presence of perhydroxy modification in the Ser324Thr variant at pH 5.7 has been attributed to an inductive effect of the extra methyl group of Thr324 facilitating indole oxidation (Carpena *et al.*, 2006).

1.7.3.2. Presence of three large loops in the catalytic region of KatGs

Apart from having a deeply buried heme, a longer and more constricted proposed access route for H_2O_2 and an unusual Met-Tyr-Trp covalent adduct, KatGs also have a short stretch and three large loop (LL) insertions (LL1-LL3) which differs them from peroxidases (Yamada *et al.*, 2002). The short stretch occurs at position 102–113 with the sequence pattern 'SQXWWPADXGXY' on the distal side of the heme, and is highly conserved (>95%) among all known KatGs (Zàmocký *et al.*, 2001). It is positioned in the region homologous to the connection between helices A and B. The first large insertion, which is of variable length among KatGs, occurs between positions 210 and 251 with a length of 36–43 residues between helices D and E situated between the distal and proximal catalytic domains. There is a conserved sequence on the C-terminus of this loop comprising residues 'AXXMGLIYVN'. The second large insertion at positions 300–334 between helices F and G has the same length for all known KatGs (35 or 36 residues) and is, relatively conserved among all KatGs with a signature sequence 'GXXPXXAXXEXQGLGW'. The third large insertion between residues 357 and 392 (between helices G and H) seems not to be highly conserved among KatGs on the other hand there exist a similar although shorter insertion in cytochrome *c* peroxidase. The

conservation evident in the inserts suggests that the first and the second insertions as well as the short distal stretch are of functional importance for KatGs (Zàmocký *et al.*, 2001). Recent crystal structure analysis of KatGs supports this hypothesis. Constriction of the access channel has been attributed to the LL1 and LL2 insertions, as LL2 is positioned at one edge of the heme between helices D and E connecting the distal and proximal catalytic domains. The LL1 insertion contains a number of residues neighboring the covalently linked Tyr249 that are highly conserved in KatGs *viz* Ile248, Asn 152, Pro252 and Glu253 (Jakopitsch *et al.*, 2005). Asp152 has been reported to be hydrogen-bonded to the LL1 residue Ile248 providing stability to the heme architecture and its substitution markedly changes the proximal His291-Asp402 hydrogen bond interaction (Santoni *et al.*, 2004), underlining the role of the LL1 insertion in linking the distal and proximal heme sites.

1.7.3.3. Substrate access channel

The crystal structure analysis of HmKatG (Yamada *et al.*, 2002) BpKatG (Carpena *et al.*, 2003), SyKatG (Wada *et al.*, 2002), MtKatG (Bertrand *et al.*, 2004), and the BpKatG Ser324Thr variant (Deemagaran *et al.*, 2005) has revealed several KatG specific peculiarities distinguishing these enzymes from other heme peroxidases. These peculiarities have also been shown to play an important role in the substrate access to the active site. An access route, for the substrate hydrogen peroxide, to the distal side of the heme through a pronounced funnel shaped channel positioned similarly to, but longer and more constricted than the access route of monofunctional peroxidases, has been proposed (Carpena *et al.*, 2003). This channel is narrowest near the residues Ser324 and Asp141,

about 14 Å from the heme iron atom. The constriction of the access channel results from the LL1 and LL2 insertions which are lacking in both ascorbate peroxidase and cytochrome *c* peroxidase. Hydrogen peroxide entering the distal side cavity of BpKatG through the constricted portion of the channel will immediately come into contact with the active-site residues Arg109, Trp111 and His112 leading to generation of compound I in both the catalatic and peroxidatic modes of reaction, or for reduction of compound I in the catalatic reaction (Carpena *et al.*, 2003). Most peroxidases have a second access route, approximately in the plane of the heme, leading to the distal heme cavity, but the equivalent route in KatGs is blocked by loops in this larger protein.

However, there is another funnel-shaped access channel that approaches a small central cavity containing a single metal ion, which, in BpKatG, was tentatively identified as sodium (Carpena *et al.*, 2003). This second channel provides direct access to the core of the protein and to a region that encompasses two other structural features with possible functional significance. The first is a large cleft between the two domains and could be a potential substrate binding site with a clear intra subunit pathway for electron transfer to the heme through the Met-Tyr-Trp adduct. A second feature is that the side chain of Arg426, which can exist in two orientations and the predominant conformation (>70%) differs from that in HmKatG.

Contributing to the complexity of this region are two conformations of the side chain of Thr119, of which the minor (<30%) is similar to the conformation in HmKatG. A co-ordination between the conformations of the Arg426 and Thr1119 side chains has been suggested (Carpena *et al.*, 2003). Changes in the structure of BpKatG relative to HmKatG (the single ion, rotated Asp427 carbonyl group, and the displaced Thr119 and

Arg 426 side-chains) are in close proximity to one another, are associated directly or indirectly through hydrogen bonds or ionic interactions, and represent the only changes in structure relative to HmKatG in this region of the protein. This correlation suggests that the changes may be functionally related, and that the region of the protein may have an, as yet undefined function. This possibility is reinforced by the fact that there is a region of undefined electron density located in the cavity vacated by the Arg426 side chain in direct contact with the oxygen atom of the side chain from Tyr238, the central residue of the covalent cross link (Carpena *et al.*, 2003).

Although, the main access channel in KatGs is more restricted compared to the monofunctional peroxidases, it is not as pronounced as in monofunctional catalases. Similar to monofunctional catalases, there are conserved acidic amino acids in the main access channel: Glu242 at the entrance of the channel and Asp141 at the 3–4 Å wide constriction in the access channel. Exchange of both residues significantly reduced the catalase, but did not alter the peroxidase activity, suggesting that they are critical for stabilizing the solute matrix in the channel and possibly for orienting the water dipoles. In addition, Asp141 controls the access to the distal residues Arg108, His112 and Trp111, an indication that it may also participate in actual oxidation of H_2O_2 to molecular oxygen (Jakopitsch *et al.*, 2004).

Recently Jakopitsch *et al.* (2005) have reported the involvement of LL1 specific residues (Ile248, Asn251, Pro252, and Glu253) in the catalysis of SyKatG based upon their exposure to the solute matrix of the access channel. These authers proposed the existence of a very rigid and ordered structure built up by interactions of LL1 residues with both distal and proximal residues and the heme itself. Mutation Ile248Phe

significantly altered the heme pocket similar to one involving Asp152Ser leading to the alteration of the hydrogen bonding between Ile248 and Asp152 and subsequent reduced catalase activity by 87%, similar to Asp152Ser variant [97%] (Jakopitsch *et al.*, 2003). They also reported that mutation at Ile248 brings changes in the proximal heme site mediated by LL1 and its connection with helices E and F, with helix F accommodating the proximal histidine. Mutations at Asn251 and Pro252 affected the coordination of the iron atom, although the variations were less pronounced and RR spectra were very similar to those of native SyKatG in both ferric and ferrous state. Mutations at Glu253, which is located at the entrance of the funnel shaped access channel ~9 Å from the constriction formed by Asp152 and Ser335, did not alter the spin and coordination state of the enzyme but altered the bifunctionality of the enzyme by significantly reducing the catalase activity. From the crystal structures of BpKatG and MtKatG, it is known that both Asn251 and Glu253 are connected by a hydrogen bond between the amide oxygen of Asn251 and the main chain nitrogen of Glu253 as well as via at least two water molecules in their vicinity and mutations at these residues changes and disrupts this hydrogen bonding network proposed to be essential for the catalase activity of KatGs (Jakopitsch *et al.*, 2005). These reports suggest that in KatGs, compound I reduction (not formation) depends strongly on a defined and oriented water matrix maintained by the channel architecture and highly conserved residues at the KatG specific loop LL1 (Jakopitsch *et al.*, 2005).

1.7.3.4. pH induced changes in catalase-peroxidases

BpKatG exhibits different pH optima for three different activities, pH 5.5 for peroxidase activity, pH 6.5 for catalase activity and pH 8.75 for oxidase activity (Singh *et al.*, 2004 and see below). Loewen and coworkers have recently demonstrated pH induced changes in the structure of BpKatG which might be playing a key role in modulating different activities in KatGs (Carpena *et al.*, 2005; Carpena *et al.*, 2006). A conserved arginine at position 426 in BpKatG, situated about ± 20 Å from the active-site heme, has been shown to act as a molecular switch moving between two conformations, the relative proportions of which vary among the different crystal structures. In one position, the guanidinium group forms an ionic association with Tyr238 in the Trp-Tyr-Met adduct [conformation Y], and in the second position, it is shifted to a region containing two other arginine residues [conformation R] (Carpena *et al.*, 2005). The proportion of conformation Y varies form about 0% in MtKatG (Berthand *et al.*, 2004), to 30% in BpKatG (Carpena *et al.*, 2003), to 80% in SyKatG (Wada *et al.*, 2002) and 100% in HmKatG (Yamada *et al.*, 2002), presenting the striking correlation with the pH values of crystallization, pH 4.5 for MtKatG, pH 5.6 for BpKatG, pH 6.3 for SyKatG and pH 8.1 for HmKatG. The apparent correlation between the conformation of Arg426 and the pH of crystallization was tentatively confirmed by increasing the pH for a crystal of BpKatG to 8.0 causing an increase in the amount of conformation Y to about 100% (Carpena *et al.*, 2005). This apparently facile movement of the side chain of Arg426 coupled with its key role in catalase activity suggested that it can act as a molecular switch reversibly interacting with the Trp-Tyr-Met adduct to inductively alter heme reactivity. Another pH induced change observed in BpKatG was a perhydroxy modification on the indole

nitrogen of Trp111, situated on the distal side of the heme which increases from 0% at pH 4.5 to 100% at pH 8.5, correlating with the NADH oxidase activity (Singh *et al.*, 2004). The covalent attachment of oxygen to the indole creates a very different molecular species compared to its noncovalent bonding to heme iron in other oxygen binding proteins. The fact that NADH is too large to fit into the heme cavity necessitates electron transfer from a remotely bound NADH to the oxygen most likely through protein, and covalent linkage of the oxygen to the indole makes possible direct electron transfer from the protein. The perhydroxy modification was detected by both X-ray crystallography and EPR spectroscopy (Carpena *et al.*, 2006).

The pH induced shift from conformation R to Y of Arg426 can be correlated with and explains at least in part, the pH optima for the peroxidase, catalase, and NADH oxidase reactions of 4.5, 6.5, and 8.75, respectively (Singh *et al.*, 2004). At pH 4.5, Arg is predominantly in R conformation, remote from Tyr238, allowing the tyrosinate charge to delocalize onto the heme, enhancing oxyferryl formation and peroxidase reaction (Carpena *et al.*, 2005). The equal proportions of Y and R at pH 6.5 suggests a facile equilibrium providing optimum conditions for both oxyferryl formation (conformation R) and oxyferryl reduction (conformation Y) by H_2O_2 required for the catalase reaction. At pH 8.5, Arg426 occupies predominantly conformation Y, associated with Tyr238, which inductively lowers electron density on the heme and adduct favoring perhydroxy-indole reduction in the oxidase reaction (Carpena *et al.*, 2006)

1.7.4. Protein radicals in catalase-peroxidases

Electron transfer reactions between metalloproteins play critical roles in many important biological processes. However these reactions are poorly understood due to their dependence on so many factors, including the kinetics of complex formation and dissociation, the electronic properties of the redox centers, the distance and the pathway for electron transfer, and the driving force and the reorganization energy (Millett et al., 1995). One such widely studied reactions is that of cytochrome *c* peroxidase with cytochreome *c*, in which the electron transfer pathway extends form the heme methyl group on cytochrome *c* through CcP residues Ala194, Ala193, and Gly192 to the indolyl radical on Trp191, which is in van der Waals contact with the heme (Pelletier and Kraut, 1992). This tryptophanyl radical, exchange-coupled with the oxyferryl heme iron [Fe(IV)=O $Trp^{\circ+}$] is necessary for the electron transfer from cytochrome c to the heme, because cytochrome *c* can not directly access the C*c*P heme active site (Pelletier and Kraut, 1992). This was identified as the relevant intermediate acting as an electron sink for the substrate (cytochrome *c*) oxidation in CcP (Sivaraja *et al.*, 1889).

In lignin peroxidase, a tryptophanyl radical located close to the enzyme surface has been identified as the oxidation site for veratryl alcohol (Smith and Veitch, 1998; Sollewiyn *et al.*, 2002). The formation of an oxyferryl-tyrosyl radical intermediate [Fe(IV)=O Tyr°] by means of intramolecular electron transfer between the heme and a tyrosine residue has been observed in catalases (Ivanicich *et al.*, 1997), peroxidases (Ivanicich *et al.*, 2001; Ivanicich *et al.*, 2001a) and prosthaglandin H synthase (Tsai *et al.*, 1999; Shi *et al.*, 2000).

Formation of such radicals on specific Tyr and/or Trp strongly favors their role as an alternate oxidation site, other than heme, in both catalases and peroxidases. In catalase-peroxidases, the exact nature and positions of such protein based radicals is poorly understood. Different groups are investigating the catalatic intermediates of KatGs. Hillar *et al.*, 2000, attributed the observed 9-GHz EPR signal of the Compound I intermediate in EcKatG to an oxoferryl-porphyrin radical [Fe(IV)=O $Por^{\circ+}$]. Magliozzo and coworkers in their study on MtKatG assigned an EPR signal to a tyrosyl radical (Chouchane *et al.*, 2002) and later, using nitric oxide as a radical scavenging reagent, identified Tyr353 to be the radical site (Zhao *et al.*, 2004). Interestingly, the residue at this position is conserved as Trp in all other KatGs used in the current study (Figure 4.2). The side chain of Tyr353 lies in the interior of MtKatG on the proximal side and close to the heme suggesting that Tyr 353 could be a site for radical formation, although proximity alone can not be the sole criterion for an electron transfer reaction pathway between Compound I and a Tyr residue (Zhao *et al.*, 2004). The authors did not rule out formation of radicals at other residues and this remains the subject of debate (Ivanicich *et al.*, 2003). The atypical formation of compound I intermediate [Fe(IV)=O $Por^{\circ+}$] as well as two subsequent protein based radical intermediates indentified as Tyr° and $Trp^{\circ+}$ were identified in *Synechocystis* PCC6803 catalase-peroxidase of catalase and peroxidases, using a combination of multifrequency EPR spectroscopy, isotope labeling and site directed mutagenesis. The position of the Trp° was assigned to Trp106 (SyKatG numbering) located on the distal side of the heme belonging to the highly conserved short stretch of KatGs. Existence of an extensive hydrogen bonding network on the distal side of the heme, involving Trp122, His123, Arg119, seven structural waters, and the heme 6-

propionate group has been identified as a possible path for electron transfer from the tryptophanyl radical (Ivanicich *et al.*, 2003). This notion was further supported (Jakopitsch *et al.*, 2006) in a demonstration that the variant Trp122His (thus maintaining the hydrogen bond network) allowed the radical formation but the Trp122Phe mutation did not.

1.7.5. Catalase-peroxidase from different organisms

The complete sequences are known for catalase–peroxidases from various prokaryotes, both eubacteria and archaea. The systematic analysis of KatGs reveals that these enzymes are distributed unequally among closely related genomes whereas in some complete genomes, no KatG is present (such as *Bacillus subtilis*). Some bacteria even contain two different ones (e.g. *Mycobacterium fortuitum*) (Zámocký, 2004). In my study I studied catalase-peroxidase from: *Burkholderia pseudomallei*, *Mycobacterium tuberculosis*, *Escherichia coli*, *Synechocystis* PCC6803, *Archaeoglobus fulgidus*, *Bacillus stearothermophilus* and *Rhodobacter capsulatus*.

1.7.5.1. Catalase-peroxidase of *Burkholderia pseudomallei* (BpKatG)

B. pseudomallei (formally known as *Pseudomonas pseudomallei*), the causative agent of melioidosis, is a gram-negative soil bacillus endemic mainly in Southeast Asia and northern Australia, although cases have been reported in India, China, Taiwan, and Laos (Cheng and Currie., 2005). The disease may manifest itself in an acute, subacute, or chronic form; and the acute form of melioidosis is often fatal despite aggressive antibiotic treatment (Chen *et al.*, 2004). In this era of biological weapons, *B. pseudomallei* is being

increasingly recognized as a potential biological weapon (Leelarasamee, 2004). At a cellular level, this gram-negative bacterium can survive and multiply in both phagocytic and non-phagocytic cells and after internalisation, it can readily escape from the membrane-bound phagosome into the cytoplasm (Jone *et al.*, 1996). The internalised *B. pseudomallei* can also induce a cell-to-cell fusion, resulting in multinucleated giant cell (MNGC) formation and cell death (Kespichayawattana *et al.*, 2000). The *rpoS* null mutants of *B. pseudomallei* exhibits an increased sensitivity to oxidative stress (Subsin *et al.*, 2003) and also demonstrate abnormal modulation of the host cell response, particularly with regard to the macrophage antimicrobial capacity to control the intracellular fate of *B. pseudomallei* (Utaisincharoen *et al.*, 2006). There is also mention of a nonspecific DNA-binding protein (DpsA) whose expression increases in response to oxidative stress through increased transcription from the upstream *katG* (catalase–peroxidase) promoter, which is OxyR dependent (Loprasert *et al.*, 2004).

Catalase-peroxidase of *B. pseudomallei* (BpKatG) is one of the antioxidant enzymes that are part of the oxidative stress response (Loprasert *et al.*, 2003). The nucleotide sequence of *katG* gene appeared in 2002 (Loprasert *et al.*, 2002), and this was followed by the purification and crystallization of the enzyme (Carpena *et al.*, 2002). BpKatG shows high sequence similarity to other catalase-peroxidases of bacterial, archaebacterial and fungal origin including 65% similarity to KatG from *M. tuberculosis* and lesser sequence similarity to members of plant peroxidase family (Carpena *et al.*, 2002). In 2003, the 1.7 Å crystal structure of BpKatG was reported (Carpena *et al.*, 2003).demonstrating that BpKatG is a homodimer of 79 kDa subunits with one modified

heme group and one metal ion, likely sodium, per subunit. Each subunit has distinct N- and C- terminal domains that are structurally related and are similar to plant peroxidases.

1.7.5.2. Catalase-peroxidase of *Mycobacterium tuberculosis* (MtKatG)

First purified and described by Diaz and Wayne (1974), this enzyme attracted the attention of researchers because of the correlation of isoniazid resistance in *Mycobacterium tuberculosis* strains with loss of catalase and peroxidase activity in the cells (Winder, 1982). Following the characterization and cloning of the structural gene for the *M. tuberculosis* KatG (MtKatG) (Zhang *et al.*, 1992), purification of the recombinant form of the catalase-peroxidase has been reported by a number of groups (Nagy *et al.*, 1995; Johnsson *et al.*, 1997; Nagy *et al.*, 1997a; Saint-Joanis *et al.*, 1999; Young *et al.*, 2003), and purification of KatG from *M. intracellulare* (Morris *et al.*, 1992), *M. smegmatis* (Marcinkeviciene *et al.*, 1995), *M. fortuitum* (Menendez *et at.*, 1997), *M. leprae* (Eiglmeier *et al.*, 1997), *M. avium* (Li *et al.*, 2005), *M. bovis* (Garnier *et al.*, 2003), *M. canettii* (Gutierrez *et al.*, 2005) has also been carried out. Recent success in solving the crystal structure of catalase-peroxidases from *Haloarcula marismortui* (Yamada *et al.*, 2002), *B. pseudomallei* (Carpena *et al.*, 2003) and *Synechococcus* Pcc 7942 (Wada and Tada, 2003) was followed by the structure of *M. tuberculosis* KatG, MtKatG (Bertrand *et al.*, 2004) and its Ser315Thr variant (Yu and Sacchettini, 2006), one of the key variants thought to be involved in INH resistance.

1.7.5.3. Catalase-peroxidase of *Escherichia coli* (EcKatG)

E. coli has three different enzymes withj catalase activity and the monofunctional catalase HPII of *E. coli* has already been discussed in Section 1.4. The bifunctional catalase-peroxidase "hydroperoxidase I [HPI or EcKatG]" (Claiborne and Fridovich, 1979) and monofunctional catalase "hydroperoxidase II (HPII)" (Claiborne *et al.*, 1979) are chromosomally encoded enzymes, both of which has been extensively studied (Chelikani *et al.*, 2004). In 1996, a third enzyme from enterohemorrhagic *E. coli* O157:H7 was characterized as a periplasmic catalase–peroxidase called KatP (Brunder *et al*,. 1996). KatP has a molecular mass of 81.8 kDa and the presence of an N-terminal signal sequence suggests that KatP is exported to and functions in the periplasm. Production of KatP by highly virulent bacterial pathogens but not by their less pathogenic or non-pathogenic relatives, suggests that these enzymes may be used as virulence factors (Cornelius *et al.*, 2003).

HPI or EcKatG is encoded by the *katG* gene located at 89.2 min on the *E. coli* chromosome (Loewen *et al.*, 1985b). Originally it was described as a tetrameric enzyme made up of identical 80 kDa subunits containing two heme *b* prosthetic groups per tetramer (Claiborne and Fridovich, 1979). Later partial heme occupation of HPI like some other catalase-peroxidases was shown with an average of 0.5 heme per subunit in a heterogenous mixture of dimers and tetramers with 0, 1, 2 and 3 hemes respectively (Hillar *et al.*, 2000). EcKatG has a specific catalase activity of about 2000 U/mg (Loewen *et al.*, 1990; Hillar *et al.*, 2000) which is only about one seventh of that reported for the large subunit catalase HPII also from *E. coli* (Loewen and Switala, 1986). To date,

success in crystallizing EcKatG remains elusive although the crystal structure of its C-terminal domain has been published (Carpena *et al.*, 2004).

1.7.5.4. Catalase-peroxidase of *Synechocystis* PCC 6803 (SyKatG)

Cyanobacteria represent one of the major phylogenetic lines of bacteria, comprising a large and heterogeneous group of phototrophic prokaryotes. It is widely accepted that they were the first oxygen-evolving organisms and were responsible for the conversion of the atmosphere of the earth from an anoxic to an oxic one. Microfossil evidence of cyanobacteria-like cells is well documented for the Precambrian era i.e. more than three billion years ago (Schopf, 1993), and there is evidence that cyanobacteria occupied large areas of the earth in those ancient times. The evolution of oxygenic photosynthesis had enormous consequences for the environment and survival was dependent on either occupying an anaerobic habitat or developing defense strategies against the reactive oxygen species, such as superoxide anion, hydrogen peroxide, and hydroxyl radical.

Cyanobacterial catalase-peroxidases have been subjected to extensive characterization. Mutsuda *et al* (1996) reported the purification and nucleotide sequence analysis of a catalase-peroxidase from *Synechococcus* PCC 7942, and Obinger *et al* (1997) described the characterization of a catalase-peroxidase from *Anacystis nidulans* (*Synechococcus* PCC 6301). The enzymes from both cyanobacteria showed peroxidase activity with *o*-dianisidine and pyrogallol, but no reaction was detected with guaiacol, ascorbate, NADH or NADPH. They are homodimeric enzymes with a molecular mass of

approximately 80 kDa per subunit. Both are very efficient catalases with a K_m for H_2O_2 in the millimolar range.

1.7.5.5. Catalase-peroxidase of *Archaeoglobus fulgidus* (AfKatG)

Archaeoglobus fulgidus is a strict anaerobic hyperthermophilic archaeon that has been isolated from marine hydrothermal environments as well as subsurface oil fields. This sulfate reducer can grow organoheterotrophically with a variety of carbon sources, or lithoautotrophically on hydrogen, thiosulfate, and CO_2 (Stetter, 1988). Besides its ability to grow at extremely high temperatures, this organism is unusual in that it is unrelated to other sulfate reducers. The sequencing of the entire genome of *A. fulgidus* was completed in 1997 (Klenk *et al.* 1997), which revealed the presence of an open reading frame that was putatively identified as a catalase-peroxidase on the basis of its high similarity (62.9% nucleotide identity; 49.5% amino acid similarity) to the *perA* gene of *Bacillus stearothermophilus* (Klenk *et al.*, 1997; Loprasert *et al.*, 1989). The purified AfKatG is a homodimer with a subunit molecular mass of 85 kDa.

1.7.5.6. Catalase-peroxidase of *Bacillus stearothermopohilus* (BsKatG)

B. stearothermopohilus is Gram-positive bacteria found in soil, hot springs, Arctic waters, ocean sediments, and spoiled food products. BsKatG is a dimeric enzyme with 731 amino acids per subunit and has 48% homology with EcKatG. It has an optimum temperature of 70°C and is stable for a month at 30°C (Loprasert *et al.*, 1997).

1.7.5.7. Catalase-peroxidase of *Rhodobacter capsulatus* (RcKatG)

R. capsulatus is a photosynthetic, facultatively anaerobic bacterium that is capable of fixing molecular nitrogen. It has two hydroperoxidases: a peroxidase and a catalase-peroxidase which make it suitable as a test organism for studying oxidative damage and protection mechanisms (Hochman *et al.*, 1991). *R. capsulatus katG* (cpeA) was initially sequenced incorrectly in 1993 (Forkl *et al.*, 1991) and later corrected (Nestor Cortez personal communication).

1.7.6. Catalase-peroxidase and isoniazid activation

M. tuberculosis, the causative agent of tuberculosis (TB), is a tenacious and remarkably successful pathogen that has latently infected a third of the world's population. Each year there are eight million new TB cases and two million deaths (Zhang *et al.*, 2006). The increasing emergence of drug resistant TB, and HIV infection, which compromises host defense and allows latent infection to reactivate or render individuals more susceptible to TB, pose further challenges for effective control of the disease (Corbett *et al.*, 2003).

Isonicotinic acid hydrazide (isoniazid or INH) [Figure 1.7 A] is one of the front line drugs used in the treatment of tuberculosis, but the mode of action of this 55 year old drug is still poorly understood (Kapetanaki *et al.*, 2005). INH is a prodrug that requires *in vivo* activation by KatG upon entering *M. tuberculosis* (Zhang *et al.*, 1992). The need for KatG activation was deduced soon after the introduction of INH therapy when INH-resistant strains were correlated with the loss of catalase-peroxidase activity (Middlebrook, 1952 and 1954). This observation was confirmed by the molecular and

genetic studies of Zhang and colleagues which demonstrated that INH-sensitivity could be restored by the introduction of a functional *katG* gene into an INH-resistant, catalase-deficient strain of *M. tuberculosis* and in *Mycobacterium smegmatis* (Zhang *et al.*, 1992 and 1993). This was followed by numerous reports demonstrating that mutation in, or deletion of, the *katG* gene results in the acquisition of isoniazid resistance (Heym *et al.*, 1995; Morris *et al.*, 1995; Rouse *et al.*, 1996; Saint-Joanis *et al.*, 1999).

The second gene found in *M. tuberculosis* to be associated with INH resistance is *inhA* (Banerjee *et al.*, 1994). InhA, the product of *inhA*, is an NADH-dependent enoyl-acyl carrier protein reductase. Mutations within the *inhA* structural gene (Ristow *et al.*, 1995) or promoter (Kapur *et al.*, 1995) have been identified and shown to be associated with both INH and ethionamide (ETH), a structural analog of the isoniazid, resistance (Larsen *et al.*, 2002). Missense mutations within the *inhA* structural gene cause INH resistance by reducing the NADH [Figure 1.7B] binding affinity of InhA and thus protecting the enzyme from INH inactivation (Rozwarski *et al.*, 1998). Formation of isonicotinoyl-NAD [Figure 1.7C], the active form of the drug, involves loss of hydrazine (N_2H_2) from INH promoted by KatG (Zhang *et al.*, 1992) and binding of the isonicotinoyl group to NAD^+ (Johnsson *et al.*, 1995). Isonicotinoyl-NAD mimics the NADH and binds to InhA [Figure 1.7D] (Rozwarski *et al.*, 1998), and possibly to KasA, a β-ketoacyl acyl carrier protein synthase (Mdluli *et al.*, 1998), blocking their NADH-binding sites and interfering with the cell wall synthesis.

The central role of KatG in INH activation is evident from the significant number of INH-resistant cases of tuberculosis attributable to mutations in *katG* and from biochemical studies that have demonstrated a direct role for KatG in the generation of

various isonicotinoyl derivatives (Johnsson and Schultz, 1994). Much of the literature related to the activation of INH by KatG has focused on the fate of INH and possible intermediates involved in the process (Johnsson and Schultz, 1995; Wilming and Johnsson, 1999; Magliozzo and Marcinkeviciene, 1996). With NAD^+ included in the mix, the generation of the isonicotinoyl-NAD adduct was observed both with and without KatG present (Wilming and Johnsson, 1999; Magliozzo and Marcinkeviciene, 1996; Lei *et al.*, 2000), leading to the suggestions that the role of KatG is limited to the hydrazine lyase of INH and that the subsequent reaction of the isonicotinoyl radical with NAD^+ is a nonenzymatic event involving a homolytic aromatic substitution (Wilming and Johnsson, 1999; Minisci *et al.*, 1989). Reactive oxygen species have also been implicated in INH activation both *in vivo* (Mitchison *et al.*, 1989; Youatt 1969) and *in vitro* (Johnsson and Schultz, 1995), and an elevated level of intracellular superoxide (Wang *et al.*, 1998) have also been associated with the high sensitivity of *M. tuberculosis* to INH (Deretic *et al.*, 1996). However, the absence of H_2O_2 involvement in INH activation implies that a reaction different from either the peroxidase or the catalase reactions may be involved, and some reports have suggested that the active participation of KatG in INH activation involves more than just hydrazinolysis (Lei *et al.*, 2000).

1.7.6.1. KatG mutations involved in isoniazid resistance

Analysis of patient isolates resistant to INH has led to the conclusion that a relatively minor subset entirely lacks catalase-peroxidase activity. Typically this subset of strains has deletions or frame-shifts in *katG* and are resistant to high levels of INH (Payton *et al.*, 1999). Small insertions, partial deletions, and missense mutations are

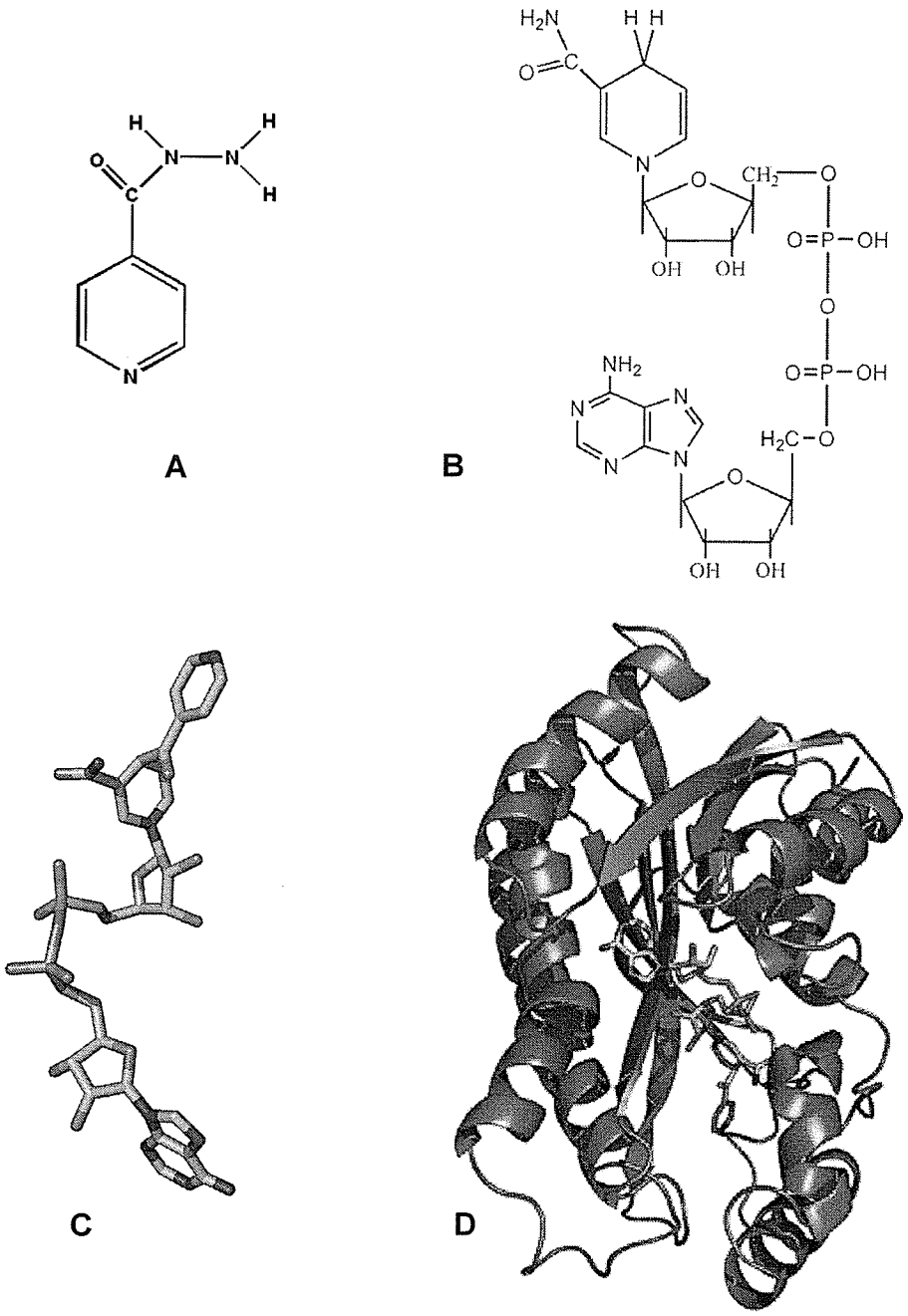

Figure 1.7. Structures of isoniazid (INH) (A), NADH (B), isonicotinoyl-NAD adduct (C) and isonicotinoyl-NAD adduct in bound form with InhA protein of *M. tuberculosis* (D). The structures were created using Chem Draw software and using Pymol (Deleno, 2003) and using the coordinates submitted to the protein data bank.

observed at a low frequency in INH-resistant clinical isolates. In contrast to these complete loss of function events, *in vivo* mutations in *katG* that result in diminished or altered catalase-peroxidase activity are much more frequently observed amongst patient isolates (Victor *et al.*, 1996; Heym *et al.*, 1995; Kelley *et al.*, 1997; Stoeckle *et al.*, 1993; Altamirano *et al.*, 1994).

Although, the real occurrence of these events *in vivo* is unknown, presumably these are more on the order of typical point mutation rates, occurring in perhaps one in 10^{8-9} organisms. The most commonly observed mutation is a point mutation replacing serine at location 315 with threonine (S315T). Estimates are that this mutation occurs in between 30 and 60% of all INH resistant isolates (Musser *et al.*, 1996; Marttila *et al.*, 1996; Marttila *et al.*, 1998). Studies on recombinant wild type MtKatG and the variant Ser315Thr demonstrated that the mutation results in somewhat reduced enzyme activity (Wengenack *et al.*, 1997; Saint-Joanis *et al.*, 1999; Rouse *et al.*, 1996) but more recent studies on the Ser315Thr variant and its equivalent Ser324Thr in *B. pseudomallei* have shown that this mutation maintains catalase and peroxidase-specific activities similar to the native enzyme with only subtle differences among the kinetic parameters (Deemagarn *et al.*, 2005).

The basis of the resistance of isoniazid became evident with the determination of crystal structures of different KatGs (Yamada *et al.*, 2002; Carpena *et al.*, 2003; Wada *et al.*, 2002; Bertrand *et al.*, 2004) and the crystal structure report of BpKatG variant Ser324Thr (equivalent of Ser315Thr) (Deemagaran *et al.*, 2005). A calculated surface diagram reveals that the channel in native BpKatG adjacent to Ser324 is significantly wider than the channel in its variant Ser324Thr to the extent that a number of water

molecules present in the native enzyme are absent from the variant. Consequently, it is interference with INH accessibility to the heme cavity that best explains the reduced affinity and reactivity of KatG towards INH, although the possibility of INH binding in the channel cannot be excluded, in which case the methyl group of Thr324 would interfere with INH binding. Other mutations of Ser324 might cause a similar blockage of the channel, but the situation may be more complex because the hydrogen bond between the hydroxyl group of Ser (and Thr) and the propionate carbonyl group would disappear. The effect that this would have on the structural integrity of the enzyme, particularly in the channel region, and the electronic environment of the heme is not clear. For example, the complete lack of isonicotinoyl-NAD synthase activity and INH hydrazinolysis activity in the Ser315Asn variant of MtKatG may be a result of the larger Asn side-chain situated in the channel or of some other distortion in the subunit arising from the lack of interaction with the heme propionate group (Deemagarn *et al.*, 2005).

Although *katG* mutations resulting in Ser315Thr are the most common mechanism of INH resistance as determined by sequencing, additional mutations also occur in functionally important residues such as Ser315Asn, Asp63Glu, His108Gln, Thr262Arg, Ala350Ser and Gly629Ser. Biochemical characterization of some of these variant proteins has confirmed their importance to protein stability and catalytic properties. An amino acid polymorphism involving the change of Arg463 to Leu, was initially thought to be associated with INH resistance but couln't be associated with the INH resistance by biochemically or epidemiologically (Johnsson *et al.*, 1997; Heym *et al.*, 1995; Musser *et al.*, 1996; Rouse *et al.*, 1995; Pretorius *et al.*, 1995; Lee *et al.*, 1997; Nagy *et al.*, 1998).

1.7.6.2. Analysis of the potential isoniazid binding site

An area of wide dispute centers on the location of isoniazid binding to KatG although the recent success with the crystallization of KatG has provided some insight into this. The crystal structure report of BpKatG shows a region of undefined electron density located just before the constricted region in the main channel leading to the distal heme cavity of BpKatG over 10 Å further away from the heme in close proximity to Ser324. This unidentified electron density was evident both in the structure obtained after a short soaking with INH and in the structure obtained without soaking and is thought to be the result of a metabolic constituent of *E. coli*, which may closely resemble INH such as pyridoxol or vitamin B6.

The location of this undefined electron density is the same in the crystal structures of native BpKatG and its variants (Deemagaran *et al.*, 2005; unpublished data) and is consistence with the observation of a small peak of electron density in the same site in MtKatG (Bertrand *et al.*, 2004). Bertrand *et al* argued this region to be too small to accommodate a pyridine-like metabolite and suggested it as solvent or a small hydrophobic molecule. Bertrand *et al* (2004) concluded that the binding site for aromatic compounds is near the δ-*meso* edge of the heme based on a comparison with the crystal structures of monofunctional peroxidases from all three classes (APX with salicylhydroxamic acid (Sharp *et al.*, 2004); *Arthromyces ramosus* peroxidase with salicylhydroxamic acid (Tsukamoto *et al.*, 1999); HRPC with benzhydroxamic acid (Henriksen *et al.*, 1998).

1.8. Objectives of the thesis

Since the first report characterizing the purified catalase peroxidase HPI [EcKatG] of *E. coli* (Claiborn and Fridovich, 1979), KatGs have been purified and characterized from a large number of organisms. Even after almost three decades, there is still more to know about this fascinating enzyme. Two important issues that need to be addressed include the role of KatG in isoniazid activation against *M. tuberculosis* with specific interest in the drug protein interaction at the molecular level and the location of the binding site of INH. Another key area is the reaction mechanism by which this enzyme maintains its bifunctionality, particularly the fate and role of the intermediates formed during the catalase and peroxidase reactions. The *in vivo* peroxidatic substrate(s) for KatGs need(s) to be identified so as to determine the physiological role for the peroxidatic activity of KatGs. The recent success in crystallization of KatGs is promising in understanding their structure function.

This study reports the comparison of catalase-peroxidases from seven different organisms, *M. tuberculosis, B. pseudomallei*, *E. coli*, *B. stearothermophilus*, *A. fulgidus*, *Synechosystis* PCC 6803, and *R. capsulatus*. The KatG gene product from these organisms was over expressed from the katG gene cloned in a suitable vector. The over expressed protein was purified and characterized for its biochemical and biophysical properties such as pH profile and enzyme kinetics. The major focus was on KatG mediated isoniazid activation, the formation of intermediates and subsequently the formation of isonicotinoyl-NAD adduct the active form of isoniazid. Two key mutations involved in isoniazid resistance, Ser315Thr and Ser315Asn, were also constructed, purified, characterized and compared with the native MtKatG for drug activation.

2. MATEIALS AND METHODS

2.1. *Escherichia coli* strains, plasmids and bacteriophage

E. coli strains, plasmids and bacteriophage used in this study are listed in Table 2.1. Phagemid pKS+/- from Stratagene cloning system were used as a vector for mutagenesis, sequencing and cloning. The *M. tuberculosis katG* gene encoding MtKatG, originally in pYZ55 (Zhang *et al.*, 1992) was recloned as an *EcoR*V-*Kpn*I fragment into pKS+ as pAH1 (Hiller, 1999). Two different sub-clones were constructed for the site-directed mutagenesis in *M. tuberculosis katG*. A 600bp *EcoR*V-*Cla*I fragment from pAH1 was sub-cloned into pKS+ to generate pMt-EC (Fragment I, Figure 2.1) and a 470bp *Xho*I-*Cla*I fragment from pAH1 was sub-cloned into pKS+ to generate pMt-XC (Fragment II, Figure 2.1). The *B. pseudomallei katG* gene, encoding catalase-peroxidase BpKatG, was inserted into plasmid pKS- to generate the plasmid pBpG (Deemagaran, 2004). For site-directed mutagenesis purposes, pBpG was subcloned as pBpG-KH and further sub-cloned as pBpG-CH, containing fragment II and I respectively of *B. pseudomallei katG* (Figure 2.2). Strain CJ236 was used to generate single stranded uracil containing DNA templates from pMt-EC, pMt-CX and pBpG-CH. The *E. coli katG* gene encoding HPI (EcKatG) was cloned into a pBR322 derived plasmid to generate pBT22 (Triggs-rain and Loewen, 1987). The *A. fulgidus katG* was cloned into a pET-28b+ vector as pLUW640 (Kengen *et al.,* 2001). The *B. stearothermophilus katG* was cloned as pBR322 (Loprasert *et al.*, 1989) to over express BsKatG. The S*ynechocytis katG* encoding SyKatG was cloned into pET-3a vector and over expressed in *E. coli* BL21- (DE3) pLysS (Jakopitsch *et al.*, 1999).

Table 2.1. Genotypes and sources of *Escherichia coli* strains, plasmids and bacteriophage used in this study.

	Genotype		Source
***E. coli* strains**			
CJ236	*dut*1 *ung*1 *thi*-1 *rel*A1/pCJ105/*cam*^{r}F'		Kunkel *et al.*, 1987
NM522	*sup*E Δ(*lac-pro*AB) *hsd*-5 [F' *pro*AB *lacI*^{q} *lacZ*Δ15]		Mead *et al.*, 1985
JM109	*rec*A1 *sup*E44 *end*A1 *hsd*A1 *had*R17 *gyr*A96 *rel*A1 *thi* Δ(*lac-pro*AB)		Yanisch-Perron *et al.*, 1985
UM262	*rec*A *katG*::Tn10 *pro leu rps*L *hsd*M *hsd*R *end*I *lac*Y		Loewen *et al.*, 1990
BL21trxB(DE3) pLysS	F^{-} *ompT hsdS*$_b$(r_b^{-} m_b^{-}) *gal dcm trxB*15::kan (DE3) pLys(Cm^R)		Novagen
Plasmids			
pKS-		Ampr^R	Stratagene Cloning System
pAH1(pSK+, *M. tuberculosis katG* clone)		Ampr^R	Hillar *et al.*, 1999
pBpG (pKS-, *B. pseudomallei katG* clone)		Ampr^R	Deemagarn M.Sc. thesis, 2004
pBT22 (pBR322, *E. coli katG* clone)		Ampr^R	Triggs and Loewen 1987
pOD10 (pBR322, *B. stearothermophilus katG* clone)		Ampr^R	Loprasert *et al.*, 1997
pLUW640 (pET9d *A. fulgidus katG* clone)		Kan^R	Kengen *et al.*, 2001
pET3a (*Synechosystis* PCC 6803 *katG* clone)		Ampr^R	Jakopitsch *et al.*, 1999
pHF100 (*R. capsulatus katG* clone)		Ampr^R	Hochman *et al.*, 1986
pMt-CX (pSK+, *M. tuberculosis katG* subclone I)		Ampr^R	This study
pMt-EC(pSK+, *M. tuberculosis katG* subclone I)		Ampr^R	This study
pBpG-KH (subclone I)		Ampr^R	This study
pBpG-CH (subclone II)		Ampr^R	This study
pEMt (pET28b^{+}, *M. tuberculosis katG* clone)		Kan^R	This study
Bacteriophage			
R408 (helper phage)			Stratagene Cloning System

Table 2.2a Sequence of oligonucleotides and restriction fragments used for the site directed mutagenesis of *M. tuberculosis katG*

Primer	Bases changed	Oligonucleotide sequence[a]	Restriction fragment
Ser315Thr	AGC-ACC	GCGATCACC**ACC**GGCATCG	*Cla*I-*Xho*I (590-1064)
Ser315Asn	AGC-AAC	GCGATCACC**AGC**GGCATCG	*Cla*I-*Xho*I (590-1064)
Trp321Phe[b]	TGG-TTC	GAGGTCGTA**TTC**ACGAACACC	*Cla*I-*Xho*I (590-1064)
Trp91Phe[b]	TGG-TTC	CAGCCGTGG**TTC**CCCGCCGAC	*Ecor*V-*Cla*I (1-490)

Table 2.2b Sequence of oligonucleotides and restriction fragments used for the site directed mutagenesis of *B. pseudomallei katG*

Primer	Bases changed	Oligonucleotide sequence[a]	Restriction fragment
His279Asn[b]	CAC-AAC	CGCGGCGGC**AAC**ACGTTCGGC	*Cla*I-*Hind*III (990-1710)
His279Tyr[b]	CAC-TAC	CGCGGCGGC**TAC**ACGTTCGGC	*Cla*I-*Hind*III (990-1710)

Table 2.2c Primers used for the polymerase chain reaction for the cloning of *katG* from *M. tuberculosis* into pET28b+ vactor.

Primer name	Oligonucleotide sequence	Restriction site generated
I8NT9S[b]	AACACCCACC**GAATTC**AGAAACCAC	*EcoR*I
MtKatG-2[b]	CGACTAA**TTCGAA**CTAGCC	*Hind*III

[a] The sequences in bold are the codons that have been modified.

[b] Results from the variants His279Asn, His279Tyr, Trp321Phe, Trp91Phe and *M. tuberculosis katG* gene cloned in the vector pET28b+ have not been reported in the thesis.

express cyanobacterium catalase-peroxidase in *E.coli* (Jakopitsch *et al.,* 1999). *Rhodobactor capsulatus* catalase-peroxidase was cloned as pHF100 in pBlusescript (Forkl *et al.,* 1992). Helper Phage R408 was used for the infection of the strain CJ236 to generate single-stranded DNA. Strain NM522 was used for cloning and plasmid propagation. Strain JM109 was used for the production of plasmid DNA for double stranded DNA sequencing. Strain UM262, an *E.coli* strain with a *katG* gene interruption, was used for routine expression of KatG from various plasmids. Genes cloned on pET expression vectors were expressed in *E.coli* strain BL21(DE3) pLysS.

2.2. Biochemical and reagents

All biochemicals and reagents, as well as antibiotics used in the course of these studies were purchased from either Sigma Chemical Company (St. Louis, Missouri), or from Fischer Scientific Limited (Mississauga, Ontario). Restriction endonucleases, polynucleotide kinase, T4 DNA ligase and most of other enzymes used in these studies were purchased from Invitrogen Canada Inc. (Burlington, Ontario). The T7 sequencing kit was purchased from USB Corporation (Cleveland, Ohio). Components of the media used for growth of bacterial cell cultures were purchased from DIFCO, U.S.A. Reverse osmosis distilled water was used in preparing all solutions.

2.3. Media, growth conditions and storage of cultures

E. coli cultures were routinely grown in LB (Luria-Bertani) medium containing 10 g/L Tryptone, 5 g/L Yeast Extract and 5 g/L NaCl. Solid LB medium contained 15 g/L agar. For strains harboring plasmids bearing the ampicillin resistance gene, ampicillin was added to a concentration of 100 μg/mL for maintenance of selection pressure while

growing in both liquid and solid LB medium. For induction of expression, cells were grown for 2-3 h until the absorbance at 600 nm reached ~ 0.6 and then 1 mM IPTG was added for induction. In addition, chloramphenicol was added to a concentration of 40 μg/ mL, in order to maintain the presence of F' episome for the growth of the strain CJ236.

E.coli strains in general were grown in solid media at 37°C. However, cell cultures in liquid media for expression of wild type and variant proteins were grown at either 28°C or at 37°C in shake flasks with good aeration depending what was optimum for a particular variant. Bacterial strains were stored at -60°C in 24% dimethylsulfoxide (DMSO). Bacteriophage R408 was stored at 4°C in LB culture supernatant.

2.4. DNA manipulation

2.4.1. Preparation of synthetic oligonucleotides

Oligonucleotides used for mutagenesis were purchased from Invitrogen (Burlington, Ontario) in non-phosphorylated form. The concentration of oligonucleotide DNA was determined spectrophotometrically at 260 nm, where 1 absorbance unit = 40 μg/mL single strand DNA (Sambrook *et al.*, 1998). Oligonucleotides used for the site-directed mutagenesis were phosphorylated at the 5' end using T_4 kinase (Invitrogen) according to Ausubel *et al.* (1989). Approximately 100 ng of oligonucleotide DNA in a volume of 25 mL containing 1mM ATP and 10 units of kinase were incubated at 37°C for 30 min in appropriately diluted buffer supplied by the manufacturers. The reaction was terminated by heat inactivation at 65°C for 5 min.

2.4.2. Site-directed mutagenesis strategy

Targeted base changes on phagemid-borne *M. tuberculosis katG* and *B. pseudomallei katG* were generated according to the in-vitro mutagenesis protocol described by Kunkel *et al.* (1987). Sub-clones were constructed from parts of the chromosomal insert containing the *katG* gene on KS (+/-) vector. Simplified restriction maps of *MtkatG* gene and *BpkatG* gene indicating the location of individual sub-clones are shown in Figures 2.1 and 2.4, respectively. The sub-clone rather than the whole gene was mutagenized in order to limit the amount of subsequent sequencing required to confirm the mutation in the subclone both after mutagenesis and after reinsertion into *MtkatG* and *BpkatG* gene for protein expression. Target codons for mutagenesis were selected from the DNA sequence of *MtkatG* and *BpkatG* gene shown in the Figures 2.3 and 2.6, respectively. DNA sequences for oligonucleotides used in the mutagenesis procedure are listed in Table 2.2. Mutagenesis was performed by annealing the phosphorylated oligonucleatides encoding the desired base modifications to uracil containing single strand DNA templates obtained from the appropriate Bluescript phagemid sub-clone. The complementary DNA strand was then synthesized *in vitro* by unmodified T7 DNA polymerase (New England Biolabs) using the annealed oligonucleotoide as a primer. The 3' and 5' ends of the completed complementary strand were ligated by adding T4 DNA ligase (Invitrogen Canada Inc) to the reaction mixture. Subsequently, the DNA was transformed into NM522 cells where the uracil-containing templates were degraded. Plasmid DNA recovered from the transformants was further transformed into JM109, recovered from this strain and used to screen for the desired mutation in the plasmid sub-clone by DNA sequencing.

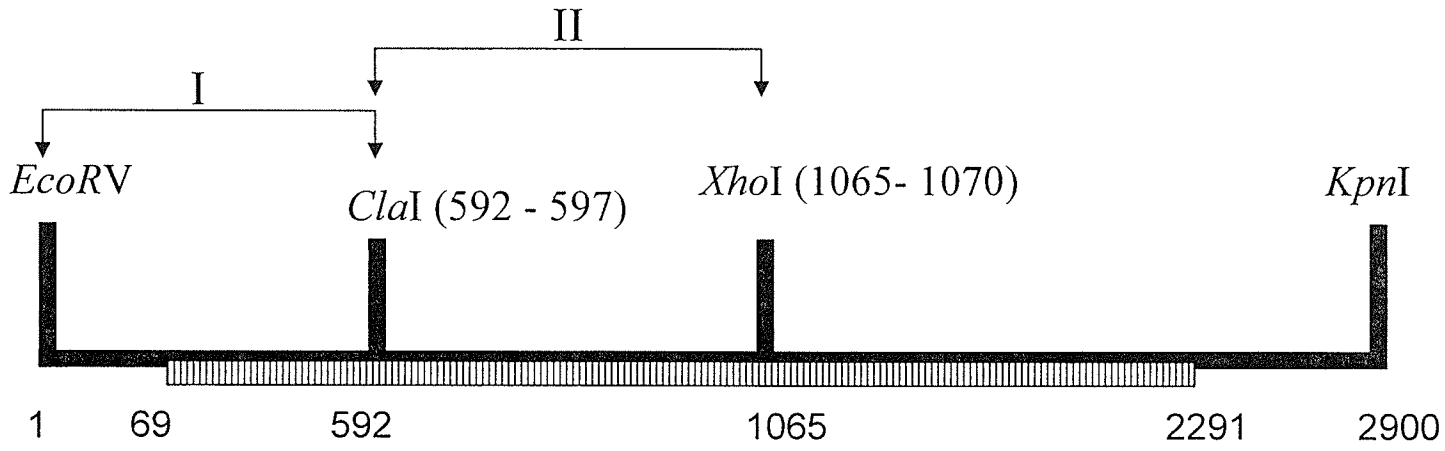

Figure 2.1. Simplified restriction map of the chromosomal insert containing the *M. tuberculosis katG* gene in plasmids pAH1 and pMt-EC(Fragment **I**) and pMtG-CX (Fragmaent **II**). The 2222 bp long katG open reading frame is indicated as the part of the chromosomal insert as is the insert as are the two insert fragments **I** and **II** used to construct the subclone vectors employed in site directed mutagenesis of *M. tuberculosis katG* .

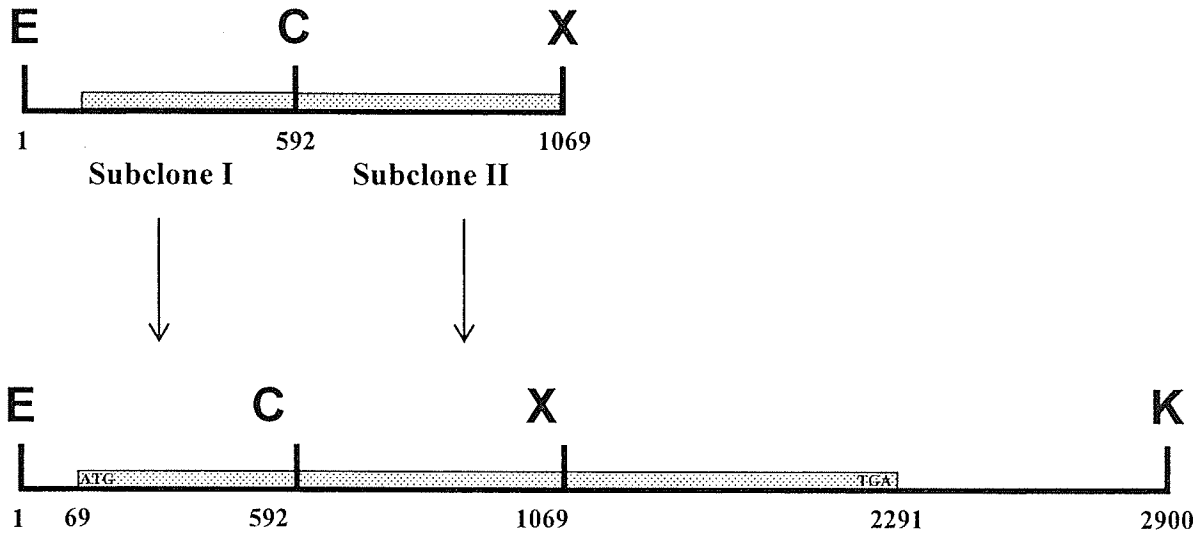

Figure 2.2 General reconstruction protocol used for the generation of variant MtKatG's from mutagenized subclone I for protein expression. (E:*EcoR*V, K:*Kpn*I, C:*Cla*I, X:*Xho*I,)

Figure 2.3. The DNA sequence and corresponding amino acid sequence of *M. tuberculosis* showing the restriction sites and the target codones selected for mutagenesis in this study. The sequencing primers are also shown.

M. tuberculosis katG (MtKatG)

```
GATATCCGACACTTCGCGATCACATCCGTGATCACAGCCCGATAACACCAACTCCTGGAA        60
CTATAGGCTGTGAAGCGCTAGTGTAGGCACTAGTGTCGGGCTATTGTGGTTGAGGACCTT
 EcoRV                          BclI

          V  P  E  Q  H  P  P  I  T  E  T  T  T  G  A  A  S         (17)
GGAATGCTGTGCCCGAGCAACACCCACCCATTACAGAAACCACCACCGGAGCCGCTAGCA        120
CCTTACGACACGGGCTCGTTGTGGGTGGGTAATGTCTTTGGTGGTGGCCTCGGCGATCGT
                                                NheI
                     ----------GAATTC---------->I8NT9S
                               EcoRI

N  G  C  P  V  V  G  H  M  K  Y  P  V  E  G  G  G  N  Q  D         (37)
ACGGCTGTCCCGTCGTGGGTCATATGAAATACCCCGTCGAGGGCGGCGGAAACCAGGACT       180
TGCCGACAGGGCAGCACCCAGTATACTTTATGGGGCAGCTCCCGCCGCCTTTGGTCCTGA

W  W  P  N  R  L  N  L  K  V  L  H  Q  N  P  A  V  A  D  P         (57)
GGTGGCCCAACCGGCTCAATCTGAAGGTACTGCACCAAAACCCGGCCGTCGCTGACCCGA       240
CCACCGGGTTGGCCGAGTTAGACTTCCATGACGTGGTTTTGGGCCGGCAGCGACTGGGCT
     CCCAACCTGCAGAATCTGA-MtyG5
           PstI

M  G  A  A  F  D  Y  A  A  E  V  A  T  I  D  V  D  A  L  T         (77)
TGGGTGCGGCGTTCGACTATGCCGCGGAGGTCGCGACCATCGACGTTGACGCCCTGACGC       300
ACCCACGCCGCAAGCTGATACGGCGCCTCCAGCGCTGGTAGCTGCAACTGCGGGACTGCG

R  D  I  E  E  V  M  T  T  S  Q  P  W  W  P  A  D  Y  G  H         (97)
GGGACATCGAGGAAGTGATGACCACCTCGCAGCCGTGGTGGCCCGCCGACTACGGCCACT       360
CCCTGTAGCTCCTTCACTACTGGTGGAGCGTCGGCACCACCGGGCGGCTGATGCCGGTGA
                               ---------TTC--------->W91F

Y  G  P  L  F  I  R  M  A  W  H  A  A  G  T  Y  R  I  H  D         (117)
ACGGGCCGCTGTTTATCCGGATGGCGTGGCACGCTGCCGGCACCTACCGCATCCACGACG       420
TGCCCGGCGACAAATAGGCCTACCGCACCGTGCGACGGCCGTGGATGGCGTAGGTGCTGC

G  R  G  G  A  G  G  G  M  Q  R  F  A  P  L  N  S  W  P  D         (137)
GCCGCGGCGGCGCCGGGGGCGGCATGCAGCGGTTCGCGCCGCTTAACAGCTGGCCCGACA       480
CGGCGCCGCCGCGGCCCCCGCCGTACGTCGCCAAGCGCGGCGAATTGTCGACCGGGCTGT
                     SphI                       PvuII
```

```
N  A  S  L  D  K  A  R  R  L  L  W  P  V  K  K  K  Y  G  K        (157)
ACGCCAGCTTGGACAAGGCGCGCCGGCTGCTGTGGCCGGTCAAGAAGAAGTACGGCAAGA      540
TGCGGTCGAACCTGTTCCGCGCGGCCGACGACACCGGCCAGTTCAACTTCATGCCGTTCT

K  L  S  W  A  D  L  I  V  F  A  G  N  C  A  L  E  S  M  G        (177)
AGCTCTCATGGGCGGACCTGATTGTTTTCGCCGGCAACTGCGCGCTGGAATCGATGGGCT      600
TCGAGAGTACCCGCCTGGACTAACAAAAGCGGCCGTTGACGCGCGACCTTAGCTACCCGA
                                                    ClaI
                                    MtK5---------------------->
F  K  T  F  G  F  G  F  G  R  V  D  Q  W  E  P  D  E  V  Y        (197)
TCAAGACGTTCGGGTTCGGCTTCGGCCGGGTCGACCAGTGGGAGCCCGATGAGGTCTATT      660
AGTTCTGCAAGCCCAAGCCGAAGCCGGCCCAGCTGGTCACCCTCGGGCTACTCCAGATAA
                                SalI  <MtK-4

W  G  K  E  A  T  W  L  G  D  E  R  Y  S  G  K  R  D  L  E        (217)
GGGGCAAGGAAGCCACCTGGCTCGGCGATGAGCGTTACAGCGGTAAGCGGGATCTGGAGA      720
CCCCGTTCCTTCGGTGGACCGAGCCGCTACTCGCAATGTCGCCATTCGCCCTAGACCTCT

N  P  L  A  A  V  Q  M  G  L  I  Y  V  N  P  E  G  P  N  G        (237)
ACCCGCTGGCCGCGGTGCAGATGGGGCTGATCTACGTGAACCCGGAGGGGCCGAACGGCA      780
TGGGCGACCGGCGCCACGTCTACCCCGACTAGATGCACTTGGGCCTCCCCGGCTTGCCGT

N  P  D  P  M  A  A  A  V  D  I  R  E  T  F  R  R  M  A  M        (257)
ACCCGGACCCCATGGCCGCGGCGGTCGACATTCGCGAGACGTTTCGGCGCATGGCCATGA      840
TGGGCCTGGGGTACCGGCGCCGCCAGCTGTAAGCGCTCTGCAAAGCCGCGTACCGGTACT
          NcoI            SalI

N  D  V  E  T  A  A  L  I  V  G  G  H  T  F  G  K  T  H  G        (277)
ACGACGTCGAAACAGCGGCGCTGATCGTCGGCGGTCACACTTTCGGTAAGACCCATGGCG      900
TGCTGCAGCTTTGTCGCCGCGACTAGCAGCCGCCAGTGTGAAAGCCATTCTGGGTACCGC
                                                    NcoI

A  G  P  A  D  L  V  G  P  E  P  E  A  A  P  L  E  Q  M  G        (297)
CCGGCCCGGCCGATCTGGTCGGCCCCGAACCCGAGGCTGCTCCGCTGGAGCAGATGGGCT      960
GGCCGGGCCGGCTAGACCAGCCGGGGCTTGGGCTCCGACGAGGCGACCTCGTCTACCCGA


L  G  W  K  S  S  Y  G  T  G  T  G  K  D  A  I  T  S  G  I        (317)
TGGGCTGGAAGAGCTCGTATGGCACCGGAACCGGTAAGGACGCGATCACCAGCGGCATCG     1020
ACCCGACCTTCTCGAGCATACCGTGGCCTTGGCCATTCCTGCGCTAGTGGTCGCCGTAGC
          SstI                PinAI
                                        ---------ACC-------
                                        ---------AAC-------
```

```
E  V  V  W  T  N  T  P  T  K  W  D  N  S  F  L  E  I  L  Y          (337)
AGGTCGTATGGACGAACACCCCGACGAAATGGGACAACAGTTTCCTCGAGATCCTGTACG        1080
TCCAGCATACCTGCTTGTGGGGCTGCTTTACCCTGTTGTCAAAGGAGCTCTAGGACATGC
                                                 XhoI
                                    MtK6---------------------->

---->S315T
---->S315N
-------TAT------------>W321F

G  Y  E  W  E  L  T  K  S  P  A  G  A  W  Q  Y  T  A  K  D          (357)
GCTACGAGTGGGAGCTGACGAAGAGCCCTGCTGGCGCTTGGCAATACACCGCCAAGGACG        1140
CGATGCTCACCCTCGACTGCTTCTCGGGACGACCGCGAACCGTTATGTGGCGGTTCCTGC

G  A  G  A  G  T  I  P  D  P  F  G  G  P  G  R  S  P  T  M          (377)
GCGCCGGTGCCGGCACCATCCCGGACCCGTTCGGCGGGCCAGGGCGCTCCCCGACGATGC        1200
CGCGGCCACGGCCGTGGTAGGGCCTGGGCAAGCCGCCCGGTCCCGCGAGGGGCTGCTACG

L  A  T  D  L  S  L  R  V  D  P  I  Y  E  R  I  T  R  R  W          (397)
TGGCCACTGACCTCTCGCTGCGGGTGGATCCGATCTATGAGCGGATCACGCGTCGCTGGC        1260
ACCGGTGACTGGAGAGCGACGCCCACCTAGGCTAGATACTCGCCTAGTGCGCAGCGACCG
                          BamHI                  AflIII(MluI)

L  E  H  P  E  E  L  A  D  E  F  A  K  A  W  Y  K  L  I  H          (417)
TGGAACACCCCGAGGAATTGGCCGACGAGTTCGCCAAGGCCTGGTACAAGCTGATCCACC        1320
ACCTTGTGGGGCTCCTTAACCGGCTGCTCAAGCGGTTCCGGACCATGTTCGACTAGGTGG

R  D  M  G  P  V  A  R  Y  L  G  P  L  V  P  K  Q  T  L  L          (437)
GAGACATGGGTCCCGTTGCGAGATACCTTGGGCCGCTGGTCCCCAAGCAGACCCTGCTGT        1380
CTCTGTACCCAGGGCAACGCTCTATGGAACCCGGCGACCAGGGGTTCGTCTGGGACGACA
    --------GAATTC-------->pMtKatG1
            EcoRI
         GGTCCCGTCGACAGATACCT>pMtkatG4
                SalI
       MtyG7<GCAACGCTTCGAAGAACCC
                     HindIII
W  Q  D  P  V  P  A  V  S  H  D  L  V  G  E  A  E  I  A  S          (457)
GGCAGGATCCGGTCCCTGCGGTCAGCCACGACCTCGTCGGCGAAGCCGAGATTGCCAGCC        1440
CCGTCCTAGGCCAGGGACGCCAGTCGGTGCTGGAGCAGCCGCTTCGGCTCTAACGGTCGG
     BamHI
```

```
L  K  S  Q  I  R  A  S  G  L  T  V  S  Q  L  V  S  T  A  W          (477)
TTAAGAGCCAGATCCGGGCATCGGGATTGACTGTCTCACAGCTAGTTTCGACCGCATGGG       1500
AATTCTCGGTCTAGGCCCGTAGCCCTAACTGACAGAGTGTCGATCAAAGCTGGCGTACCC
AflII

A  A  A  S  S  F  R  G  S  D  K  R  G  G  A  N  G  G  R  I          (497)
CGGCGGCGTCGTCGTTCCGTGGTAGCGACAAGCGCGGCGGCGCCAACGGTGGTCGCATCC       1560
GCCGCCGCAGCAGCAAGGCACCATCGCTGTTCGCGCCGCCGCGGTTGCCACCAGCGTAGG
                                        ---------------------->MtK7

R  L  Q  P  Q  V  G  W  E  V  N  D  P  D  G  D  L  R  K  V          (517)
GCCTGCAGCCACAAGTCGGGTGGGAGGTCAACGACCCCGACGGGGATCTGCGCAAGGTCA       1620
CGGACGTCGGTGTTCAGCCCACCCTCCAGTTGCTGGGGCTGCCCCTAGACGCGTTCCAGT


I  R  T  L  E  E  I  Q  E  S  F  N  S  A  A  P  G  N  I  K          (537)
TTCGCACCCTGGAAGAGATCCAGGAGTCATTCAACTCCGCGGCGCCGGGGAACATCAAAG       1680
AAGCGTGGGACCTTCTCTAGGTCCTCAGTAAGTTGAGGCGCCGCGGCCCCTTGTAGTTTC

V  S  F  A  D  L  V  V  L  G  G  C  A  A  I  E  K  A  A  K          (557)
TGTCCTTCGCCGACCTCGTCGTGCTCGGTGGCTGTGCCGCCATAGAGAAAGCAGCAAAGG       1740
ACAGGAAGCGGCTGGAGCAGCACGAGCCACCGACACGGCGGTATCTCTTTCGTCGTTTCC

A  A  G  H  N  I  T  V  P  F  T  P  G  R  T  D  A  S  Q  E          (577)
CGGCTGGCCACAACATCACGGTGCCCTTCACCCCGGGCCGCACGGATGCGTCGCAGGAAC       1800
GCCGACCGGTGTTGTAGTGCCACGGGAAGTGGGGCCCGGCGTGCCTACGCAGCGTCCTTG
                                        SmaI

Q  T  D  V  E  S  F  A  V  L  E  P  K  A  D  G  F  R  N  Y          (597)
AAACCGACGTGGAATCCTTTGCCGTGCTGGAGCCCAAGGCAGATGGCTTCCGAAACTACC       1860
TTTGGCTGCACCTTAGGAAACGGCACGACCTCGGGTTCCGTCTACCGAAGGCTTTGATGG

L  G  K  G  N  P  L  P  A  E  Y  M  L  L  D  K  A  N  L  L          (617)
TCGGAAAGGGCAACCCGTTGCCGGCCGAGTACATGCTGCTCGACAAGGCGAACCTGCTTA       1920
AGCCTTTCCCGTTGGGCAACGGCCGGCTCATGTACGACGAGCTGTTCCGCTTGGACGAAT
```

```
T  L  S  A  P  E  M  T  V  L  V  G  G  L  R  V  L  G  A  N          (637)
CGCTCAGTGCCCCTGAGATGACGGTGCTGGTAGGTGGCCTGCGCGTCCTCGGCGCAAACT       1980
GCGAGTCACGGGGACTCTACTGCCACGACCATCCACCGGACGCGCAGGAGCCGCGTTTGA
Y  K  R  L  P  L  G  V  F  T  E  A  S  E  S  L  T  N  D  F          (657)
ACAAGCGCTTACCGCTGGGCGTGTTCACCGAGGCCTCCGAGTCACTGACCAACGACTTCT       2040
TGTTCGCGAATGGCGACCCGCACAAGTGGCTCCGGAGGCTCAGTGACTGGTTGCTCAAGA
   Eco47III

F  V  N  L  L  D  M  G  I  T  W  E  P  S  P  A  D  D  G  T          (677)
TCGTGAACCTGCTCGACATGGGTATCACCTGGGAGCCCTCGCCAGCAGATGACGGGACCT       2100
AGCACTTGGACGAGCTGTACCCATAGTGGACCCTCGGGAGCGGTCGTCTACTGCCCTGGA

Y  Q  G  K  D  G  S  G  K  V  K  W  T  G  S  R  V  D  L  V          (697)
ACCAGGGCAAGGATGGCAGTGGCAAGGTGAAGTGGACCGGCAGCCGCGTGGACCTGGTCT       2160
TGGTCCCGTTCCTACCGTCACCGTTCCACTTCACCTGGCCGTCGGCGCACCTGGACCAGA

F  G  S  N  S  E  L  R  A  L  V  E  V  Y  G  A  D  D  A  Q          (717)
TCGGGTCCAACTCGGAGTTGCGGGCGCTTGTCGAGGTCTATGGCGCCGATGACGCGCAGC       2220
AGCCCAGGTTGAGCCTCAACGCCCGCGAACAGCTCCAGATACCGCGGCTACTGCGCGTCG

P  K  F  V  Q  D  F  V  A  A  W  D  K  V  M  N  L  D  R  F          (737)
CGAAGTTCGTGCAGGACTTCGTCGCTGCCTGGGACAAGGTGATGAACCTCGACAGGTTCG       2280
GCTTCAAGCACGTCCTGAAGCAGCGACGGACCCTGTTCCACTACTTGGAGCTGTCCAAGC
                                          pMtKatG3⌐ CTGTCCAAGT

D  V  R  *                                                          (740)
ACGTGCGCTGATTCGGGTTGATCGGCCCTGCCCGCCGATCAACCACAACCCGCCGCAGCA       2340
TGCACGCGACTAAGCCCAACTAGCCGGGACGGGCGGCTAGTTGGTGTTGGGCGGCGTCGT
                                ⌐MtK-2
     ⌐-------TTCGAA------pMtKatG2
             HindIII
TCGAACGCTGAT
HindIII
       <-------------------CCATGGCCATGG<MTG3'Kpn

CCCCGCGAGCTGACCGGCTCGCGGGGTGCTGGTGTTTGCCCGGCGCGATTTGTCAGACCC       2400
GGGGCGCTCGACTGGCCGAGCGCCCCACGACCACAAACGGGCCGCGCTAAACAGTCTGGG

CGCGTGCATGGTGGTCGCACGGACGCACGAGACGGGGATGACGAGACGGGGATGAGGAGA       2460
GCGCACGTACCACCAGCGTGCCTGCGTGCTCTGCCCCTACTGCTCTGCCCCTACTCCTCT

AAGGGCGCCGAAATGTGCTGGATGTGCGATCACCCGGAAGCCACCGCCGAGGAGTACCTC       2520
TTCCCGCGGCTTTACACGACCTACACGCTAGTGGGCCTTCGGTGGCGGCTCCTCATGGAG
                                    ⌐MtK-1
```

GACGAGGTGTACGGGATAATGCTCATGCATGGCTGGGCGGTACAGCACGTGGAGTGCGAG 2580
CTGCTCCACATGCCCTATTACGAGTACGTACCGACCCGCCATGTCGTGCACCTCACGCTC
*Nsi*I

CGACGGCCATTTGCCTACACGGTTGGTCTAACCCGGCGCGGCTTGCCCGAACTGGTGGTG 2640
GCTGCCGGTAAACGGATGTGCCAACCAGATTGGGCCGCGCCGAACGGGCTTGACCACCAC

ACTGGCCTCTCGCCACGACGTGGGCAGCGGTTGTTGAACATGCCGTCGAGGGCTCTGGTC 2700
TGACCGGAGAGCGGTGCTGCACCCGTCGCCAACAACTTGTACGGCAGCTCCCGAGACCAG

GGTGACTTGCTGACTCCCGGTATGTAGACCACCCTCAAAGCCGGCCCTCTTGTCGAAACG 2760
CCACTGAACGACTGAGGGCCATACATCTGGTGGGAGTTTCGGCCGGGAGAACAGCTTTGC

GTCCAGGCTACACATCCGGACGCGCATTTGTATTGTGCGATCGCCATCTTTGCGCACAAG 2820
CAGGTCCGATGTGTAGGCCTGCGCGTAAACATAACACGCTAGCGGTAGAAACGCGTGTTC

GTGACGGCCTTGCAGTTGGTGTGGGCCGACCGCGTGGTCGCTGGCCGTGGGCGGCGGACT 2880
CACTGCCGGAACGTCAACCACACCCGGCTGGCGCACCAGCGACCGGCACCCGCCGCCTGA

TCGACGAAGGTCGCGGTACC 2900
AGCTGCTTCCAGCGCCATGG
*Kpn*I

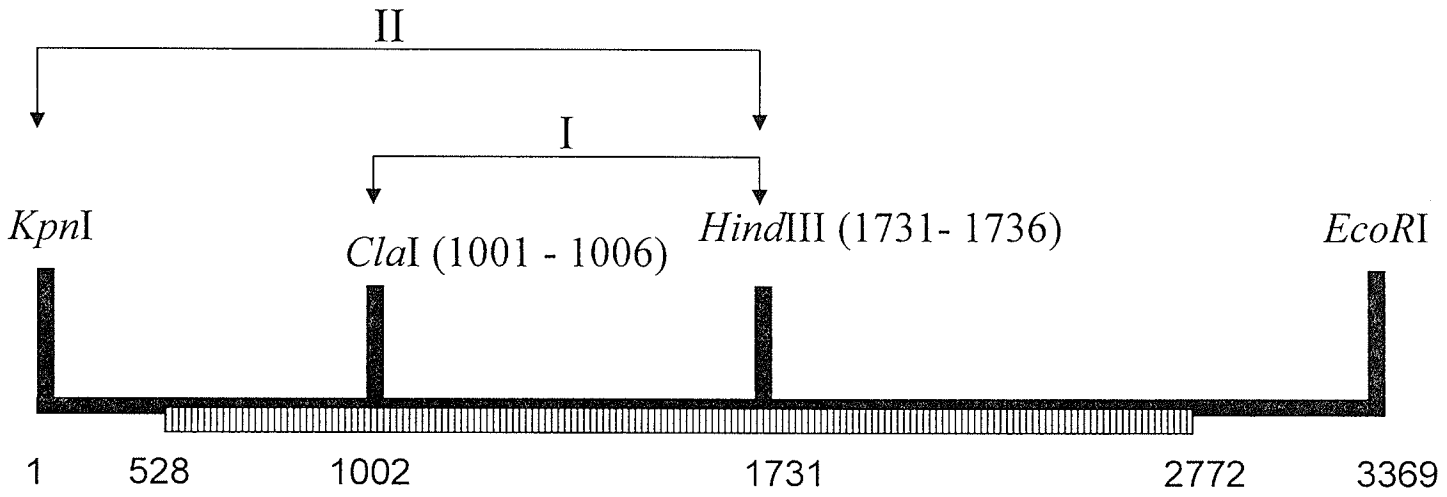

Figure 2.4. Simplified restriction map of the chromosomal insert containing the *B. pseudomallei katG* gene in plasmids pBpG and pBpG-KH (Fragment **I**) and pBpG-CH (Fragmaent **II**). The 1134 bp long katG open reading frame is indicated as the part of the chromosomal insert as is the insert fragment **I** used to construct the subclone vectors employed in site directed mutagenesis of *B. pseudomallei katG*.

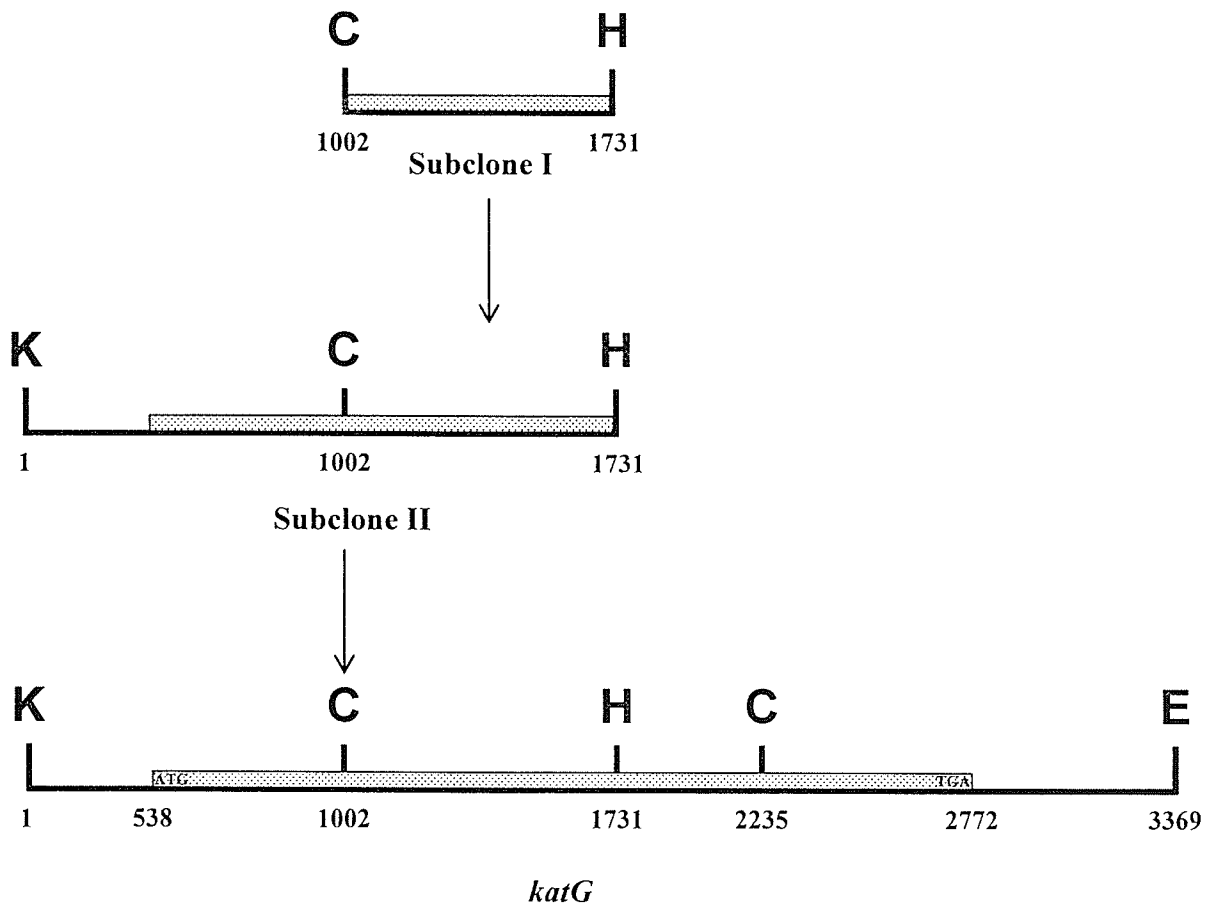

Figure 2.5 General reconstruction protocol used for the generation of variant BpKatG's from mutagenized subclone I for protein expression. (K:*Kpn*I, C:*Cla*I, *Hind*III, E: *EcoR*I)

Figure 2.6. The DNA sequence and corresponding amino acid sequence of *B. pseudomallei* showing the restriction sites and the target codones selected for mutagenesis in this study. The sequencing primers are also shown.

Burkholderia pseudomallei KatG (BpKAtG)

```
   CGGGGTGACGAAGCTCGATATCCCGGCGACGGTGAATTGAGCGCGGCGAGCGCAGCTG        60
   GCCCCACTGCTTCGAGCTATAGGGCCGCTGCCACTTAACTCGCGCCGCTCGCGACGAC

CGGGCCGCCGCGCGCCATGATCGGACGGGGCTTCGGGGCCCCGTTTATTTTTGCCTATCG        120
GCCCGGCGGCGCGCGGTACTAGCCTGCCCCGAAGCCCCGGGGCAAATAAAAACGGATAGC

GATAAATAAAATTTATTAAATTACATATATCAATAGCAAATAATAGAATGCTTCGCATGG        180
CTATTTATTTTAAATAATTTAATGTATATAGTTATCGTTTATTATCTTACGAAGCGTACC

ATCGGCGCAGCGCCGCCGGACGGTAACTGCAAGCGTCAAGGGAGGATGTCATGATGCAAC        240
TAGCCGCGTCGCGGCGGCCTGCCATTGACGTTCGCAGTTCCCTCCTACAGTACTACGTTG

CGGCATTGTCGCGCGCGCGGCGGAACATTGCGCCGCGCCCGGCGGTCATTGATCGTGCCA        300
GCCGTAACAGCGCGCGCGCCGCCTTGTAACGCGGCGCGGGCCGCCAGTAACTAGCACGGT

AGGCTGCCATCCGGAGCCTGCGTCCGATTGCGTTCGCTTATCTGGCGGACCGCGCCCACG        360
TCCGACGGTAGGCCACGGACGCAGGCTAACGCAAGCGAATAGACCGCCTGGCGCGGGTGC

GCGGCTGAGCGCCGCCGCGTGCCGGGCCGCTTTTTTCGCGCCGCGCGTCGCGTCGCACGC        420
CGCCGACTCGCGGCGGCGCACGGCCCGGCGAAAAAAGCGCGGCGCGCAGCGCAGCGTGCG
                                                      ------

                                                    M  P  G  S        (4)
AGGAGGGGTCAACCTGTTTGTTTCCCCGCAAAGTCGCCCCCCGAACGATGCCCGGCTCCG        480
TCCTCCCCAGTTGGACAAACAAAGGGGCGTTTCAGCGGGGGGCTTGCTACGGGCCGAGGC
               ------------------>BpG2
--------------->BpG5

G  A  G  P  R  R  R  G  V  H  E  Q  R  R  N  R  M  S  N  E        (24)
ATGCCGGGCCCCGCAGGCGGGGCGTACACGAACAAAGGAGAAATCGCATGTCGAATGAAG        540
TACGGCCCGGGGCGTCCGCCCCGCATGTGCTTGTTTCCTCTTTAGCGTACAGCTTACTTC


A  K  C  P  F  H  Q  A  A  G  N  G  T  S  N  R  D  W  W  P        (44)
CGAAGTGCCCGTTCCATCAAGCCGCAGGCAACGGCACGTCGAACCGGGACTGGTGGCCCA        600
GCTTCACGGGCAAGGTAGTTCGGCGTCCGTTGCCGTGCAGCTTGGCCCTGACCACCGGGT
```

```
N  Q  L  D  L  S  I  L  H  R  H  S  S  L  S  D  P  M  G  K          (64)
ATCAGCTGGACCTGAGCATCCTGCATCGGCACTCGTCGCTGTCCGATCCGATGGGCAAGG       660
TAGTCGACCTGGACTCGTAGGACGTAGCCGTGAGCAGCGACAGGCTAGGCTACCCGTTCC

D  F  N  Y  A  Q  A  F  E  K  L  D  L  A  A  V  K  R  D  L          (84)
ATTTCAACTACGCGCAGGCGTTCGAGAAGCTCGACCTCGCGGCGGTGAAGCGCGACCTCC       720
TAAAGTTGATGCGCGTCCGCAAGCTCTTCGAGCTGGAGCGCCGCCACTTCGCGCTGGAGG


H  A  L  M  T  T  S  Q  D  W  W  P  A  D  F  G  H  Y  G  G          (104)
ACGCGCTGATGACGACGTCGCAGGACTGGTGGCCGGCCGATTTCGGCCACTACGGCGGCC       780
TGCGCGACTACTGCTGCAGCGTCCTGACCACCGGCCGGCTAAAGCCGGTGATGCCGCCGG
----------------->BpG6                                              -

L  F  I  R  M  A  W  H  S  A  G  T  Y  R  T  A  D  G  R  G          (124)
TGTTCATCCGCATGGCATGGCACAGCGCGGGCACGTACCGCACGGCCGACGGCCGCGGCG       840
ACAAGTAGGCGTACCGTACCGTGTCGCGCCCGTGCATGGCGTGCCGGCTGCCGGCGCCGC

G  A  G  E  G  Q  Q  R  F  A  P  L  N  S  W  P  D  N  A  N          (144)
GCGCGGGCGAAGGGCAGCAGCGCTTCGCGCCGCTCAACAGCTGGCCCGACAACGCGAACC       900
CGCGCCCGCTTCCCGTCGTCGCGAAGCGCGGCGAGTTGTCGACCGGGCTGTTGCGCTTGG

L  D  K  A  R  R  L  L  W  P  I  K  Q  K  Y  G  R  A  I  S          (164)
TCGACAAGGCGCGCCGGCTGCTGTGGCCGATCAAGCAGAAGTACGGCCGCGCCATCTCGT       960
AGCTGTTCCGCGCGGCCGACGACACCGGCTAGTTCGTCTTCATGCCGGCGCGGTAGAGCA

W  A  D  L  L  I  L  T  G  N  V  A  L  E  S  M  G  F  K  T          (184)
GGGCCGACCTGCTGATCCTGACGGGCAACGTCGCGCTCGA*ATCGAT*GGGCTTCAAGACCT     1020
CCCGGCTGGACGACTAGGACTGCCCGTTGCAGCGCGAGCTTAGCTACCCGAAGTTCTGGA
                                          *Cla*I

F  G  F  A  G  G  R  A  D  T  W  E  P  E  D  V  Y  W  G  S          (204)
TCGGCTTCGCGGGCGGCCGCGCGGACACGTGGGAGCCCGAGGACGTCTACTGGGGCTCGG       1080
AGCCGAAGCGCCCGCCGGCGCGCCTGTGCACCCTTCGGGCTCCTGCAGATGACCCCGAGC

E  K  I  W  L  E  L  S  G  G  P  N  S  R  Y  S  G  D  R  Q          (224)
AAAAGATCTGGCTGGAACTGAGCGGCGGCCCGAACAGCCGCTATTCGGGCGACCGCCAGC       1140
CTTTTCTAGACCGACCTTGACTCGCCGCCGGCTTGTCGGCGATAAGCCCGCTGGCGGTCG

L  E  N  P  L  A  A  V  Q  M  G  L  I  Y  V  N  P  E  G  P          (244)
TCGAGAACCCGCTCGCCGCCGTGCAGATGGGCCTCATCTACGTGAATCCGGAAGGCCCGG       1200
AGCTCTTGGGCGAGCGGCGGCACGTCTACCCGGAGTAGATGCACTTAGGCCTTCCGGGCC

D  G  N  P  D  P  V  A  A  A  R  D  I  R  D  T  F  A  R  M          (264)
```

```
ACGGCAATCCCGATCCGGTCGCCGCGGCGCGCGACATTCGTGACACCTTCGCGCGCATGG      1260
TGCCGTTAGGGCTAGGCCAGCGGCGCCGCGCGCTGTAAGCACTGTGGAAGCGCGCGTACC
                                                  ------------


A  M  N  D  E  E  T  V  A  L  I  A  G  G  H  T  F  G  K  T       (284)
CGATGAACGACGAAGAGACGGTCGCGCTGATCGCGGGCGGCCACACGTTCGGCAAGACGC    1320
GCTACTTGCTGCTTCTCTGCCAGCGCGACTAGCGCCCGCCGGTGTGCAAGCCGTTCTGCG
----->BpG3
                                    ---------TAC--------->H279Y
                                    ---------AAC--------->H279N

H  G  A  G  P  A  S  N  V  G  A  E  P  E  A  A  G  I  E  A       (304)
ACGGCGCGGGGCCCGCGTCGAACGTCGGCGCCGAGCCGGAGGCCGCGGGCATCGAAGCGC    1380
TGCCGCGCCCCGGGCGCAGCTTGCAGCCGCGGCTCGGCCTCCGGCGCCCGTAGCTTCGCG

Q  G  L  G  W  K  S  A  Y  R  T  G  K  G  A  D  A  I  T  S       (324)
AGGGCCTCGGCTGGAAGAGCGCGTACCGCACGGGCAAGGGCGCGGACGCGATCACGAGCG    1440
TCCCGGAGCCGACCTTCTCGCGCATGGCGTGCCCGTTCCCGCGCCTGCGCTAGTGCTCGC

G  L  E  V  T  W  T  T  T  P  T  Q  W  S  H  N  F  F  E  N       (344)
GGCTCGAAGTCACGTGGACGACGACGCCGACGCAGTGGAGCCACAACTTCTTCGAGAACC    1500
CGGAGCTTCAGTGCACCTGCTGCTGCGGCTGCGTCACCTCGGTGTTGAAGAAGCTCTTGG

L  F  G  Y  E  W  E  L  T  K  S  P  A  G  A  H  Q  W  V  A       (364)
TGTTCGGCTACGAGTGGGAGCTGACGAAGAGCCCGGCGGGCGCGCACCAGTGGGTCGCGA    1560
ACAAGCCGATGCTCACCCTCGACTGCTTCTCGGGCCGCCCGCGCGTGGTCACCCAGCGCT

K  G  A  D  A  V  I  P  D  A  F  D  P  S  K  K  H  R  P  T       (384)
AGGGCGCCGACGCGGTGATTCCCGACGCGTTCGATCCGTCGAAGAAGCATCGTCCGACGA    1620
TCCCGCGGCTGCGCCACTAAGGGCTGCGCAAGCTAGGCAGCTTCTTCGTAGCAGGCTGCT

M  L  T  T  D  L  S  L  R  F  D  P  A  Y  E  K  I  S  R  R       (404)
TGCTCACGACCGACCTGTCGCTGCGCTTCGATCCGGCGTACGAAAAGATCTCGCGCCGCT    1680
ACGAGTGCTGGCTGGACAGCGACGCGAAGCTAGGCCGCATGCTTTTCTAGAGCGCGGCGA

F  H  E  N  P  E  Q  F  A  D  A  F  A  R  A  W  F  K  L* T       (424)
TCCACGAGAACCCGGAGCAGTTCGCCGACGCGTTCGCGCGCGCCTGGTTC AAGCTT ACGC  1740
AGGTGCTCTTGGGCCTCGTCAAGCGGCTGCGCAAGCGCGCGCGGACCAAGTTCGAGTGCG

H  R  D  M  G  P  R  A  R  Y  L  G  P  E  V  P  A  E  V  L       (444)
ACCGCGACATGGGCCCGCGCGCGCGCTATCTCGGCCCGGAAGTGCCGGCCGAGGTGCTGC    1800
TGGCGCTGTACCCGGGCGCGCGCGCGATAGAGCCGGGCCTTCACGGCCGGCTCCACGACG
-->BpG1
```

```
L  W  Q  D  P  I  P  A  V  D  H  P  L  I  D  A  D  A  A  A          (464)
TGTGGCAGGACCCGATTCCGGCCGTCGACCATCCGCTGATCGACGCCGCGGACGCCGCCG       1860
ACACCGTCCTGGGCTAAGGCCGGCAGCTGGTAGGCGACTAGCTGCGGCGCCTGCGGCGGC

E  L  K  A  K  V  L  A  S  G  L  T  V  S  Q  L  V  S  T  A          (484)
AGCTGAAGGCAAAGGTGCTCGCGTCGGGGCTGACCGTGTCGCAGCTCGTTTCCACCGCGT       1920
TCGACTTCCGTTTCCACGAGCGCAGCCCCGACTGGCACAGCGTCGAGCAAAGGTGGCGCA

W  A  A  A  S  T  F  R  G  S  D  K  R  G  G  A  N  G  A  R          (504)
GGGCGGCGGCGTCCACCTTCCGCGGCTCGGACAAGCGCGGCGGCGCGAACGGCGCGCGCA       1980
CCCGCCGCCGCAGGTGGAAGGCGCCGAGCCTGTTCGCGCCGCCGCGCTTGCCGCGCGCGT

I  R  L  A  P  Q  K  D  W  E  A  N  Q  P  E  Q  L  A  A  Y          (524)
TTCGCCTTGCGCCGCAGAAGGACTGGGAGGCGAACCAGCCCGAGCAGCTCGCGGCGGTGC       2040
AAGCGGAACGCGGCGTCTTCCTGACCCTCCGCTTGGTCGGGCTCGTCGAGCGCCGCCACG

L  E  T  L  E  A  I  R  T  A  F  N  G  A  Q  R  G  G  K  Q          (544)
TCGAGACGCTCGAGGCAATTCGCACGGCGTTCAACGGCGCGCAGCGCGGCGGCAAGCAAG       2100
AGCTCTGCGAGCTCCGTTAAGCGTGCCGCAAGTTGCCGCGCGTCGCGCCGCCGTTCGTTC

V  S  L  A  D  L  I  V  L  A  G  C  A  G  V  E  Q  A  A  K          (564)
TGTCGCTCGCCGATCTGATCGTGCTGGCCGGCTGCGCGGGCGTCGAGCAGGCGGCGAAGA       2160
ACAGCGAGCGGCTAGACTAGCACGACCGGCCGACGCGCCCGCAGCTCGTCCGCCGCTTCT

N  A  G  H  A  V  T  V  P  F  A  P  G  R  A  D  A  S  Q  E          (584)
ACGCGGGCCACGCGGTGACCGTGCCGTTCGCGCCGGGCCGCGCGGACGCATCGCAGGAGC       2220
TGCGCCCGGTGCGCCACTGGCACGGCAAGCGCGGCCCGGCGCGCCTGCGTAGCGTCCTCG
-------------------->BpG7

Q  T  D  V  E  S  M  A  V  L  E  P  V  A  D  G  F  R  N  Y          (604)
AGACCGACGTCGAATCGATGGCCGTGCTCGAGCCGGTGGCCGACGGTTTTCGCAACTACC       2280
TCTGGCTGCAGCTTAGCTACCGGCACGAGCTCGGCCACCGGCTGCCAAAAGCGTTGATGG
               ClaI

L  K  G  K  Y  R  V  P  A  E  V  L  L  V  D  K  A  Q  L  L          (624)
TGAAGGGCAAGTATCGGGTGCCCGCCGAGGTGCTGCTCGTCGACAAGGCGCAACTGCTGA       2340
ACTTCCCGTTCATAGCCCACGGGCGGCTCCACGACGAGCAGCTGTTCCGCGTTGACGACT

T  L  S  A  P  E  M  T  V  L  L  G  G  L  R  V  L  G  A  N          (644)
CGCTGAGCGCGCCGGAGATGACGGTGCTGCTGGGCGGCCTGCGCGTGCTGGGCGCGAACG       2400
GCGACTCGCGCGGCCTCTACTGCCACGACGACCCGCCGGACGCGCACGACCCGCGCTTGC
```

```
V  G  Q  S  R  H  G  V  F  T  A  R  E  Q  A  L  T  N  D  F          (664)
TCGGGCAGAGCCGGCACGGCGTGTTCACCGCGCGCGAGCAGGCATTGACCAACGACTTCT       2460
AGCCCGTCTCGGCCGTGCCGCACAAGTGGCGCGCGCTCGTCCGTAACTGGTTGCTGAAGA

F  V  N  L  L  D  M  G  T  E  W  K  P  T  A  A  D  A  D  V          (684)
TCGTGAACCTGCTCGACATGGGCACCGAGTGGAAGCCGACGGCGGCCGACGCGGACGTGT       2520
AGCACTTGGACGAGCTGTACCCGTGGCTCACCTTCGGCTGCCGCCGGCTGCGCCTGCACA

F  E  G  R  D  R  A  T  G  E  L  K  W  T  G  T  R  V  D  L          (704)
TCGAAGGGCGCGACCGCGCGACGGGCGAGCTCAAGTGGACGGGCACGCGCGTCGATCTCG       2580
AGCTTCCCGCGCTGGCGCGCTGCCCGCTCGAGTTCACCTGCCCGTGCGCGCAGCTAGAGC

V  F  G  S  H  S  Q  L  R  A  L  A  E  V  Y  G  S  A  D  A          (724)
TGTTCGGCTCGCACTCGCAGTTGCGCGCGCTCGCGGAGGTCTACGGCAGCGCGGACGCGC       2640
ACAAGCCGAGCGTGAGCGTCAACGCGCGCGAGCGCCTCCAGATGCCGTCGCGCCTGCGCG

Q  E  K  F  V  R  D  F  V  A  V  W  N  K  V  M  N  L  D  R          (744)
AGGAGAAGTTCGTGCGCGACTTCGTCGCGGTCTGGAACAAGGTGATGAACCTCGACCGCT       2700
TCCTCTTCAAGCACGCGCTGAAGCAGCGCCAGACCTTGTTCCACTACTTGGAGCTGGCGA

F  D  L  A  *                                                      (748)
TCGATCTCGCGTGATCGCGCCGCCGCGCCGCCGGAGCGGCGGCGCGCGGCGGCGGGGAAC       2760
AGCTAGAGCGCACTAGCGCGGCGGCGCGGCGGCCTCGCCGCCGCGCGCCGCCGCCCCTTG
                          BpG4<------------------

GGCCGGCTGACGCGGGCCGCTTCCCGCCGGGCCGCTGATATCGTTTCAAGGAGTGACGAT       2820
CCGGCCGACTGCGCCCGGCGAAGGGCGGCCCGGCGACTATAGCAAAGTTCCTCACTGCTA
BpG6<--------------------

CATGACGCAAATGATTCTCGACCTGCGCGGGGCGCTCGCGGCGCCGGCCAGGCGCGCGGG       2880
CGCCGCGGCGTGGCGGCGGCTGATCGGCCTCGCGATCGCGGGCGGCGGCGCGGCCGTGCT       2940
GGCCGCGCAGGCCGCGCGCTACTTCACGGCGGCCGCCGGCGGTTGAGCGGGCCTGCGTTT       3000
CGCGCAAATCGCGCGCTCGCGATCTACGCTAAACTGGTGCGGCGCTCGGCGGGCAGCCGC       3060
ACGCGCGTCTGCCGCCTCTGCATAGGCTGCCCATGCGCATGTCGCCTGCGCGCATCCCGC       3120
ATCGGGCATGCGGATCTTTCGATGCATTTTCGTCGGTTCGAACCATCGGACAAGGAGTTT       3180
CGAGGATGGCCAAGAAAAGCAACGCAACCCAGATCAACATCGGCATCAGCGACAAGGATC       3240
GCAAGAAGATCGCGGCGGGGCTGTCGCGTCTGCTCGCCGATACGTACACGCTGTACCTGA       3300
AGACGCACAATTTCCACTGGAACGTGACCGGCCCGATGTTCAACACGCTGCACCTGATGT       3360
TCGAGGAGCAGTACAACGAACTGTGGCTCGCCGTCGATCTCGTCGCGGAGCGCATCCGCA       3420
CGCTCGGGGTCGTCGCGCCGGGCACGTATCGCGAATTCGCGAAGCTGTCGTCGATTCCCG       3480
AGGCCGACGGCGTGCCGGCCGCCGAGGAGATGATTCGCCAGCTCGTCGAAGGGCATGAGG       3540
CTGTCGTGCGCACCGCGCGCGCGATCTTCCCGGACGCCGACGCGGCGAGCGACGAGCCCA       3600
CCGCCGATCTGCTGACGCAGCGCCTGCAG                                       3629
```

Once the correct mutation was identified, the complete sub-clone sequence was determined to ensure that no base changes apart from those desired had been introduced. The mutated sub-clone was used to reconstruct the complete *MtkatG* or *BpkatG* gene. The complete gene was sequenced over the region containing the mutation for final confirmation. Reconstructed mutant *MtkatG* and *BpkatG* clones were transformed into UM262 for determination of enzyme activities and visualization of protein from crude extracts or whole cells by SDS-PAGE. Clones over expressing significant levels of variant MtKatG and BpKatG enzyme were grown on a large scale (4-6 liters) for purification and characterization of the enzymes.

2.4.3. Reconstruction of *M. tuberculosis katG* subclones with desired mutation

An outline of the reconstruction protocol is illustrated in Figure 2.2a. The plasmids was drawn in a linearized form for reasons of simplicity. Reconstruction of mutant *katG* genes was done in a single step. Plasmid pMt-CX (subclone I) with the desired mutation was cut with *Xho*I and *Cla*I. The 474 bp *Xho*I-*Cla*I fragment from pMt-CX was then ligated into pAH1 that was also cut with *Xho*I and *Cla*I to generate the plasmid containing the mutant *katG* gene. All the variant constructs were verified for correct restriction sites using various restriction digestion studies at each step in the construction process.

2.4.4. Reconstruction of *B. pseudomallei katG* subclones with desired mutation

An outline of the reconstruction protocol is illustrated in Figure 2.2b. The plasmids have been drawn in a linearized form for reasons of simplicity. Reconstruction

of mutant *katG* genes was done in two stages. In the first stage, plasmid pBpG-CH (subclone I) with the desired mutation was cut with *Cla*I and *Hind*III. The 730 bp *Cla*I-*Hind*III fragment from pBpG-CH was then ligated into pBpG-KH (subclone II) that was also cut with *Cla*I and *Hind*III. In the second stage, plasmid pBpG-KH (subclone II) with the desired mutation was cut with *Kpn*I and *Hind*III. The 1731 bp *Kpn*I-*Hind*III fragment from pBpG-KH (subclone II) was then ligated into pBpG that was also cut with *Kpn*I and *Hind*III to generate the plasmid containing mutant *katG* gene. All the variant constructs were verified for correct restriction sites using various restriction digestion studies at each step in the construction process.

2.4.5. DNA isolation and purification

Isolation of plasmid DNA was according to Sambrook *et al.* (1989). Plasmid harboring cells were grown in tubes containing 5 mL LB medium to stationary phase and were pelleted by centrifugation and resuspended in 200 μL Tris-glucose-EDTA buffer (25 mM Tris-HCL, pH 8.0, 1% glucose, 10 mM Na-EDTA). Resuspended cells were lysed by addition of 400 μL 1% SDS (w/v), 0.2 M NaOH solution and gentle mixing. This was then neutralized by addition of 300 μL 6.2 M ammonium acetate, pH 6.2. After 10 min incubation, the mixture was centrifuged twice to remove the precipitate. Plasmid were pelleted by centrifugation and resuspended in 200 μL Tris-glucose-EDTA buffer (25 mM Tris-HCL, pH 8.0, 1% glucose, 10 mM Na-EDTA). Resuspended cells were lysed by addition of 400 μL 1% SDS (w/v), 0.2 M NaOH solution and gentle mixing. This was then neutralized by addition of 300 μL 6.2 M ammonium acetate, pH 6.2. After 10 min incubation, the mixture was centrifuged twice to remove the precipitate. Plasmid

DNA was then precipitated by the addition of 550 µL isopropanol to the remaining supernatant followed by 15 min incubation at room temperature. Plasmid DNA was pelleted by centrifugation, washed twice with 1 mL of 70% (v/v) ice cold ethanol, and then dried under vacuum. The DNA pellet was either stored under these conditions at -20°C or was resuspended in HPLC grade distilled water or TE buffer (10 mM Tris, pH 8.0, 1 mM Na-EDTA) prior to being stored at -20°C until further use.

2.4.6. Restriction endonuclease digestion of DNA

Restriction digestions were performed at 37°C for 2-5 h in a total volume of 10 µL containing 1 µL RNAse, 1 µL of 10X appropriate buffer provided by the supplier, ~ 1-5 µg DNA, and 0.5-1 µl (50-2500 Units) of endonuclease.

2.4.7. Agarose gel electrophoresis

Electrophoresis of the restriction endonuclease digested DNA were performed according to Sambrook *et al.*, (1989). Agarose gels containing 1% (w/v) agarose and 0.9 µg/mL ethidium bromide were prepared in TAE buffer (40 mM Tris-Acetate and 1 mM EDTA, pH 8.0) and cast in Bio-Rad Mini Sub cell plexiglass horizontal electrophoresis trays (6.5 cm x 10 cm). Samples of 10 µl volumes were mixed with 2 µl stop buffer (40% [v/v] glycerol, 10 mM EDTA pH 8.0, 0.25% [w/v] bromophenol blue). 1kb or 1 kb plus DNA ladders (Invitrogen Canada Inc) were used as molecular weight size standards. Electrophoresis was carried out at 40-60 mA constant current in TAE buffer until the bromophenol blue marker dye front had migrated approximately two thirds of the length of the gel. Following electrophoresis, the DNA bands were visualized with ultraviolet

light and recorded in a digitized form using a Gel Doc 1000 image capture system (Bio-Rad) or FluorChem^{TM}8900 image capture system (Alpha Innotech).

2.4.8. Ligation

DNA fragments to be ligated were excised from agarose gels and purified using the Ultraclean^{TM} 15 DNA purification kit (Bio/Can Scientific Inc.) according to the instructions supplied by the manufacturer. Ligation of insert DNA into vectors was carried out according to the procedure of Sambrook *et al* (1989). Purified DNA was mixed in a ratio of 2-3 of insert to vector in 10 µl volumes containing 1 unit of T4 DNA ligase (Invitrogen Canada Inc.), and the manufacturer's supplied buffer at the appropriate concentration. Ligation mixtures were incubated overnight at 15°C. A mixture without added insert DNA was used as control.

2.4.9. Transformation

Transformation of *E. coli* cells with the various plasmids was achieved according to Chung *et al* (1989). 5 mL LB cultures of cells grown to exponential phase (2-4 h) were harvested by centrifugation and made competent by resuspension in 500 µL ice-cold 0.1 M $CaCl_2$ for at least 30 min on ice. 2-10 mg DNA was added to 100 µL of this cell suspension, followed by additional 30 min incubation on ice, and a 90 second heat shock at 42°C. 0.9 mL LB was added to the cell suspension and incubated at 37°C for one hour without aeration. The mixture was either spread, or (in the case of ligation mixtures transformations) mixed with 3 mL of molten (50°C) R-Top agar (0.125 g of yeast extract, 1.25 g of tryptone, 1 g of NaCl, 1 g of agar per 125 mL volume with 0.25 mL of 1 M

$CaCl_2$ and 0.42 mL of 30% glucose sterile solutions added after autoclaving) and poured onto ampicillin-containing LB plates.

2.4.10. DNA sequencing

Sequencing of DNA was performed according to the method of Sanger *et al.* (1977). Sequencing was carried out manually with double stranded DNA templates using the primers shown in Table 2.2. For preparation of double stranded DNA template, 5 μg plasmid DNA was resuspended and denatured in a 40 μL volume of freshly prepared 2 M NaOH. This mixture was incubated for 10 min at 37°C, reprecipated by addition of 10 μL of 3 M sodium acetate (pH 4.8) and 140 μL of ice-cold 95% ethanol. Following incubation at -20°C for 30 min, the DNA pellet was recovered by centrifugation, washed once with 1 mL of 95% ice-cold ethanol, and once with 200 μL of 70% ice-cold ethanol, and then evaporated to dryness under vacuum in a desiccator. Annealing and sequencing reactions were carried out using a 10 μCi [α-^{35}S] dATP (Amersham biosciences). Reaction mixtures were separated and resolved on 8% (w/v) polyacrylamide vertical slab gels containing 7 M urea, 0.13 M Tris, 0.13 M boric acid, and 10 mM EDTA. Electrophoresis was carried out using 18-24 mA constant current in TBE buffer (90mM Tris, 89 mM borate, 2.2 mM EDTA) for 1.5-4 h as required. Gels were mounted on 3 mm paper (Whatman), covered with clear plastic film, and dried at 80°C for about 1 hour on a slab gel drier vacuum (Savant). Dried gels were exposed to X-ray film (Kodak X-OMAT AR) in order to visualize and record the DNA bands.

2.5. Purification of catalase-peroxidases

For small scale crude extracts used to determine relative levels of protein expression and catalase activity, plasmid-containing cells were grown in either 5 mL of LB medium in test tubes, or in 30 mL of LB medium in shaking flasks at 28°C and 37°C for 16-20 h. The cells were pelleted and resuspended in 1-2 mL of 50 mM potassium phosphate buffer, pH 7.0 (buffer A), sonically disrupted, and centrifuged to remove unbroken cells and debris. This was followed by an assay for catalase activity and a protein expression profile by electrophoresis on sodium dodecyl sulfate polyacrylamide gels (SDS-PAGE). If only protein visualization was to be carried out (in the case of mutations that had low or no catalase activity), 10-15 μl aliquots of the cell suspensions were pelleted by centrifugation, directly resuspended in SDS protein sample buffer, and analyzed via SDS-PAGE.

For large scale preparations of KatG and their variant proteins, UM262 cells over expressing the desired protein from the appropriate plasmid borne genes were grown in 4-6 liters of LB media, in 2 L shake flasks (500 mL LB per flask) supplemented with 100 μg/mL of ampicillin and 40 μg/mL hemin (Sigma), for 16-20 h, at either 28°C or 37°C with good aeration. Isolation and purification of KatGs were done according to the procedure of Loewen and Switala (1986) with modifications. All isolation and purification steps were carried out at 4°C. Cells were harvested from the growth medium by centrifugation at 7000 rpm. The cell pellet (approximately 30 g wet weight from 6 l culture) was either stored at -60°C or resuspended in about 150-250 mL of buffer A containing 5 mM EDTA. The cells were disrupted by a single pass through a French pressure cell press at 20,000 psi. Unbroken cells and debris were removed by

centrifugation, yielding the crude extract, which was treated with streptomycin sulfate to a final concentration of 2.5% (w/v). In case of protein preparations from *A. fulgiduis* KatG and *B. stereothermopilus* KatG, the crude extract was heat treated at 80°C in a water bath for 45 min followed by centrifugation prior to streptomycin sulfate treatment. The resulting precipitants were removed by centrifugation and discarded. Solid $(NH_4)_2SO_4$ was added in appropriate amounts with gentle stirring, to precipitate the desired protein. Most of the KatG proteins were found to precipitate in $(NH_4)_2SO_4$ at 40-50% saturation. Pellets from the $(NH_4)_2SO_4$ precipitations were resuspended in 10-20 mL of buffer A. The presence of the desired protein in the pellets was confirmed by assays for catalytic activity and visualization on SDS gels. Resuspensions were centrifuged to remove any remaining precipitate, and dialyzed overnight against 2 liters of buffer A using a 12,000-14,000 molecular weight cutoff membrane,.

The dialyzed resuspensions were centrifuged and loaded onto a 2.5 cm x 23 cm column of DEAE-cellulose A-500 (Cellufine, Amicon) equilibrated with buffer A. The column was washed with buffer A until the A_{280} of the eluting solution was below 0.04. The protein was then eluted with a 0-0.4 M NaCl linear gradient in buffer A, usually to a volume of 1 L. Eighty drops (5 mL) fractions of the eluted proteins from the column were collected throughout. The purity of the recovered column fractions was determined using A_{280}, A_{407} and catalase activity and the fractions with higher A_{280}, A_{407} and higher catalase activity were selected. Selected fractions were pooled and concentrated under nitrogen in a stirred pressure cell (Model 8050, Amicon) using a YM-30 (Amicon) membrane, to volumes between 5-10 mL. The concentrated protein sample was dialyzed against approximately 1 L of buffer A. The concentrated, dialyzed proteins were checked

for purity using catalase activity, the Rz (Reinheitzahl) values as determined by $A_{407/280}$ ratios and visualization using SDS-PAGE. The protein was loaded on to a 2.5 x 15 cm hydroxyapatite column (Bio-Rad) equilibrated with potassium phosphate 5 mM (pH 7.0). The protein was eluted with potassium phosphate 5-200 mM, pH 7.0 usually in a final volume of 500 mL. Fifty drop fractions of the eluted proteins from the column were collected through out. Selected fractions were pooled and concentrated as previously. The purified samples were aliquoted into centrifuge tubes in 0.5 mL volumes and stored frozen at -60°C until use.

2.6. Polyacrylamide gel electrophoresis (PAGE) of proteins and staining

Denaturing SDS-PAGE was carried out according to Weber *et al* (1972). Discontinuous 4% stacking and 8% separating polyacrylamide gels were cast as vertical slabs of dimensions 10 x 10 cm and 0.5 mm thickness (mini gels). Samples loaded onto the mini gels usually contained about 10-20 μg protein for crude extracts or 2-5 μg protein for purified protein. Protein samples were mixed with equal volumes of reducing and denaturing sample buffer (3.4 mg/mL NaH_2PO4, 10.2 mg/mL Na_2HPO_4, 10 mg/mL SDS, 0.13 mM 2-mercaptoethanol, 0.36 g/mL urea and 0.15% bromophenol blue) and boiled for 3 min before loading on the gels. Samples were run with 150 V constant voltage in a vertical BIO-RAD Mini Protean II electrophoresis system, using a running buffer containing 14 g glycine, 3 g Tris base and 1 g SDS per L. Gels were stained in a solution containing 0.5 g/l Coomassie Brilliant Blue R-250, 30% ethanol and 10% acetic acid for one hour and destained with repeated changes of destaining solution containing 15% methanol and 7% acetic acid and 1% glycerol for 30 min. Gels were then mounted

on 3 mm (Whatman) paper, covered with a clear plastic film, and dried at 80°C for 1 hour on a slab gel drier under vacuum (Savant).

Non-denaturing PAGE was carried out according to Davis (1964). 8% acrylamide continuous gels were cast as vertical slabs as described for SDS-PAGE. When protein was to be visualized on the gels, sample amounts loaded were as described for SDS-PAGE. When enzymatic activity was to be visualized on the gels, samples were loaded in amounts corresponding to 1 unit of catalase activity, or 40 units of peroxidase activity. Samples were mixed with equal volumes of 2X sample buffer containing 0.125 M Tris, pH 6.8, 10% (w/v) glycerol, and 0.2% bromophenol blue (modified from Bio-Rad Mini-Protean II instruction manual). Electrophoresis was performed as described for SDS-PAGE, but using a running buffer containing 4.8 g Tris base, 20.8 g glycine per 4 L.

Gels were stained for peroxidase activity according to the method of Gregory and Fridovich (1974) using 3,3'-diaminobenzidine (DAB) as the electron donor species. Gels were soaked in a solution containing 20 mg DAB in 80 mL of 50 mM potassium phosphate buffer, pH 7.0 for 45 min, followed by a brief wash with water and then a second soak in the same buffer containing 20 mM H_2O_2. Peroxidase activity was visualized as brown band on the gels. Colour development was usually complete within 30 min.

Gels were stained for catalase activity according to the method of Clare *et al.* (1984) with minor modifications. Gels were soaked in a solution containing 50 μg/mL horseradish peroxidase (Sigma) in 50 mM potassium phosophate, pH 7.0 for 45 min, then briefly washed with water, incubated in 20 mM H_2O_2 for 10 min, and lastly, soaked in a solution of 50 mg/mL DAB in 80 mL water containing 1 mL glycerol. Catalase activity

was visualized as zones of clearing on brown background. Color development was usually complete within 30-60 min.

Staining for KatG-mediated oxidation of isoniazid (INH) was performed by soaking the gels in 200 mL Tris-HCl, pH 8.0 containing 10 mM INH (Sigma), and 0.2 mM Nitro Blue tetrazolium (NBT). INH oxidation was visualized as purple bands on the gels. Color development was usually complete between 30-60 min. When staining of gels was judged to be complete, they were rinsed with water, and soaked in 7% acetic acid, 1% glycerol for several h or overnight prior to mounting.

Staining for KatG mediated NADH oxidation was performed by soaking the gels in 200 mL 50 mM Tris-HCl, pH 8.75 containing 200 μM NADH and 0.2 mM NBT. NADH oxidation was visualized as purple bands on the gels. Color development was complete in 1-2 h. When staining of gels was judged to be complete, they were rinsed with water, and soaked in 7% acetic acid, 1% glycerol for several h or overnight prior to mounting.

2.7. Enzyme assay and protein quantitation

2.7.1. Catalase activity

Calalase activity was determined by the method of Rorth and Jensen (1967) in a Gilson oxygraph equipped with a Clark electrode. One unit of catalase is defined as the amount of enzyme that decomposes 1 μM H_2O_2 in 1 min in 60 mM H_2O_2 at 37°C, pH 7.0. Appropriately diluted samples of enzyme or cell cultures aliquots were incubated in 1.8 mL 50 mM phosphate buffer, pH 7.0 for 0.5-1.0 min at 37°C followed by the addition of H_2O_2 to a final concentration of 60 mM. Catalase activity as units/mL was determined

from the slope of the plot representing oxygen evolution. Specific catalase activity was expressed as units/mL per mg purified protein or units per mg dry cell weight. Specific activities were always determined as the average of a minimum of three or more individual determinations. The data was fitted to Michaelis-Menton equation using Sigma Plot to determine the V_{max} and K_m values.

2.7.2. Peroxidase activity

Peroxidase activity was determined spectrophotometrically by the *o*-dianisidine method described in the Worthington Enzyme Catalogue (Worthington Chemicals Co., 1969). Assays were carried out at room temperature in 1 mL final assay volumes containing 1 mM H_2O_2, 0.34 mM o-dianisidine in 50 mM sodium acetate buffer pH 4.5. Aliquots (1-5 µl) of the appropriately diluted enzymes were added to initiate the reaction. Peroxidase activity was determined by the ΔA_{560}/min over periods of 2 min and expressed as units•mg^{-1}•mL^{-1} purified protein calculated as: (ΔA460/min)/11.3 x mg enzyme/mL reaction mixture), using a molar extinction coefficient at A_{460} nm for *o*-dianisidine product of 11,300 $M^{-1}cm^{-1}$. Peroxidase activity was also determined spectrophotometrically by the 2,2'-*azinobis*{3-ethylbenzoathiazolinesulfonic acid} (ABTS) method (Smith *et al.*, 1990) with minor modifications. Assays were carried out at room temperature in 1 mL final assay volumes containing 2.5 mM H_2O_2, 0.4 mM ABTS in 50 mM sodium acetate buffer pH 4.5. Aliquots (1-5 µl) of the appropriately diluted enzymes were added to initiate reaction. Peroxidase activity was determined by the ΔA_{405}/min average over a period of 2 min and expressed as units•mg^{-1}•mL^{-1} purified protein calculated as: (ΔA_{405}/min)/36.8 x mg enzyme/mL reaction mixture), using a

molar extinction coefficient of ABTS product at A_{405} nm of 36,800 $M^{-1}cm^{-1}$. One unit of peroxidase activity is defined as the amount that decomposes 1 μmole of electron donor (ABTS or *o*-dianisidine) in 1 minute at pH 4.5 and room temperature.

2.7.3. INH hydrazine lyase activity

INH hydrazine lyase activity has been referred to the formation of radical species from a reaction mixture containing INH, KatG and NBT under the conditions described below. The reaction involves removal of the hydrazine moiety from INH (Figure 4.3) resulting in the formation of isonicotinoyl radical which could subsequently form amide, acid and aldehyde derivatives of INH (Nguyen *et al.*, 2001).

Isoniazid (INH) hydrazine lyase by KatG was determined spectrophotometrically at 560 nm by monitoring the reduction of NBT to a monoformazan dye (ε = 15,000 $M^{-1}cm^{-1}$) (Auclair and Voicin, 1985) through an enzymatically oxidized radical species of isoniazid. Assays were carried out in 1 mL final volumes containing 10 mM INH and 200 μM NBT in 50 mM Tris buffer, pH 8.0, at room temperature. Aliquots of 1.2 μM enzymes were added to initiate the reaction. Effect of manganese on INH hydrazine lyase activity was assayed both in the presence and absence of KatG by the addition of 2 μM $MnCl_2$ to the reaction mixture carrying 10 mM INH in 50 mM Tris pH 8.0. The synergistic effect of INH and NADH on NBT reduction was also followed by monoformazan formation (Auclair and Voicin, 1985) by oxidized radical species of INH and NADH. Assays were carried out in 1 mL final volumes containing 10 mM INH, 250 μg NADH and 200 μM NBT in 50 mM Tris buffer, pH 8.0 at room temperature. Aliquots of 1.2 μM enzymes were added to initiate the reaction.

2.7.4. NADH oxidation

NADH oxidase activity was determined spectrophotometrically at 560 nm by monitoring the reduction of NBT to a monoformazan dye by enzymatically oxidized radical species of NADH. Assays were carried out in 1 mL final volumes containing 250 μg NADH and 200 μM NBT in 50 mM Tris buffer, pH 8.75 at room temperature. Aliquots of 1.2 μM enzymes were added to initiate the reaction.

NADH oxidation was directly observed spectrophotometrically at 340 nm to monitor the rate of NADH disappearance. Assays were carried out in 1 mL final volumes containing 100 μM NADH in 50 mM Tris buffer, pH 8.75 at room temperature. Aliquots of 1.2 μM enzymes were added to initiate the reaction. NADH oxidase activity was determined by the Δ_{340}/min average over periods of 15 min. NADH oxidase activities were expressed as units.mL^{-1}.mg^{-1} purified protein, using a molar extinction coefficient of 6,300 M^{-1}.cm^{-1} for NADH (DeChatelet *et al.*, 1975). One unit of NADH activity is defined as the amount that decomposes 1 nmol of NADH in 1 minute in a solution of 100 μM NADH at pH 8.75 and room temperature. NADH oxidation was also assayed under anaerobic conditions by flushing the reaction mixture, sealed in a glass tube with rubber cork, with nitrogen before initiating the reaction by the addition of the enzyme.

2.7.5. Isonicotinoyl NAD synthase activity

Isonicotinoyl NAD synthase activity was measured from a reaction mixture carrying 200 μM INH, 100 μM NAD^+, 2 μM $MnCl_2$ and 1.2 μM KatG in 50 mM Tris pH 8.0. The adduct formation was monitored at 326 nm for a period of 30 min and rates were calculated using the extinction coefficient ε = 6.9 $mM^{-1}cm^{-1}$(Rawat *et al.*, 2004).

2.7.6. Protein Concentration

Protein concentration (mg/mL) was estimated spectrophotometrically based on A_{280} calculated as (A_{280} x MW/ε) where MW is the molecular weight of KatG and ε is the molar extinction coefficient (Lyane, 1957).

2.8. Absorption spectrophotometry pf KatGs

Absorption spectra, time courses, and enzyme assays were performed using a Pharmacia Ultrospec 4000 Spectrophotometer, a Milton Roy MR300 Spectrophotometer, Ultrospec 3100 pro or Biochrom Novaspec II visible spectrophotometer (for assaying samples under anaerobic conditions). All experiments were performed at ambient temperature in 1 mL quartz, semi micro cuvettes. Proteins were diluted in 50 mM potassium phosphate buffer, pH 7.0, unless otherwise stated, and the same buffer was used as reference. For the peroxidase assays using ABTS and *o*-dianisidine, proteins were diluted in 50 mM sodium acetate buffer, pH 4.5 and the same buffer was used as reference. For NADH oxidation and INH hydrazine lyase activity assays, 50 mM Tris buffer, pH 8.75 and 8.0 respectively were used and the same buffers were used as reference. For preparation of spectral and time course plots, data collected were transferred to Sigma Plot software.

2.9. Effects of inhibitors

The effects of classical heme inhibitors, KCN and NaN_3 on catalase, peroxidase and oxidase activities of KatG and variants were studied. The enzyme was incubated with

different concentrations of KCN and NaN_3 for 1 min in the reaction mixture prior to initiation of the reaction by addition of the substrate.

The effect of superoxide dismutase (SOD) on NADH oxidase activity was assayed by adding 200 μg of SOD in the 1 mL reaction mixture carrying 250 μM NADH, 200 μM NBT and appropriately diluted enzyme. The assay was performed as described for NADH oxidation.

The effect of pyridoxine and pyridoxal-5-phosphate on NADH oxidase activity was determined by incubating the appropriately diluted enzyme with different concentrations of pyridoxine and pyridoxal-5-phosphate and initiating the reaction by addition of the substrate.

2.10. High Performance Liquid Chromatography (HPLC) characterization of reaction products.

Reaction products of INH hydrazine lyase activity and isonicotinoyl-NAD adduct formation were characterization using HPLC. For INH hydrazine lyase activity, reaction mixtures carrying 1 mM INH and 1.2 μM KatG in 50 mM Tris pH 8 were incubated for 3-4 h. Aliquots were kept frozen after the incubation until ready to use.

For NADH oxidation, reaction mixture containing 200 μM NADH and 1.2 μM KatG in 50 mM Tris pH 8.75 were incubated for 3-4 h and aliquots were kept frozen at -20°C until ready to use.

Isonicotinoyl-NAD synthase activity was characterized using different permutations and combinations of reactants. Adduct formation was analyzed in the presence and absence of KatG and in the presence and absence of $MnCl_2$ using INH and

$NADH/NAD^+$ as substrates. In all the reactions, 100 μM $NADH/NAD^+$, 200 μM INH, 1.2 μM KatG and 2 μM $MnCl_2$ were used in 50 mM Tris pH 8.0. Samples were incubated for 3-4 h and aliquots were kept frozen at -20°C until ready to use.

For HPLC analysis samples were centrifuged and transferred into the tubes made for automated sample injection (Waters Corporation, MA, USA). Samples were loaded on a 4.6 x 250 mm column equilibrated with buffer A (11.7 g KH_2PO_4, 2.4 g K_2HPO_4 and 2.72 g tert-butyl ammonium hydrogen sulfate in 1 L HPLC grade water) packed with Whatman 5 μM ODS-3 (C18 coated, Altech HPLC column) and eluted with a gradient of 0-100% buffer B (buffer A + Methanol to a final concentration of 30%) over a period of 52 min and the 100-0% buffer B from 53-78 min in a Waters HPLC system with detection at 260 nm. Fractions showing peaks were collected to determine the mass of the reaction products. For preparation of elution profiles, data collected were transferred to Sigma Plot computer software.

2.11. Mass Spectrometry

Mass spectrometric analysis was kindly carried out by Dr. LG Donald. KatG was dialyzed into 5 mM ammonium acetate, and NADH was dialyzed against three changes of 1 L 0.1 M ammonium bicarbonate, after which the concentration was determined by A_{340}. The matrix solution was freshly prepared each day at 160 mg/mL 2,5-dihydroxybenzoic acid in a 3:1 water:acetonitrile, 2% formic acid solution. A 20-μl reaction mixture contained 200 μg KatG, 128 μM NADH, and 10 mM INH in 0.1 M NH_4HCO_3 at room temperature. 0.5 μl aliquots were removed at 1 min, 2 h, 4 h, and 18 h and immediately mixed with 0.5 μl of matrix solution on a metal target. Different

fractions collected from HPLC column were also analyzed in a similar fashion to characterize the reaction products. All samples were analyzed on a quadrupole time of flight (QqTOF) mass spectrometer (Clare *et al.*, 1984).

3. RESULTS

3.1. Introduction

The appearance of three crystal structure reports of catalase-peroxidases (KatGs) from *Haloarcula marismortui*, *Burkholderia pseudomallei* and *Synechococcus* PCC 7942 just prior to the beginning of this study, revived interest in these bi-functional heme proteins. The objective of this study was to gain a better understanding of how catalase and peroxidase activities are modulated by the same enzyme, and more importantly their role in the activation of isoniazid (INH). KatGs from seven different organisms including *B. pseudomallei* (BpKatG), *M. tuberculosis* (MtKatG), *E. coli* (EcKatG), *Synechocystis* PCC6803 (SyKatG), *A. fulgidus* (AfKatG), *B. stereothermophilus* (BsKatG), and *R. capsulatus* (RcKatG), each belonging to a different environmental niche, were selected. Plasmid borne *katG* gene from each organism was over expressed in *E. coli* host cells and purified enzyme was compared for various biochemical and biophysical properties such as pH optimum and enzyme kinetics for catalase and peroxidase activities. Spectral properties and sensitivity to various heme inhibitors, such as cyanide and azide, were also compared for seven KatGs.

Another focus of this study was the role of KatGs in the activation of isoniazid and subsequent formation of isonicotinoyl-NAD adduct. Much of the literature related to the activation of INH by KatG has focused on the fate of INH and possible intermediates involved in the process (Johnsson and Schultz, 1994; Wilming and Johnsson, 1999; Magliozzo and Marcinkeviciene, 1996; Lei *et al.*, 2000). With NAD^+ included in the mix, the generation of the isonicotinoyl-NAD adduct was observed both with and without KatG present (Wilming and Johnsson, 1999; Magliozzo and Marcinkeviciene, 1996; Lei

et al., 2000), leading to the suggestions that the role of KatG is limited to the hydrazinolysis of INH and that the subsequent reaction of the isonicotinoyl radical with NAD^+ is a nonenzymatic event and subsequent formation of isonicotinoyl-NAD adduct is considered as a non-enzymatic event. During this study, pyridine derivatives such as INH, NADH, NADPH, pyridoxine etc were used to analyze their interaction with KatGs and their possible involvement in the formation of isonicotinoyl-NAD.

3.2. Purification and characterization of BpKatG, MtKatG, EcKatG, SyKatG, BsKatG, AfKatG and RcKatG.

3.2.1. Purification of KatGs

For the over expression of catalase-peroxidase, the *katG* genes from the seven organisms used in this study were first cloned into high expression plasmid vectors and subsequently over-expressed in *E.coli* host cells (UM262 or BL21). The plasmids used are listed in the Table 2.1. Heme incorporation in the apoprotein has always been a cause of concern in the over expressed KatG as heme production by the cellular machinery appears insufficient. Over expressed protein often results in lower heme-to-protein ratios, which is also called "reinheitzahl" (Rz) (Dunnford, 1999). To solve this problem, exogenous heme was added to the growth medium to support heme formation and hence incorporation. Table 3.2.1 describes the effect of δ-aminolevulinic acid (ALA), $FeCl_3$ and hemin chloride and temperature on the catalase specific activity of MtKatG. Iron and ALA are precursors in the biosynthesis of heme whereas hemin is a direct source of ferric heme for the apoprotein. Addition of both ALA and $FeCl_3$ to the growth medium or the

Table 3.2.1. Effect of $FeCl_3$, δ-aminolevulinic acid (ALA) and hemin chloride on the catalase activity of MtKatG. *E.coli* strain UM262 containing plasmids pAH1 (MtKatG) were grown for 16-18 h at 37° or 28° C in 30 mL LB medium supplemented with ampicillin. Activity assays were performed on whole cells and the activity at 37°C was considered 100%.

Growth temperature (°C)	Supplement added			% Catalase activity (units/mg)
	ALA (mM)	$FeCl_3$ (μM)	Hemen (μM)	
28	—	—	—	40
37	—	—	—	100
28	1	50	—	50
37	1	50	—	130
28	—	—	60	40
37	—	—	60	130

Table 3.2.2.a Purification of wild type BpKatG and MtKatG from *E. coli* strain UM262 harboring plasmid encoded *katG* of *B. pseudomallei* and *M. tuberculosis*.

Purification Step	Total protein (mg)	Total catalase activity (units x 10^3)	Specific catalase activity (units/mg)	Recovery (%)	Purification (fold)
BpKatG					
Crude extract	5380	2200	290	100	1
$(NH_4)_2SO_4$ Precipitation	600	700	980	32	3
Anion exchange (DEAE-A-500)	95	360	3000	16	10
Hydroxyapatite column	60	200	3800	9	13
MtKatG					
Crude extract	12300	3050	250	100	1
$(NH_4)_2SO_4$ Precipitation	600	830	1360	27	5
Anion exchange (DEAE-A-500)	200	630	3240	21	13
Hydroxyapatite column	130	460	4450	15	18

Table 3.2.2b Purification of wild type EcKatG and AfKatG from *E. coli* strain UM262 harboring plasmid encoded *katG* of *E. coli* and *A. fulgidus*.

Purification Step	Total protein (mg)	Total catalase activity (units x 10^3)	Specific catalase activity (units/mg)	Recovery (%)	Purification (fold)
EcKatG					
Crude extract	4265	6410	1500	100	1
$(NH_4)_2SO_4$ Precipitation	196	420	2140	7	1.4
Anion exchange (DEAE-A-500)	73	200	5050	3	3.4
Hydroxyapatite column	27	170	6150	3	4.1
AfKatG					
Crude extract [a]	3100	2850	260	100	1
$(NH_4)_2SO_4$ Precipitation	220	460	2100	16	8
Anion exchange (DEAE-A-500)	70	400	3500	16	13
Hydroxyapatite column	30	380	5300	13	20

[a] crude extract was heated at 55°C for 30 min after determining catalsae activity

addition of hemin alone increased the catalase specific activity in the whole cells by ~30%. Following these results, hemin chloride was added regularly to the growth medium assuming that its addition allows more efficient incorporation of heme into the overexpressed KatGs. Table 3.2.2a & b describe the typical purification procedure of BpKatG, MtKatG, EcKatG and AfKatG. The purification procedure is essentially the same for all the KatGs with the exception of the KatG from the thermophile *A. fulgidus*. In this case the crude extract was heated at 55°C for 30 min in order to precipitate contaminating protein without loss of catalase activity. The difference in the total protein obtained from each enzyme is proportional to the volume of medium used to grow the cells, for example total protein in the crude extract of MtkatG, which was obtained from cells grown in 6 L of LB was almost four times higher than the total protein in the crude extract of AfkatG which was obtained from cells grown in 2 L of LB. Passing the protein through hydroxyapatite column also helped in achieving the higher Rz ratio and yield. SyKatG and BsKatG were purified by Mr. Jack Switala, while purified RcKatG was a gift from Dr. Anabella Ivancich from CEA, Saclay, France.

3.2.2. Polyacrylamide gel electrophoresis (PAGE) of the catalase-peroxidases

PAGE of purified KatGs under denaturing conditions is shown in Figure 3.1. All the KatGs migrate as a predominantly single bands with an apparent molecular mass ~78 kDa. A band at approximately 160 kDa appeared in all the lanes and could be attributed to a small amount of slower migrating crosslink dimer which is not reduced by either β-mercaptoethanol or dithiothreitol added to the sample buffer. In case of EckatG this 160 kDa band is more prominent presumably because homotetrameric EcKatG resulted in

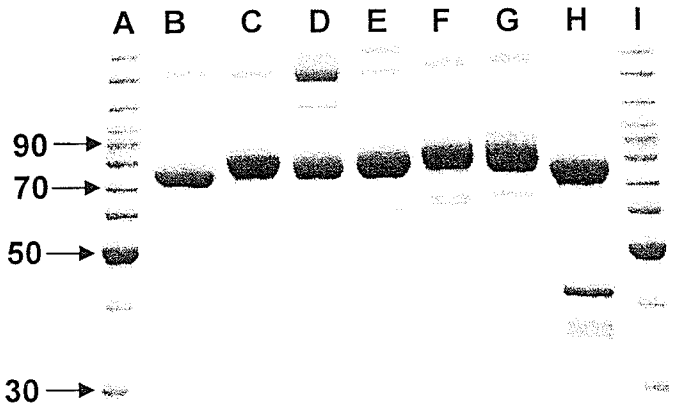

Figure 3.2.1. SDS-polyacrylamide analysis of purified KatGs. Approximately 5 μg of sample were run on an 8% polyacrylamide gel and stained with Coomassie blue. Lanes A-I contains protein MW ladder, BpKatG, MtKatG, EcKatG, SyKatG, BsKatG, AfKatG, RcKatG and protein MW ladder, respectively.

Table 3.2.3. Comparison of observed optical absorbance maxima, $A_{407/280}$ ratio and heme/subunit ratio for purified KatGs.

KatG	Sorêt maximum (nm)	$A_{407/280}$ ratio	Theoritical $A_{407/280}$ ratios[a]	Heme/subunit ratio
BpKatG	408	0.58	0.72	0.81
MtKatG	408	0.60	0.61	0.98
EcKatG	407	0.60	0.68	0.88
SyKatG	407	0.47	0.56	0.84
BsKatG	406	0.47	0.58	0.81
AfkatG	404	0.54	0.60	0.90
RcKatG	406	0.52	0.66	0.79

[a] ε at 280 nm calculated based on ε_{TRP} = 5500 and ε_{TYR} = 1490, ε at 407 nm for heme estimated to be 100.000 M^{-1} cm^{-1}

Figure 3.2.2. Absorption spectra of KatGs. The left axis is for the range from 350 to 500 nm while the right axis is for the range from 500 to 700 nm.

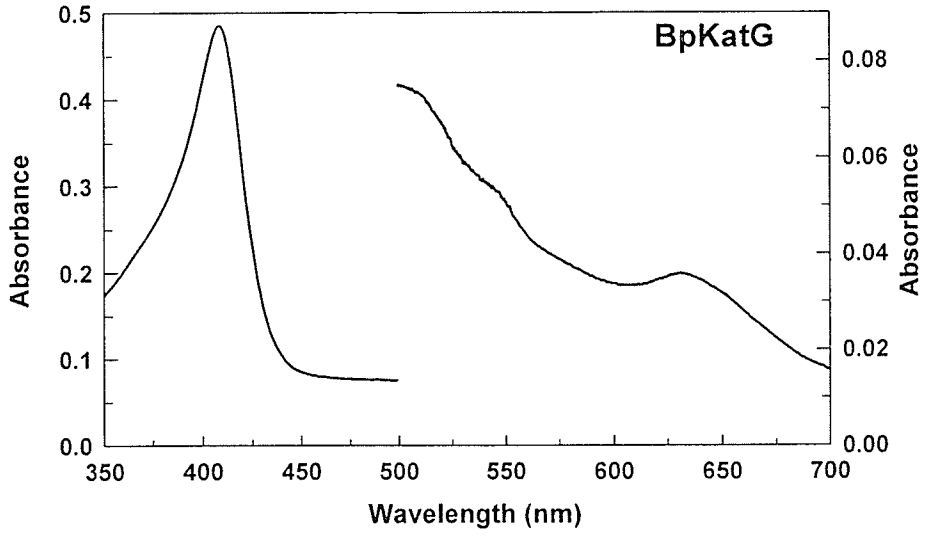
BpKatG
Absorbance
Absorbance
Wavelength (nm)
0.0
0.1
0.2
0.3
0.4
0.5
0.00
0.02
0.04
0.06
0.08
350
400
450
500
550
600
650
700

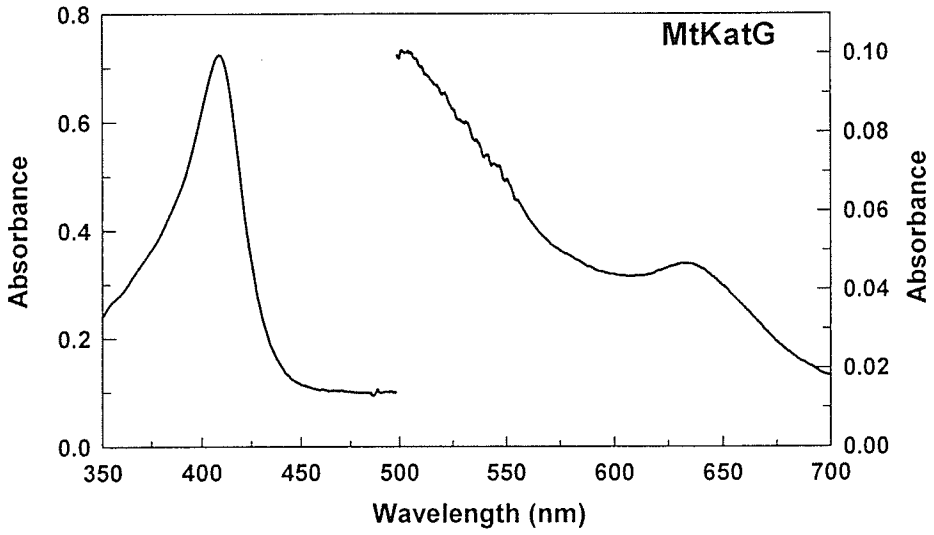
MtKatG
Absorbance
Absorbance
Wavelength (nm)
0.0
0.2
0.4
0.6
0.8
0.00
0.02
0.04
0.06
0.08
0.10
350
400
450
500
550
600
650
700

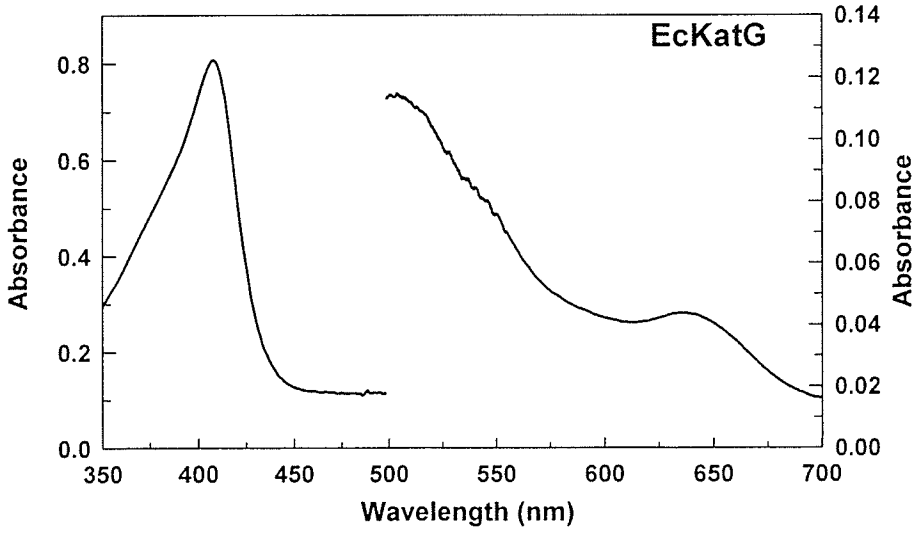
EcKatG
Absorbance
Absorbance
Wavelength (nm)
0.0
0.2
0.4
0.6
0.8
0.00
0.02
0.04
0.06
0.08
0.10
0.12
0.14
350
400
450
500
550
600
650
700

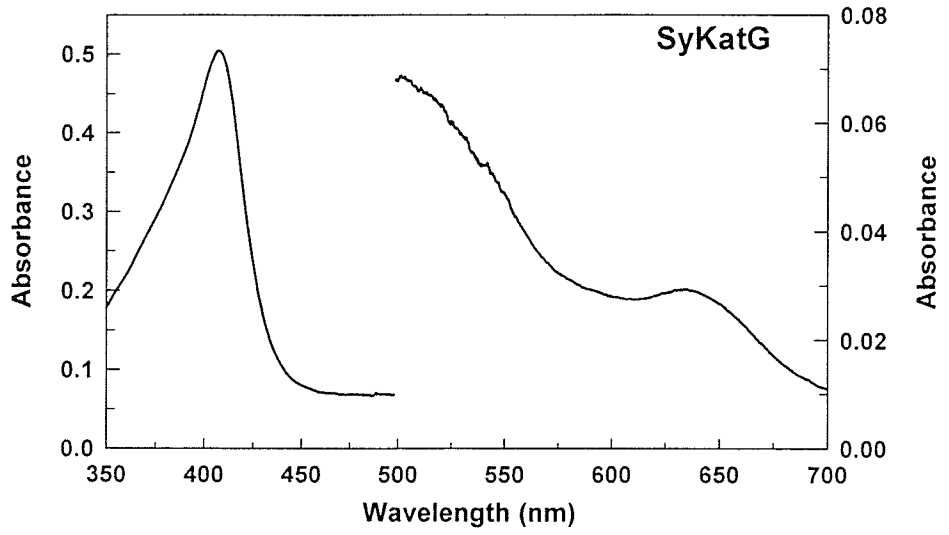
SyKatG
Absorbance
Absorbance
Wavelength (nm)
0.0
0.1
0.2
0.3
0.4
0.5
0.00
0.02
0.04
0.06
0.08
350
400
450
500
550
600
650
700

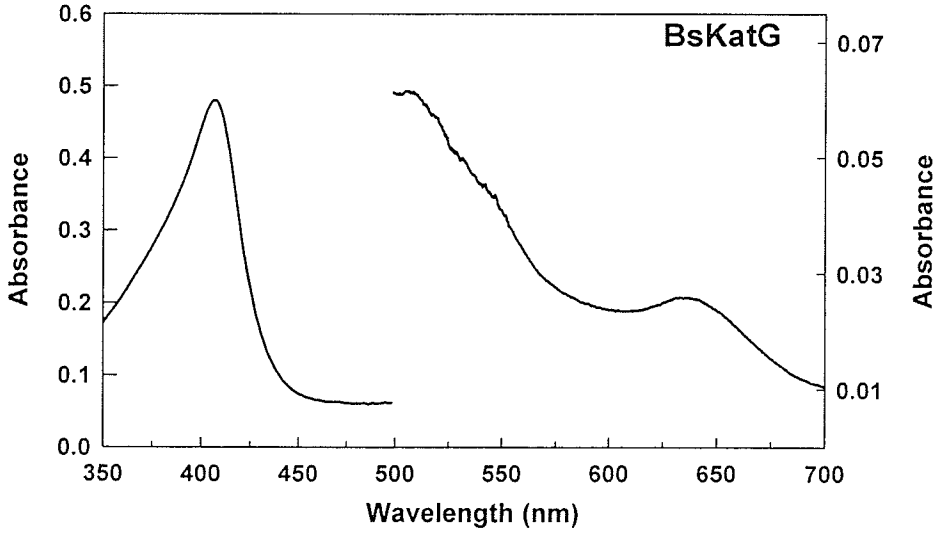
BsKatG
Absorbance
Absorbance
Wavelength (nm)
0.0
0.1
0.2
0.3
0.4
0.5
0.6
0.01
0.03
0.05
0.07
350
400
450
500
550
600
650
700

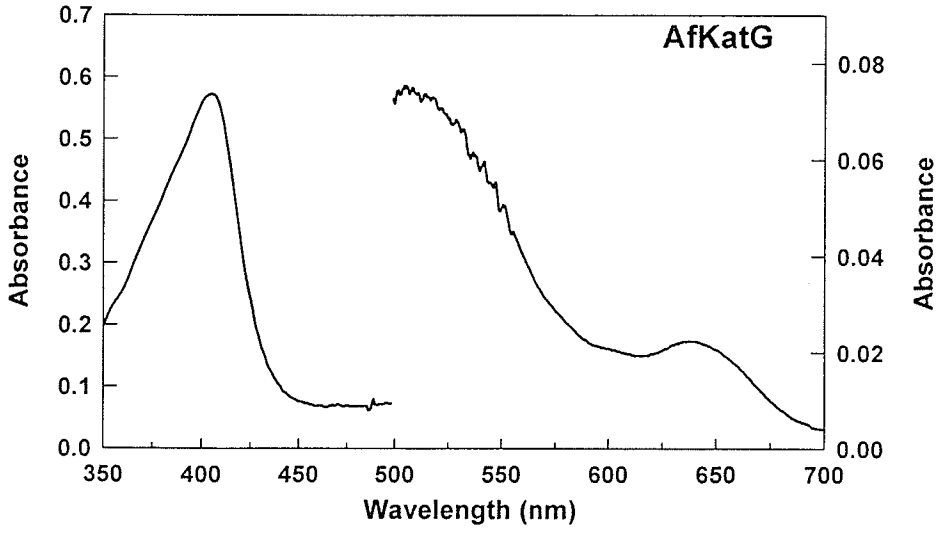
AfKatG
Absorbance
Absorbance
Wavelength (nm)
0.0
0.1
0.2
0.3
0.4
0.5
0.6
0.7
0.00
0.02
0.04
0.06
0.08
350
400
450
500
550
600
650
700

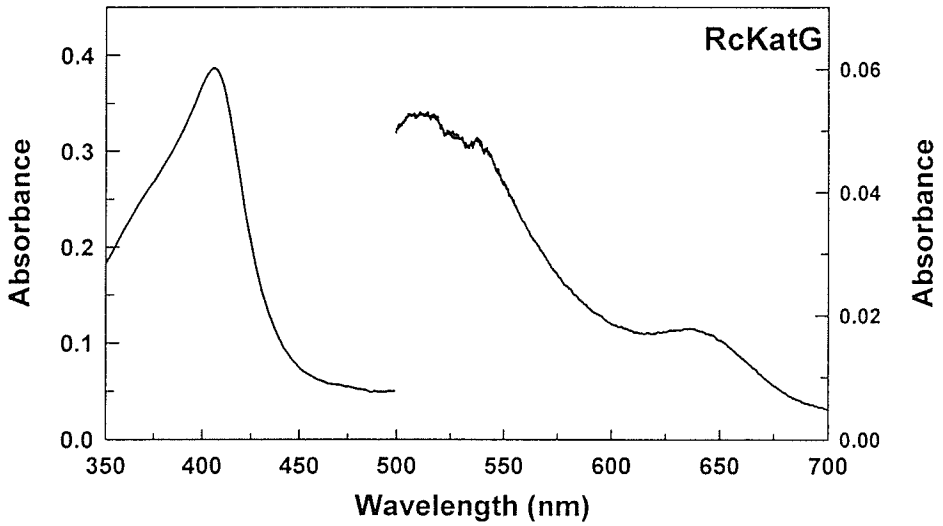
RcKatG
Absorbance
0.0
0.1
0.2
0.3
0.4
0.00
0.02
0.04
0.06
Absorbance
350
400
450
500
550
600
650
700
Wavelength (nm)

higher dimer formation as compared to the rest of the homodimeric KatGs. In case of RcKatG, a single band at ~ 46 kDa is also visible without any explanation.

3.2.3. UV-visible absorption spectroscopy of catalase-peroxidases

Absorbance spectra of the purified KatGs in the Sorêt and visible regions of the spectrum are shown in Figure 3.2.2 while the positions of absorption maxima, heme/protein ratio ($A_{Sorêt/280}$) and heme/subunit ratio has been summarized in Table 3.2.3. There is a variation of 4 nm between the seven KatGs in the Sorêt band with BpKatG and MtKatG showing Sorêt band at 408 nm whearas AfKatG having the same at 404 nm. EckatG and SyKatG have a Sorêt band at 407 nm and RckatG and BsKatG show Sorêt band at 406 nm. The spectra in 500-700 nm region show the charge transfer (CT) bands at ~500 (CT 1) and ~630 nm (CT 2). These charge transfer bands generally indicate the changes in the hydrogen bonding network in the vicinity of the heme. Purified KatGs showed a heme/protein ($A_{407/280}$) ratio or the Rz value of 0.5 or higher with heme/subunit occupancy > 0.8, maximum being 1.0 for MtKatG, suggesting better heme incorporation.

3.2.4. pH profile for the catalase and peroxidase activities

The pH profiles for the catalase and peroxidase activities of the KatGs are shown in Figure 3.3. All KatGs show different pH optimum for catalase and peroxidase activities. The pH optima for peroxidase activity are between pH 4 and 5 for all seven KatGs using ABTS as peroxidatic substrate whereas catalatic pH optimum is between 6.25 and 6.5 as shown in Table 3.2.4.

Table 3.2.4. pH optima for catalatic and peroxidatic activities of KatGs

KatG	pH Optimum	
	Peroxidase activity (ABTS)	**Catalase activity**
BpKatG	4.5	6.5
MtKatG	4.75	6.5
EcKatG	4.25	6.25
SyKatG	4.25	6.5
BsKatG	4	6.5
AfkatG	4.5	6.25
RcKatG	5	6.5

Figure 3.2.3. pH profile for catalase and peroxidase activities of KatGs

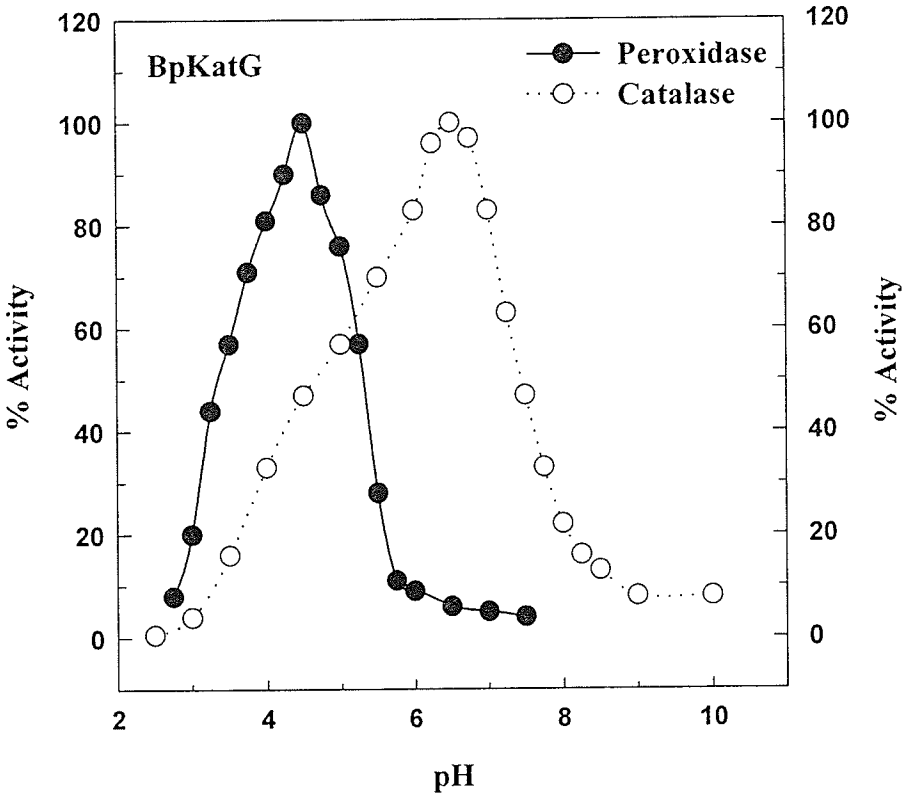
BpKatG
Peroxidase
Catalase
% Activity
% Activity
pH
0
20
40
60
80
100
120
2
4
6
8
10

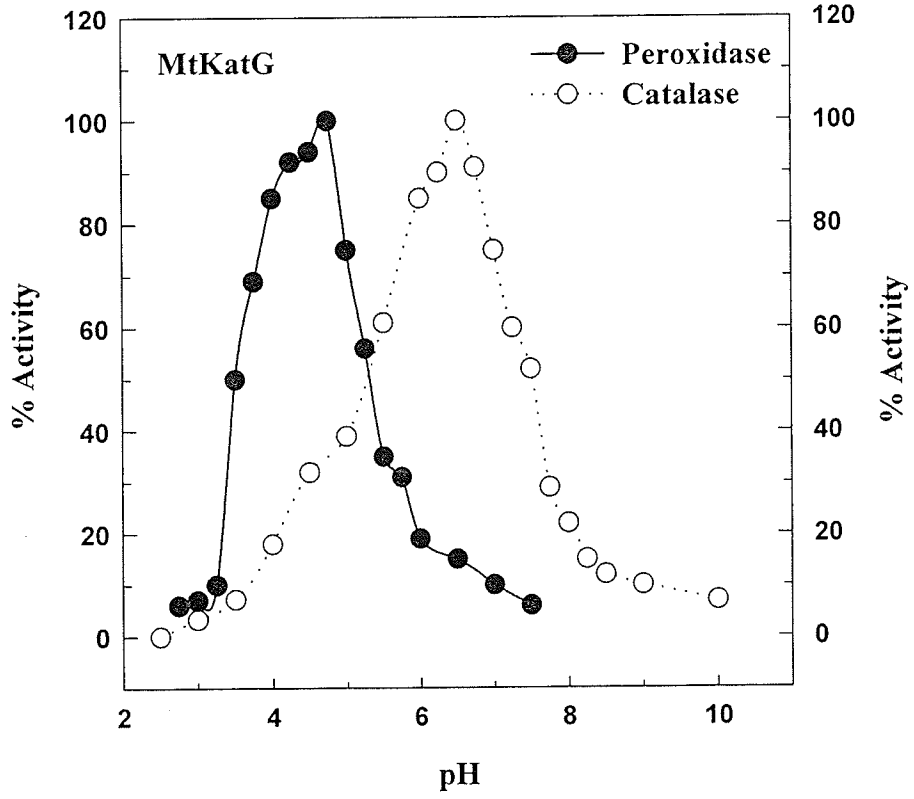
MtKatG
Peroxidase
Catalase
% Activity
% Activity
pH
0
20
40
60
80
100
120
2
4
6
8
10

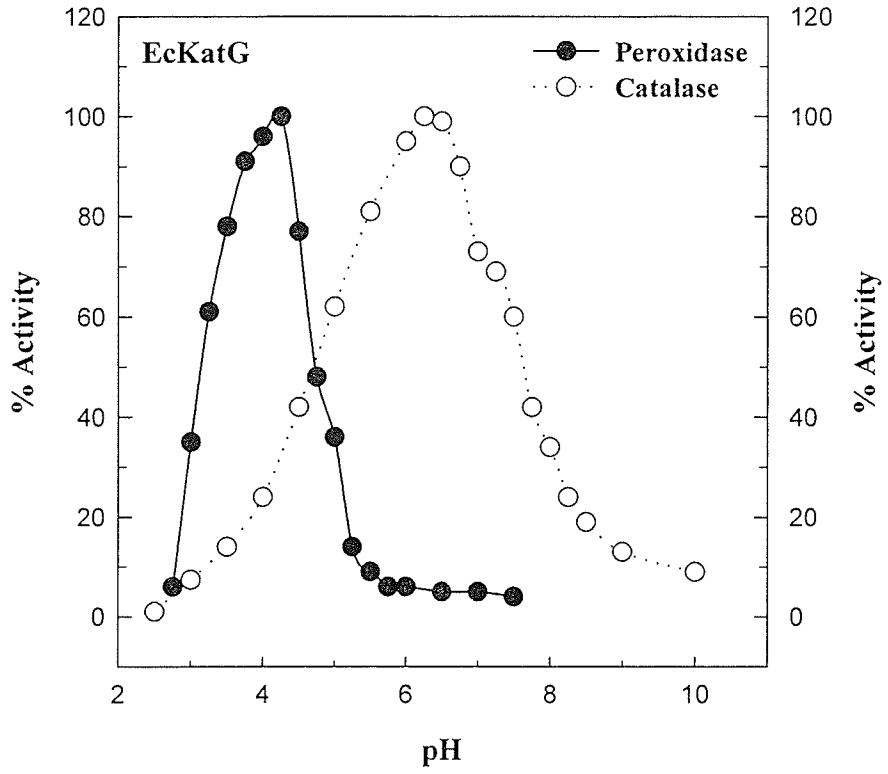
EcKatG
Peroxidase
Catalase
% Activity
% Activity
pH
120
100
80
60
40
20
0
2
4
6
8
10

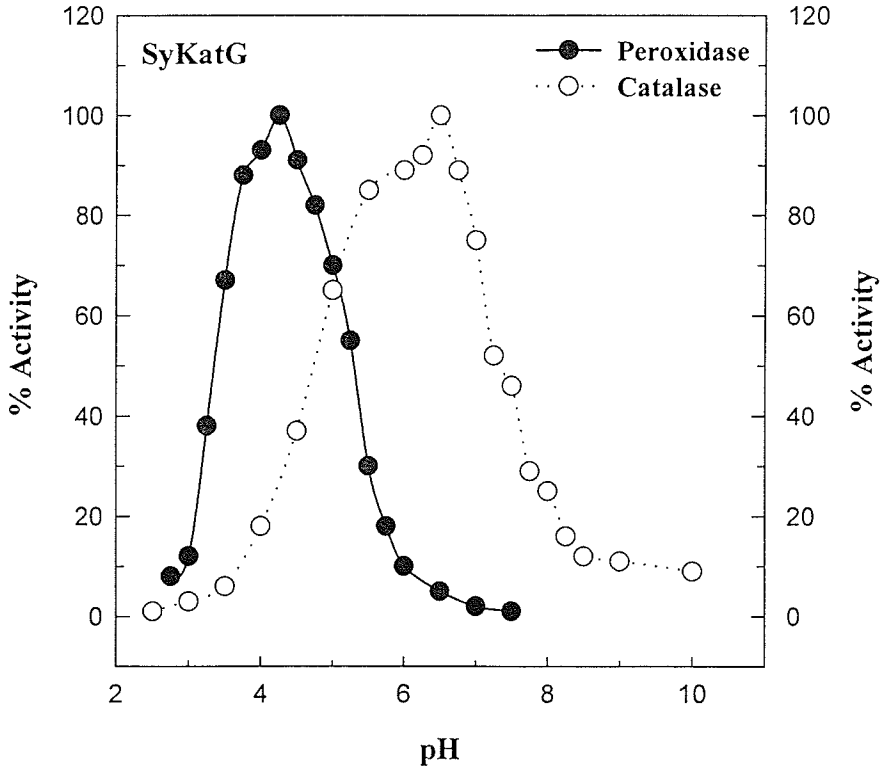
SyKatG
Peroxidase
Catalase
% Activity
% Activity
pH
120
100
80
60
40
20
0
2
4
6
8
10

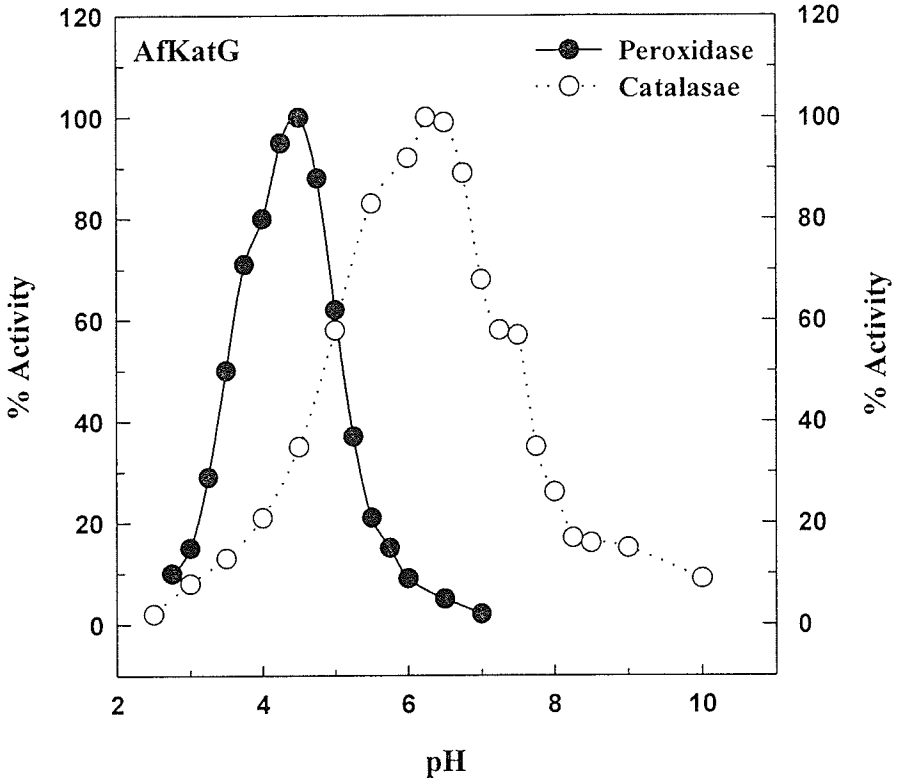
AfKatG
Peroxidase
Catalasae
% Activity
% Activity
pH
0
20
40
60
80
100
120
2
4
6
8
10

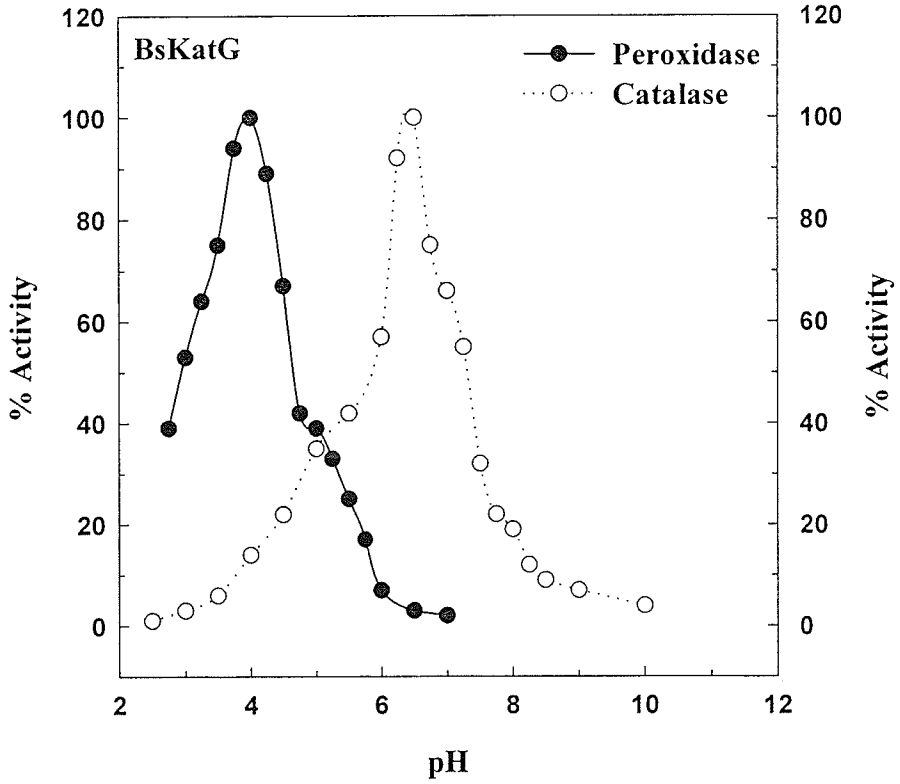
BsKatG
Peroxidase
Catalase
% Activity
% Activity
pH
0
20
40
60
80
100
120
2
4
6
8
10
12

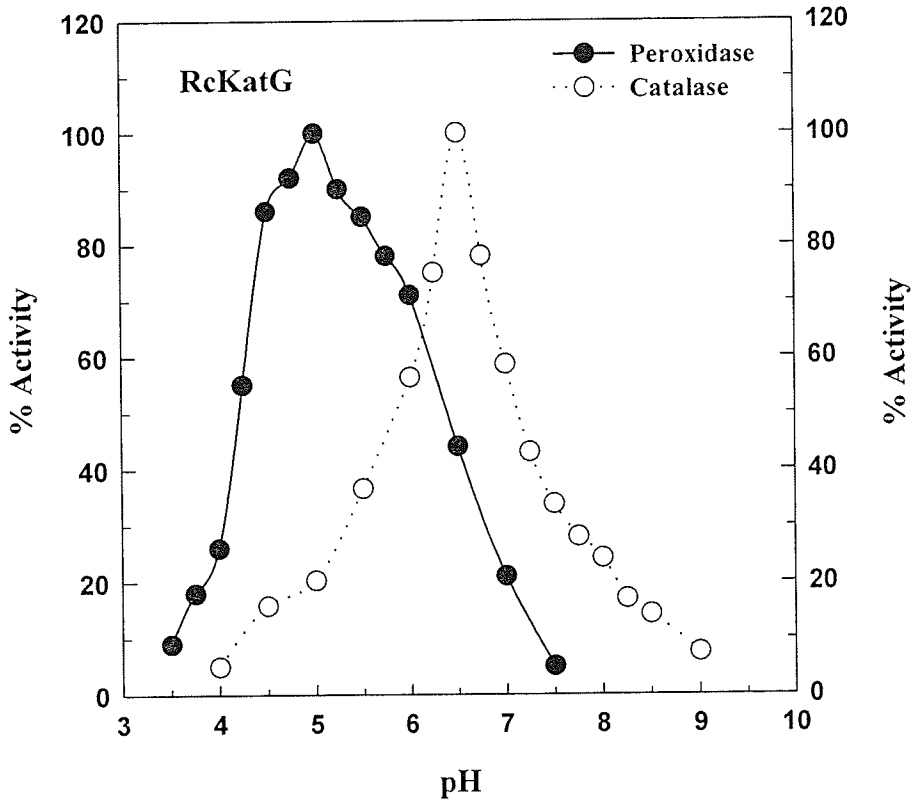
RcKatG
Peroxidase
Catalase
% Activity
% Activity
pH
0
20
40
60
80
100
120
3
4
5
6
7
8
9
10

3.2.5. Specific catalase and peroxidase activities of KatGs

Table 3.2.5 summarizes the specific enzymatic activities of KatGs. All the KatGs show substantial catalase activity ranging from 3634 U/mg by BpKatG to 5985 U/mg by EcKatG. The latter shows significantly higher activity from the previous reports where the activity was reported from EcKatG produced without exogenous addition of hemin in the growth medium. Peroxidase activity was determined using two different organic electron donors (ABTS and *o*-dianisidine) as peroxidatic substrate. All the KatGs show a broad specificity in peroxidase activity ranging from 2 U/mg for RcKatG to 11.7 U/mg for AfkatG using ABTS as substrate and for o-dianisidine ranging from 1 U/mg for RckatG to 8.8 U/mg for MtKatG.

3.2.6. Kinetic Characterization of KatGs

Kinetic constants for the catalase and peroxidase reactions of seven KatGs were determined by titrating enzyme with different concentrations of substrate. Figure 3.4 shows the effect of various concentrations of H_2O_2 on the rate of catalase reaction of KatGs. The initial velocities shown are expressed as μmoles of H_2O_2 decomposed per min per μmole of heme. The kinetic constants for catalase activity are shown in Table 3.2.6. Kinetic constants for peroxidase activity, using ABTS as an electron donor, were determined by titrating KatGs against concentrations of ABTS and results are expressed as μmole of ABTS oxidized per min per μmole of heme as shown in Figure 3.5 and the kinetic constants are shown in Table 3.2.7.

Both catalase and peroxidase reactions require H_2O_2 for compound I formation. In order to determine the kinetic constants for compound I formation during peroxidase

Table 3.2.5. Comparison of catalase and peroxidase activities of KatGs

KatG	Catalase (units/mg)[a]	Peroxidase	
		ABTS (units/mg)[a]	***o*-dianisidine (units/mg)[a]**
BpKatG	3630 ± 150	4.8 ± 0.9	5.3 ± 0.9
MtKatG	4450 ± 150	10 ± 2.5	8.8 ± 1.5
EcKatG	5990 ± 180	11 ± 1.3	8.3 ± 2.1
SyKatG	5150 ± 500	6.4 ± 2.1	5.5 ± 2.1
BsKatG	3690 ± 380	5.9 ± 1.6	5.3 ± 2.0
AfkatG	5280 ± 250	12 ± 3.3	3.2 ± 0.6
RcKatG	5520 ± 226	2.0 ± 0.3	1.0± 0.2

[a](1 unit = 1 μmol/min)

Figure 3.2.4. Effect of H_2O_2 concentration on the initial catalatic velocities of KatGs

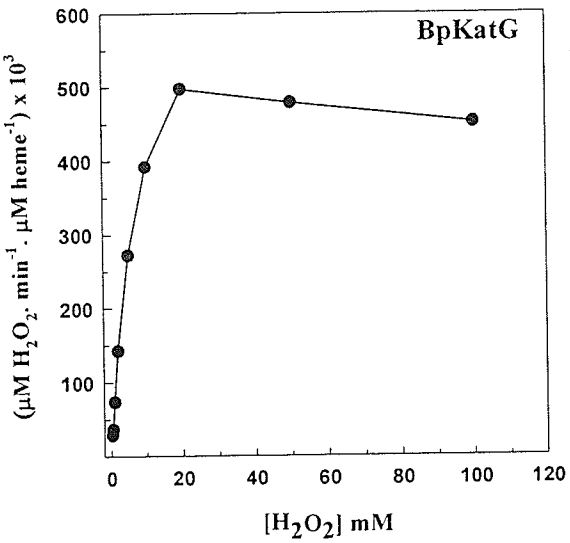
BpKatG
600
500
400
300
200
100
0
20
40
60
80
100
120
(μM H2O2. min-1. μM heme-1) x 10-3
[H2O2] mM

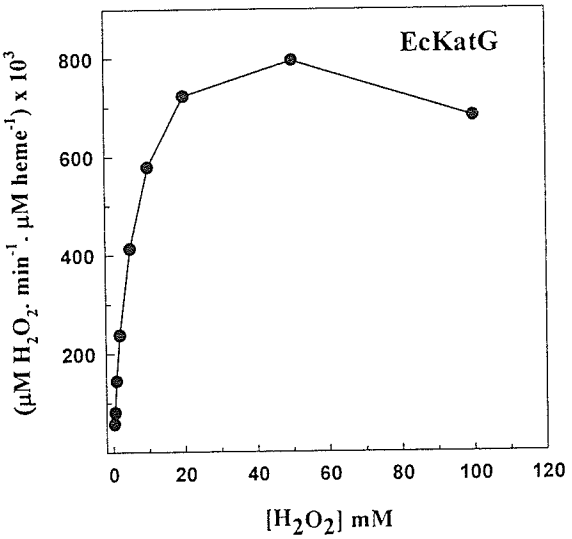
EcKatG
800
600
400
200
0
20
40
60
80
100
120
(μM H2O2. min-1. μM heme-1) x 10-3
[H2O2] mM

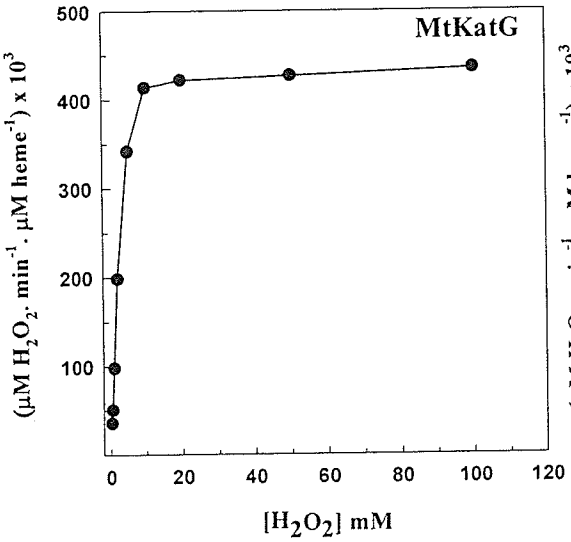
MtKatG
500
400
300
200
100
0
20
40
60
80
100
120
(μM H2O2. min-1. μM heme-1) x 10-3
[H2O2] mM

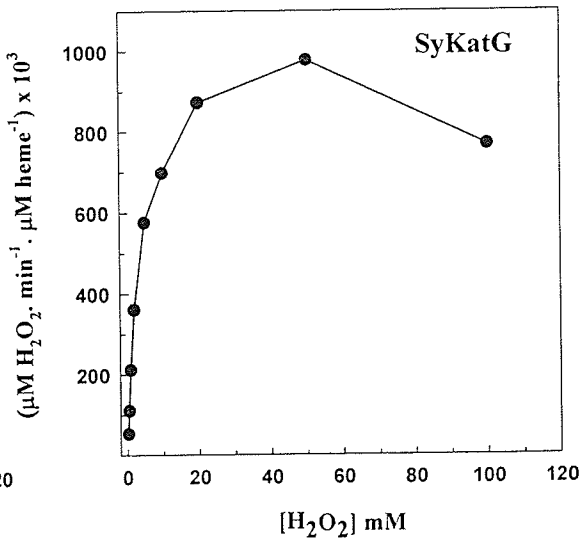
SyKatG
1000
800
600
400
200
0
20
40
60
80
100
120
(μM H2O2. min-1. μM heme-1) x 10-3
[H2O2] mM

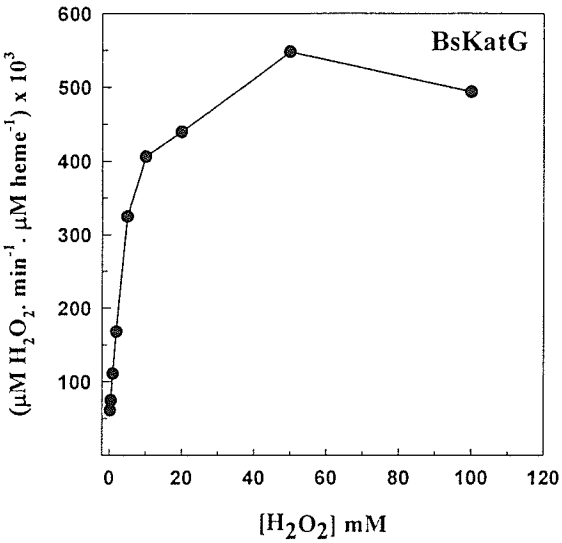
BsKatG
(μM H2O2. min-1 . μM heme-1) x 10^3
[H2O2] mM
600
500
400
300
200
100
0
20
40
60
80
100
120

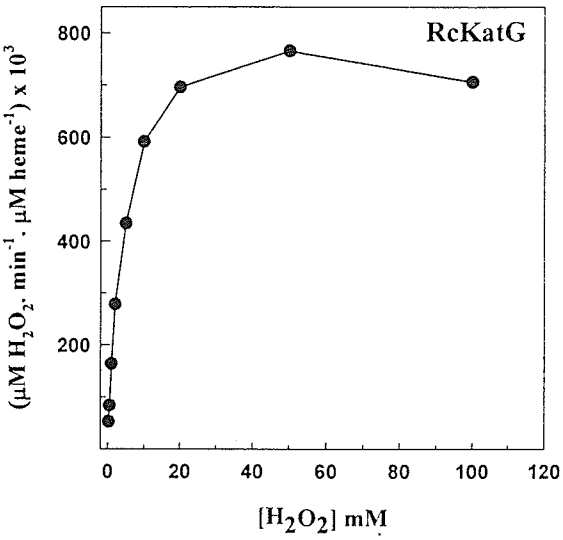
RcKatG
(μM H2O2. min-1 . μM heme-1) x 10^3
[H2O2] mM
800
600
400
200
0
20
40
60
80
100
120

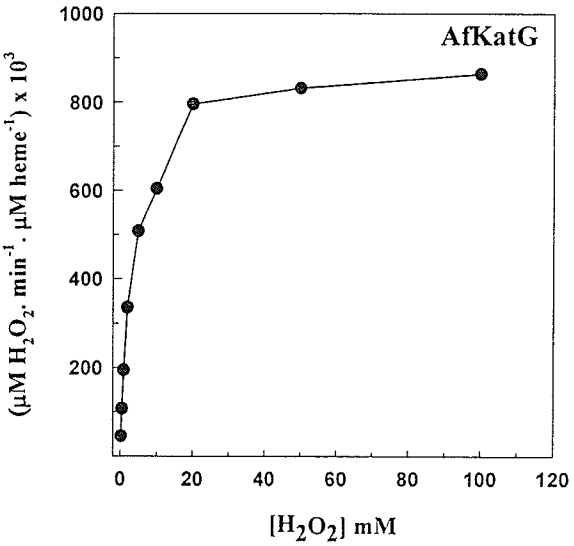
AfKatG
(μM H2O2. min-1 . μM heme-1) x 10^3
[H2O2] mM
1000
800
600
400
200
0
20
40
60
80
100
120

Table 3.2.6. Comparison of the observed catalatic kinetic parameters of purified KatGs, using H_2O_2 as substrate.

KatG	V_{max}[a] (x 10^3)	K_m (mM)	k_{cat} (s^{-1})	k_{cat}/K_m ($M^{-1}s^{-1}$)
BpKatG	525 ± 29	4.3 ± 0.9	8750 ± 483	2.0 x 10^6
MtKatG	455 ± 22	2.4 ± 0.5	7600 ± 367	3.2 x 10^6
EcKatG	800 ± 32	4.2 ± 0.8	13400 ± 543	3.2 x 10^6
SyKatG	1010 ± 50	3.1 ± 0.7	17300 ± 837	5.6 x 10^6
BsKatG	540 ± 19	3.7 ± 0.7	9050 ± 317	2.5 x 10^6
AfKatG	900 ± 19	3.8 ± 0.3	14960 ± 317	3.9 x 10^6
RcKatG	820 ± 22	3.7 ± 0.9	13600 ± 367	3.7 x 10^6

[a] V_{max} is expressed as μmoles of H_2O_2 decomposed min^{-1} μmole $heme^{-1}$

Figure 3.2.5. Effect of ABTS concentration on the initial peroxidatic velocities of KatGs.

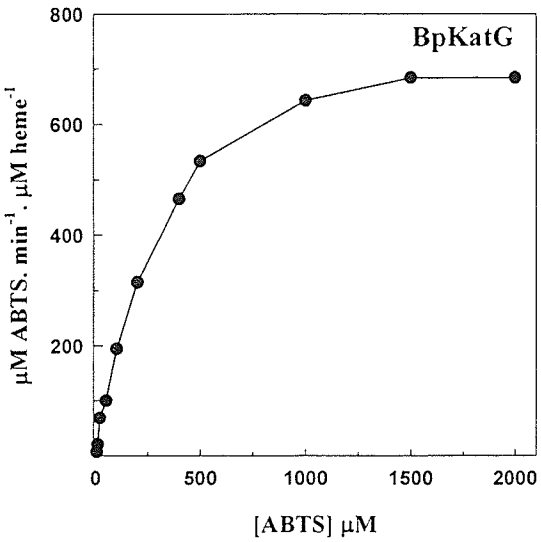
BpKatG
μM ABTS. min-1 . μM heme-1
[ABTS] μM
0
500
1000
1500
2000
200
400
600
800

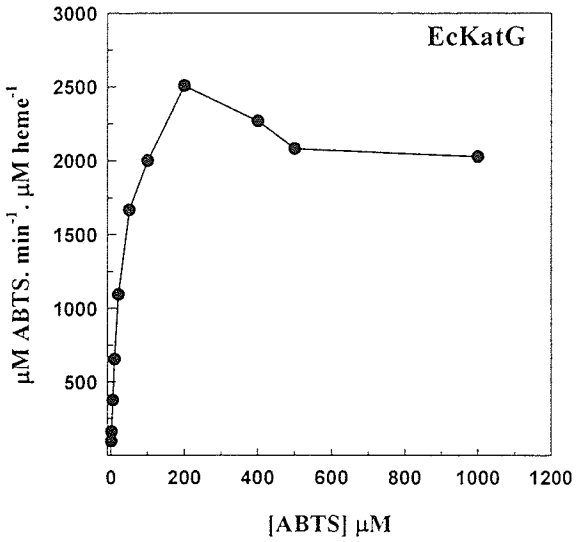
EcKatG
μM ABTS. min-1 . μM heme-1
[ABTS] μM
0
200
400
600
800
1000
1200
500
1000
1500
2000
2500
3000

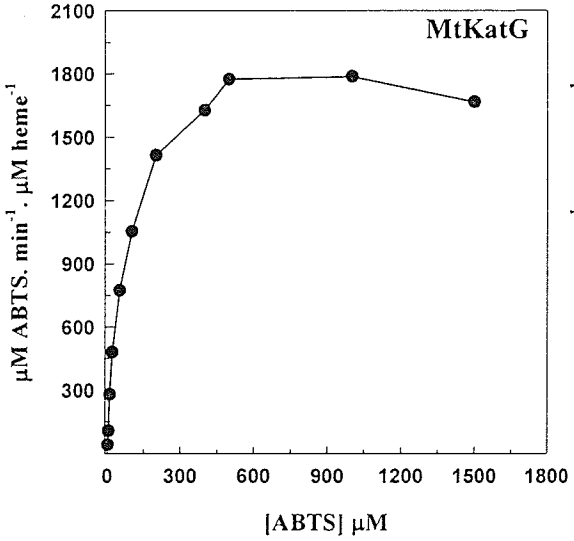
MtKatG
μM ABTS. min-1 . μM heme-1
[ABTS] μM
0
300
600
900
1200
1500
1800
2100

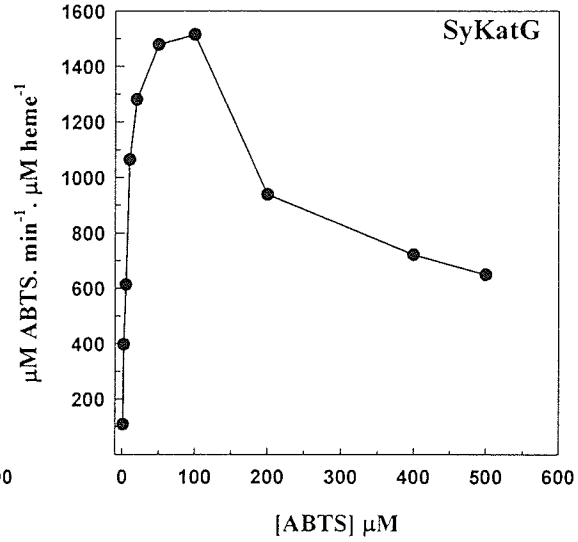
SyKatG
μM ABTS. min-1 . μM heme-1
[ABTS] μM
0
100
200
300
400
500
600
200
400
600
800
1000
1200
1400
1600

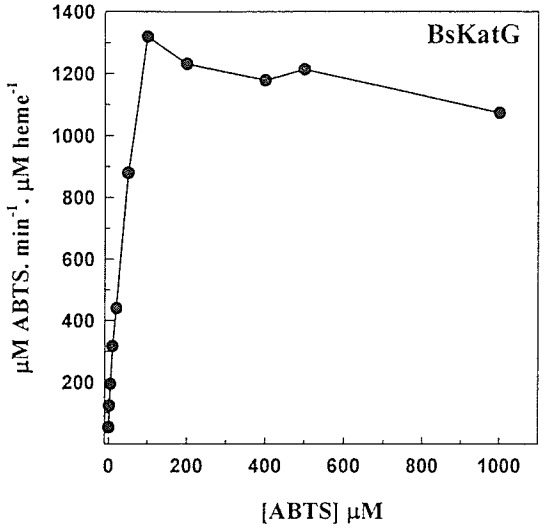
BsKatG
μM ABTS. min-1 . μM heme-1
[ABTS] μM
1400
1200
1000
800
600
400
200
0
200
400
600
800
1000

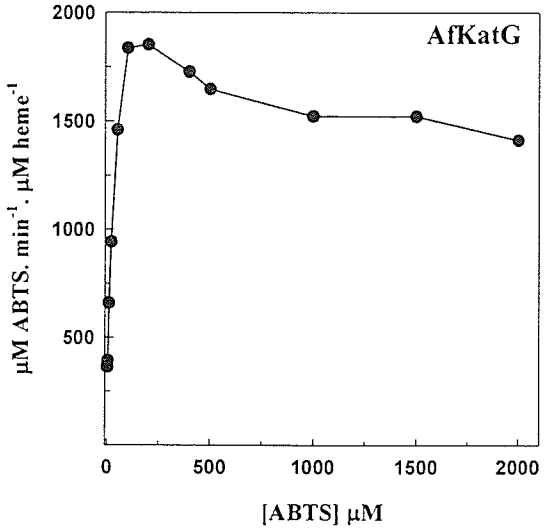
AfKatG
μM ABTS. min-1 . μM heme-1
[ABTS] μM
2000
1500
1000
500
0
500
1000
1500
2000

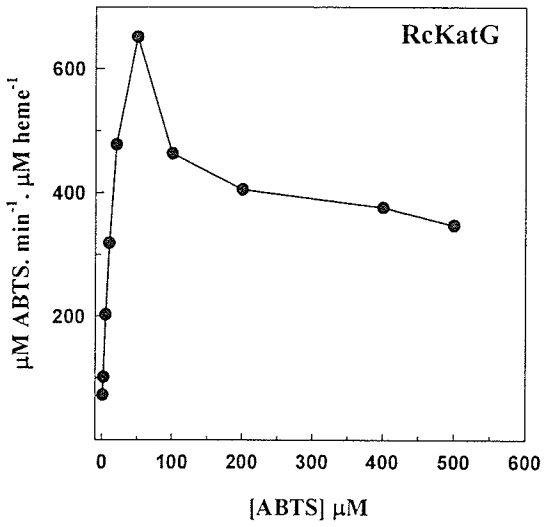
RcKatG
μM ABTS. min-1 . μM heme-1
[ABTS] μM
600
400
200
0
100
200
300
400
500
600

Table 3.2.7 Comparison of the observed peroxidatic kinetic parameters of purified KatGs, using ABTS as substrate.

KatG	V_{max}[a]	K_m (μM)	k_{cat} (s^{-1})	k_{cat}/K_m ($M^{-1}s^{-1}$)
BpKatG	810 ± 14	300 ± 21	14 ± 0.2	0.5 x 10^5
MtKatG	1870 ± 53	67 ± 7	31 ± 0.9	4.5 x 10^5
EcKatG	2450 ± 107	24 ± 5	41 ± 1.8	17 x 10^5
SyKatG	1680 ± 72	7 ± 1	28 ± 1.2	40 x 10^5
BsKatG	1420 ± 105	31 ± 8	24 ± 1.8	7.6 x 10^5
AfKatG	1870 ± 94	16 ± 4	31 ± 1.6	19 x 10^5
RcKatG	890 ± 30	16 ± 1	15 ± 0.5	9.3 x 10^5

[a]V_{max} is expressed as μmoles of ABTS oxidized min^{-1} μmole $heme^{-1}$

Figure 3.2.6. Effect of H_2O_2 concentration on the initial peroxidatic velocities of KatGs.

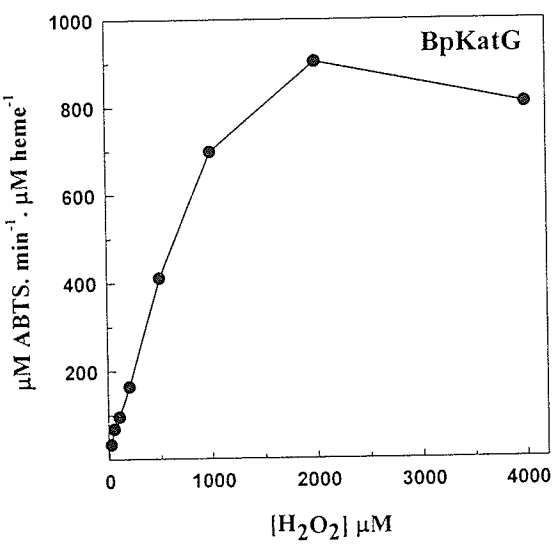
BpKatG
μM ABTS. min-1 . μM heme-1
[H2O2] μM
1000
800
600
400
200
0
1000
2000
3000
4000

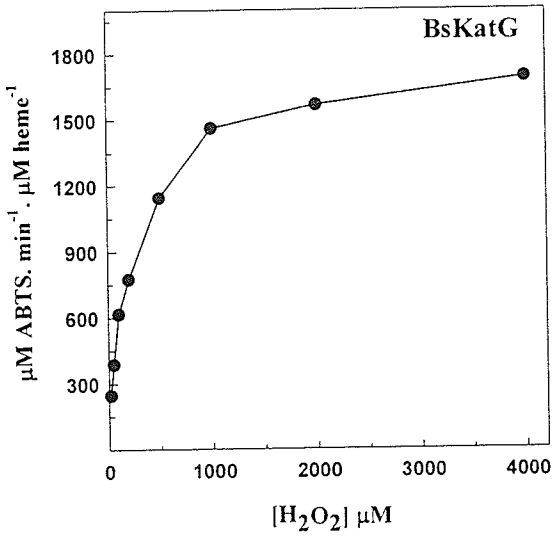
BsKatG
μM ABTS. min-1 . μM heme-1
[H2O2] μM
1800
1500
1200
900
600
300
0
1000
2000
3000
4000

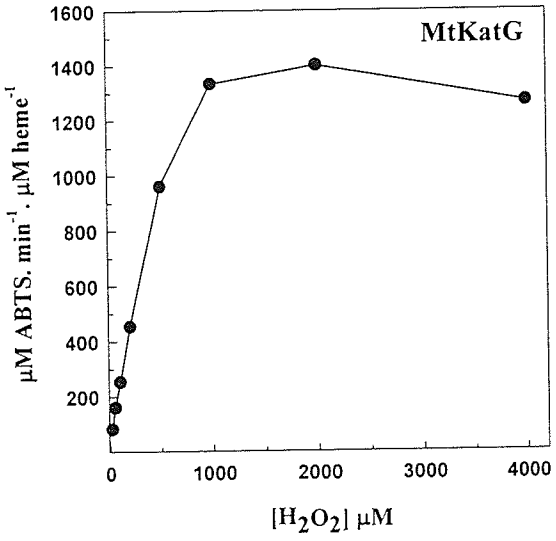
MtKatG
μM ABTS. min-1 . μM heme-1
[H2O2] μM
1600
1400
1200
1000
800
600
400
200
0
1000
2000
3000
4000

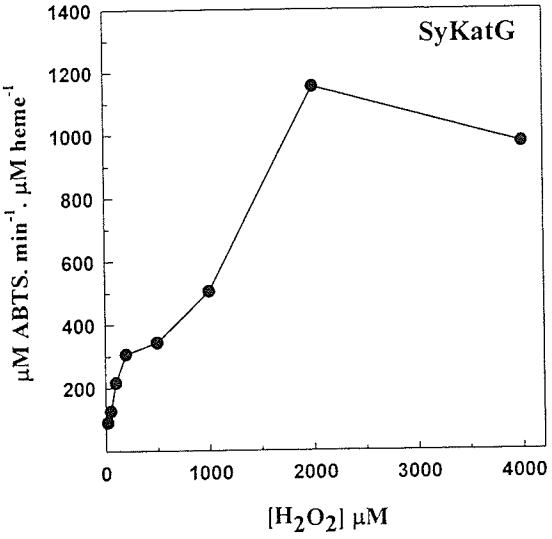
SyKatG
μM ABTS. min-1 . μM heme-1
[H2O2] μM
1400
1200
1000
800
600
400
200
0
1000
2000
3000
4000

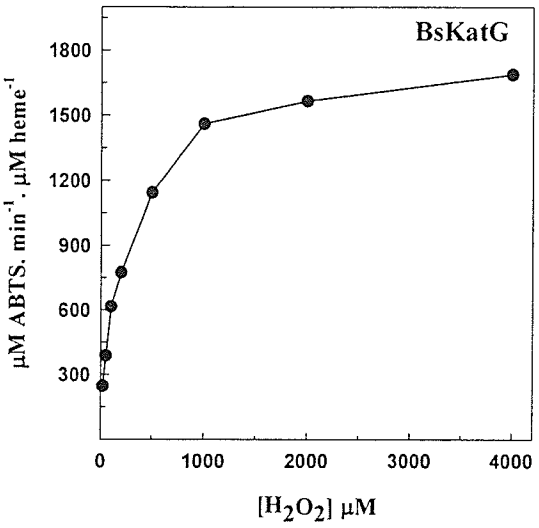
BsKatG
µM ABTS. min-1. µM heme-1
1800
1500
1200
900
600
300
0
1000
2000
3000
4000
[H2O2] µM

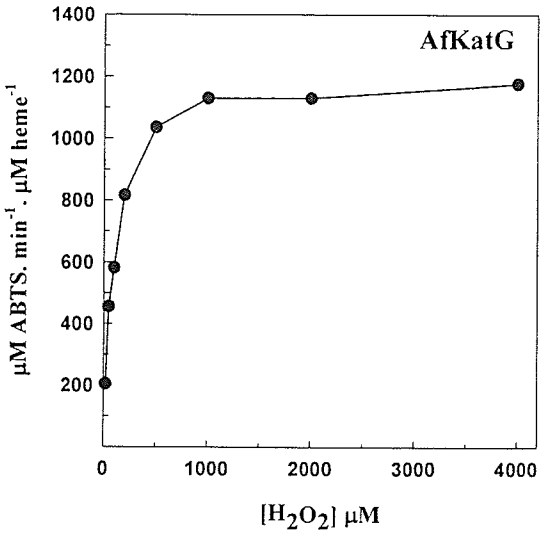
AfKatG
µM ABTS. min-1. µM heme-1
1400
1200
1000
800
600
400
200
0
1000
2000
3000
4000
[H2O2] µM

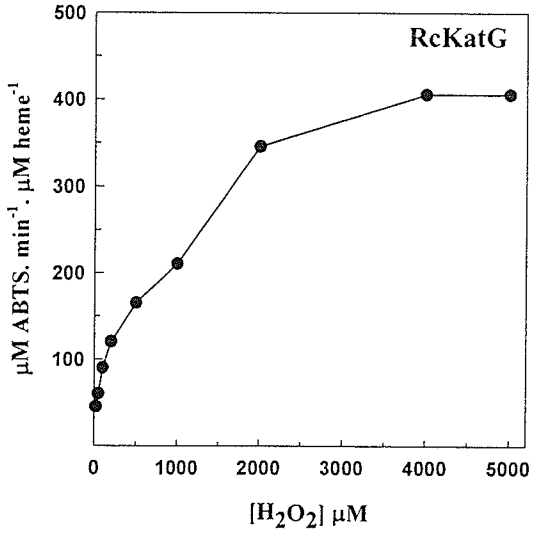
RcKatG
µM ABTS. min-1. µM heme-1
500
400
300
200
100
0
1000
2000
3000
4000
5000
[H2O2] µM

Table 3.2.8 Comparison of the observed peroxidatic kinetic parameters of purified KatGs, using H_2O_2 as substrate for the compound I formation.

KatG	V_{max} [a]	K_m [b] (μM)	k_{cat} (s^{-1})	k_{cat}/K_m ($M^{-1}s^{-1}$)
BpKatG	1070 ± 110	700 ± 220	18 ± 1.8	0.3×10^5
MtKatG	1570 ± 120	360 ± 100	26 ± 1.7	0.7×10^5
EcKatG	2080 ± 160	60 ± 20	35 ± 2.7	6.0×10^5
SyKatG	1440 ± 54	1000 ± 60	24 ± 1	0.2×10^5
BsKatG	1740 ± 53	210 ± 27	29 ± 1	1.4×10^5
AfKatG	1210 ± 9	95 ± 6	20 ± 0.2	2.1×10^5
RcKatG	470 ± 60	830 ± 80	8 ± 1	0.1×10^5

[a] V_{max} is expressed as μmoles of ABTS oxidized min^{-1} μmole $heme^{-1}$
[b] K_m is shown for H_2O_2

activity of KatGs, initial velocities for peroxidase activity were determined at various concentrations of H_2O_2 as shown in Figure 3.2.6, the kinetic constants are summarized in the table 3.2.8. At lower substrate concentrations (100 to 200 mM), KatGs follow Michaelis-Menten kinetics for catalase reaction while higher concentrations tend to inhibit the enzyme activity as shown in Figure 3.2.4. The *Km* value for all seven KatGs studied was found to be in milimolar range, between 2.4 and 4.8, with a very high turnover rate (k_{cat}).

Figure 3.2.5 shows that KatGs follow Michaelis-Menten kinetics for peroxidase activity even at higher concentration of substrate (ABTS). The exceptions to this were SyKatG and RcKatG which showed significant inhibition in the activity at higher substrate (ABTS) concentration. The K_m values for ABTS (Figure 3.2.7.) were determined in μmolar range for all seven KatGs but the variantion among enzymes was prominent ranging from 300 μM (BpKatG) to 7μM (SyKatG). The turnover rate or k_{cat} values also were much lower for peroxidsae reaction as compared to catalase reaction. Figure 3.2.6 shows that KatGs follow Michaelis-Menten kinetics for compound I formation with an exception of SyKatG and RcKatG both of which show significant increase in the initial velocity at H2O2 concentration higher that 1 mM. The K_m values for H_2O_2 are found in μmolar range except for SyKatG which showed a high K_m of ~1 mM.

3.2.7. Effect of heme inhibitor on catalase activity of KatGs

Cyanide and azide are classical heme protein inhibitors that bind to the active-site heme iron reversibly to form stable complexes. Figure 3.2.7 compares the effect of KCN

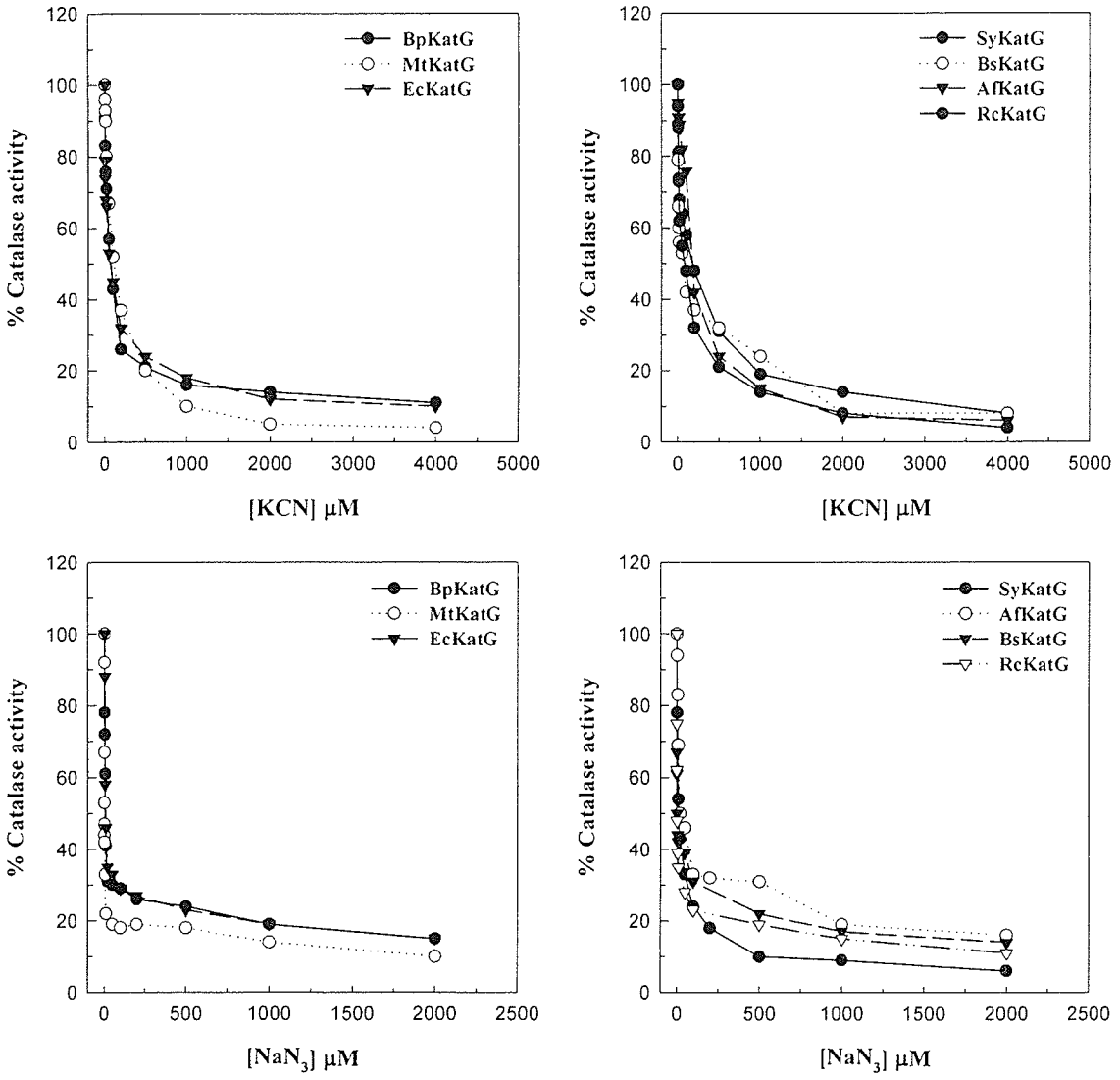

Figure 3.2.7. Comparison of the sensitivity of KatGs to cyanide (KCN) or azide (NaN_3).

Table 3.2.9. Comparison of the sensitivity of KatGs to cyanide (KCN) or azide (NaN_3).

KatG	[KCN] causing 50% inhibition (μM)	[NaN_3] causing 50% inhibition (μM)
BpKatG	40	8
MtKatG	100	0.2
EcKatG	50	7
SyKatG	170	13
BsKatG	50	2
AfKatG	150	20
RcKatG	80	8

reversibly to form stable complexes. Figure 3.7 compares the effect of KCN and NaN_3 on the catalase activity of KatGs and the IC_{50} for both KCN and NaN_3 are summarized in Table 3.9. Both KCN and NaN_3 show similar inhibition patterns for catalase activity but the IC_{50} for KCN is higher than that of NaN_3 though, it remains in the μmolar region.

3.3. KatGs and isoniazid activation

Isonicotinic acid hydrazide (isoniazid or INH) is a widely used pro-drug effective against *Mycobacterium tuberculosis* (Deretic *et al.*, 1996). Formation of isonicotinoyl-NAD, the active form of the drug, involves removal of hydrazine from INH by KatG (Zhang *et al.*, 1992) and ligation of the isonicotinoyl group with NAD^+ (Johnsson *et al.*, 1995). Isonicotinoyl-NAD interferes with the synthesis of mycolic acid and therefore cell wall synthesis by binding to InhA, an enoyl-acyl carrier protein reductase (Rozwarski *et al.*, 1998), and possibly to KasA, a β-ketoacyl acyl carrier protein synthase (Mdluli *et al.*, 1998), blocking their NADH-binding sites. The central role of KatG in INH activation is evident in the significant fraction of INH-resistant cases of tuberculosis attributable to mutations in *katG* and in biochemical studies that have demonstrated a direct role for KatG in the generation of various isonicotinoyl derivatives (Johnsson and Schultz, 1994). Much of the literature related to the activation of INH by KatG has focused on the fate of INH and possible intermediates involved in the process (Johnsson and Schultz, 1994; Wilming and Johnsson, 1995; Magliozzo and Marcinkeviciene, 1996). With NAD^+ included in the mix, the generation of the isonicotinoyl-NAD adduct was observed both with and without KatG present (Wilming and Johnsson, 1995; Magliozzo and Marcinkeviciene, 1996; Lie *et al.*, 2000), leading to the suggestions that the role of KatG is limited to the hydrazine lyase of INH and that the subsequent reaction of the isonicotinoyl radical with NAD^+ is a nonenzymatic event involving a homolytic aromatic substitution (Wilming and Johnsson, 1995; Minisci, *et al.*, 1989). Reactive oxygen species have been implicated in INH activation both *in vivo* (Mitchison and Selkon, 1956; Youatt, 1959) and *in vitro* (Johnsson and Schultz, 1994), and an elevated level of

superoxide (Wang, *et al.*, 1998) was identified as a possible reason for the high sensitivity of *M. tuberculosis* to INH (Deretci *et al.*, 1996). However, the absence of H_2O_2 involvement in INH activation implies that a reaction different from either the peroxidase or the catalase reactions is involved, and some reports have suggested that the active participation of KatG in INH activation involves more than just hydrazine lyase (Lei et al., 2000). During this study a comparative analysis of their interaction with INH and some other pyridine derivatives such as NADH, NADPH and pyridoxine revealed striking peculiarities of KatGs.

3.3.1. Catalase-peroxidases (KatG) exhibit NADH oxidase activity

NADH oxidases are widely distributed in nature, being found in species ranging from bacteria (Ashrafuddin and Claiborne, 1989; Zoldak *et al.*, 2003) and archaebacteria (Kengen *et al.*, 2003) to mammals (Xia *et al.*, 2003). The enzymes can be both soluble and membrane-bound, and although NADH is the common electron donor, water, hydrogen peroxide, or superoxide may be formed as products depending on the enzyme. The physiological role of NADH oxidases in many instances is unknown, but the reaction has been described as a detoxifier of oxygen in nitrogen fixing organisms and archaebacteria (Kengen *et al.*, 2003) and as a possible sensor of oxygen levels in the regulation of muscle contractility (Xia *et al.*, 2003). A variation of the NADH oxidase reaction, a "peroxidase-oxidase" reaction has been well characterized in horseradish peroxidase (HRP) to require a catalytic amount of H_2O_2 that is alternately used and regenerated during the reaction of NAD radicals with molecular oxygen (Akazawa and Conn, 1958; Yokota and Yamazaki, 1965; Yokota and Yamazaki, 1977; Dunford, 1999).

Plant peroxidases, including HRP, have about 20% sequence similarity and remarkable structural similarity to the N-terminal domain of KatG proteins, particularly in the vicinity of the heme active site, raising the possibility that KatG proteins may also exhibit an NADH peroxidase-oxidase activity. Indeed, there are reports of NADH being oxidized to NAD^+ by KatG in both peroxidase (Ro *et al.*, 2003) and an oxidase-like (Wilming and Johnsson, 1999) reactions, but the reaction of KatG with NADH has not been characterized. Keeping in mind the potential importance of any reaction involving NADH in isonicotinoyl-NAD formation, the interactions of KatG with NADH was investigated and an oxygen-dependent NADH oxidase activity was demonstrated along with a direct role for KatG in the formation of isonicotinoyl-NAD.

3.3.1.1. NADH Oxidation by KatG

NAD^+ replaces the hydrazine moiety of the anti-tubercular pro-drug INH to generate the active form of the drug, isonicotinoyl-NAD. In an attempt to define the role of KatG in the formation of isonicotinoyl-NAD, the potential utilization of NADH and NAD^+ as substrates was investigated, revealing that NADH supports BpKatG-mediated radical generation (Figure 3.3.1a) in the absence of H_2O_2 using NBT as radical sensor at a rate approximately equal to the rate of NADH disappearance (Figure 3.3.1b). A similar comparison of other KatGs used in this study demonstrated a similar fate of NADH but at a much slower rate as compared to BpKatG (Table 3.3.1 & Figure 3.3.1). In all cases the radical formation, using NBT as radical sensor, can be clearly differentiated from the background activity of the control lacking KatG. Among KatGs, RcKatG, MtKatG and SyKatG show substantial rates of radical production from a reaction mixture containing

Table 3.3.1. Comparison of NADH oxidase activity of KatGs

KatG	NADH oxidase @ Δ340nm pmole NADH. min^{-1}. $nmol^{-1}$	NADH oxidase @ 560nm pmole NBT. min^{-1}. $nmol^{-1}$
BpKatG	510 ± 85	640 ± 96
MtKatG	30 ± 3	100 ± 15
EcKatG	15 ± 6	13 ± 4
SyKatG	10± 3	80 ± 6
BsKatG	6 ± 6	60 ± 6
AfkatG	38 ± 6	65 ± 4
RcKatG	30 ± 9	240 ± 20

Figure 3.3.1. NADH oxidation by catalase-peroxidases. *a*, the rates of radical production in a reaction mixture containing 100 μM NADH, 1.2 μM KatG, 200 μM NBT and 50 mM Tris, pH 8.75, were followed by formazan appearance measured at 560 nm. Separate assays contain no enzyme (control), BpKatG, MtKatG, EcKatG, SyKatG, BsKatG, AfKatG, & RcKatG. *b*, the rates of NADH oxidation in a solution containing 100 μM NADH, 1.2 μM KatG, and 50 mM Tris, pH 8.75 were followed by NADH disappearance measured at 340 nm. Separate assays contain no enzyme (control), BpKatG, MtKatG, EcKatG, SyKatG, BsKatG, AfKatG, & RcKatG.

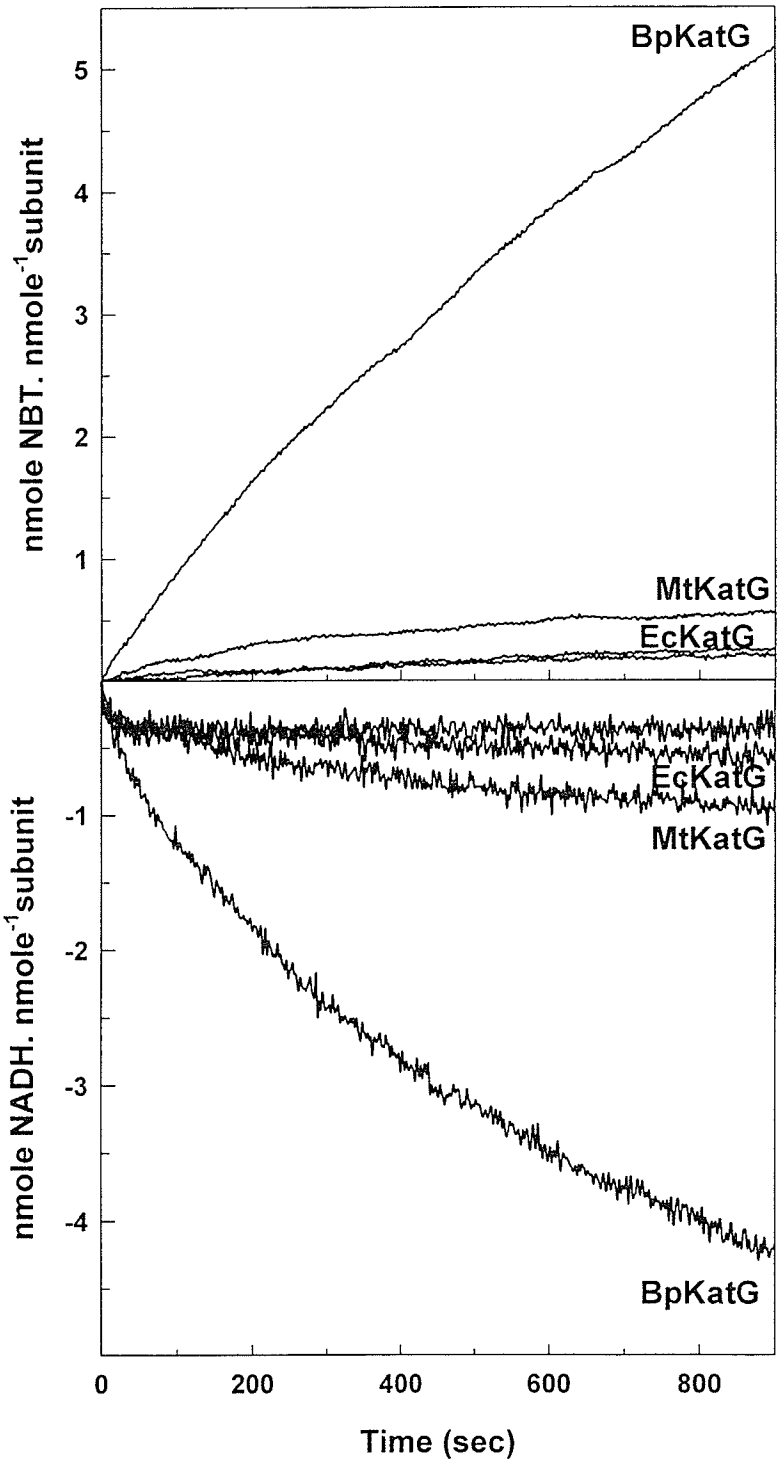
BpKatG
MtKatG
EcKatG
EcKatG
MtKatG
BpKatG
nmole NBT. nmole^{-1}subunit
nmole NADH. nmole^{-1}subunit
5
4
3
2
1
-1
-2
-3
-4
0
200
400
600
800
Time (sec)

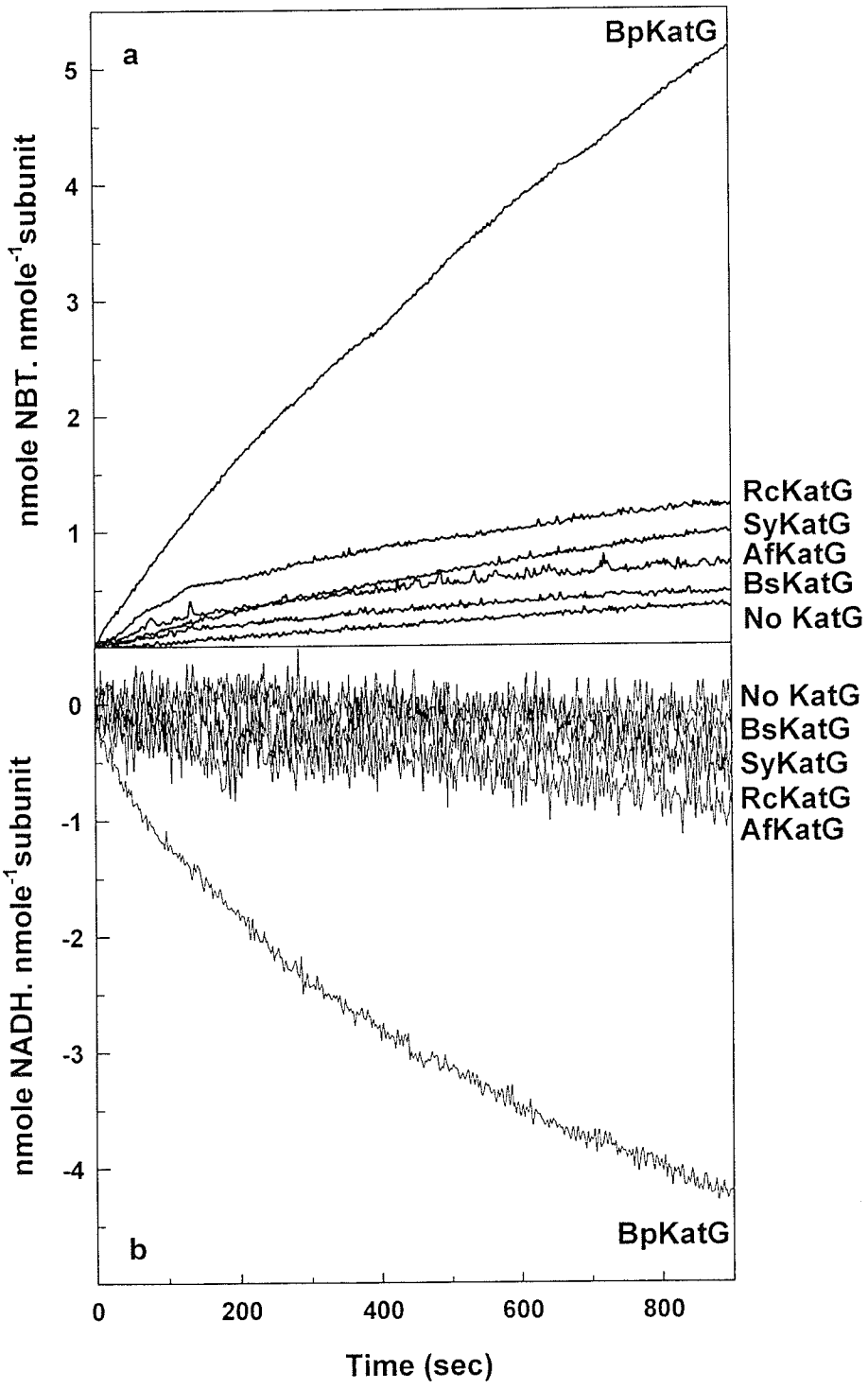
a
BpKatG
RcKatG
SyKatG
AfKatG
BsKatG
No KatG
nmole NBT. nmole-1subunit
5
4
3
2
1
0
-1
-2
-3
-4
No KatG
BsKatG
SyKatG
RcKatG
AfKatG
b
BpKatG
nmole NADH. nmole-1subunit
0
200
400
600
800
Time (sec)

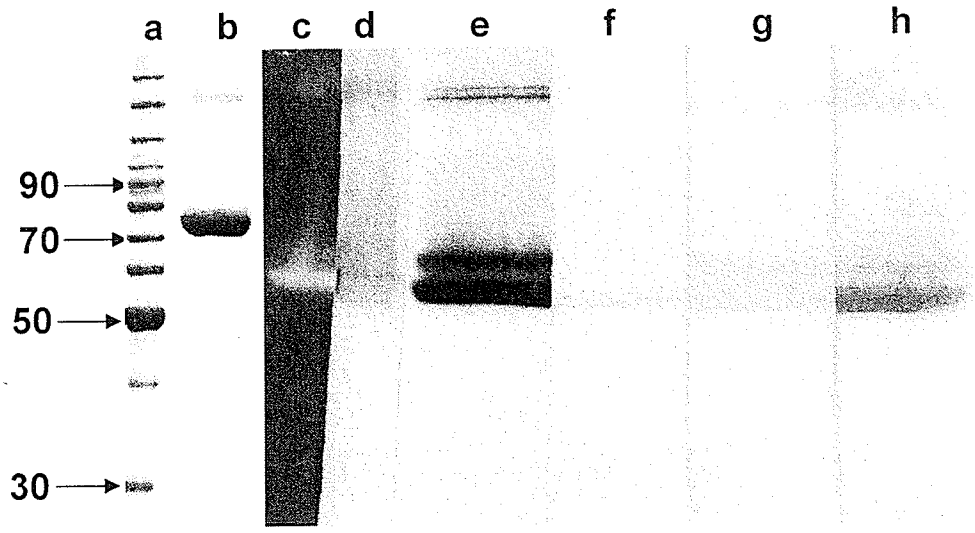

Figure 3.3.2. Migration of purified BpKatG on a 8% SDS-polyacrylamide gel (*lane a and b*) and a nondenaturing 8% polyacrylamide gel (*lanes c–h*). *Lane b* (SDS-polyacrylamide gel) was stained with Coomassie Brilliant Blue dye. A single 200 μg amount of BpKatG was loaded in one large lane for *lanes c–h*, and after electrophoresis, the gel was cut into six strips for separate staining. *Lane c* was stained for catalase activity (a *clear band* on a *brown background*). *Lane d* was stained for peroxidase activity (*brown bands* on a *clear background*). *Lane e* was stained with Coomassie Brilliant Blue. *Lane f* was stained for oxidase activity in a mixture of 200 μM NADH and 200 μM NBT. *Lane g* was stained for INH hydrazine lyase activity in a mixture of 10 mM INH and 200 μM NBT. *Lane h* was stained for combined INH hydrazine lyase and NADH oxidase activity in a mixture of 10 mM INH, 200 μM NADH, and 200 μM NBT.

Table 3.3.2. KatG-mediated radical production in the presence of different substrates

	No enzyme[a]	BpKatG[b]	MtKatG[b]	EcKatG[b]
	pmol. min^{-1}	*pmole. min^{-1}. nmole^{-1} subunit*		
NADH	3.0 ± 0.2	640 ± 96	100 ± 15	13 ± 4
NADH + Mn^{2+}	2.0 ± 0.1	540 ± 23	99 ±4	10 ± 4
NADH – O_2[c]	1.0 ± 0.2	320 ± 15	9 ± 2	7 ± 2
NADH + SOD	1.0 ± 0.1	350 ± 8	58 ± 6	5 ± 2
NADPH	1.0 ± 0.1	260 ± 2	1.0 ± 0.1	1.0 ± 0.1
NAD^+	3.0 ± 0.6	ND[d]	ND[d]	ND[d]
NADH + INH	8.0 ± 2	1140 ± 76	260 ± 21	100 ± 6
NADH + INH + Mn^{2+}	290 ± 16	2940 ± 29	830 ± 17	930 ± 91
NAD^+ + INH	4.0 ± 0.3	82 ± 1	79 ± 8	74 ± 19
NADH + INH + Mn^{+2}	140 ± 4	230 ± 12	340 ± 5	220 ± 9
INH	5 ± 0.2	76 ± 2	78 ± 9	38 ± 2
INH + Mn^{2+}	190 ± 18	410 ± 3	460 ± 5	450 ± 2
INH – O_2[c]	6 ± 2	75 ± 5	78 ± 5	40 ± 3
INH + SOD	5.2 ± 1	90 ± 2	65 ± 5	38 ± 3
INH + pyridoxine	4.0 ± 1	9.0 ± 2	20 ± 5	18 ± 3

[a] All the reactions contained 200 μM NBT in 50 mM Tris pH 8.75 or pH 8.0 (for reactions involving INH), supplemented with 10 mM INH, 250 μM NADH, 250 μM NADPH, and 250 μM NAD^+, and 200 μM of superoxide dismutase as indicated. O_2 was reduced by flushing the reaction mixture with N_2 gas.

[b] KatG was added 1.2 μM.

[c] For anaerobic reactions, the reaction mixtures were flushed with nitrogen to remove dissolve oxygen.

[d] ND, not detected

NADH, NBT and KatG as well as upon direct observation of NADH disappearance at 340 nm (Figure 3.3.1a and b) and BsKatG shows the lowest level of NADH oxidase activity at both 560 and 340 nm. NADPH supports a slower rate of radical generation, and NAD^+ does not support any radical production (Table 3.3.2). NAD^+ was confirmed as the product of the reaction with NADH by HPLC analysis (Figure 3.3.4). Both superoxide dismutase and a lower molecular oxygen concentration reduce radical generation (Table 3.3.2) from NADH. The pH optima for both radical production and NADH disappearance are 8.75, but the curves are not perfectly superimposable (Figure 3.3.3), suggesting two different, pH-dependent, fates for the reduced oxygen, most likely H_2O_2 at lower pH and superoxide radical at higher pH. Unfortunately, the rapid degradation of H_2O_2 by both the catalase and peroxidase activities of BpKatG precluded its identification or even the observation of any spectral changes in the enzyme during the reaction. The optimum pH for the oxidase reaction is significantly different from the optimum pH levels for the peroxidase (pH 4.5) and catalase (pH 6.5) reactions (Figure 3.3.3). These results are consistent with BpKatG having an NADH oxidase activity producing NAD^+ and either superoxide ion or H_2O_2 and with a similar activity existing in MtKatG, EcKatG, SyKatG, BsKatG, AfKatG and RcKatG, but at a much lower level.

3.3.1.2 Visualization of NADH oxidase activity by PAGE under non-denaturating conditions.

Purified BpKatG migrates as a single band (apparent mass of 78 kDa) on denaturing gels (Figure 3.3.2, *lane a*) with only a small amount of slower migrating dimer. On a nondenaturing gel (Figure 3.3.1, *lanes b–g*), catalase, peroxidase, and

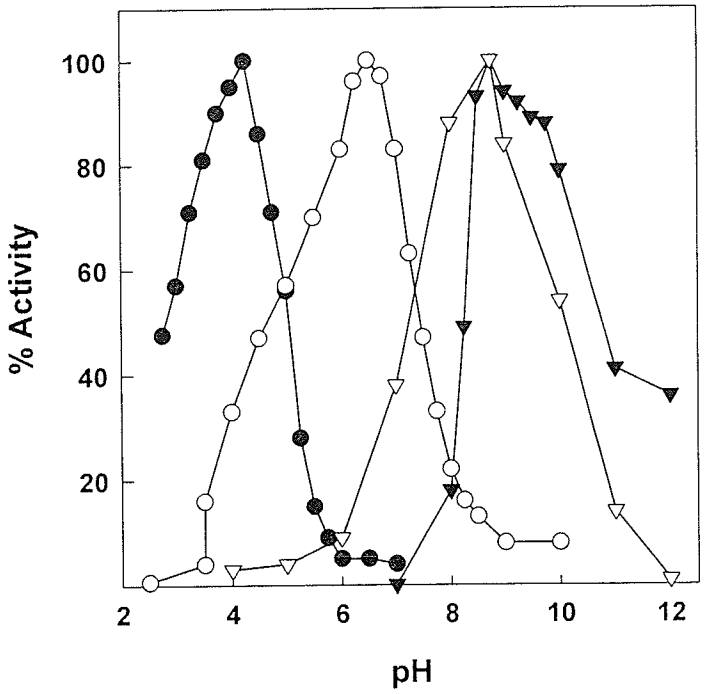

Figure 3.3.3. pH dependence of NADH oxidation by BpKatG determined by radical formation at 560 nm (▼) and NADH disappearance at 340 nm (▽) compared with the pH dependence of the catalase (○) and peroxidase (●) reactions. Buffered solutions contained 50 mM each of sodium acetate, pH 3, 4, 5; potassium phosphate, pH 6 and 7; Tris-HCL, pH 8 and 9; and CHES, pH 10.

Figure 3.3.4. Elution profiles from reverse phase HPLC of reaction products from mixtures containing 100 μM NADH and no enzyme (a); 1.2 μM BpKatG (b); 1.2 μM MtKatG (c); 1.2 μM EcKatG (d). *N-H*, NADH; *N-D*, NAD^+.

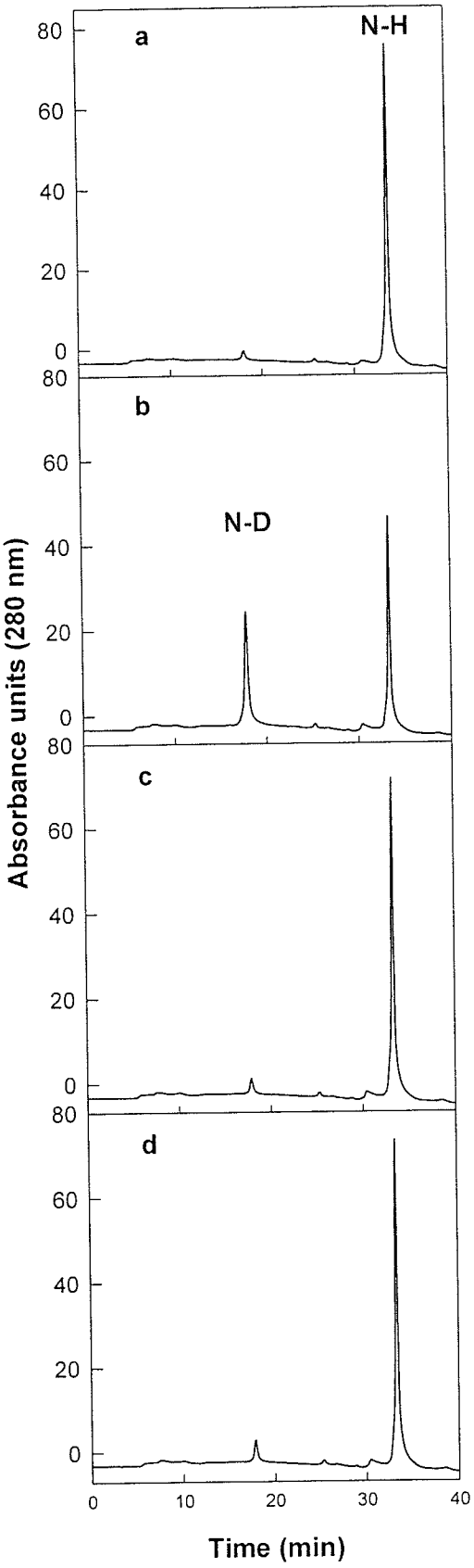
a
N-H
b
N-D
c
d
Absorbance units (280 nm)
Time (min)
0
20
40
60
80
0
10
20
30
40

oxidase activities all co-migrate with the main bands of protein (*lanes b–e*). The presence of two bands of catalase-peroxidase with the same mass on nondenaturing gels has been noted previously but not explained.

3.3.1.3. Kinetic characterization of NADH oxidase activity

Titration of BpKatG with different concentrations of NADH demonstrates that BpKatG follows Michaelis-Menton kinetics for the NADH oxidase reaction (Figure 3.3.5). The kinetic parameters (Table 3.3.3) reveal a relatively high affinity (K_m) for NADH but a very slow turnover rate (k_{cat}) in comparison with the catalase and peroxidase reactions. NAD^+ and pyridoxine act as competitive inhibitors of the NADH oxidase reaction (Table 3.3.2 & Figure 3.3.6).

3.3.1.4. Comparison of NADH oxidase activity with NADH peroxidase-oxidase reaction by HRP

HRP catalyzes an NADH peroxidase-oxidase reaction in which H_2O_2 is required to initiate the reaction, after which there is a cycling of $O_2^{\bullet-}$, H_2O_2, and compound III (Dunford, 1999). Given the sequence similarity between plant peroxidases and catalase-peroxidases, particularly in the active site, the possibility that the NADH oxidase activity of KatG is similar to the peroxidase-oxidase reaction was investigated (Table 3.3.4). The HRP peroxidase-oxidase reaction is characterized by a need for a catalytic amount of H_2O_2, by inhibition by SOD or catalase, and by long lag periods in the presence of low NADH concentrations and high HRP concentrations. NADH oxidation by BpKatG does not exhibit anyof these characteristics (Table 3.3.4). For

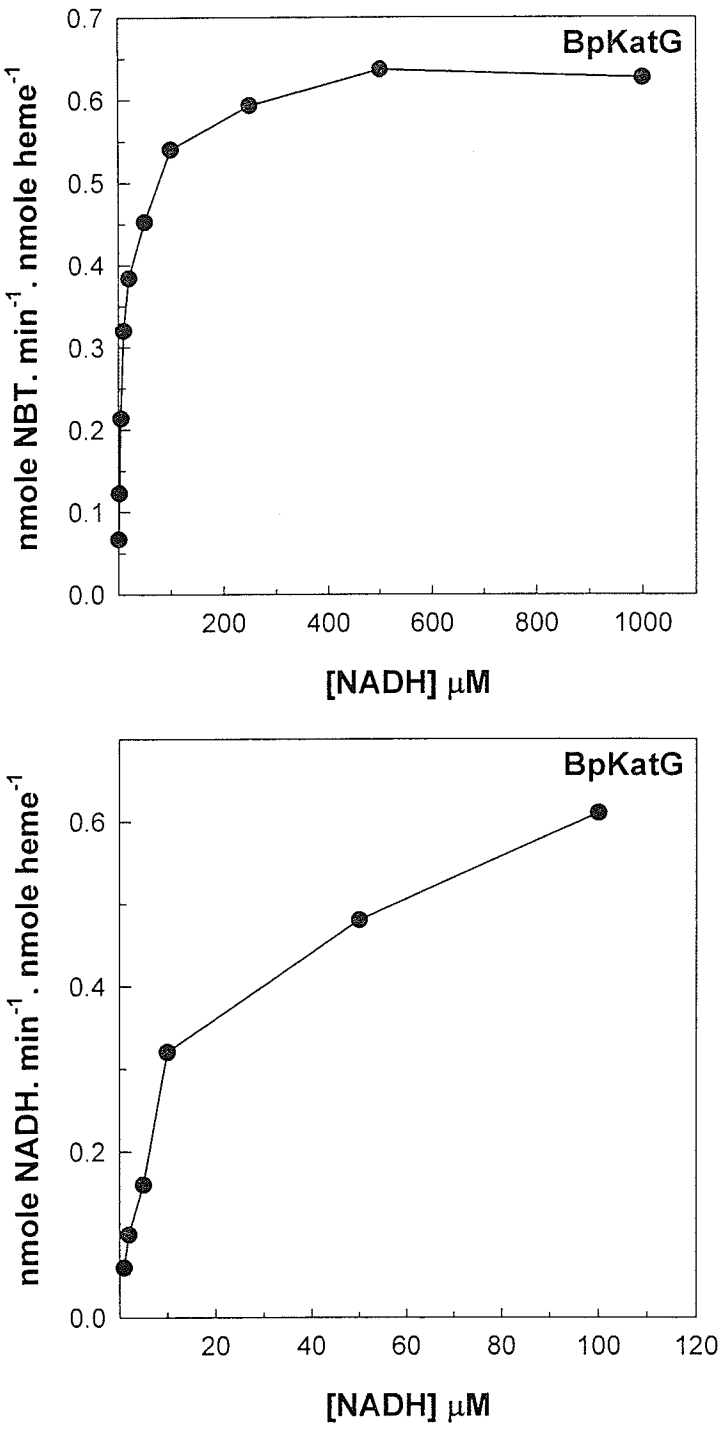

Figure 3.3.5. Effect of NADH concentration on the initial NADH oxidase velocities of BpKatG at 560 nm (top panel) and 340 nm (bottom panel).

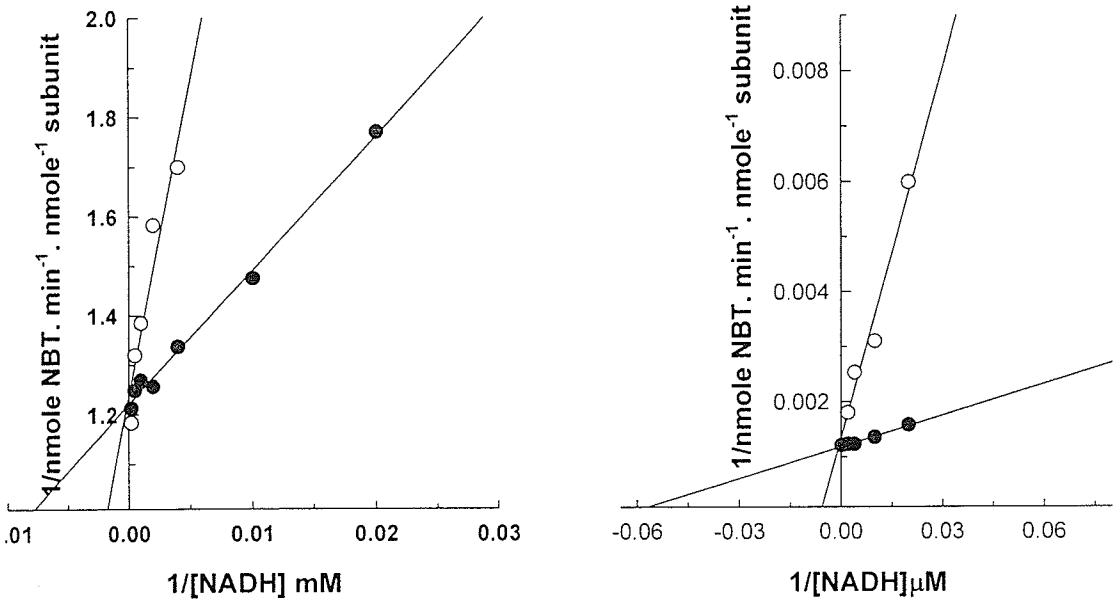

Figure 3.3.6. Effects of $NAD^+$and pyridoxine on NADH oxidase activity. 1.2 μM BpKatG was equilibrated with 5 mM NAD^+ or pyridoxine before titrating with different concentrations of NADH at pH 8.75. Lineweaver-Burk plots (double reciprocal) are shown.

Table 3.3.3. Comparison of kinetic constants for NADH oxidase, catalase and, peroxidase activities of BpKatG

	V_{max}	K_m	k_{cat}	k_{cat}/K_m
	$\mu mole.min^{-1}.\ \mu mole\text{-}heme^{-1}$	μM^a	s^{-1}	$M^{-1}.s^{-1}$
Oxidase (Δ A_{340})	$540 \pm 96 \times 10^{-3}$	12.5 ± 2.0	$9.0 \pm 0.4 \times 10^{-3}$	7.2×10^{2}
Peroxidase	1083 ± 29	330 ± 30	10.1 ± 0.27	3.1×10^{4}
Catalase	$902 \pm 20 \times 10^{3}$	7700 ± 400	$8.4 \pm 0.2 \times 10^{3}$	1.1×10^{6}

[a] [NADH] for the oxidase reaction, [ABTS] for the peroxidase reaction, and [H_2O_2] for the catalase reaction

Table 3.3.4. Comparison of NADH oxidation by HRP, BpKatG, and the Trp111Phe variant. Reactions mixtures contained 100 μM NADH, and 1.2 μM either of HRP, BpKatG or Trp111Phe in 50 mM Tris, pH 8.75. 10 μM H_2O_2, 300 nM HPII or 6 μM SOD was added as indicated. NADH oxidation was followed by decrease in absorbance at 340 nm.

	HRP	**BpKatG**	**Trp111Phe**
NADH	110 ± 18[a]	490 ± 16	500 ± 41
NADH + H_2O_2	360 ± 22	490 ± 24	2160 ± 180
NADH + HPII[b]	30 ± 4	480 ± 16	392 ± 16
NADH + HPII + H_2O_2	54 ± 4	480 ± 16	290 ± 16
NADH + SOD[c]	86 ± 16	400 ± 24	460 ± 16
NADH + SOD + H_2O_2	540 ± 29	400 ± 16	2200 ± 190

[a] The data expressed as *pmol NADH. min^{-1} $nmole^{-1}$ heme*

[b] Monofunctional catalase of *E. coli*

[c] Superoxide dismutase

Figure 3.3.5. Effect of NADH or NAD^+ on the peroxidase activity of BpKatG, MtKatG and EckatG using ABTS or *o*-dianisidine as peroxidatic substrate.

	ABTS					
	Activity after 1min (U/mg)			Activity after 15 min (U/mg)		
	BpKatG	MtkatG	EckatG	BpKatG	MtkatG	EckatG
NO NADH/NAD^+	3.8 ± 0.1	15 ± 0.2	12 ± 0.4	3.7 ± 0.3	15 ± 0.3	12 ± 0.2
NADH	3.3 ± 0.1	15 ± 0.2	10 ± 0.6	2.9 ± 0.1	14 ± 0.1	11 ± 0.4
NAD^+	4.9 ± 0.1	12 ± 0.4	10 ± 0.3	4.6 ± 0.1	14 ± 0.6	10 ± 0.3

	o-dianisidine					
	Activity after 1min (U/mg)			Activity after 15 min (U/mg)		
	BpKatG	MtkatG	EckatG	BpKatG	MtkatG	EckatG
NO NADH/NAD^+	5.3 ± 0.1	10 ± 0.2	10 ± 0.4	5.3 ± 0.3	9.9 ± 0.3	10 ± 0.2
NADH	5.4 ± 0.1	10 ± 0.2	9.9 ± 0.6	4.9 ± 0.1	10 ± 0.1	9.0 ± 0.4
NAD^+	6.9 ± 0.2	11 ± 0.4	10 ± 0.3	6.7 ± 0.1	9.8 ± 0.6	9.7 ± 0.3

comparison, NADH oxidation by the Trp111Phe variant, which lacks catalase activity, is reduced slightly by catalase, but not SOD, and is significantly enhanced by added H_2O_2, attributable to NADH serving as a peroxidatic substrate. No lag in the initiation of NADH oxidation was evident over a broad range of NADH concentrations or enzyme concentrations for either BpKatG or the Trp111Phe variant.

3.3.1.5 Effect of NADH on the peroxidase activity of KatGs

Effect of NADH and NAD^+ on the peroxidase activity of BpKatG, MtKatG and EckatG was observed in order to determine the probability of NADH or NAD^+ having the similar binding site as that for the peroxidatic substrate such as ABTS or *o*-dianisidine in KatGs. A mixture of KatG equilibrated with NADH or NAD^+ was assayed at different time intervals for peroxidase activity using either ABTS or *o*-dianisidine as substrate. The results demonstrated only very subtle changes in peroxidase activity even after 15 min of incubation for both ABTS and *o*-dianisidine (Table 3.3.5), suggesting a separate binding site for NADH/NAD^+. Slight decrease in the peroxidase activity can be debated and the most plausible explanation could be the proximity between the binding sites for ABTS/o-dianisidine and NADH/NAD^+ but this needs confirmation by structural analysis of the ligand-enzyme complex.

3.3.2 INH hydrazine lyase activity by KatGs

The activation of INH as an anti-tubercular drug by catalase-peroxidases involves removal of the hydrazine moiety and proceeds via a radical producing reaction that can be monitored using NBT as a radical sensor (Hillar and Loewen, 1995). The H_2O_2

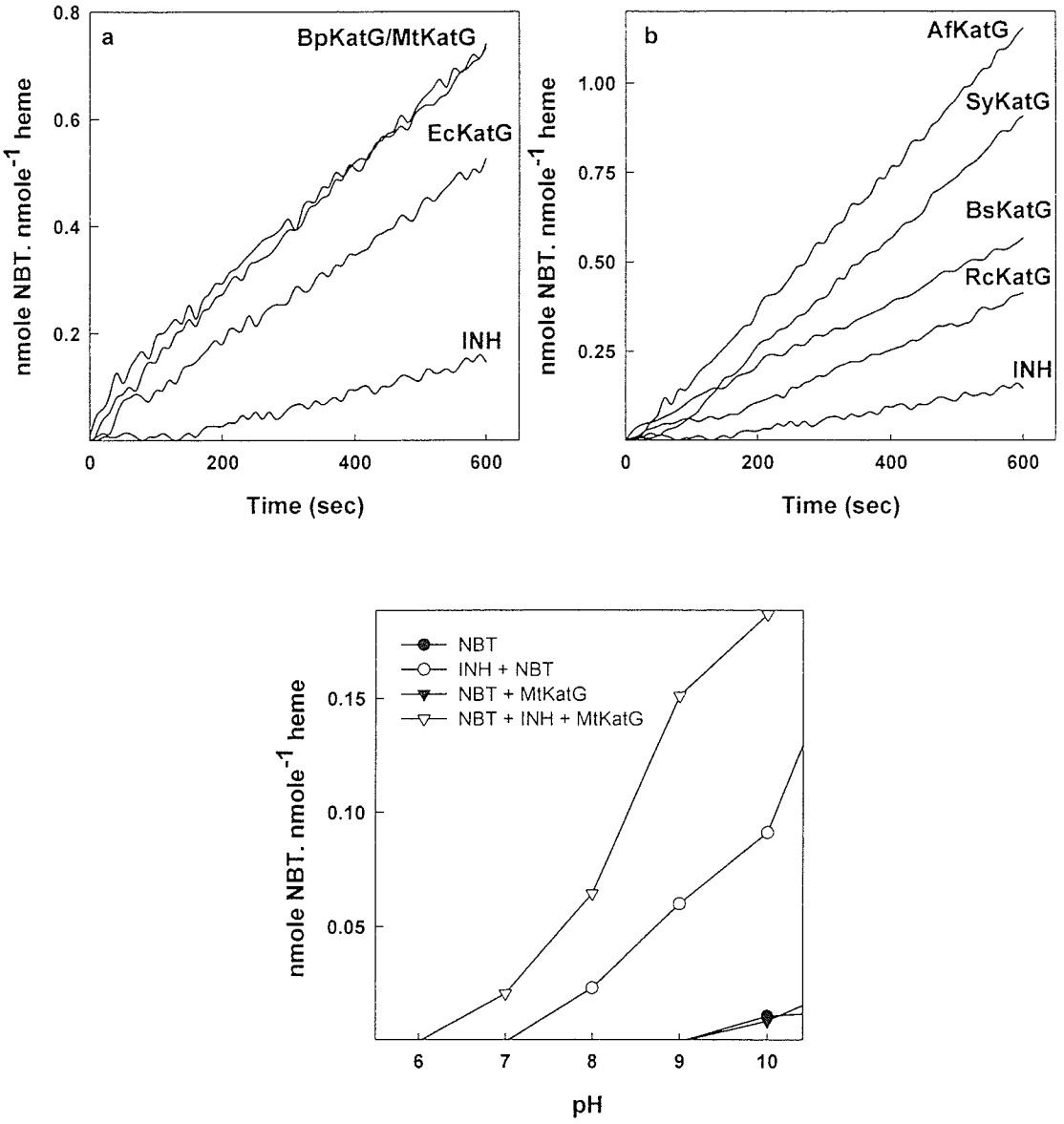

Figure 3.3.7. Removal of hydrazine form isoniazid. *a* and *b*, Radical generation in a solution containing 10 mM INH, 200 μM NBT as radical sensor in 50 mM Tris, pH 8.0, was followed by formazan appearance measured at 560 nm. Separate assays contain no enzyme (control), BpKatG, MtKatG, EcKatG, SyKatG, BskatG, AfKatG or RckatG. *c*, pH dependence of radical generation in a solution of 200 μM NBT with and without MtKatG and a solution of 200 μM NBT and 10 μM INH with and without MtKatG is shown.

Figure 3.3.8. Effect of manganese on the removal of hydrazine lyase activity by KatG. *a* and *b*, radical generation in a solution containing 10 mM INH, 2 μM $MnCl_2$ and 200 μM NBT in 50 mM Tris, pH 8.0, was followed by formazan appearance measured at 560 nm. Separate assays contain no enzyme (control), BpKatG, MtKatG, EcKatG, SyKatG, BskatG, AfKatG or RckatG.

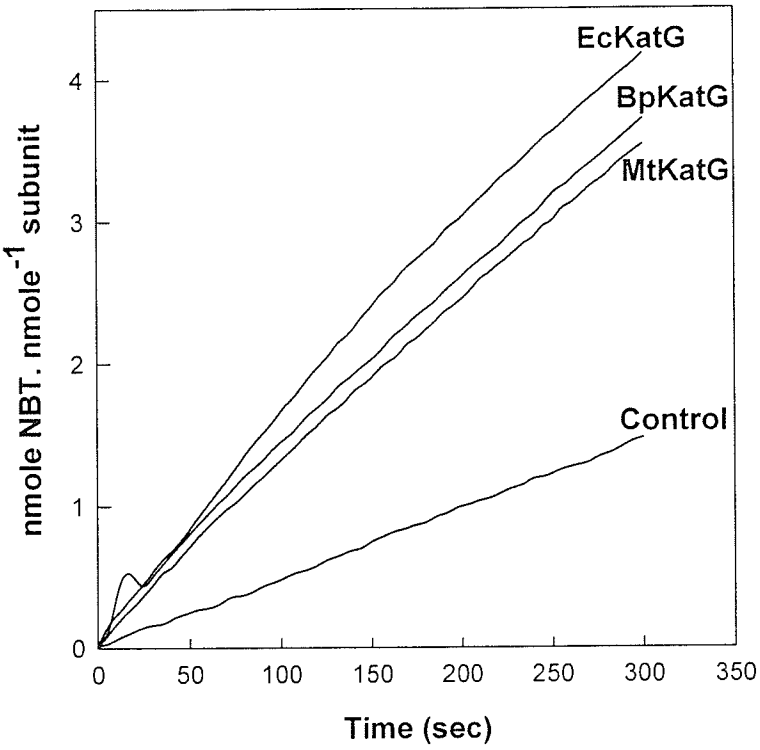
EcKatG
BpKatG
MtKatG
Control
nmole NBT. nmole^{-1} subunit
Time (sec)
0
1
2
3
4
0
50
100
150
200
250
300
350

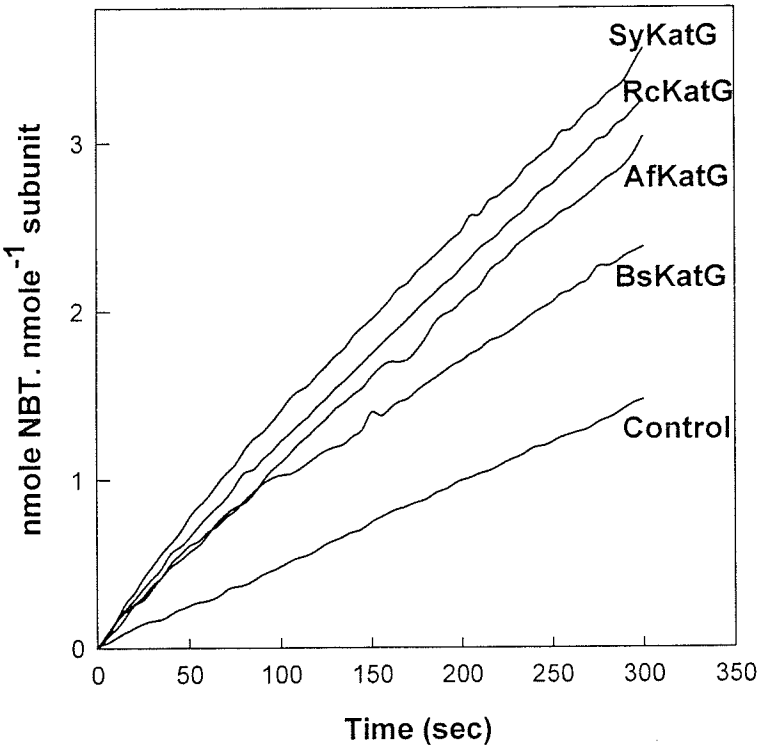
SyKatG
RcKatG
AfKatG
BsKatG
Control
nmole NBT. nmole^{-1} subunit
Time (sec)
0
1
2
3
0
50
100
150
200
250
300
350

Table 3.3.6. Comparison of effect of $MnCl_2$ and NADH on the hydrazine lyase activity of catalase-peroxidases.

KatG	Hydrazine lyase (units/mg)[a]	Hydrazine lyase (with 2 μM Mn^{2+}) (units/mg)[a]	INH-NADH synergistic reaction(units/mg)[a]
BpKatG	76	410	1140
MtKatG	78	460	260
EcKatG	38	450	100
SyKatG	57	500	190
BsKatG	62	420	220
AfkatG	88	370	190
RcKatG	14	270	140

[a] data expressed as pmole NBT. min^{-1} $nmole^{-1}$ heme.

independence (Figures 3.3.7a & b) and enhanced rates at alkaline pH (Figure 3.3.7c) of the KatG-mediated INH hydrazine lyase reaction differentiate it from the catalase and peroxidase reactions (Figure 3.3.3). There is a pH-dependent, nonenzymatic generation of radicals from INH, but in the pH 7–9 range, the contribution of the enzymatic reaction is clear and suggests a pH optimum between 8 and 9, albeit not well defined (Figure 3.3.7 c). To minimize the nonenzymatic contribution, all subsequent assays and reactions involving INH were carried out at pH 8. Oxygen levels do not affect the KatG-mediated radical generation from INH, and superoxide dismutase does not reduce radical production (Table 3.3.2), confirming that molecular oxygen does not have a role in the reaction. AfKatG demonstrates the highest rate of hydrazine lyase whereas MtKatG shows almost the same rate as BpKatG, but the EcKatG-mediated reaction is slowest among the seven KatGs studied (Figure 3.3.7 and Table 3.3.6). Despite having a pyridine ring as part of its structure, NAD^+ does not inhibit INH hydrazine lyase (Table 3.3.2). Addition of 2 μM Mn^{2+} to a reaction mixture carrying INH and NBT resulted in a 4-5 fold increase in the radical production even in the absence of KatG, but the addition of KatG significantly increased the rates as compared to the control lacking KatG (Figure 3.3.8 and Table 3.3.6).

3.3.3 Interaction of KatG with a mixture of INH and NADH

Radical generation in a mixture of BpKatG, INH, and NADH is about two times faster than the cumulative rate of the individual reactions of INH and NADH (Figures 3.3.9a and b). A similar pattern was observed for other KatGs which show significantly higher rates of radical formation as compared to the individual rates by

Figure 3.3.9. Synergistic effect of INH and NADH on radical generation in a solution containing 10 mM INH, 100 μM NADH, 200 μM NBT as radical sensor in 50 mM Tris, pH 8.0, was followed by formazan appearance measured at 560 nm. Separate assays contain, no enzyme (control), BpKatG, MtKatG, EcKatG, SyKatG, BskatG, AfKatG or RckatG.

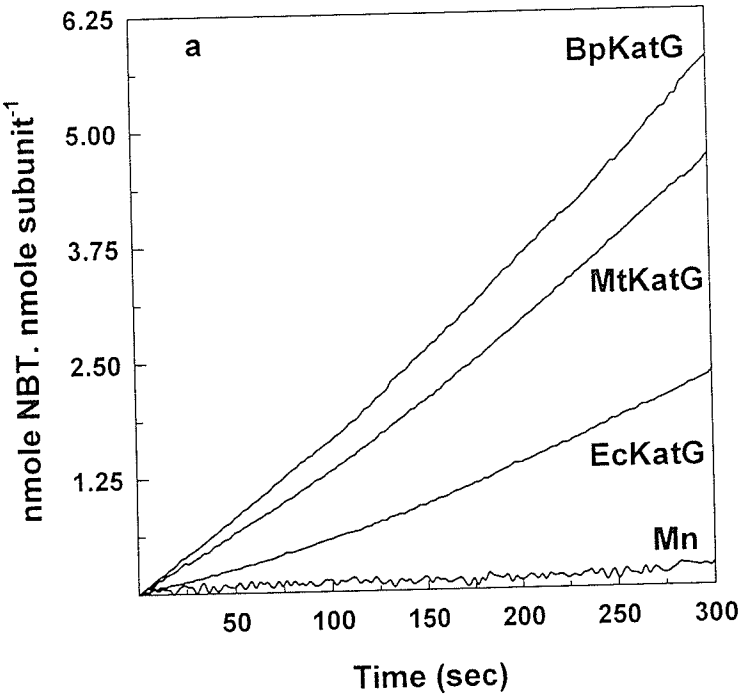
a
BpKatG
MtKatG
EcKatG
Mn
6.25
5.00
3.75
2.50
1.25
nmole NBT. nmole subunit-1
50
100
150
200
250
300
Time (sec)

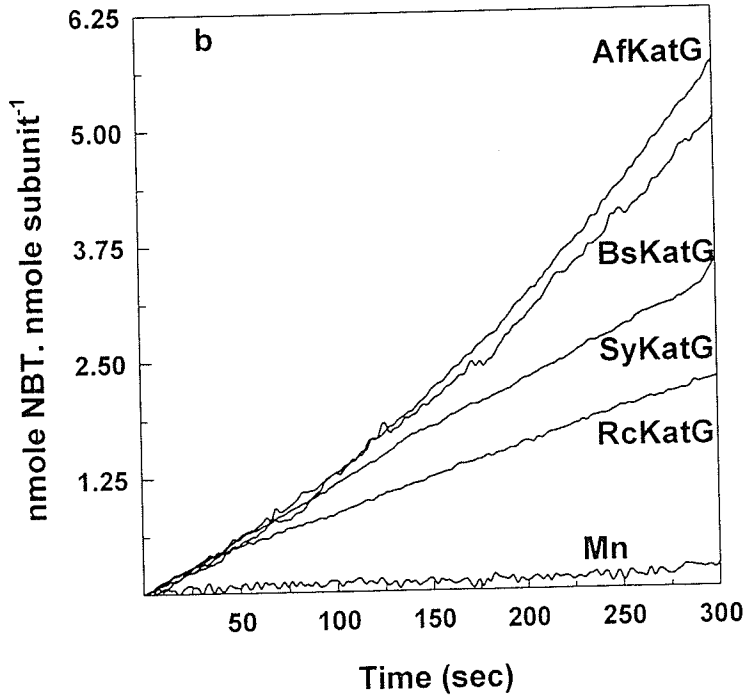
b
AfKatG
BsKatG
SyKatG
RcKatG
Mn
6.25
5.00
3.75
2.50
1.25
nmole NBT. nmole subunit-1
50
100
150
200
250
300
Time (sec)

Figure 3.3.10. Elution profiles from reverse phase HPLC of reaction products from mixtures containing 100 μM NADH, 200 μM INH and no enzyme (a); 1.2 μM BpKatG (b); 1.2 μM MtKatG (c); 1.2 μM EcKatG (d). *I*, isonicotinic acid hydrazide; *N-H*, NADH; *N-D*, NAD^+; *I-N*, isonicotinoyl-NAD.

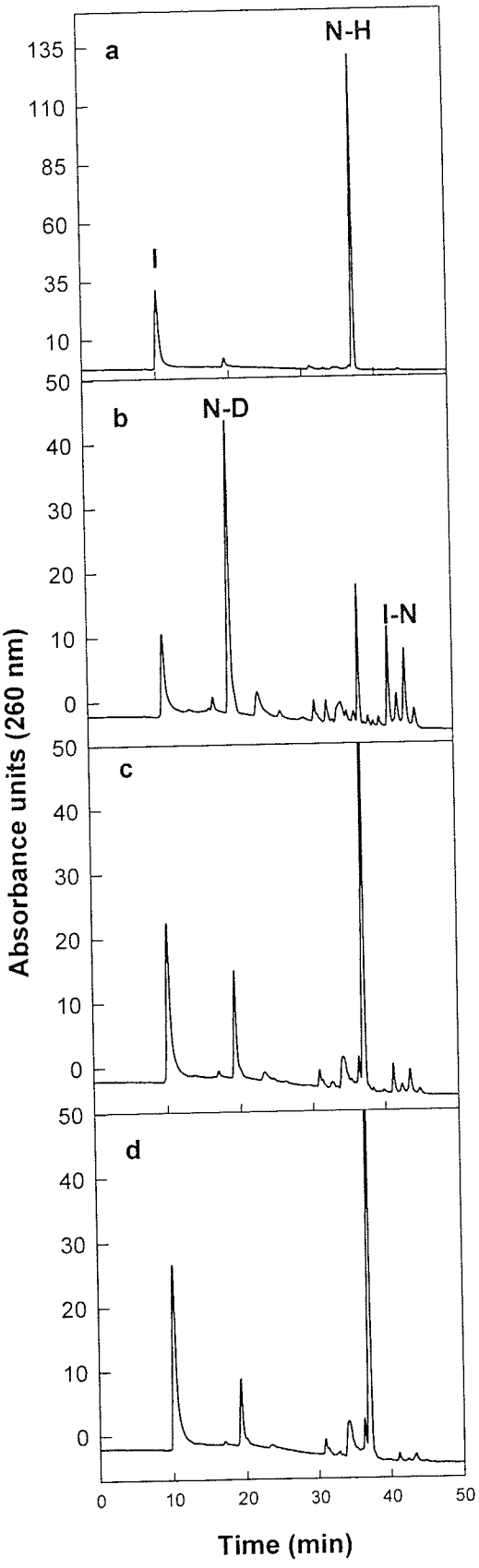
a
N-H
I
b
N-D
I-N
c
d
Absorbance units (260 nm)
Time (min)

Figure 3.3.11. Elution profiles from reverse phase HPLC of reaction products from mixtures containing 100 mM NADH, 200 μM INH, 2μM $MnCl_2$ and no enzyme (a); 1.2 μM BpKatG (b); 1.2 μM MtKatG (c); 1.2 μM EcKatG (d). *I*, isonicotinic acid hydrazide; N-D, NAD^+; *N-H*, NADH; *I-N*, isonicotinoyl-NAD.

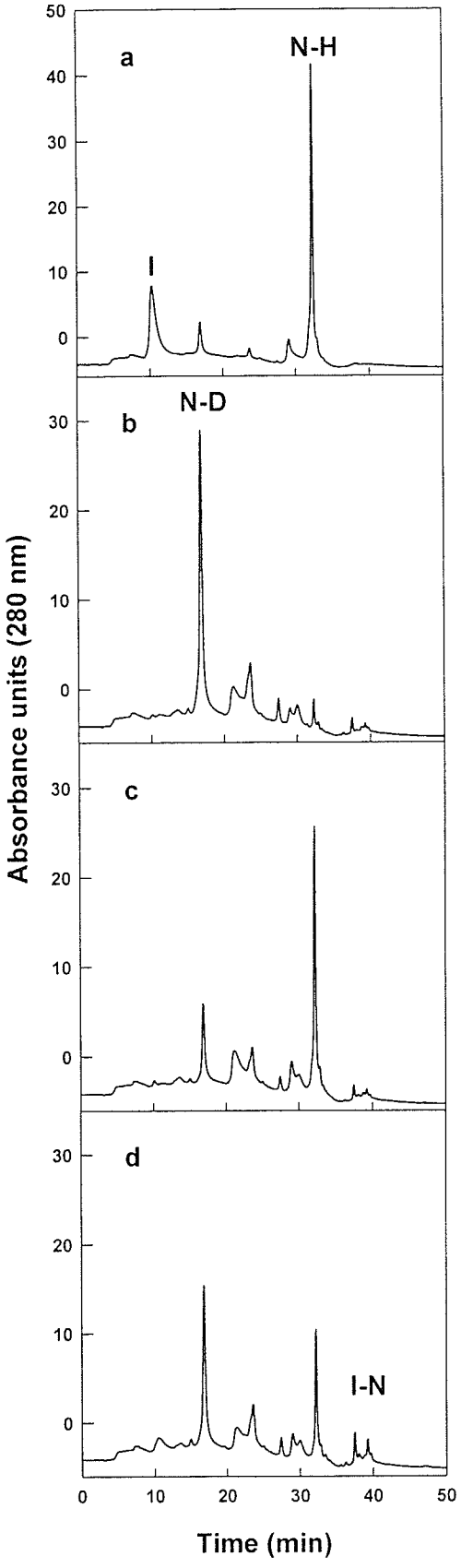
a
N-H
I
b
N-D
c
d
I-N
Absorbance units (280 nm)
Time (min)
0
10
20
30
40
50

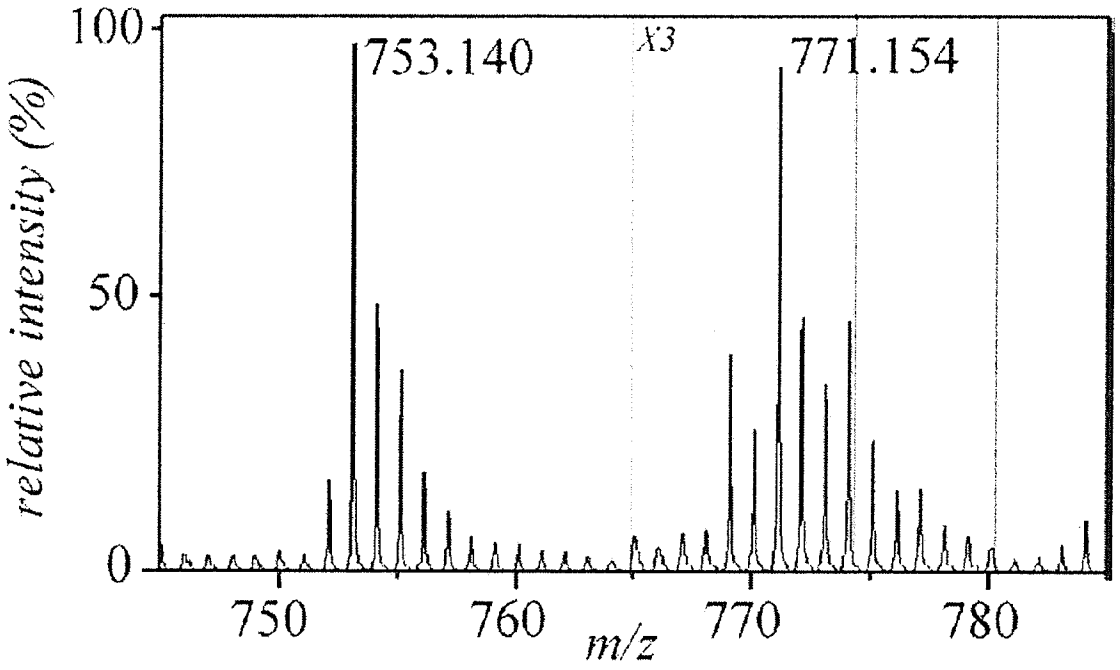

Figure 3.3.12. Part of a matrix-assisted laser desorption ionization mass spectrum of a reaction mixture after 18 h of incubation showing the isonicotinoyl-NAD product ion at *m/z* 771 and the decay product at *m/z* 753. *N*, NAD; *I-N*, isonicotinoyl-NAD.

Table 3.3.7. Comparison of expected and observed m/z values of ions in the MS/MS spectra of NADH and the product of the reaction of KatG with INH and NADH identified as isonicotinoyl-NAD

	Product ions (*m/z*) from parent ion[a]			Assigned structure[b]	Formula to calculate expected ion	Expected *m/z*
	m/z 771	*m/z* 753	*m/z* 666			
Parent ions	771.154			IN-NRPPA	$C_{27}H_{33}N_8O_{15}P_2$	771.154
	753.140	753.166		IN-NRPPA-H_2O	$C_{27}H_{31}N_8O_{14}P_2$	753.144
			666.090	NHRPPA (NADH)	$C_{21}H_{30}N_7O_{14}P_2$	666.133
Fragmentation from the adenine end ("y" ions)			530.061	NHRPPR	$C_{16}H_{24}N_2O_{14}P_2$	530.070
			514.059	NHRPPR-NH_3	$C_{16}H_{22}NO_{14}P_2$	514.052
	424.093	424.101		IN-NRP	$C_{17}H_{19}N_3O_8P$	424.091
			319.073	NHRP	$C_{11}H_{16}N_2O_7P$	319.070
	229.044			IN-N	$C_{12}H_{10}N_3O_2$	229.085
			123.063	NH	$C_6H_7N_2O$	123.056
Fragmentation from the nicotinamide end ("b" ions)			649.109	NHRPPA-NH_3	$C_{21}H_{27}N_6O_{14}P_2$	649.106
	664.126			NRPPA	$C_{21}H_{28}N_7O_{14}P_2$	664.117
	542.078	542.072	542.082	RPPA	$C_{15}H_{22}N_5O_{13}P_2$	542.069
	524.059	524.067	524.067	RPPA-H_2O	$C_{15}H_{20}N_5O_{12}P_2$	524.058
	428.041	428.023	428.040	PPA	$C_{10}H_{16}N_5O_{10}P_2$	428.037
	348.073	348.070	348.071	PA	$C_{10}H_{15}N_5O_7P$	348.071
	250.094	250.087	250.100	A	$C_{10}H_{12}N_5O_3$	250.094
	136.070	136.065	136.064	Adenine	$C_5H_6N_5$	136.062

[a] The parent ions at m/z 771.153, 753.166, and 666.090 were selected individually and fragmented by tandem mass spectrometry.

[b] A, adenosine; N, nicotinamide; IN, isonicotinoyl group; R, ribose

using NADH or INH as substrate (Figure 3.3.9a and b and Table 3.3.6). This rate is further enhanced by the inclusion of 2 μM manganese ion (either Mn^{2+} or Mn^{3+}) (Table 3.3.2). NAD^+ is not a substrate for radical generation, and the rate of radical formation from a mixture of NAD^+ and INH is the same as with INH alone (Table 3.3.2) and is enhanced by Mn^{2+} (Table 3.3.2). The MtKatG and EcKatG mediated reactions of INH and NADH are both slower in the absence of Mn^{2+} (Table 3.3.2) but approach or exceed the BpKatG-mediated reaction in the presence of Mn^{2+} (Table 3.3.2). Based on HPLC retention times (Figure 3.3.10) combined with mass spectrometry and tandem mass spectrometry analysis (Table 3.3.9), the main products of the combined NADH and INH reaction with KatG are NAD^+ and isonicotinoyl-NAD with other products being present in smaller amounts. Isonicotinoyl-NAD elutes from the column as four peaks, all exhibiting an ion at *m/z* 771, consistent with a previous report (Wilming and Johnsson, 1999), which explained the elution pattern as the result of two stereoisomers, arising from the addition of the isonicotinoyl group to opposite faces of the nicotinamide ring, each with two rotamers, resulting from restricted rotation of the isonicotinoyl group. The time course of appearance and identity of isonicotinoyl-NAD were confirmed by mass spectrometry analysis of the reaction mixture, and the product ion at *m/z* 771, coincident with the mass of isonicotinoyl-NAD, was evident only in mixtures containing all three of KatG, INH, and NADH or NAD^+ (discussed in the next section). Tandem mass spectrometry measurements of the ions at *m/z* 753 and 771 produced almost identical fragmentation patterns, confirming that the ion at *m/z* 753 is a product of the parent ion at *m/z* 771 (Table 3.3.9). The difference in mass between the two ions, 18.014 Da, suggests the loss of H_2O (18.016 Da) but offers no clue as to the structural basis for the decay or

its cause. Comparison with the fragmentation pattern of NADH clearly confirms the presence of NAD in the pattern of fragments from the *m/z* 771 and 753 ions (Figure 3.3.12 and Table 3.3.9) degraded from the nicotinamide end and by inference allowing for the isonicotinoyl group, also after degradation from the adenine end (Table3.3.9).

3.3.3.1. NAD^+ as Precursor for Isonicotinoyl-NAD

The facile KatG-mediated oxidation of NADH and lack of apparent reaction with NAD^+ initially suggested that NADH, not NAD^+, is the precursor to isonicotinoyl-NAD. However, isonicotinoyl-NAD is formed in a KatG-mediated reaction more efficiently from a mixture of NAD^+ and INH (Figure 3.3.14) than from a mixture of NADH and INH, both with 2 μM Mn^{2+} (Figure 3.3.11). Therefore, NAD^+ is the probable precursor for isonicotinoyl-NAD as concluded earlier (Wilming and Johnsson, 1999), but NADH oxidation by KatG to NAD^+ will lead to the same product in an NADH mixture. The presence of 2 μM Mn^{2+} greatly speeds the NAD^+-dependent formation of isonicotinoyl-NAD by all seven KatGs: BpKatG, MtKatG, EcKatG, SyKatG, BsKatG, AfKatG and RcKatG (Table 3.3.7).

3.3.3.2. Comparison of the rate of isonicotinoyl-NAD synthase activity by KatGs

The synthesis of the isonicotinoyl-NAD adduct was monitored at 326 nm and the rate was determined using an extinction coefficient of 6900 M^{-1} cm^{-1} (Rawat *et al.*, 2003). All seven KatGs shows substantially higher rates for the synthase activity as compared to the control containing INH, NAD^+, and Mn^{2+} but no KatG (Figure 3.3.13 and Table 3.3.7) clearly demonstrating the significant role of KatGs in the formation of

Figure 3.3.13. Elution profiles from reverse phase HPLC of reaction products from mixtures containing 100 μM NAD^+, 200 μM INH, 2μM $MnCl_2$ and no enzyme (a); 1.2 μM BpKatG (b); 1.2 μM MtKatG (c); 1.2 μM EcKatG (d).*I*, isonicotinic acid hydrazide; *N-D*, NAD^+; *I-N*. isonicotinoyl-NAD. l_2(d).*I*,

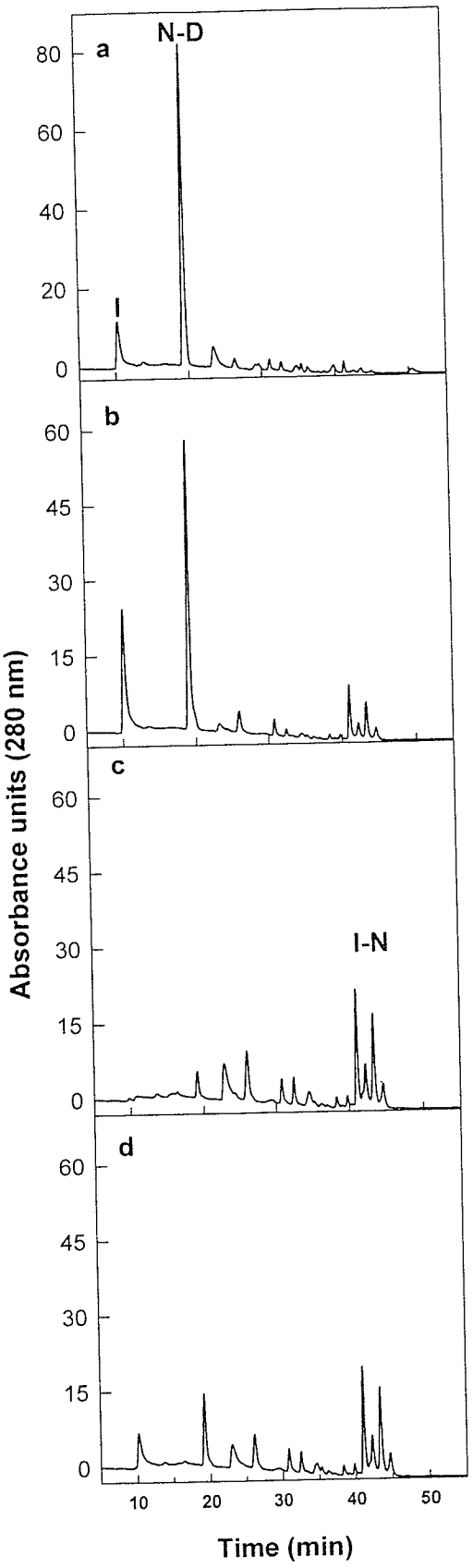
N-D
a
I
b
c
I-N
d
Absorbance units (280 nm)
Time (min)
0
20
40
60
80
15
30
45
10
50

Figure 3.3.14. Rate of synthesis of the isonicotinoyl-NAD adduct, a and b. The reaction mixture contained 100 μM NAD^+, 200 μM INH, 2μM $MnCl_2$, in 50 mM Tris-HCL (pH 8.0). Separate assays contain, no KatG, or 1.2 μM of BpKatG, MtKatG, EcKatG, SyKatG, BsKatG, AfKatG, RcKatG. Absorbance at 326 nm was monitored and an extinction coefficient of 6900 $M^{-1}cm^{-1}$ was used to calculate the amount of isonicotinoyl-NAD formed, assuming no interference from other minor products formed in the reaction.

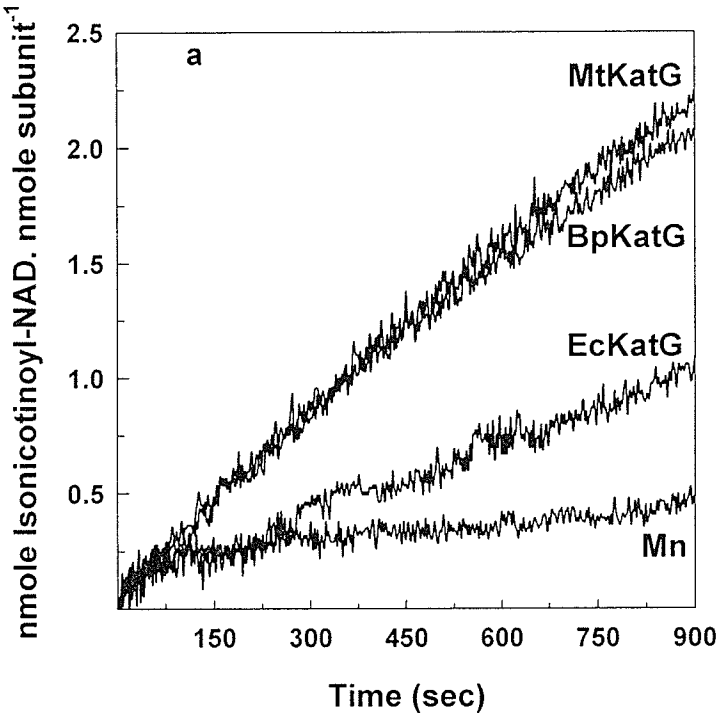
a
MtKatG
BpKatG
EcKatG
Mn
2.5
2.0
1.5
1.0
0.5
150
300
450
600
750
900
Time (sec)
nmole Isonicotinoyl-NAD. nmole subunit-1

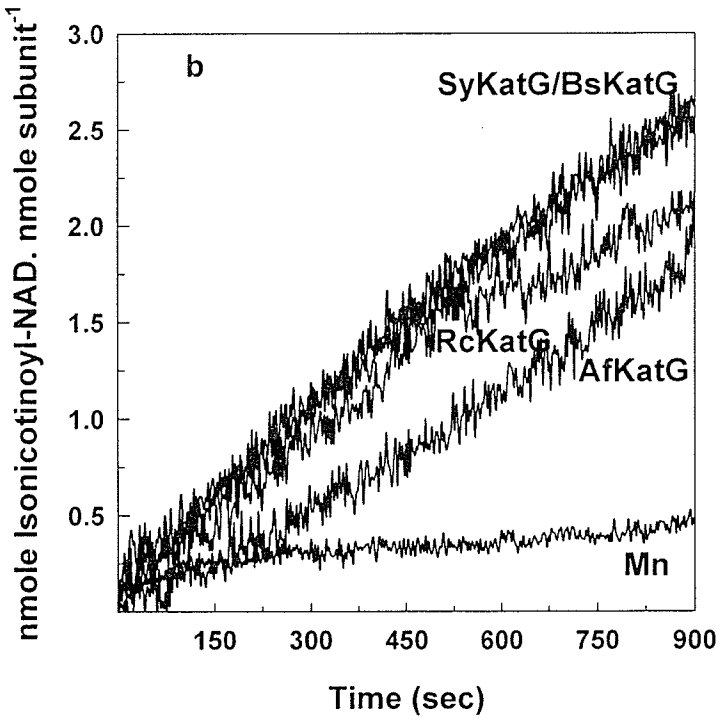
b
SyKatG/BsKatG
RcKatG
AfKatG
Mn
3.0
2.5
2.0
1.5
1.0
0.5
150
300
450
600
750
900
Time (sec)
nmole Isonicotinoyl-NAD. nmole subunit-1

isonicotinoyl-NAD adduct. Among the seven KatGs compared in this study, SyKatG demonstrates the highest rate for synthase activity followed by BsKatG, RcKatG, MtKatG, BpKatG, AfKatG and the EcKatG being the lowest.

3.3.5. NADH Oxidation Can Be Uncoupled from Superoxide Formation

It has been well documented that changing any one of a number of residues in KatG reduces catalase activity with minimal effect on peroxidase activity (Jakopitsch *et al.*, 2003; Yu *et al.*, 2003, Jakopitsch *et al.*, 2003; Regelsberger *et al*, 2000; Hillar *et al.*, 2000). A number of variants of BpKatG with residues changed in the active site cavity and in the Met-Tyr-Trp cross-linked structure (Yamada *et al.*, 2002; Carpena *et al.*, 2003) were assayed for oxidase and hydrazine lyase activities for comparison with their catalase and peroxidase activities (Table 3.6.8). The hydrazine lyase reaction was largely unaffected by any of the changes except the change of His112 to Ala. By contrast, the oxidase reaction was affected in several of the variants, and two groups with different properties can be discerned. One group, including those with changes in any of the three residues in the cross-linked structure of Trp111, Tyr238, and Met264, exhibits normal rates of NADH disappearance but significantly reduced rates of radical production. The apparent uncoupling of NADH oxidation from superoxide generation could be a result of a broken electron tunnel or of a change in the reaction chemistry to favor H_2O_2 over superoxide formation. Unfortunately, the unambiguous identification or quantification of H_2O_2 formed in the reaction is not possible because it is immediately utilized in a peroxidatic reaction. Indeed, an inconclusive 13% hypochromic and 3–5-nm red shift in the Soret band and little change in the 500–700 nm region are observed for the

Table 3.3.8. Comparison of catalase, peroxidase, and oxidase activities of BpKatG and its variants.

	Catalase	Peroxidase	Oxidase$_{(340nm)}$	Oxidase$_{(560nm)}$	Hydrazine lyase
			units/mg		
BpKatG	4100 ± 200	4.4 ± 0.5	6.9 ± 1.0	7.7 ± 1.2	0.9 ± 0.02
Arg108Ala	1250 ± 110	1.0 ± 0.1	3.7 ± 0.5	2.2 ± 0.4	0.3 ± 0.01
Arg108Lys	320 ± 20	09 ± 0.1	2.2 ± 0.2	1.3 ± 0.1	0.32 ± 0.01
His112Ala	1 ± 0.2	0.1 ± 0.01	ND[a]	ND[a]	ND[a]
His112Asn	2 ± 0.6	0.1 ± 0.01	3.1 ± 0.2	1.3 ± 0.5	0.2 ± 0.06
Trp111Phe	2 ± 0.1	3.3 ± 0.6	7.7 ± 2.4	ND[a]	0.5 ± 0.04
Asp141Ala	60 ± 10	5.8 ± 0.4	2.2 ± 0.1	0.7 ± 0.1	0.5 ± 0.1
Asp141Asn	390 ± 20	5.4 ± 0.3	2.8 ± 0.2	1.2 ± 0.2	0.6 ± 0.1
Asp141Glu	3290 ± 40	6.3 ± 1.7	3.4 ± 0.1	2.8 ± 0.2	0.8 ± 0.02
Tyr238Ala	2 ± 0.1	6.1 ± 0.1	10.8 ± 2.0	0.4 ± 0.1	0.5 ± 0.04
Tyr238Phe	6 ± 1.1	2.8 ± 0.3	10.3 ± 2.0	ND[a]	1.1 ± 0.05
Met264Ala	6 ± 1.1	7.0 ± 1.4	4.3 ± 0.1	ND[a]	0.6 ± 0.04
Met264Leu	2 ± 0.9	6.1 ± 1.3	11.0 ± 1.5	4.9 0.6	1.0 ± 0.06
MtKatG	3550 ± 160	9.7 ± 0.2	2.4 ± 0.8	1.2 ± 0.2	1.0 ± 0.06
EcKatG	2320 ± 230	9.9 ± 0.3	1.1 ± 0.4	0.2 ± 0.05	0.5 ± 0.02

[a] ND, not determined.

BpKatG variants Arg108Ala, Arg108Lys, His112Ala, His112Asn, Asp141Ala, Asp141Asn, Asp141Glu were constructed and characterized by MR. Taweewat Deemagarn; Tyr238Ala, Tyr238Phe, Met264Ala, Met264Lys were constructed and characterized by MR. Ben Wiseman; Trp111Phe was constructed by MR. Jack Switala

Trp111Phe and Tyr238Phe variants during the oxidase reaction, whereas no change in native BpKatG. The second group exhibits reduced rates of both NADH disappearance and superoxide formation, consistent with reduced NADH oxidation. This group includes those with changes in the active site residues Arg108, His112, and Asp141. The changes in catalase and peroxidase activities caused by the sequence changes are consistent with those reported previously for KatGs from *Synechocystis* (Regelsberger *et al*, 2000; Yu *et al*, 2003; Regelsberger *et al*, 2000), *M. tuberculosis* (Yu *et al*, 2003), and *E. coli* (Hillar *et al*., 2000).

3.4. Resistance against isoniazid in *Mycobacterium tuberculosis*.

3.4.1. Introduction

Multidrug-resistant strains of *Mycobacterium tuberculosis* seriously threaten tuberculosis (TB) control and prevention efforts. Resistance against isoniazid was reported soon after its first use in 1951 (Middlebrook, 1954). Simultaneously a correlation between INH resistance and the loss of catalase-peroxidase activity was discovered in the early 1950's from the clinical isolates of *M. tuberculosis* (Middlebrook *et al*., 1954a; Middlebrook, 1954b; Middlebrook, 1954c). There was also a report mentioning *katG* deletion from the chromosome of two strains with high level INH-resistance isolates (MIC > 50 mg/ml) (Zhang *et al*., 1992). However, many subsequent studies have shown that the vast majority of INH resistance strains contain the *katG* gene, a result indicating that deletion of this gene is very rare among patient isolates (Ramaswamy and Musser, 1998 and other reviews therein). Almost 50–60% INH

resistance patient isolates have missense mutations, or small deletions or insertions that are not represented among INH sensitive control strains (Musser, 1995). A wide array of distinct KatG mutations have been reported among INH resistance isolates but a point mutation of Ser at position 315 is the most abundant. Statistically, the most common amino acid substitution is AGC (Ser)->ACC (Thr), but ACA (Thr), ATC (Ile),AGA (Arg), CGC (Arg), AAC (Asp), and GGC (Gly) changes also have been identified (Ramaswamy and Musser, 1998). As a result, Ser315Thr is one of the most characterized variants of MtKatG and has recently had its crystal structure determined (Zhao *et al.*, 2006). To determine the effect of Ser315 mutation on hydrazine lyase, NADH oxidase and isonicotinoyl-NAD synthase activities of KatGs, Ser315Thr and Ser315Asn variants of MtKatG were constructed and characterized.

3.4.2. Purification of Ser315Thr, Ser315Asn variants of *M. tuberculosis* catalase-peroxidase

Purification of Ser315Thr and S315Asn variants employed the same protocol as described in section 3.2.1. Purified variants migrate on denaturing SDS-PAGE predominantly as a single band with a molecular mass of ~ 80 kDa (Figure 3.4.1). Comparative absorption spectra of the native MtkatG and the variants revealed similar absorbance peaks in the Sorêt region at 408 nm and in the charge transfer region (Figure 3.4.2 and Table 3.4.1). The Rz ratio of both Ser315Thr and Ser315Ans was comparable to that of native enzyme (Table 3.4.1) demonstrating more than 90% occupancy of heme.

3.4.3. Catalase and peroxidase specific activities of MtKatG and variants

Purified Ser315Thr variant exhibited catalase specific activity comparable to that of the native enzyme, while the Ser315Asn variant exhibited a 50 % decrease in the catalase specific activity (Table 3.4.2). The peroxidase specific activities of the variants are significantly lower than those of the native enzyme with Ser315Thr being only 50% and 60% as active with ABTS and *o*-dianisidine respectively as electron donors. Even more striking, Ser315Asn variant is only 10% and 35% as active as the native enzyme with ABTS and *o*-dianisidine, respectively (Table 3.4.2).

3.4.4. Kinetic characterization of Ser315Thr and Ser315Asn variants.

A comparative analysis of the catalatic kinetic constants for native MtKatG and variants has been demonstrated in the Table 3.4.3 and Figure 3.4.3. They reveal comparable V_{max} values for both the MtKatG and Ser315Thr variants with Ser315Asn about 50% lower. Surprisingly the K_m of the Ser315Thr variant for H_2O_2 is six times higher than that of the native enzyme whereas the K_m of the Ser315Asn variant for H_2O_2 is lower by 60% than the native enzyme. The changes in the V_{max} and K_m values are indicative of the changes caused by these mutations in the heme environment and disruption in the substrate access channel to the active site heme. Ser315Thr consistent with the specific activities, exhibits a turnover rate comparable to that of native enzyme with a much reduced turnover rate, whereas Ser315Asn is reduced to almost 50% but with a specificity constant similar to that of the native enzyme.

Peroxidatic kinetic constants for native MtKatG and Ser315Thr and Ser315Asn variants are shown in the Table 3.4.4 and Figures 3.4.5 and 3.4.6. Both variants exhibit a

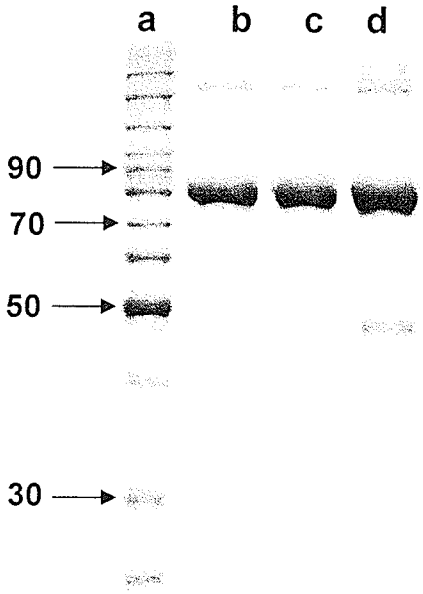

Figure 3.4.1. SDS-polyacrylamide analysis of purified MtKatG and variants Ser315Thr and Ser315Asn. Approxmately 5 μg of protein was loaded and run on an 8% polyacrylamide gel and stained with Coomassie brilliant blue. Lane *a*, protein ladder; *b* MtKatG; *c*, Ser315Thr; *d*, Ser315Asn.

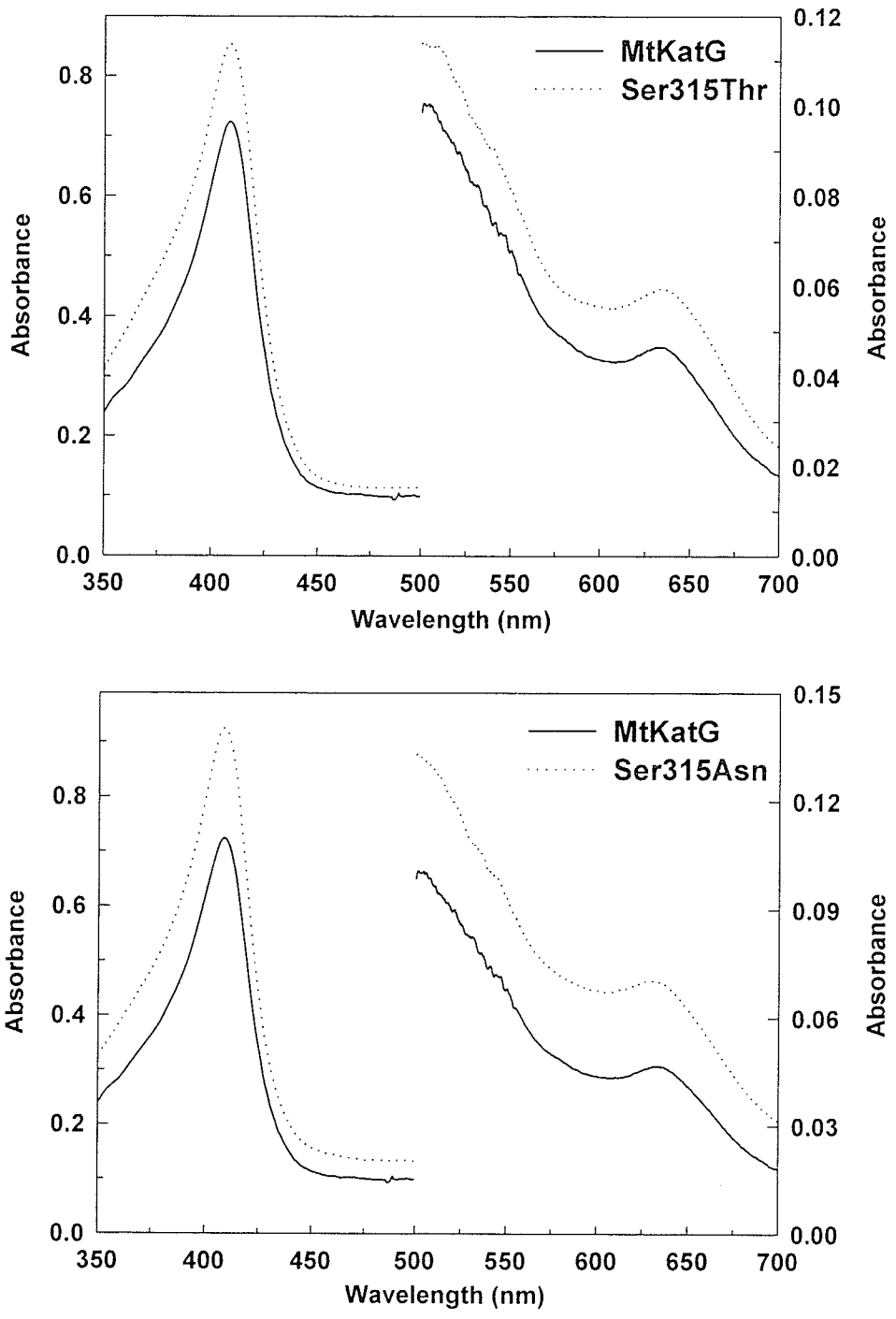

Figure 3.4.2. Absorption spectra of MtKatG and variants Ser315Thr and Ser315Asn. The left axis is for the range from 350 to 500nm while the right axis is for the range from 500 to 700 nm.

Table 3.4.1. Comparison of observed optical absorbance maxima, A407/280 ratio and heme/subunit ratio for purified KatGs.

KatG	Sorêt maximum (nm)	$A_{407/280}$ ratio	Theoretical $A_{407/280}$ ratios[a]	Heme/subunit ratio
MtKatG	408	0.60	0.61	0.98
Ser315Thr	408	0.54	0.61	0.88
Ser315Asn	408	0.56	0.61	0.92

[a] ε at 280 nm calculated based on the $\varepsilon_{TRP} = 5500\ M^{-1}\ cm^{-1}$ and $\varepsilon_{TYR} = 1490\ M^{-1}\ cm^{-1}$ and ε at 407 nm for heme estimated to be $100{,}000\ M^{-1}\ cm^{-1}$

Table 3.4.2. Comparison of catalase and peroxidase activities of MtKatGs and Ser315Thr and Ser315Asn variants.

KatG	Catalase (units/mg)[a]	Peroxidase	
		ABTS[b] (units/mg)[a]	***o*-dianisidine**[c] (units/mg)[a]
MtKatG	4450 ± 140	10 ± 2.5	8.8 ± 1.5
Ser315Thr	4200 ± 480	4.3 ± 0.3	5.4 ± 0.8
Ser315Asn	1880 ± 180	1.3 ± 0.2	3.1 ± 0.4

[a] Data expressed as μmole H_2O_2. min^{-1}. mg^{-1}

[a] Data expressed as μmole ABTS. min^{-1}. mg^{-1}

[a] Data expressed as μmole *o*-dianisidine. min^{-1}. mg^{-1}

50% reduction in the V_{max} values as compared to that of the native enzyme. The K_m of Ser315Thr for ABTS is 1.5 times higher and that for Ser315Asn is 25% lower as compared to the native enzyme. The K_m values for H_2O_2 (required only for generation of the compound I in the peroxidase activity) are similar for both native enzyme and Ser315Thr variant whereas the Ser315Asn variant has a K_m two times higher than the native enzyme.

3.4.5. Comparison of heme inhibition by cyanide and azide.

Both variants are inhibited by cyanide and azide, classical heme protein inhibitors (Figure 3.4.7 and Table 3.4.5). Ser315Thr shows 50% inhibition of catalase activity at 55 μM concentration of KCN while the Ser315Asn variant requirs 126 μM KCN for 50% inhibition as compared to 112 μM needed for native MtKatG. For NaN_3, both variants exhibit 22-25 times higher IC_{50} values than the same needed for native MtKatG (Figure 3.4.7 and Table 3.4.5) consistent with the mutation constricting the substrate access channel.

3.4.6. Effect of Ser315 mutation on NADH oxidase activity and isoniazid activation.

Neither Ser315Thr nor Ser315Asn exhibit NADH oxidase activity at 340 nm although Ser315Thr shows very low levels of radical formation using NADH as substrate and NBT as radical sensor (Figure 3.4.8 and Table 3.4.6). In addition a low level of hydrazine lyase activity is associated with both Ser315Thr and Ser315Asn as compared to the native enzyme. Similar results are evident when 2 μM of Mn^{2+} was added to the

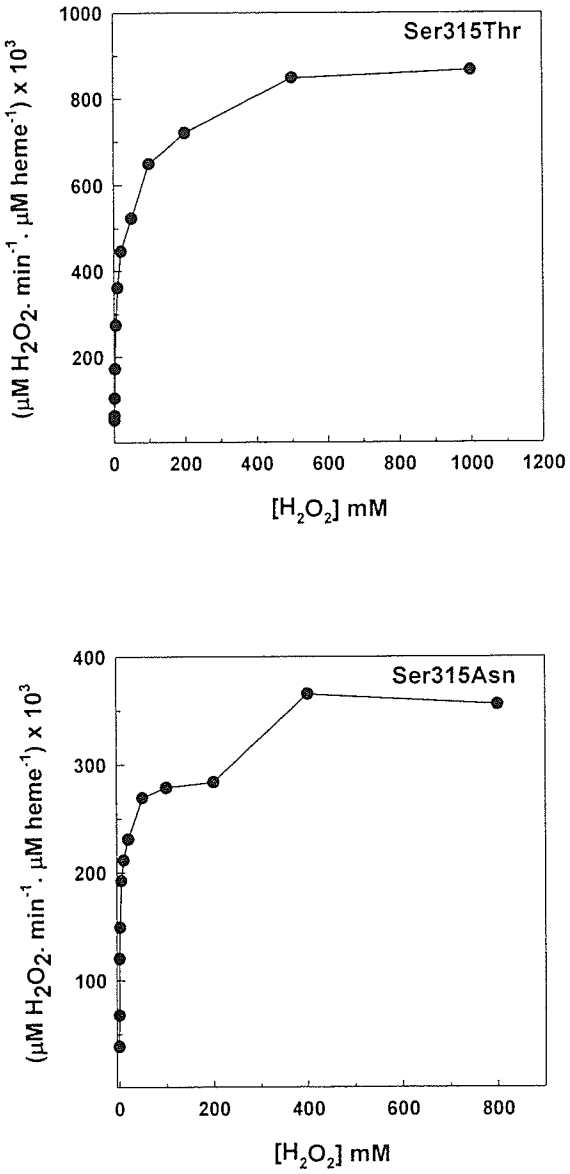

Figure 3.4.3. Effect of H_2O_2 concentration on the initial catalatic velocities of S31T and Ser315Asn variants of MtKatG.

Table 3.4.3. Comparison of the observed catalatic kinetic parameters of purified MtKatG and Ser315Thr and Ser315Asn variants using H_2O_2 as substrate.

KatG	V_{max}[a]	K_m (mM)	k_{cat} (s^{-1})	k_{cat}/K_m ($M^{-1}s^{-1}$)
MtKatG	$460 \pm 22 \times 10^3$	2.4 ± 0.5	7600	3.2×10^6
Ser315Thr	$440 \pm 27 \times 10^3$	13 ± 2.6	7300	0.6×10^6
Ser315Asn	$240 \pm 32 \times 10^3$	1.4 ± 0.9	4000	2.9×10^6

[a] V_{max} is expressed as μmoles of H_2O_2 decomposed min^{-1} μmole $heme^{-1}$

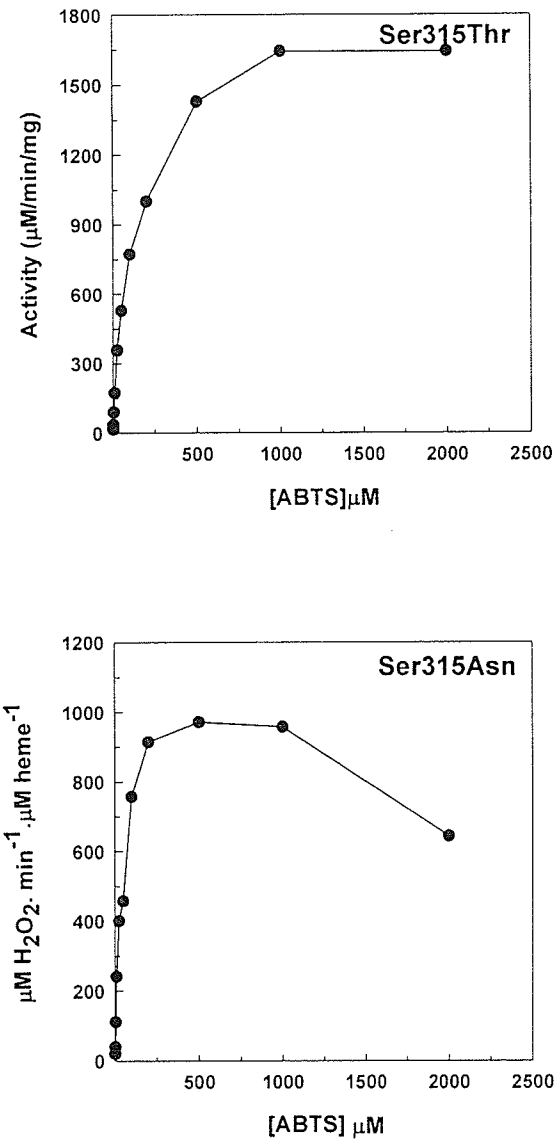

Figure 3.4.4. Effect of ABTS concentration on the initial catalatic velocities of Ser315Thr and Ser315Asn variants of MtKatG.

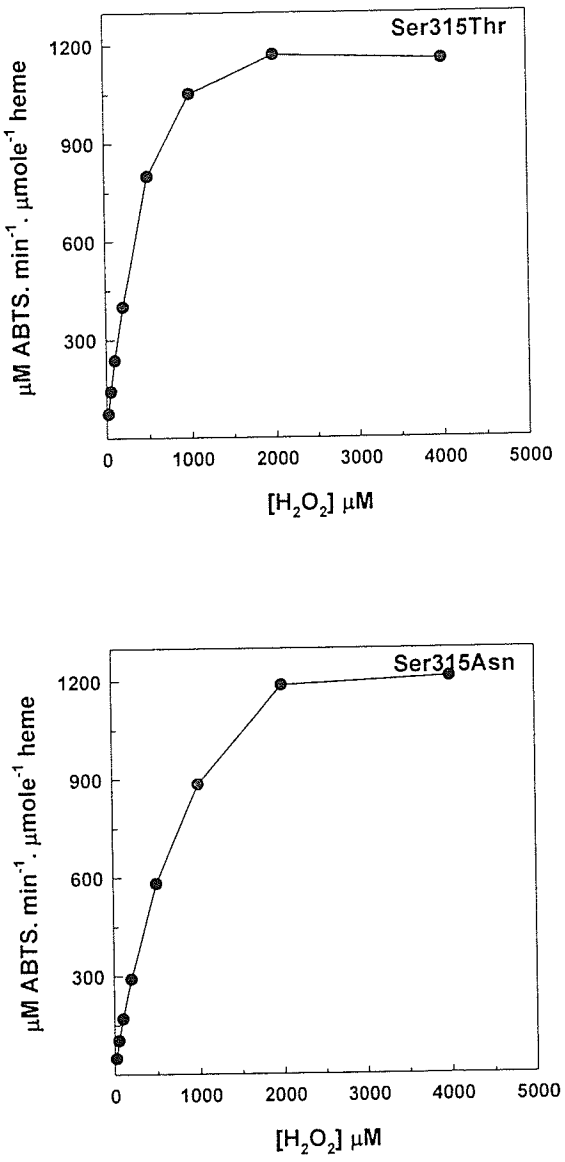

Figure 3.4.5. Effect of H_2O_2 concentration on the initial peroxidatic velocities of Ser315Thr and Ser315Asn variants of MtkatG.

Table 3.4.4. Comparison of the observed peroxidatic kinetic parameters of purified MtKatG and Ser315Thr and Ser315Asn variants using ABTS as substrate.

KatG	V_{max} [a]	K_m [b] (μM)	K_m [c] (μM)	k_{cat} (s^{-1})	k_{cat}/K_m ($M^{-1}s^{-1}$)
MtKatG	1870 ± 53	67 ± 7	360 ± 102	31 ± 0.9	4.5×10^5
Ser315Thr	940 ± 32	100 ± 16	380 ± 59	42 ± 0.5	5.0×10^5
Ser315Asn	830 ± 30	50 ± 3	740 ± 101	14 ± 0.5	2.8×10^5

[a] V_{max} is expressed as μmoles of ABTS decomposed min^{-1} μmole $heme^{-1}$

[b] K_m shown for ABTS, [c] K_m shown for H_2O_2

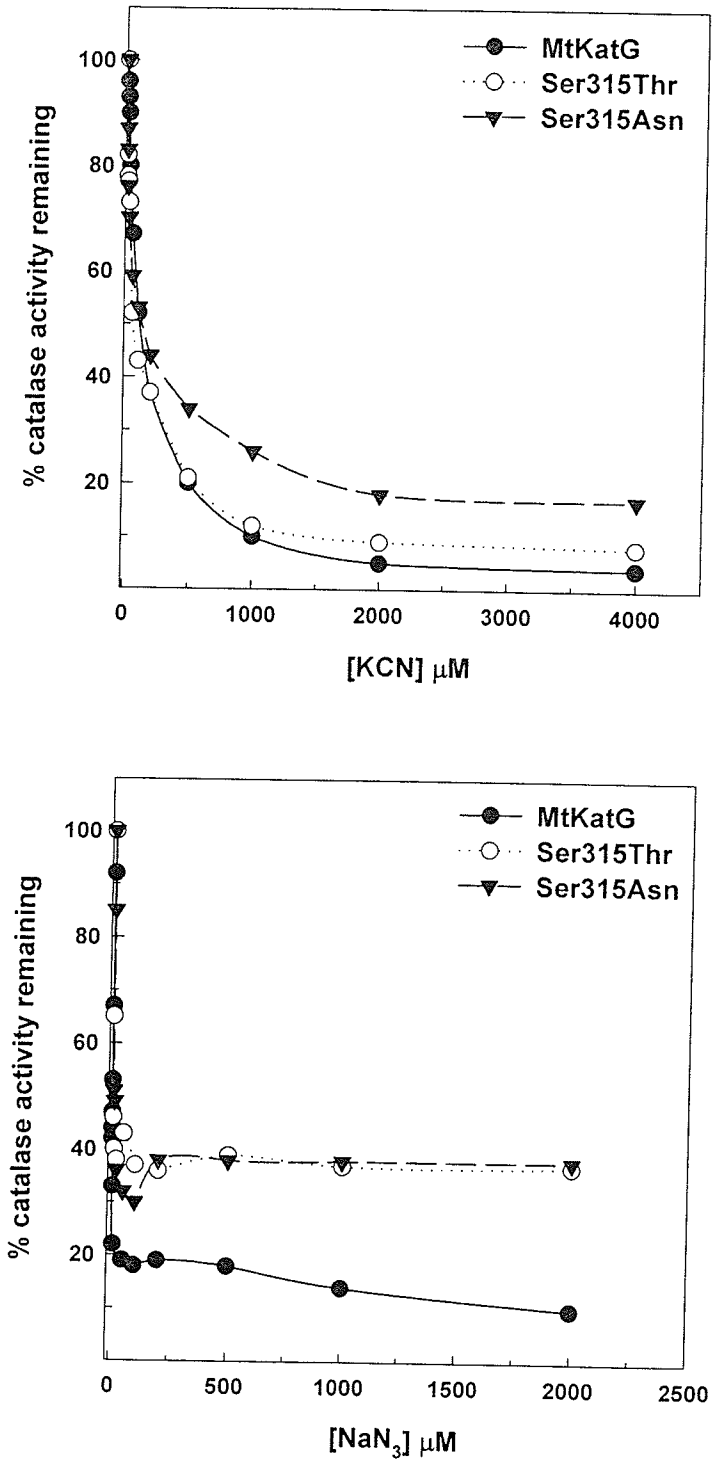

Figure 3.4.6. Comparison of sensitivity of MtKatG and its variants to cyanide (KCN) or azide (NaN_3).

Table 3.4.5. Comparison of sensitivity of KatG and its variants to cyanide (KCN) or azide (NaN_3).

KatG	[KCN] causing 50% inhibition (μM)	[NaN_3] causing 50% inhibition (μM)
MtKatG	98	0.2
Ser315Thr	55	5
Ser315Asn	110	4.5

Figure 3.4.7. NADH oxidation by MtKatG and variants Ser315Thr and Ser315Asn. *a*, the rates of radical production in a solution containing 100 μM NADH, 1.2 μM enzyme , 200 μM NBT and 50 mM Tris, pH 8.75, are followed by formazan appearance measured at 560 nm. Separate assays contain no enzyme (control), MtKatG, S315Tand Ser315Asn. *b*, the rates of NADH oxidation in a solution containing 100 μM NADH, 1.2 μM enzyme, and 50 mM Tris, pH 8.75 were followed by NADH disappearance measured at 340 nm. Separate assays contain no enzyme (control), MtKatG, S315Tand Ser315Asn.

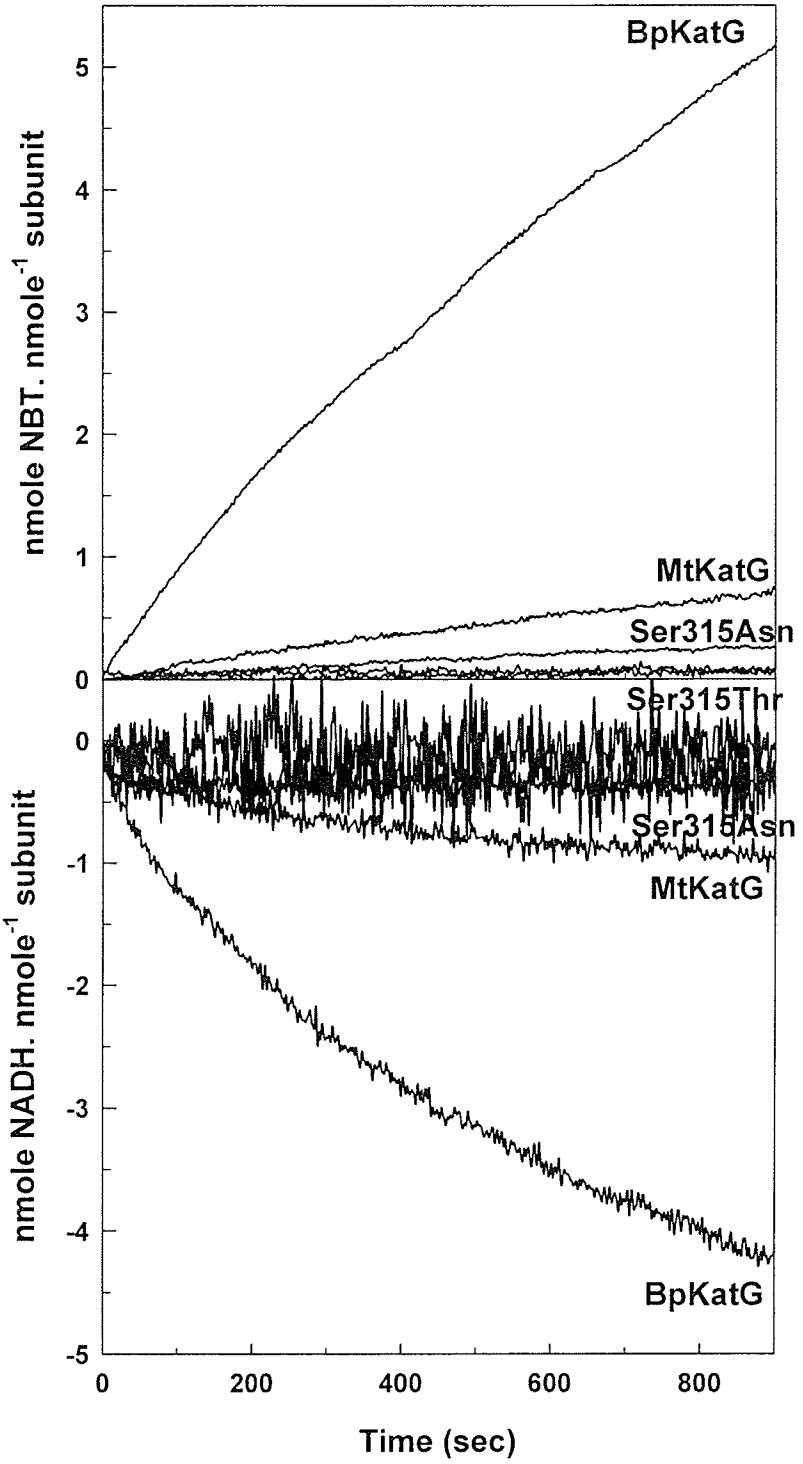
BpKatG
MtKatG
Ser315Asn
Ser315Thr
Ser315Asn
MtKatG
BpKatG
nmole NBT. nmole-1 subunit
nmole NADH. nmole-1 subunit
Time (sec)
5
4
3
2
1
0
0
-1
-2
-3
-4
-5
0
200
400
600
800

Figure 3.4.8. Removal of hydrazine form isoniazid by MtKatG and variants. *a*, radical generation in a solution containing 10 mM INH, 200 mM NBT as radical sensor in 50 mM Tris, pH 8.0, was followed by formazan appearance measured at 560 nm. Separate assays contain no enzyme (control), MtKatG and variants Ser315Thr and Ser315Asn. *b*, Similar assay conditions were employed to determine the effect of Mn^{2+} on the hydrazine lyase reaction.

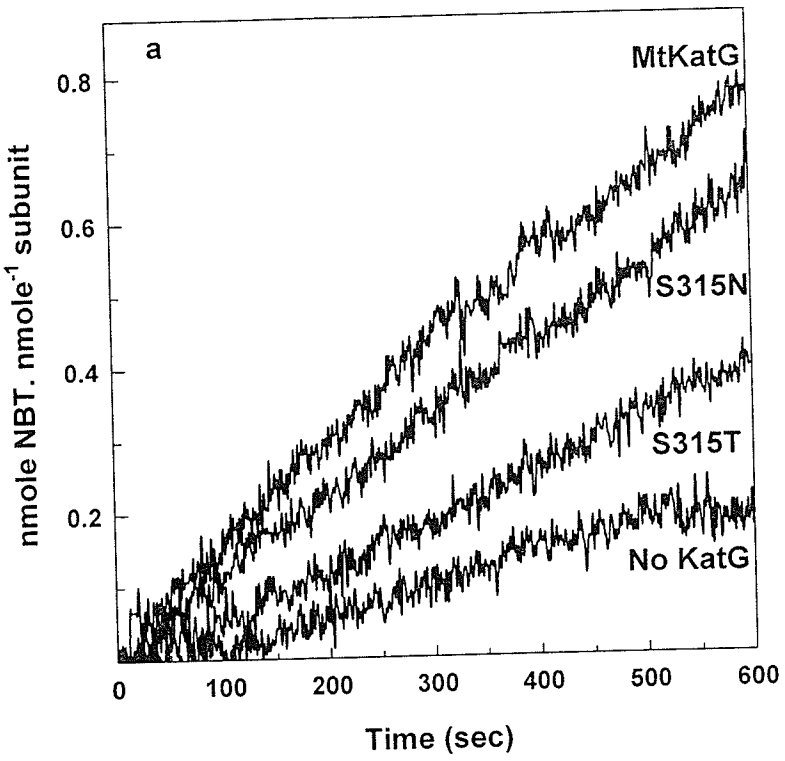
a
MtKatG
S315N
S315T
No KatG
nmole NBT. nmole^{-1} subunit
0.8
0.6
0.4
0.2
0
100
200
300
400
500
600
Time (sec)

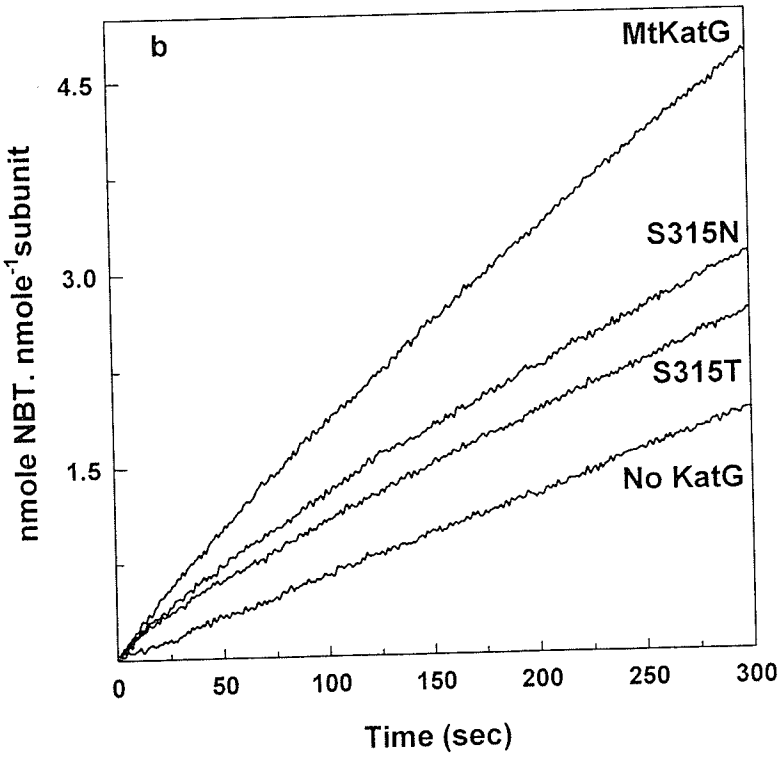
b
MtKatG
S315N
S315T
No KatG
nmole NBT. nmole^{-1}subunit
4.5
3.0
1.5
0
50
100
150
200
250
300
Time (sec)

Figure 3.4.9. Effect of NADH on the hydrazine lyase activity by MtKatG and variants *a*, Isonicotinoyl-NAD synthase activity by MtKatG and variants *b*.

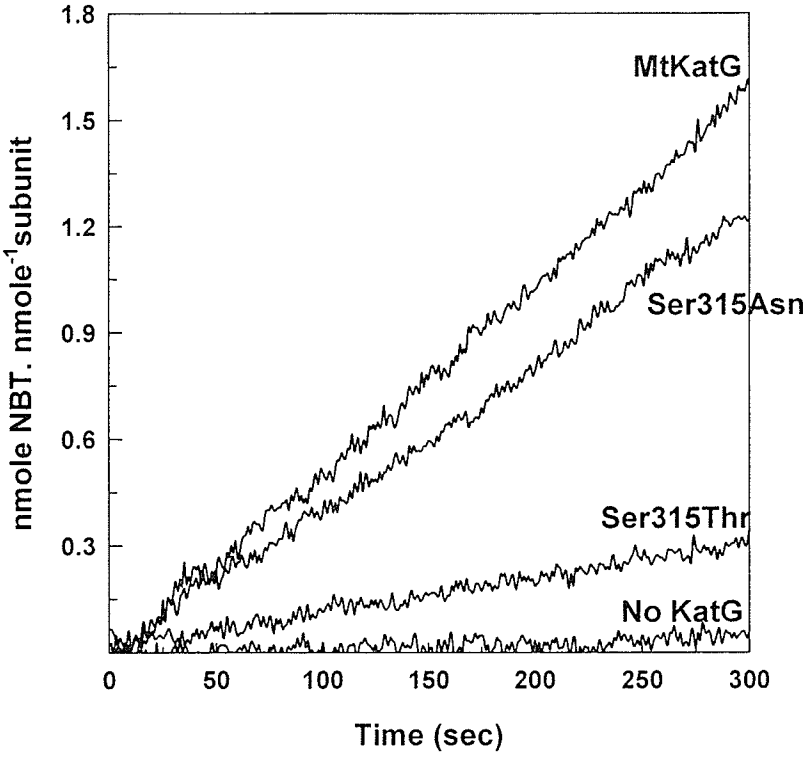
1.8
1.5
1.2
0.9
0.6
0.3
nmole NBT. nmole^{-1}subunit
MtKatG
Ser315Asn
Ser315Thr
No KatG
0
50
100
150
200
250
300
Time (sec)

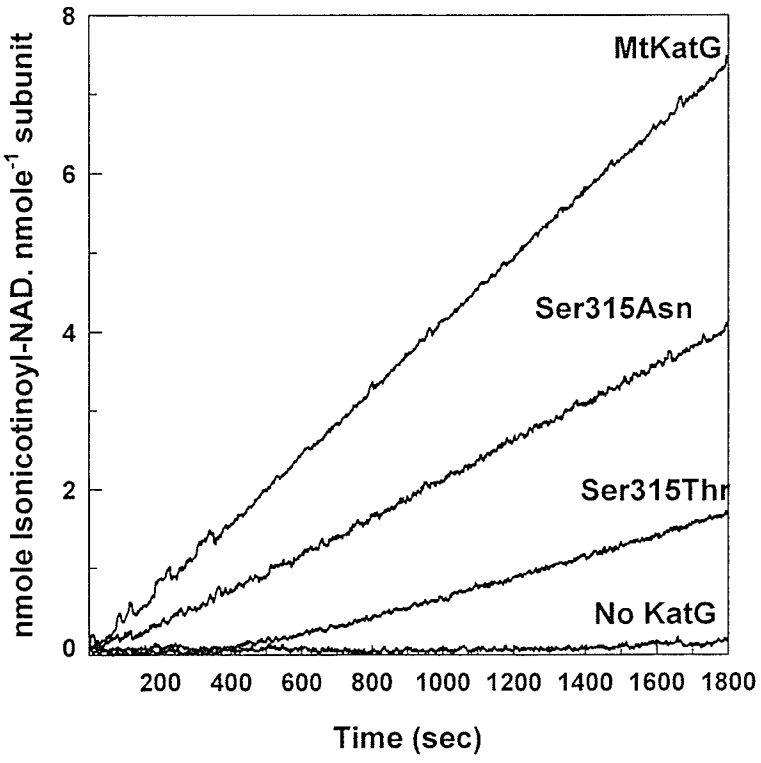
8
6
4
2
0
nmole Isonicotinoyl-NAD. nmole^{-1} subunit
MtKatG
Ser315Asn
Ser315Thr
No KatG
200
400
600
800
1000
1200
1400
1600
1800
Time (sec)

Table 3.4.6. Comparison of NADH oxidase activity, hydrazine lyase, and synthase activity by MtKatG and variants.

	MtkatG[a]	Ser315Thr[a]	Ser315Asn[a]
NADH oxidase (A_{560})	100 ± 15	ND	20
NADH oxidase (A_{340})	30 ± 3	ND	ND
INH hydrazine lyase	78 ± 9	27 ± 3	60 ± 5
INH + NADH	1140 ± 76	57 ± 5	115 ± 6
INH + Mn^{+2}	460 ± 5	250 ± 15	320 ± 10
Isonicotinoyl-NAD synthase[b]	93 ± 6	20 ± 4	30 ± 8

[a] Data expressed as pmole. min^{-1}. $nmole^{-1}$ subunit

[b] Data expressed as pmole. min-1. $mmole^{-1}$ subunit

ND, not determined

reaction mixture (Figure 3.4.9 and Table 3.4.6) demonstrating the significance of the native enzyme structure in drug activation. Following this trend, the rate of radical production from a reaction mixture including INH and NADH is 20 times lower for Ser315Thr and 10 times lower for Ser315Asn variant as compared to the native enzyme (Figure 3.4.10 and Table 3.4.6). Most significantly, the isonicotinoyl-NAD synthase activity is almost five times lower for Ser315Thr variant and three times lower for Ser315Asn variant compared to the native enzyme. These results are consistent with the reports demonstrating the lower sensitivity to isoniazid of clinical isolates carrying Ser315 mutation on *katG* of *M. tuberculosis*.

4. Discussion

4.1. Location of conserved residues in catalase-peroxidases

Because the *in vivo* peroxidase substrates remain unidentified, possible substrate-binding sites, for as yet unidentified substrates, was a topic for speculation in the original report of the BpKatG structure (Carpena *et al.*, 2002). Unambiguous identification of such sites will have to await a crystal structure determination of protein-ligand complexes. Evidence for a diversity of substrate binding sites in KatGs is shown in the high frequency of highly conserved residues (Table 4.1) and their broad distribution throughout the KatG subunit including on the surface (Figure 4.1). Over 27 and 18% of the residues, respectively, in the catalytic N-terminal domain and noncatalytic C-terminal domain of the KatG subunit are identical in more than 95% of the sequences available for KatGs. This is compared with the 8–14% frequency of nearly identical residues, all located near the active sites in pyruvate kinases, catalases, peroxidases, CuZn SODs, and FeMn SODs. Seven KatGs used in this study also have 50-70% similarity in the amino acid sequence (Figure 4.2) and, the four crystal structures that have appeared so far (Yamada *et al.*, 2002; Carpena *et al.*, 2003; Vada *et al.*, 2002; and Bertrand *et al.*, 2004) exhibit a high degree of structural integrity particularly in the vicinity of heme (Figure 1.3). All four KatGs adopt similar folds with MtKatG sharing 55% identity and 69% similarity with HmKatG and 66% identity and 77% similarity with BpKatG (Bertrand *et al.*, 2004). C α backbone superpositions show root mean square deviations of 1.18 and 0.82 Å between MtKatG with HmKatG or BpKatG, respectively. Active site residues are conserved and align well in all three structures, and there are few structural differences in the three-dimensional arrangement of the polypeptide chains. In

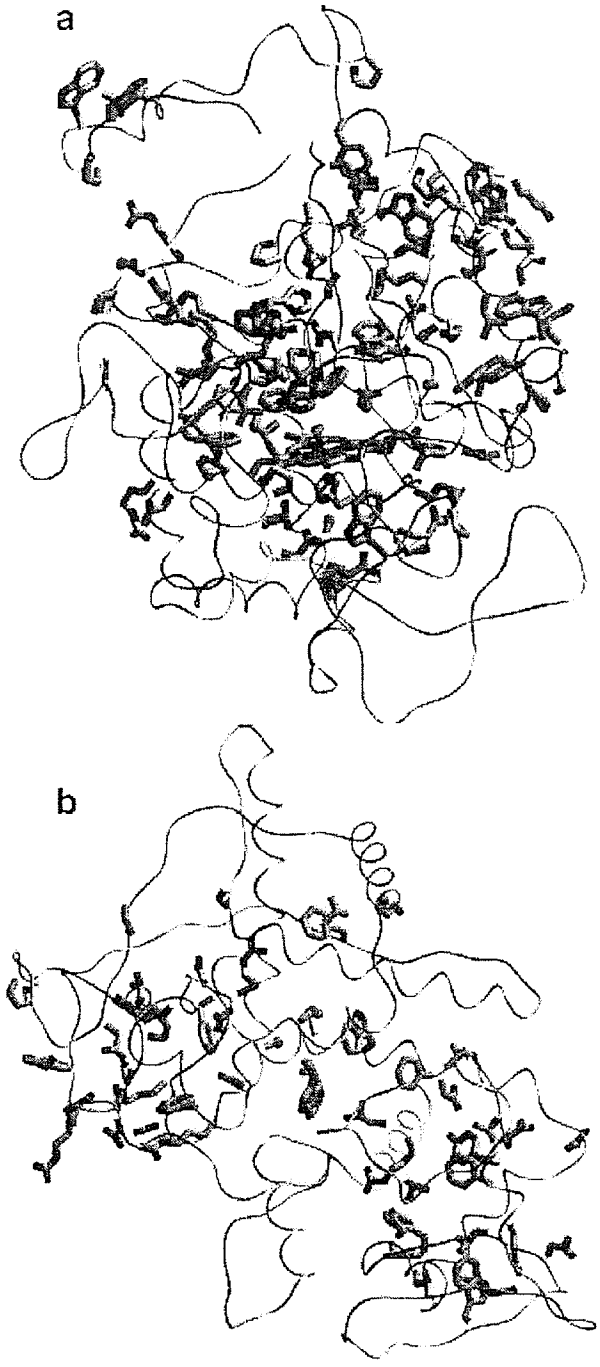

Figure 4.1. Location of residues in BpKatG that are identical in more than 95% of the 53 catalase-peroxidase sequences available. The distribution in the N-terminal domain is shown in *a*, and the distribution in the C-terminal domain is shown in *b*. The domains are treated separately for a clearer representation of the differences.

Table 4.1 Comparison of the percentage of highly conserved residues (>95% identical) in KatGs compared to other families of proteins

	KatG		SOD				
			Catalase			Peroxidase	Pyruvate kinase
	N-terminal	C-terminal		CuZn	FeMn		
No. in family	52[a]	52[a]	228[a]	22[b]	25[c]	24[d]	28[e]
Length	390	322	490	155	238	294	470
No. with >95% identity	107	59	57	22	22	24	59
Percentage with >95% identity	27.4	18.3	11.6	14.2	9.2	8.2	12.3

[a] Accession numbers are described by Klotz and Loewen (Klotz and Loewen, 2003)

[b] The accession numbers for the sequences used are: AA054860, AAR15417 AB087845, AF312586, AF312588, AF318938, AJ581746, AY428604, AY434497, BAC96317 BC061861, CAC28938 Jo2658, J04087, L13778, M15175, M84013, NM011435, NM174615, NP012638, NP231223, NP940620, P24704, X97766, and XM358882

[c] The accession numbers for the sequences used are: AAN16456 AA057908, AB093035, AB109302, AF318020, AY314980, J03511, L11707, L25675, M33119, M60401, M74242, M94879, M96560, NM013671, NM057577, NM059889, NP011872, NP231679, NP232322, NP704405, NP940564, Q8K6Y8, and X03951

[d] The accession numbers for the sequences used are: AB027752, AB009084, AB022273, AB024437, AB027752, AB027753, AF039027, AF109123, AF139910, AF149278, AF155124, AF159380, AF159629, AF175710, AJ003141, AJ011939, D11102, D11337, D14442, D83669, D84400, D90115, M60729, Y16773, and Y17192

[e] The accession numbers for the sequences used are: AAB47952 AAH16619 AAH19265 AAHY25737, AAH61541 AAO57788 AAQ57928 BAC91436 BAD01636 CAA24631 CAE07913 CAE14987 CAE20854 NP230139, NP231642, NP416191, NP416368, NP703926, NP721573, NP881869, NP934082, NP939895, Q8Z6K2, Q9Z9B4, Q89AI8, XP224416, XP341924, ZP00026409, ZP00078743, and ZP000122573

particular, the covalent modification linking the distal Trp 111, Tyr238 and Met264 residues (BpKatG numbering), which are fully conserved in all seven KatGs used in this study, plays a crucial role in the modulation of catalase activity in these heme proteins (Donald *et al.*, 2003; Jakospitch *et al.*, 2003d). This modification is unique to KatGs and has been reported in all four crystal structures and confirmed using mass spectrometry (Donald *et al.*, 2003; Jakospitch *et al.*, 2003; Ghiladi *et al.*, 2005; and Ghiladi *et al.*, 2005a). Despite these apparent structural similarities, this study demonstrates significant differences upon interaction of KatGs with various substrates and in the catalytic efficiency of the reactions indicating the importance of subtle changes within the KatG backbone in the regulation of activities.

4.2. Overview and comparison of catalase and peroxidase activities

Seven KatGs studied demonstrated different levels of catalase and peroxidase activities ranging from 3700-6000 U/mg. The enzyme kinetics reveal differences in V_{max} and K_m values. For example, the catalatic K_m for H_2O_2 of MtKatG is 2.4 mM, but for BpKatG and EckatG, the K_ms are 4.3 and 4.2 mM (Table 3.6). Similarly the turnover rates for all seven KatGs vary from 7600 to 17300 s^{-1} and k_{cat}/K_m values also vary from 2 to 5.6 $M^{-1}s^{-1}$ (Table 3.6). These variations are significant and a plausible explanation could be the differences in the substrate access channel. In KatGs there are conserved acidic residues in the main access channel: Glu242 (BpKatG numbering) at the entrance and Asp141 at the 3–4 Å wide constriction (Smuelvich *et al.*, 2006). Both residues are critical for stabilizing the solute matrix in the channel and for orienting the water dipoles. In addition, Asp141 controls the access to the distal residues Arg108, His112 and Trp111.

These residues are conserved in the seven KatGs used in this study. Thus, the differences in the affinity for the substrate could also be arising from the presence of some other access route for the substrate apart from the main channel. Interestingly there are not significant differences in the pH optimum for the catalase activity which remains between pH 6.25 and 6.5 for seven KatG studies. This suggests that highly conserved active site residues modulate the catalase activity in a similar fashion and require a similar pH environment irrespective of the type of KatG.

Although the *in vivo* peroxidatic substrate is still unknown, various organic electron donors such as ABTS and *o*-dianisidine are used as *in vitro* peroxidatic substrates. Each KatG has a different affinity for the same substrate such as ABTS, where the K_m ranges from 7 to 300 μM in the seven enzymes studied (Table 3.7). Binding of the same substrate with different affinity to different KatGs could be attributed to the differences in the binding sites on the protein. Even between two different substrates used in this study (ABTS and *o*-dianisidine), different kinetic constants for peroxidase activity were noted among the enzymes but exhibited similar optimum pHs (Table 3.4) suggesting a common reaction involving similar catalytic residues. The specificity constants (k_{cat}/K_m) and the K_m for H_2O_2 for compound I formation for the peroxidase activity of the seven KatGs varied 20-80 folds from 0.5 to 40 x 10^5 $M^{-1}s^{-1}$ and 58 μM to 1 mM respectively. The structures of the peroxidatic substrates will play an important role in their binding to the enzyme and differences in the surface topology caused by sequence variations will affect their affinity toward enzyme. Cytochrome c, the peroxidatic substrate for Cytochrome *c* peroxidase (CcP), bounds at the surface of CcP and the electron transfer between the enzyme and substrate occurs through protein based radicals

formed on the CcP (Millett *et al.*, 1995). A similar process could be a possibility with KatGs since they are closer to plant peroxidases in sequence and structure. In such a case, protein based radicals could play an important role in electron transfer from the heme to the distantly bound peroxidatic substrate. There are reports mentioning the formation of such protein based radicals in KatGs (Ivancich *et al.*, 2003; Zhao *et al.*, 2004) and determining the location and understanding the role of such protein radicals will be crucial in determining the peroxidatic reaction of KatGs. It is expected that studies such as this will eventually lead to the identification of the actual *in vivo* substrates for KatGs and as a result the significance of this activity for the organisms.

Heme inhibition by classical heme inhibitors also demonstrates different IC_{50} value for different KatGs. For example, SyKatG and AfKatG needed almost three times higher concentration of KCN as compared to that needed by BpKatG, MtKatG and EcKatG for 50% inhibition of catalase activity. On the other hand, MtKatG needed a mere 0.2 μM NaN_3 for 50% inhibition in contrast to 20 μM needed by AfKatG (Table 3.9).

4.3. The oxidase, lyase and synthase activities of KatGs

The existence of catalase, peroxidase, and oxidase activities in a single protein makes KatG a complex and fascinating enzyme, an assessment further enhanced by INH hydrazine lyase and isonicotinoyl-NAD synthase activities. A summary of these various activities (Figure 4.2) illustrates the independence of the closely related catalase and peroxidase activities from the oxidase, hydrazine lyase, and synthase activities. Not only are the pH optima very different, but, unlike the catalase and peroxidase reactions, the

oxidase, hydrazine lyase, and synthase reactions do not require H_2O_2 or involve the formation of identifiable oxidized heme intermediates. The hydrazine lyase and synthase reactions are closely linked because hydrazine lyase must occur before the ligation of NAD^+ to the isonicotinoyl radical, but the oxidase reaction is not mechanistically linked to any other reaction except that it very likely shares with the synthase the same NAD^+/NADH-binding site. In addition, the oxidase reaction may serve as a source of NAD^+ for the synthase reaction and H_2O_2 for the catalase and peroxidase reactions (Figure 4.3). The catalase and peroxidase functions of KatG are rationalized as protection against H_2O_2, and the NADH oxidase activity may present a complementary protection against molecular oxygen or a means of maintaining low cytoplasmic levels of oxygen. However, the turnover rate of the oxidase is very slow compared with the catalase and peroxidase reactions, and the oxidase activity may simply be a residual vestige of what was once a more substantial activity with metabolic significance in a particular environmental niche. Certainly, the high affinity of BpKatG for NADH is consistent with there being, or having been, a physiological significance to the activity. Among the seven KatGs in this study, the variation in NADH oxidase activity, highest in BpKatG and lower in the rest of the KatGs, might be interpreted as the result of an environmentally determined differential loss of activity. Although the KatGs can utilize NADH as a peroxidatic substrate, the NADH oxidation characterized here is clearly not a peroxidatic reaction, and it is also different in several key respects from the peroxidase-oxidase activity associated with HRP. H_2O_2 does not have a catalytic role, SOD and catalase do not inhibit the reaction, and lag periods in reaction initiation are not evident in the presence of high enzyme or low NADH concentrations. In addition, the pH dependence

Figure 4.2. Amino acid sequence alignment of BpKatG, MtKatG, EcKatG, SykatG, BskatG, AfkatG, RcKatG. Sequence alignment was created using clustal. ■ represents fully conserved residues; ▩ represents residues replaced with similar properties; and ▒ represents partially conserved residues.

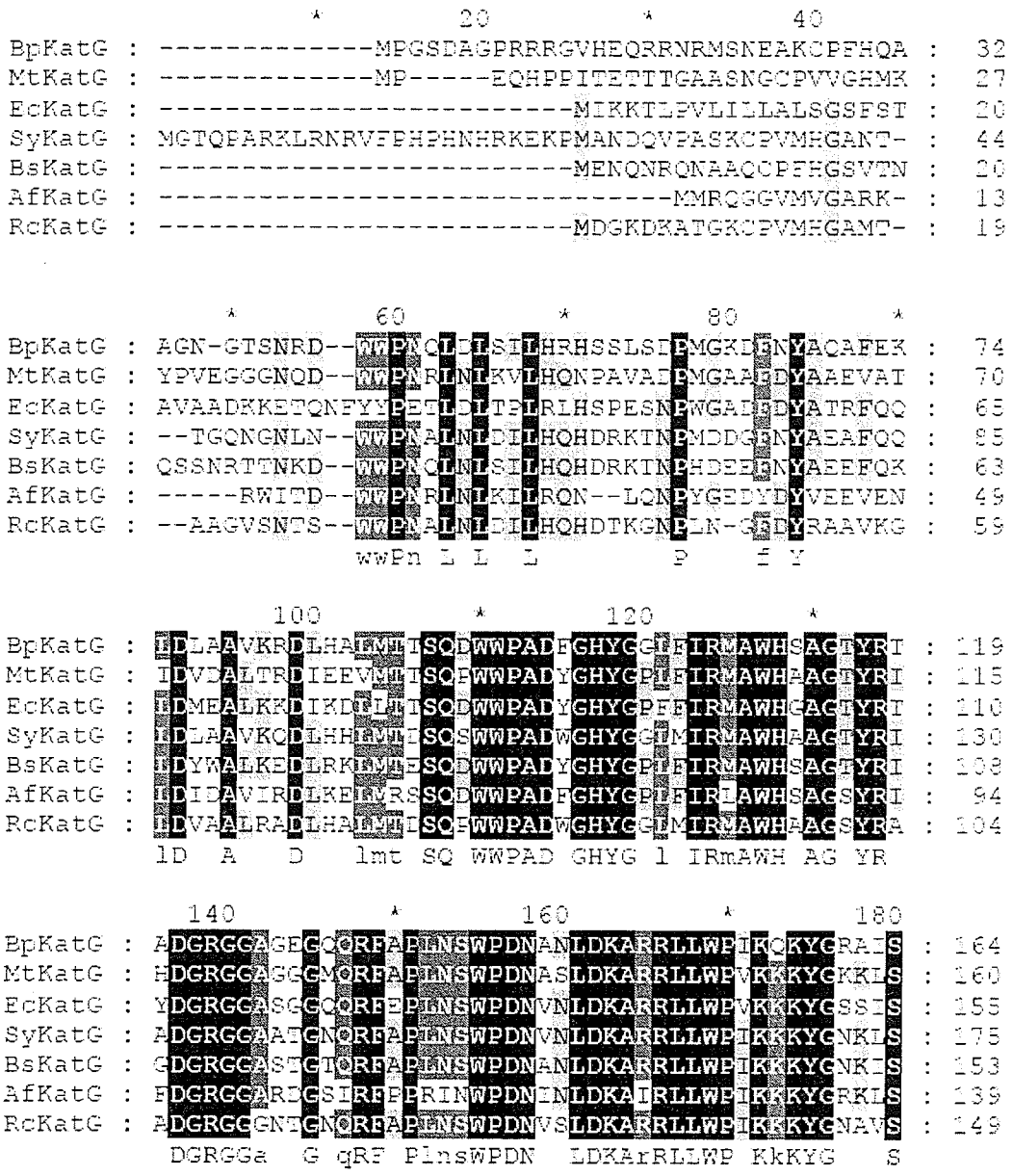
BpKatG : ----------MPGSDAGPRRRGVHEQRRNRMSNEAKCPFHQA : 32
MtKatG : ----------MP-----EQHPPITETTTGAASNGCPVVGHMK : 27
EcKatG : ----------MIKKTLPVLILLALSGSFST : 20
SyKatG : MGTQPARKLRNRVFPHPHNHRKEKPMANDQVPASKCPVMHGANT- : 44
BsKatG : ----------MENQNRQNAAQCPFHGSVTN : 20
AfKatG : ----------MMRQGGVMVGARK- : 13
RcKatG : ----------MDGKDKATGKCPVMHGAMT- : 19
BpKatG : AGN-GTSNRD--WWPNQLDLSILHRHSSLSDPMGKDGNYAQAFEK : 74
MtKatG : YPVEGGGNQD--WWPNRINIKVLHQNPAVADPMGAAGDYAAEVAI : 70
EcKatG : AVAADKKETQNFYYPETLDLTDLRLHSPESNPWGAGFDYATRFQQ : 65
SyKatG : --TGQNGNLN--WWPNALNLDILHQHDRKTNPMDDGFNYAEAFQQ : 85
BsKatG : QSSNRTTNKD--WWPNQLNLSILHQHDRKTNPHDEFGNYAEEFQK : 63
AfKatG : -----RWITD--WWPNRLNLKILRQN--LQNPYGEDYDYVEEVEN : 49
RcKatG : --AAGVSNTS--WWPNALNLDILHQHDTKGNPLN-GSDYRAAVKG : 59
BpKatG : IDLAAVKRDLHALMTISQDWWPADFGHYGGLFIRMAWHSAGTYRI : 119
MtKatG : IDVDALTRDIEEVMTLTSQEWWPADYGHYGPLFIRMAWHAAGTYRI : 115
EcKatG : IDMEALKKDIKDGLTLTSQDWWPADYGHYGPFFIRMAWHGAGTYRI : 110
SyKatG : IDLAAVKQDLHHLMTLTSQSWWPADWGHYGGLMIRMAWHAAGTYRI : 130
BsKatG : IDYWALKEDLRKLMTLPSQDWWPADYGHYGPLFIRMAWHSAGTYRI : 108
AfKatG : IDIDAVIRDLKELVRSSQDWWPADFGHYGPLFIRLAWHSAGSYRI : 94
RcKatG : IDVAALRADLHALMTISQEWWPADWGHYGGLMIRMAWHAAGSYRA : 104
BpKatG : ADGRGGAGEGQQRFAPLNSWPDNANLDKARRLLWPIKQKYGRAIS : 164
MtKatG : HDGRGGAGGGMQRFAPLNSWPDNASLDKARRLLWPVKKKYGKKLS : 160
EcKatG : YDGRGGASGGQQRFEPLNSWPDNVNLDKARRLLWPVKKKYGSSIS : 155
SyKatG : ADGRGGAAIGNQRFAPLNSWPDNVNLDKARRLLWPIKKKYGNKLS : 175
BsKatG : GDGRGGASIGTQRFAPLNSWPDNANLDKARRLLWPIKKKYGNKIS : 153
AfKatG : FDGRGGARIGSIRFEPRINWPDNINLDKAIRLLWPIKKKYGRKLS : 139
RcKatG : ADGRGGGNIGNQRFAPLNSWPDNVSLDKARRLLWPIKKKYGNAVS : 149

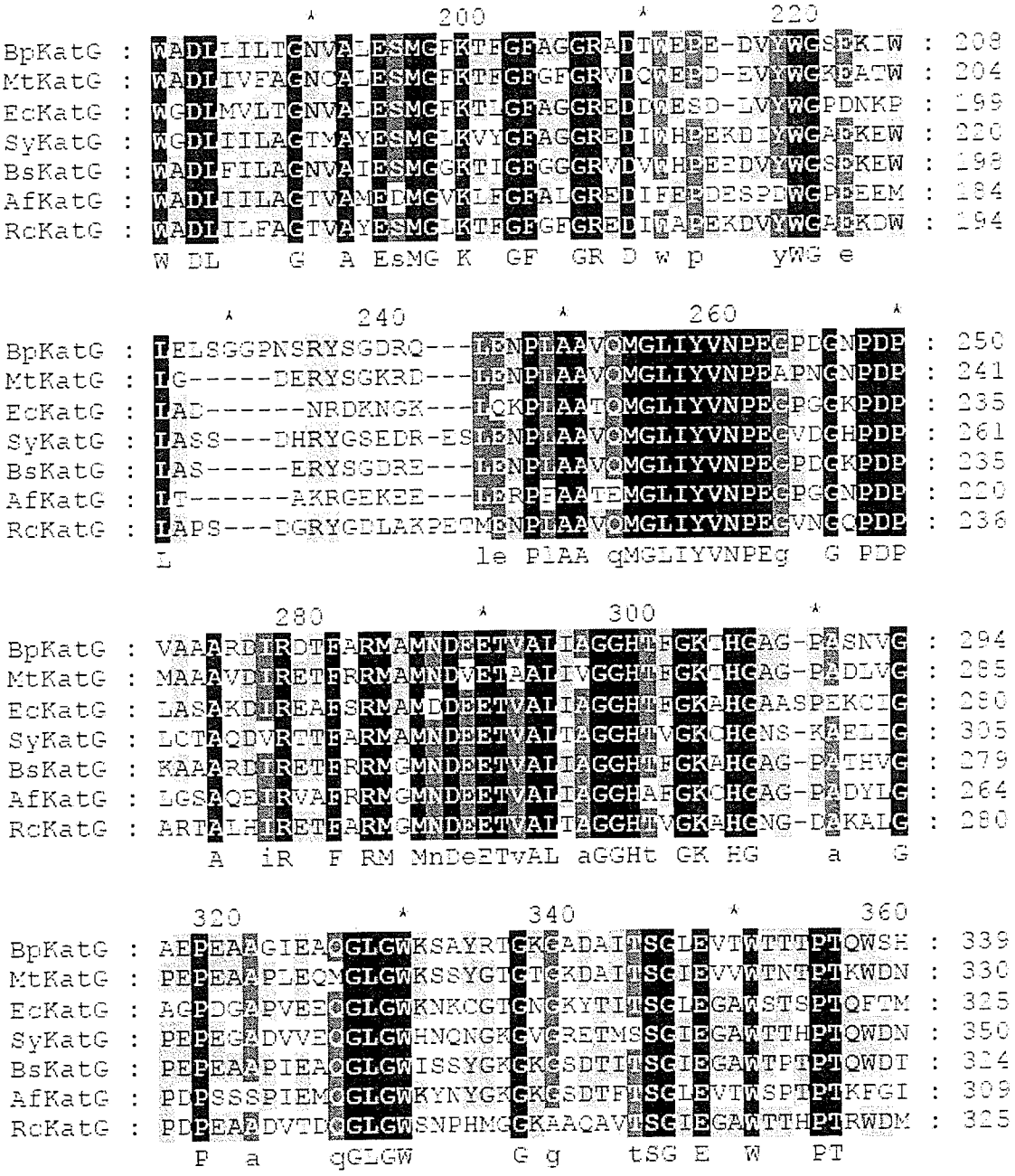
200
220
BpKatG : WADLILILIGNVALESMGFKTFGFAGGRADIWEPE-DVYWGSEKIW : 208
MtKatG : WADLIVFAGNCALESMGFKTFGFGFGRVDQWEPD-EVYWGKEATW : 204
EcKatG : WGDLMVLIGNVALESMGFKTLGFAGGREDDWESD-LVYWGPDNKP : 199
SyKatG : WGDLIILAGTMAYESMGLKVYGFAGGREDIWHPEKDIYWGAEKEW : 220
BsKatG : WADLFILAGNVAIESMGGKTIGFGGGRVDVWTHPEEDVYWGSEKEW : 198
AfKatG : WADLIILAGTVAMEDMGVKLFGFALGREDIFEPDESPDWGPEEEM : 194
RcKatG : WADLILFAGTVAYESMGLKTFGFGFGREDITAPEKDVYWGAEKDW : 194
W DL G A EsMG K GF GR D w p yWG e
240
260
BpKatG : TELSGGPNSRYSGDRQ---LENPLAAVQMGLIYVNPEGPDGNPDP : 250
MtKatG : IG-----DERYSGKRD---LENPLAAVQMGLIYVNPEAPNGNPDP : 241
EcKatG : LAD------NRDKNGK---LQKPLAATQMGLIYVNPEGPGGKPDP : 235
SyKatG : LASS---DHRYGSEDR-ESLENPLAAVQMGLIYVNPEGVDGHPDP : 261
BsKatG : LAS-----ERYSGDRE---LENPLAAVQMGLIYVNPEGPDGKPDP : 235
AfKatG : LT------AKRGEKEE---LERPFAATEMGLIYVNPEGPGGNPDP : 220
RcKatG : LAPS---DGRYGDLAKPETMENPLAAVQMGLIYVNPEGVNGCPDP : 236
L le PlAA qMGLIYVNPEg G PDP
280
300
BpKatG : VAAARDIRDTFARMAMNDEETVALIAGGHTFGKTHGAG-PASNVG : 294
MtKatG : MAAAVDIRETFRRMAMNDVETAALIVGGHTFGKTHGAG-PADLVG : 285
EcKatG : LASAKDIREAFSRMAMDDEETVALIAGGHTFGKAHGAASPEKCIG : 280
SyKatG : LCTAQDVRTTFARMAMNDEETVALIAGGHTVGKCHGNS-KAELIG : 305
BsKatG : KAAARDIRETFRRMGMNDEETVALIAGGHTFGKAHGAG-PATHVG : 279
AfKatG : LGSAQEIRVAFRRMGMNDEETVALIAGGHAFGKCHGAG-PADYLG : 264
RcKatG : ARIALHIRETFARMGMNDEETVALIAGGHTVGKAHGNG-DAKALG : 280
A iR F RM MnDeETvAL aGGHt GK HG a G
320
340
360
BpKatG : AEPEAAGIEAQGLGWKSAYRIGKGADAITSGLEVIWTTTPTQWSH : 339
MtKatG : PEPEAAPLEQMGLGWKSSYGIGTGKDAITSGIEVVWTNTPTKWDN : 330
EcKatG : AGPDGAPVEEQGLGWKNKCGIGNGKYTITSGLEGAWSTSPTQFTM : 325
SyKatG : PEPEGADVVEQGLGWHNQNGKGVGRETMSSGIEGAWTTHPTQWDN : 350
BsKatG : PEPEAAPIEAQGLGWISSYGKGKGSDTITSGIEGAWTPTPTQWDI : 324
AfKatG : PDPSSSPIEMQGLGWKYNYGKGKGSDTFTSGLEVIWSPTPTKFGI : 309
RcKatG : PDPEAADVTDQGLGWSNPHMGGKAAQAVTSGIEGAWTTHPTRWDM : 325
P a qGLGW G g tSG E W PT

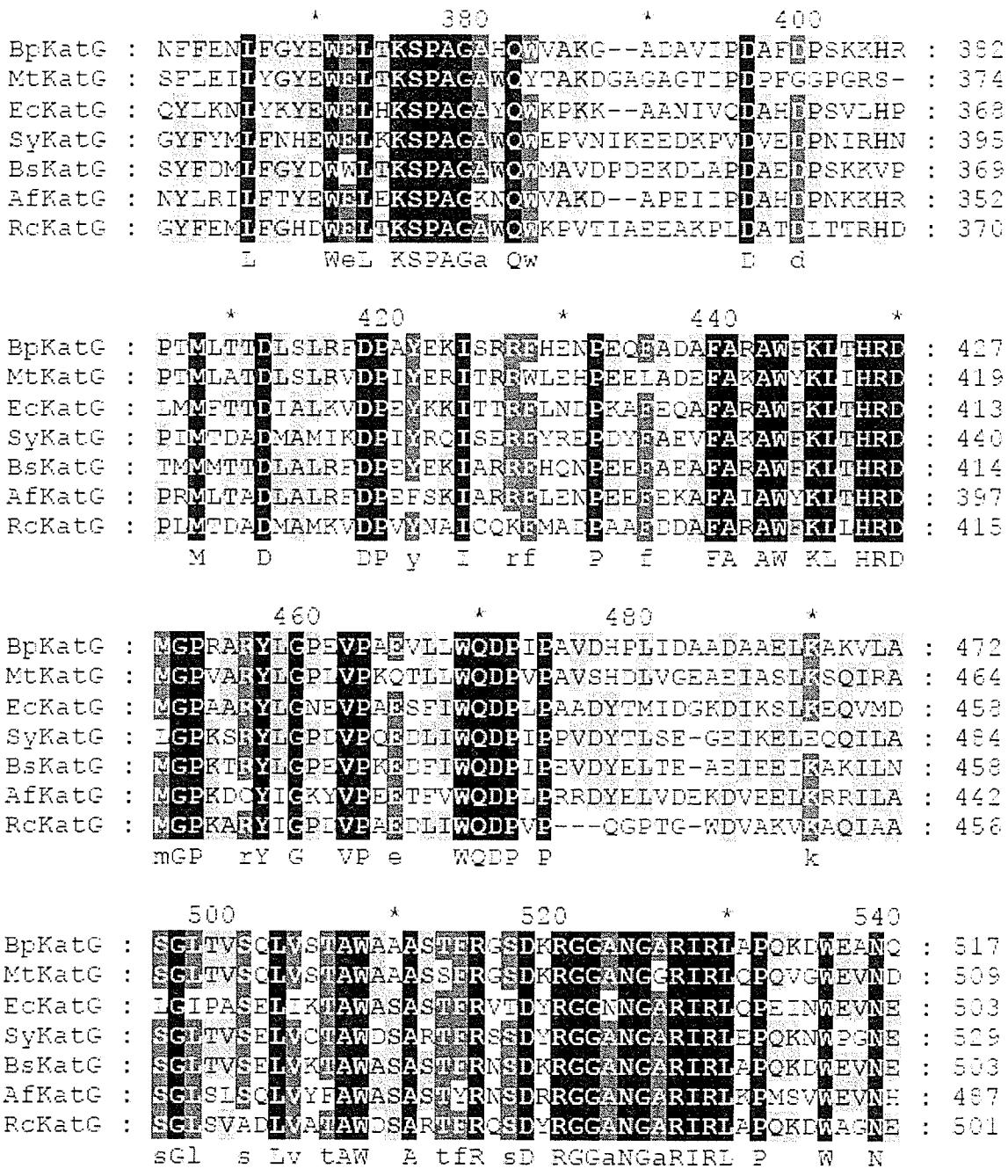
380
400
BpKatG : NFFENLFGYEWELTKSPAGAHQWVAKG--ADAVIPDAFDPSKKHR : 392
MtKatG : SFLEILYGYEWELTKSPAGAWQYTAKDGAGAGTIPDPFGGPGRS- : 374
EcKatG : QYLKNLYKYEWELHKSPAGAYQWKPKK--AANIVQDAHDPSVLHP : 368
SyKatG : GYFYMLFNHEWELKKSPAGAWQWEPVNIKEEDKPVDVEDPNIRHN : 395
BsKatG : SYFDMLFGYDWWLTKSPAGAWQWMAVDPDEKDLAPDAEDPSKKVP : 369
AfKatG : NYLRILFTYEWELEKSPAGKNQWVAKD--APEIIPDAHDPNKKHR : 352
RcKatG : GYFEMLFGHDWELTKSPAGAWQWKPVTIAEEAKPLDATDLTTRHD : 370
L WeL KSPAGa Qw D d
420
440
BpKatG : PTMLTTDLSLRFDPAYEKISRRFHENPEQFADAFARAWFKLTHRD : 427
MtKatG : PTMLATDLSLRVDPIYERITRRWLEHPEELADEFAKAWYKLIHRD : 419
EcKatG : LMMFTTDIALKVDPEYKKITTRFLNIPKAFEQAFARAWFKLTHRD : 413
SyKatG : PIMTDADMAMIKDPIYRQISERFYREPDYFAEVFARAWFKLTHRD : 440
BsKatG : TMMMTTDLALRFDPEYEKIARRFHQNPEEFAEAFARAWFKLTHRD : 414
AfKatG : PRMLTADLALRFDPEFSKIARRGLENPEEFEKAFAIAWYKLTHRD : 397
RcKatG : PLMTDADMAMKVDPVYNAICQKFMADPAAFDDAFARAWFKLLHRD : 415
M D DP y I rf P f FA AW KL HRD
460
480
BpKatG : MGPRARYLGPEVPAEVLLWQDPIPAVDHPLIDAADAAELKAKVLA : 472
MtKatG : MGPVARYLGPLVPKQTLLWQDPVPAVSHDLVGEAEIASLKSQIRA : 464
EcKatG : MGPAARYLGNEVPAESFIWQDPLPAADYTMIDGKDIKSLKEQVMD : 458
SyKatG : IGPKSRYLGPDVPQEDLIWQDPIPPVDYTLSE-GEIKELEQQILA : 484
BsKatG : MGPKTRYLGPEVPKEDFIWQDPIPEVDYELTE-AEIEEIKAKILN : 458
AfKatG : MGPKDCYIGKYVPPETFVWQDPLPRRDYELVDEKDVEELKRRILA : 442
RcKatG : MGPKARYIGPDVPAEDLIWQDEVP---QGPTG-WDVAKVKAQIAA : 456
mGP rY G VP e WQDP P k
500
520
540
BpKatG : SGITVSQLVSTAWAAASTFRGSDKRGGANGARIRLAPQKDWEANQ : 517
MtKatG : SGLTVSQLVSTAWAAASSFRGSDKRGGANGCRIRLCPQVGWEVND : 509
EcKatG : LGIPASELIKTAWASASTFRVTDYRGGNNGARIRLCPEINWEVNE : 503
SyKatG : SGLTVSELVCTAWDSARTFRSSDYRGGANGARIRLEPQKNWPGNE : 529
BsKatG : SGLTVSELVKTAWASASTFRNSDKRGGANGARIRLAPQKDWEVNE : 503
AfKatG : SGLSLSQLVYPAWASASTYRNSDRRGGANGARIRLKPMSVWEVNH : 487
RcKatG : SGLSVADLVATAWDSARTFRQSDYRGGANGARIRLAPQKDWAGNE : 501
sGl s Lv tAW A tfR sD RGGaNGaRIRL P W N

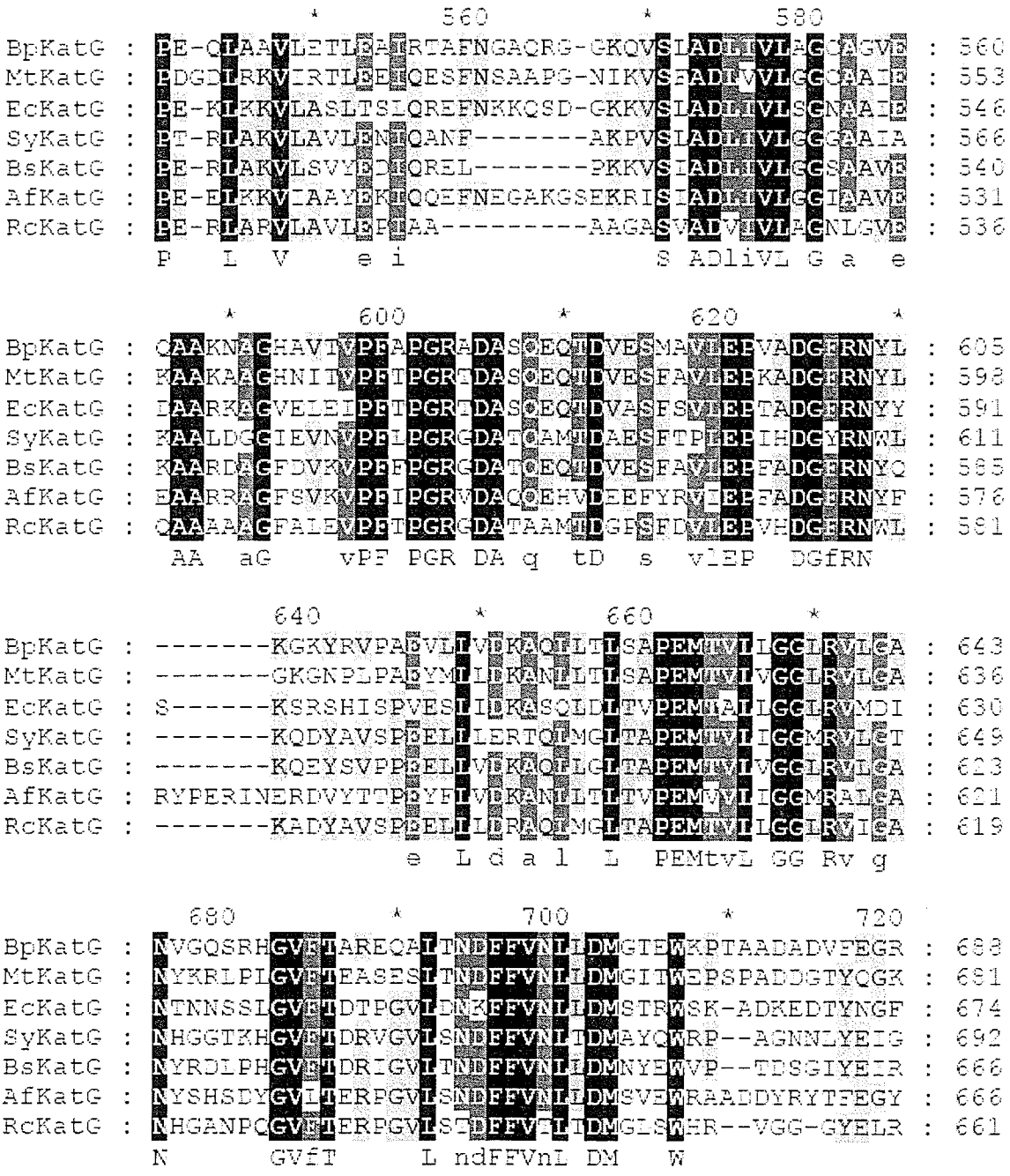
560 580
BpKatG : PE-QLAAVLETLEATRTAFNGAQRG-GKQVSLADLIVLAGCAGVE : 560
MtKatG : PDGDLRKVIRTLEEIQESFNSAAPG-NIKVSFADIVVLGGCAAIE : 553
EcKatG : PE-KLKKVLASLTSIQREFNKKQSD-GKKVSLADLIVLSGNAAIE : 546
SyKatG : PT-RLAKVLAVLENIQANF-------AKPVSLADLIVLGGCAAIA : 566
BsKatG : PE-RLAKVLSVYEDIQRFL-------PKKVSIADLIVLGGSAAVE : 540
AfKatG : PE-ELKKVIAAYEKIQQEFNEGAKGSEKRISIADIIVLGGIAAVE : 531
RcKatG : PE-RLAPVLAVLEPIAA---------AAGASVADVIVLAGNLGVE : 536
P L V e i S ADliVL G a e
600 620
BpKatG : QAAKNAGHAVIVPFAPGRADASQEQTDVESMAVLEPVADGFRNYL : 605
MtKatG : KAAKAAGHNITVPFIPGRTDASQEQTDVESFAVLEPKADGFRNYL : 598
EcKatG : IAARKAGVELEIPFTPGRTDASQEQTDVASFSVLEPTADGFRNYY : 591
SyKatG : KAALDGGIEVNVPFLPGRGDATQAMTDAESFTPLEPIHDGYRNWL : 611
BsKatG : KAARDAGFDVKVPFFPGRGDATQEQTDVESFAVLEPFADGFRNYQ : 585
AfKatG : EAARRAGFSVKVPFIPGRVDAQQEHVDEEFYRVLEPFADGFRNYF : 576
RcKatG : QAAAAAGFALEVPFTPGRGDATAAMTDGPSFDVLEPVHDGFRNWL : 581
AA aG vPF PGR DA q tD s vLEP DGfRN
640 660
BpKatG : -------KGKYRVPADVLLVDKAQFLTLSAPEMTVLLGGLRVLGA : 643
MtKatG : -------GKGNPLPADYMLLDKANFLTLSAPEMTVLVGGLRVLGA : 636
EcKatG : S------KSRSHISPVESLIDKASQLDLTVPEMTALLGGLRVMDI : 630
SyKatG : -------KQDYAVSPDELLLERTQFMGLTAPEMTVLIGGMRVLGT : 649
BsKatG : -------KQEYSVPPDELLVDKAQFLGLTAPEMTVLVGGLRVLGA : 623
AfKatG : RYPERINERDVYTTPDYFLVDKANLLTLTVPEMTVLIGGMRALGA : 621
RcKatG : -------KADYAVSPDELLLDRAQIMGLTAPEMTVLLGGLRVIGA : 619
e L d a l L PEMtvL GG Rv g
680 700 720
BpKatG : NVGQSRHGVFTAREQALTNDFFVNLLDMGIEWKPTAADADVFEGR : 688
MtKatG : NYKRLPLGVFTEAESSLTNDFFVNLLDMGITWEPSPADDGTYQGK : 681
EcKatG : NTNNSSLGVFTDTPGVLDNKFFVNLLDMSIRWSK-ADKEDTYNGF : 674
SyKatG : NHGGTKHGVFTDRVGVLSNDFFVNLIDMAYQWRP--AGNNLYEIG : 692
BsKatG : NYRDLPHGVFTDRIGVLTNDFFVNLLDMNYEWVP--TDSGIYEIR : 666
AfKatG : NYSHSDYGVLTERPGVLSNDFFVNLLDMSVEWRAADDYRYTFEGY : 666
RcKatG : NHGANPQGVFTERPGVLSQDFFVTLIDMGLSWHR--VGG-GYELR : 661
N GVfT L ndFFVnL DM W

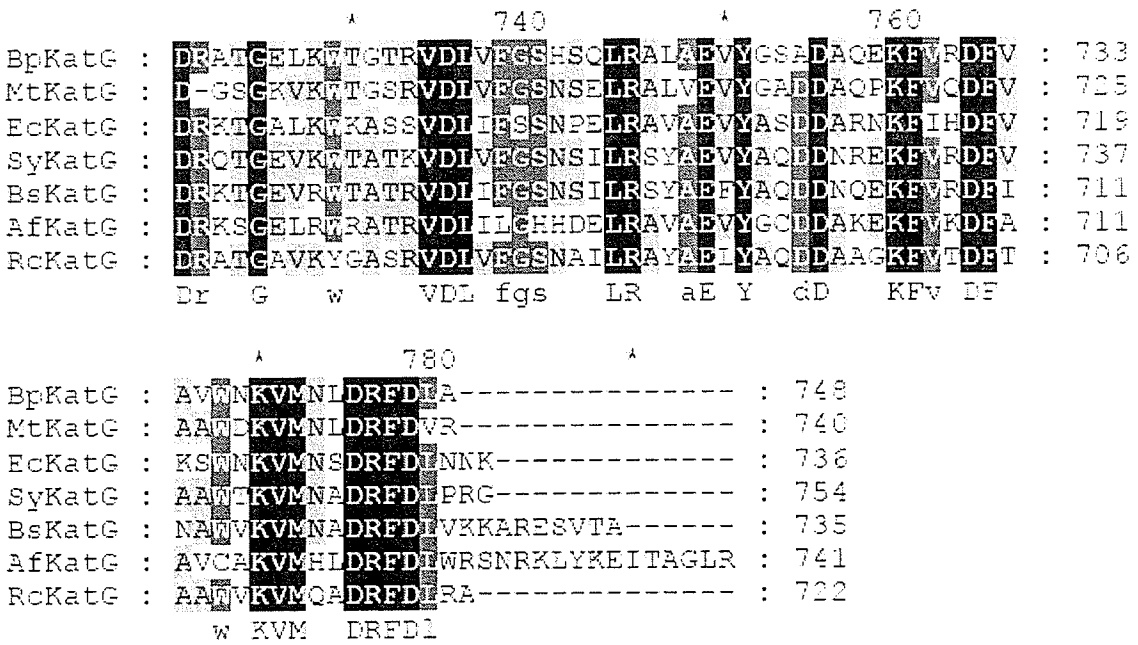
740
760
BpKatG : DRATGELKWTGTRVDIVFGSHSQLRALAEVYGSADAQEKFVRDFV : 733
MtKatG : D-GSGKVKWTGSRVDIVFGSNSELRALVEVYGADDAQPKFVQDFV : 725
EcKatG : DRKTGALKWKASSVDIIFSSNPELRAVAEVYASDDARNKFIHDFV : 719
SyKatG : DRQTGEVKWTATKVDIVFGSNSILRSYAEVYAQDDNREKFVRDFV : 737
BsKatG : DRKTGEVRWTATRVDIIFGSNSILRSYAEFYAQDDNQEKFVRDFI : 711
AfKatG : DRKSGELRWRATRVDIILGHHDELRAVAEVYGCDDAKEKFVKDFA : 711
RcKatG : DRATGAVKYGASRVDIVFGSNAILRAYAELYAQDDAAGKFVIDFT : 706
Dr G w VDL fgs LR aE Y dD KFv DF
780
BpKatG : AVWNKVMNLDRFDIA---------- : 748
MtKatG : AAWDKVMNLDRFDVR---------- : 740
EcKatG : KSWNKVMNSDRFDLNNK---------- : 736
SyKatG : AAWTKVMNADRFDFPRG---------- : 754
BsKatG : NAWVKVMNADRFDIVKKARESVTA------ : 735
AfKatG : AVCAKVMHLDRFDIWRSNRKLYKEITAGLR : 741
RcKatG : AAWVKVMQADRFDIRA---------- : 722
w KVM DRFDl

Figure 4.3. Scheme showing the relationship of the five activities of KatG. The locations of the INH hydrazine lyase, NADH oxidase, isonicotinoyl-NAD synthase, catalase, and peroxidase reactions are *underlined*. The two pH-dependent options for the NADH oxidase reaction are also indicated. The isonicotinoyl (*a*) and hydrazide (*b*) radicals from the hydrazine lyase reaction are available to radical scavengers in the absence of NAD^+. The di-imide and proton products from the synthase reaction, indicated in *parentheses* with an *asterisk*, have not been confirmed as products but provide a convenient and logical way to balance the reaction. The catalase and peroxidase cycles are shown at the *bottom* and appear to be independent of the reactions at the *top* except for the possible metabolism of H_2O_2 generated in the oxidase reaction (*dotted line*) and the possibility that molecular oxygen may also bind to the heme.

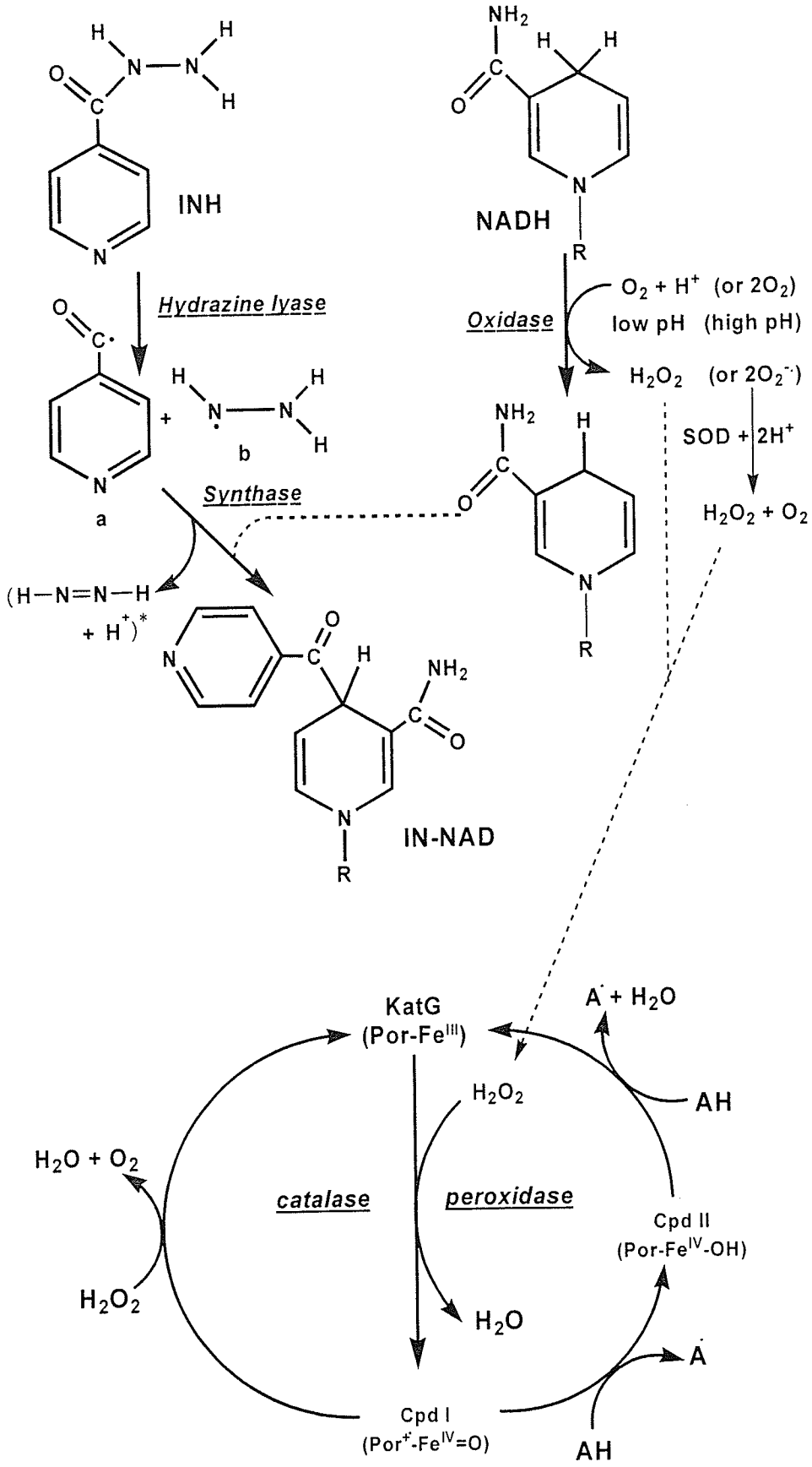
INH
NADH
Hydrazine lyase
Oxidase
O2 + H+ (or 2O2)
low pH (high pH)
H2O2 (or 2O2-·)
SOD + 2H+
H2O2 + O2
a
b
Synthase
(H–N=N–H + H+)*
IN-NAD
KatG
(Por-FeIII)
A· + H2O
AH
H2O2
catalase
peroxidase
H2O + O2
H2O2
H2O
Cpd II
(Por-FeIV-OH)
A·
Cpd I
(Por+·-FeIV=O)
AH

of superoxide radical formation in the oxidase reaction suggests the possibility of two reaction outcomes for molecular oxygen depending on proton availability. Below pH 8, with protons more readily available, a two electron transfer to oxygen takes place generating H_2O_2 (Reaction 1), whereas at higher pH, two one-electron transfers to two oxygen molecules generate two superoxide ions (Reaction 2). The protonation state of the imidazole ring of the distal side His112 (Figure 1.5) may determine the reaction pathway through presentation of a proton to the bound oxygen in the active site. Any H_2O_2 produced via reaction 1 would rapidly oxidize the heme to compound I and subsequent reduction in catalase or peroxidase reactions would give rise to H_2O.

$$NADH + O_2 + H^+ \rightarrow NAD^+ + H_2O_2 \qquad (1)$$

$$NADH + 2O_2 \rightarrow NAD^+ + 2O_2^{-\circ} \qquad (2)$$

The enhancement of INH hydrazine lyase by KatG and its importance in INH pro-drug activation is well documented. A single mutation in Ser315 of MtKatG is sufficient to reduce the affinity of the enzyme for INH (Yu *et al.*, 2003) and to prevent isonicotinoyl-NAD formation (Wei *et al.*, 2003) leading to *in vivo* isoniazid resistance. The facts that NAD^+ is a competitive inhibitor of NADH oxidation but does not inhibit the hydrazine lyase reaction and that an INH-NADH mixture supports a rate of radical production greater than the cumulative rates of the individual reactions suggest that NADH/NAD^+ and INH have separate binding sites and that there is an element of synergy between the two reactions. Manganese ions (both Mn^{2+} and Mn^{3+}) enhance both nonenzymatic and enzymatic hydrazine lyase to the extent that the manganese-mediated isonicotinoyl radical formation is faster than the KatG-mediated reaction. However,

despite this high rate of manganese-mediated hydrazine lyase, manganese-mediated isonicotinoyl-NAD formation is negligible compared with its rapid formation in the presence of KatG. The data in this thesis do not dispute the observation that there can be a nonenzymatic origin of isonicotinoyl-NAD (Wilming and Johnsson, 1999), but under the conditions employed in this work, KatGs are a much more effective catalyst of isonicotinoyl-NAD synthesis than manganese ions.

The regulatory systems controlling KatG expression, involving OxyR in *E. coli*, are generally oxidative response systems, supporting the conjecture that the primary role of KatG is the detoxification of H_2O_2 as a catalase or peroxidases. The physiological role and importance of the peroxidatic reaction in the anti-oxidant process remains unclear, in large part because the identity of the *in vivo* peroxidatic substrate(s) remains unknown. The wide variety of *in vitro* substrates that are utilized by KatG and the wide variety of substrates used by the closely related plant peroxidases, ranging from whole proteins to simple carbohydrates and metal ions, have not helped in the identification. Furthermore, the structures of KatGs present several potential substrate-binding sites on their surface topographys, and there is an abnormally high percentage of highly conserved residues close to the protein surface, consistent with the idea of important features residing in other than the heme pocket. Of the known substrates, H_2O_2 binds at the heme iron, which is also the most likely site for O_2 binding and INH binds in the heme cavity or in the entrance channel near Ser324 (equivalent to Ser315) (Deeamgarn *et al.*, 2005). The peroxidatic substrates probably also bind in the vicinity of Ser324 as suggested by benzhydroxamic acid binding in HRP (Henriksin *et al.*, 1998), although the substrates used in this study are larger and would not fit into as small a cavity as benzhydroxamic

acid. Trying to identify the NADH-binding site would be pure conjecture at this point, but the possibility that the cross-linked side chains of Trp111, Tyr238, and Met264 may have a role in electron transfer from NADH to O_2, and the observations that INH does not inhibit NADH oxidation and NAD^+ does not inhibit the hydrazine lyase reaction suggest that the NADH-binding site is some distance from the heme pocket. However, this surmise must be tempered by the logic of having NAD^+ bind in close proximity to the site of isonicotinoyl radical formation. A structural definition of the binding sites is needed.

4.4. Modulation of isoniazid activation by Ser315 variants in MtKatG

An understanding of the role of KatG in the formation of isonicotinoyl-NAD has not been advanced greatly by the four native KatG structures (Yamada *et al.*, 2002; Carpena *et al.*, 2003; Vada *et al.*, 2002; and Bertrand *et al.*, 2004). One paramount question that remains unanswered is the location of the INH and NADH/NAD^+ binding sites in KatG, although the location of INH binding in the structurally related horse-radish peroxidase suggests a site close to the δ-meso (C_{20}) edge of the heme (Pierattelli *et al.*, 2004). The Ser315Thr and Ser315Asn mutations are among the commonest causes of INH resistance (Heym *et al.*, 1995) and while retaining significant catalase and peroxidase activities the variant enzymes exhibit a reduced affinity for INH (Yu *et al.*, 2003). Both the Ser315Thr and Ser315Asn variants constructed in this study showed reduced NADH oxidase and INH hydrazine lyase activities compared to the native enzyme (Table 3.4.5), and this is mirrored in a slower rate of isonicotinoyl-NAD adduct formation by both variants (Figure 3.4.7). Recent crystallization of the Ser315Thr variant

of MtKatG (Zhao *et al.*, 2006) and the equivalent Ser324Thr from BpKatG (Deemagran *et al.*, 2005) have demonstrated that replacement of Ser with Thr causes a small change in conformation of the main-chain atoms including a small displacement of the adjacent main-chain carbonyl oxygen atoms. While these appear to be very subtle changes, their effect on isonicotinoyl-NAD synthesis and INH affinity is significant as shown in this study and in a previous report (Yu *et al.*, 2003). The proposed binding site for isoniazid lies in a cavity on the distal side of the heme close to its δ-meso edge (Pierattelli *et al.*, 2004). To reach this site in KatG, isoniazid must pass through the channel leading to the heme cavity, passing adjacent to Ser315. The mutation of Ser315 (MtkatG) or Ser324 (BpKatG) to Thr narrows the heme access channel from around 6 to 4.7 Å at its narrowest point in the mutant enzymes from both organisms (Deemagarn *et al.*, 2005; Zhao *et al.*, 2006). These observations in combination with significantly decreased INH activation in these variants suggest that drug binding within the heme pocket is a likely requirement for INH activation. Consequently, it is interference with INH accessibility to the heme cavity that best explains the reduced affinity and reactivity of KatG towards INH, although the possibility of INH binding in the channel cannot be excluded, in which case the methyl group would interfere with INH binding. Other mutations of this serine residue might cause a similar blockage of the channel.

4.5. Future directions

Recent success in the crystallization of KatGs has excited researchers studying these enzymes. In addition, the discovery of a new activity in this well studied enzyme is both interesting and intriguing. Further characterization of the NADH oxidase reactions

in KatGs other than those used in this study is needed. This would help in determining the physiological relevance of this activity. One of the observations during this study was variations in NADH oxidase activities from different batches of BpKatG. Different batch of EcKatG, prepared while writing this thesis, also demonstrated substantial NADH oxidase activity as compared to very low levels mentioned in this study. This raises the question about the requirement of specific conditions for expressing the enzyme and needs explanation. A recent report associating a pH induced perhydroxy modification of Trp 111 in BpKatG with NADH oxidase activity (Carpena *et al.*, 2006) stresses the importance of crystallization of Trp111 variants of BpKatG so as to confirm the modulation of NADH oxidase activity and its association with Trp111. This study has determined the catalytic role of KatGs in isoniazid activation and isonicotinoyl-NAD synthesis over the non-enzymatic Mn^{2+} dependent drug activation. However, the lack of identity of the binding sites for INH and NADH/NAD^+ hinders a complete understanding of how KatG's modulates NADH oxidase, hydrazine lyase and isonicotinoyl-NAD synthase activities. The identification of ligand binding sites remains the ultimate goal of future work.

5. REFERENCES

Ausubel, F.M., Brent, R., Kingston, R.E., Moore, D.D., Seidman, J.G., Smith, J.A., & Strunhl, K. (1989). *Current Protocols in Molecular Biology*. Green Publishing-Weiley Inter*Science*.. New York

Ahmed, S. A. & Claiborne, A. (1989). The streptococcal flavoprotein NADH oxidase. I. Evidence linking NADH oxidase and NADH peroxidase cysteinyl redox centers. *J. Biol. Chem.***264**, 19856-19863.

Akazawa, T. & Conn, E. E. (1958). The oxidation of reduced pyridine nucleotides by peroxidase. *J. Biol. Chem.***232**, 403-415.

Allgood, G. S. & Perry, J. J. (1986). Characterization of a manganese-containing catalase from the obligate thermophile *Thermoleophilum album*. *J. Bacteriol.* **168**, 563-567.

Altamirano, M., Marostenmaki, J., Wong, A., FitzGerald, M., Black, W. A. & Smith, J. A. (1994). Mutations in the catalase-peroxidase gene from isoniazid-resistant *Mycobacterium tuberculosis* isolates. *J. Infect. Dis.* **169**, 1162-1165.

Auclair, C., Torres, M., & Hakim, J. (1978). Superoxide anion involvement in NBT reduction catalyzed by NADPH-cytochrome P-450 reductase: a pitfall. *FEBS Lett.* **89**, 26-28

Banerjee, A., Dubnau, E., Quemard, A., Balasubramanian, V., Um, K. S., Wilson, T., Collins, D., de Lisle, G. & Jacobs, W. R., Jr. (1994). *inhA*, a gene encoding a target for isoniazid and ethionamide in *Mycobacterium tuberculosis*. *Science.* **263**, 227-230.

Basso, L. A., Zheng, R., Musser, J. M., Jacobs, W. R., Jr. & Blanchard, J. S. (1998). Mechanisms of isoniazid resistance in *Mycobacterium tuberculosis*: enzymatic characterization of enoyl reductase mutants identified in isoniazid-resistant clinical isolates. *J. Infect. Dis.* **178**, 769-775.

Berglund, G. I., Carlsson, G. H., Smith, A. T., Szoke, H., Henriksen, A. & Hajdu, J. (2002). The catalytic pathway of horseradish peroxidase at high resolution. *Nature.* **417**, 463-468.

Bertrand, T., Eady, N. A., Jones, J. N., Jesmin, Nagy, J. M., Jamart-Gregoire, B., Raven, E. L. & Brown, K. A. (2004). Crystal structure of *Mycobacterium tuberculosis* catalase-peroxidase. *J. Biol. Chem.***279**, 38991-38999.

Bravo, J., Verdaguer, N., Tormo, J., Betzel, C., Switala, J., Loewen, P. C. & Fita, I. (1995). Crystal structure of catalase HPII from *Escherichia coli*. *Structure* **3**, 491-502.

Bravo, J., Fita, I., Ferrer, J. C., Ens, W., Hillar, A., Switala, J. & Loewen, P. C. (1997). Identification of a novel bond between a histidine and the essential tyrosine in catalase HPII of *Escherichia coli*. *Protein Sci* **6**, 1016-1023.

Bravo, J., Mate, M. J., Schneider, T., Switala, J., Wilson, K., Loewen, P. C. & Fita, I. (1999). Structure of catalase HPII from *Escherichia coli* at 1.9 A resolution. *Proteins* **34**, 155-166.

Brunder, W., Schmidt, H. & Karch, H. (1996). KatP, a novel catalase-peroxidase encoded by the large plasmid of enterohaemorrhagic *Escherichia coli* O157:H7. *Microbiology* **142 (Pt 11)**, 3305-3315.

Bunkelmann, J. R. & Trelease, R. N. (1996). Ascorbate peroxidase. A prominent membrane protein in oilseed glyoxysomes. *Plant Physol.***110**, 589-598.

Buse, G., Soulimane, T., Dewor, M., Meyer, H. E. & Bluggel, M. (1999). Evidence for a copper-coordinated histidine-tyrosine cross-link in the active site of cytochrome oxidase. *Protein Sci* **8**, 985-990.

Cabiscol, E., Tamarit, J. & Ros, J. (2000). Oxidative stress in bacteria and protein damage by reactive oxygen species. *Int Microbiol* **3**, 3-8.

Carpena, X., Perez, R., Ochoa, W. F., Verdaguer, N., Klotz, M. G., Switala, J., Melik-Adamyan, W., Fita, I. & Loewen, P. C. (2001). Crystallization and preliminary X-ray analysis of clade I catalases from *Pseudomonas syringae* and *Listeria seeligeri*. *Acta. Crystallogr. D. Biol. Crystallogr.* **57**, 1184-1186.

Carpena, X., Guarne, A., Ferrer, J. C., Alzari, P. M., Fita, I. & Loewen, P. C. (2002a). Crystallization and preliminary X-ray analysis of the hydroperoxidase I C-terminal domain from *Escherichia coli*. *Acta. Crystallogr. D. Biol. Crystallogr.* **58**, 853-855.

Carpena, X., Switala, J., Loprasert, S., Mongkolsuk, S., Fita, I. & Loewen, P. C. (2002b). Crystallization and preliminary X-ray analysis of the catalase-peroxidase KatG from *Burkholderia pseudomallei*. *Acta. Crystallogr. D. Biol. Crystallogr.* **58**, 2184-2186.

Carpena, X., Loprasert, S., Mongkolsuk, S., Switala, J., Loewen, P. C. & Fita, I. (2003a). Catalase-peroxidase KatG of *Burkholderia pseudomallei* at 1.7A resolution. *J. Mol. Biol.* **327**, 475-489.

Carpena, X., Soriano, M., Klotz, M. G., Duckworth, H. W., Donald, L. J., Melik-Adamyan, W., Fita, I. & Loewen, P. C. (2003b). Structure of the Clade 1 catalase, CatF of *Pseudomonas syringae*, at 1.8 A resolution. *Proteins* **50**, 423-436.

Carpena, X., Melik-Adamyan, W., Loewen, P. C. & Fita, I. (2004). Structure of the C-terminal domain of the catalase-peroxidase KatG from *Escherichia coli*. *Acta. Crystallogr. D. Biol. Crystallogr.* **60**, 1824-1832.

Carpena, X., Wiseman, B., Deemagarn, T., Singh, R., Switala, J., Ivancich, A., Fita, I. & Loewen, P. C. (2005). A molecular switch and electronic circuit modulate catalase activity in catalase-peroxidases. *EMBO Rep.* **6**, 1156-1162.

Carpena, X., Wiseman, B., Deemagarn, T., Herguedas, B., Ivancich, A., Singh, R., Loewen, P. C. & Fita, I. (2006). Roles for Arg426 and Trp111 in the modulation of NADH oxidase activity of the catalase-peroxidase KatG from *Burkholderia pseudomallei* inferred from pH-induced structural changes. *Biochemistry.* **45**, 5171-5179.

Chance, B., Sies, H. & Boveris, A. (1979). Hydroperoxide metabolism in mammalian organs. *Physiol. Rev.* **59**, 527-605.

Chelikani, P., Carpena, X., Fita, I. & Loewen, P. C. (2003a). An electrical potential in the access channel of catalases enhances catalysis. *J. Biol. Chem.***278**, 31290-31296.

Chelikani, P., Donald, L. J., Duckworth, H. W. & Loewen, P. C. (2003b). Hydroperoxidase II of *Escherichia coli* exhibits enhanced resistance to proteolytic cleavage compared to other catalases. *Biochemistry.* **42**, 5729-5735.

Chelikani, P., Fita, I. & Loewen, P. C. (2004). Diversity of structures and properties among catalases. *Cell Mol. Life Sci.* **61**, 192-208.

Chelikani, P., Carpena, X., Perez-Luque, R., Donald, L. J., Duckworth, H. W., Switala, J., Fita, I. & Loewen, P. C. (2005). Characterization of a large subunit catalase truncated by proteolytic cleavage. *Biochemistry.* **44**, 5597-5605.

Chen, Y. S., Chen, S. C., Wu, T. R., Kao, C. M. & Chen, Y. L. (2004). Seroprevalence of anti-flagellin antibody against *Burkholderia pseudomallei* in Taiwan. *Jpn. J. Infect. Dis.* **57**, 224-225.

Cheng, A. C. & Currie, B. J. (2005). Melioidosis: epidemiology, pathophysiology, and management. *Clin. Microbiol. Rev.* **18**, 383-416.

Choi, H. J., Kang, S. W., Yang, C. H., Rhee, S. G. & Ryu, S. E. (1998). Crystal structure of a novel human peroxidase enzyme at 2.0 A resolution. *Nat. Struct. Biol.* **5**, 400-406.

Chouchane, S., Lippai, I. & Magliozzo, R. S. (2000). Catalase-peroxidase (*Mycobacterium tuberculosis* KatG) catalysis and isoniazid activation. *Biochemistry.* **39**, 9975-9983.

Chouchane, S., Girotto, S., Kapetanaki, S., Schelvis, J. P., Yu, S. & Magliozzo, R. S. (2003). Analysis of heme structural heterogeneity in *Mycobacterium tuberculosis* catalase-peroxidase (KatG). *J. Biol. Chem.***278**, 8154-8162.

Christman, M. F., Morgan, R. W., Jacobson, F. S. & Ames, B. N. (1985). Positive control of a regulon for defenses against oxidative stress and some heat-shock proteins in Salmonella typhimurium. *Cell* **41**, 753-762.

Christman, M. F., Storz, G. & Ames, B. N. (1989). OxyR, a positive regulator of hydrogen peroxide-inducible genes in *Escherichia coli* and Salmonella typhimurium, is homologous to a family of bacterial regulatory proteins. *Proc. Natl. Acad. Sci. U S A.* **86**, 3484-3488.

Chung, C. T., Niemela, S. L. & Miller, R. H. (1989). One-step preparation of competent *Escherichia coli*: transformation and storage of bacterial cells in the same solution. *Proc. Natl. Acad. Sci. U S A.* **86**, 2172-2175.

Claiborne, A. & Fridovich, I. (1979a). Purification of the o-dianisidine peroxidase from *Escherichia coli* B. Physicochemical characterization and analysis of its dual catalatic and peroxidatic activities. *J. Biol. Chem.***254**, 4245-4252.

Claiborne, A. & Fridovich, I. (1979b). Chemical and enzymatic intermediates in the peroxidation of o-dianisidine by horseradish peroxidase. 2. Evidence for a substrate radical--enzyme complex and its reaction with nucleophiles. *Biochemistry.* **18**, 2329-2335.

Claiborne, A. & Fridovich, I. (1979c). Chemical and enzymatic intermediates in the peroxidation of o-dianisidine by horseradish peroxidase. 1. Spectral properties of the products of dianisidine oxidation. *Biochemistry.* **18**, 2324-2329.

Clare, D. A., Duong, M. N., Darr, D., Archibald, F. & Fridovich, I. (1984). Effects of molecular oxygen on detection of superoxide radical with nitroblue tetrazolium and on activity stains for catalase. *Anal. Biochem.* **140**, 532-537.

Corbett, E. L., Charalambous, S., Fielding, K., Clayton, T., Hayes, R. J., De Cock, K. M. & Churchyard, G. J. (2003). Stable incidence rates of tuberculosis (TB) among human immunodeficiency virus (HIV)-negative South African gold miners during a decade of epidemic HIV-associated TB. *J. Infect. Dis. s* **188**, 1156-1163.

Cypionka, H. (2000). Oxygen respiration by Desulfovibrio species. *Annu. Rev. Microbiol.* **54**, 827-848.

Dang, P. M., Babior, B. M. & Smith, R. M. (1999). NADPH dehydrogenase activity of p67PHOX, a cytosolic subunit of the leukocyte NADPH oxidase. *Biochemistry.* **38**, 5746-5753.

Dawson, J. H., Bracete, A. M., Huff, A. M., Kadkhodayan, S., Zeitler, C. M., Sono, M., Chang, C. K. & Loewen, P. C. (1991). The active site structure of *E. coli* HPII catalase. Evidence favoring coordination of a tyrosinate proximal ligand to the chlorin iron. *FEBS Lett.* **295**, 123-126.

Deemagarn, T., Carpena, X., Singh, R., Wiseman, B., Fita, I. & Loewen, P. C. (2005). Structural characterization of the Ser324Thr variant of the catalase-peroxidase (KatG) from *Burkholderia pseudomallei. J. Mol. Biol.* **345**, 21-28.

Demple, B. & Harrison, L. (1994). Repair of oxidative damage to DNA: enzymology and biology. *Annu. Rev. Biochem.* **63**, 915-948.

Deretic, V., Philipp, W., Dhandayuthapani, S., Mudd, M. H., Curcic, R., Garbe, T., Heym, B., Via, L. E. & Cole, S. T. (1995). *Mycobacterium tuberculosis* is a natural mutant with an inactivated oxidative-stress regulatory gene: implications for sensitivity to isoniazid. *Mol. Microbiol.* **17**, 889-900.

Deretic, V., Pagan-Ramos, E., Zhang, Y., Dhandayuthapani, S. & Via, L. E. (1996). The extreme sensitivity of *Mycobacterium tuberculosis* to the front-line antituberculosis drug isoniazid. *Nat. Biotechnol.* **14**, 1557-1561.

Dhandayuthapani, S., Mudd, M. & Deretic, V. (1997). Interactions of OxyR with the promoter region of the *oxyR* and *ahpC* genes from *Mycobacterium leprae* and *Mycobacterium tuberculosis. J. Bacteriol.* **179**, 2401-2409.

Diaz, A., Horjales, E., Rudino-Pinera, E., Arreola, R. & Hansberg, W. (2004). Unusual Cys-Tyr covalent bond in a large catalase. *J. Mol. Biol.* **342**, 971-985.

Diaz, G. A. & Wayne, L. G. (1974). Isolation and characterization of catalase produced by *Mycobacterium tuberculosis. Am. Rev. Respir. Dis.* **110**, 312-319.

Donald, L. J., Krokhin, O. V., Duckworth, H. W., Wiseman, B., Deemagran, T., Singh, R., Switala, J., Carpena, X., Fita, I., Loewen, P.C. (2003). Characterization of the catalase-peroxidase KatG from *Burkholderia pseudomallei* by mass spectrometry. *J. Biol. Chem.***278**, 35687-35692.

Doroshow, J. H., Leong, L., Margolin, K., Flanagan, B., Golberg, D., Akman, S., Carr, B., Odujinrin, O., Newman, E. (1989). Refractory metastatic breast cancer: salvage therapy with fluorouracil and high-dose continuous infusion leucovorin calcium. *J. Clin. Oncol.* **7**, 439-444.

Dos Santos, D. M. & Berridge, D. M. (2000). A continuation ratio random effects model for repeated ordinal responses. *Stat. Med.* **19**, 3377-3388.

Dunford, H. B. (1999) *Heme peroxidases*. Wiley-VCH. New York

Dunford, H. B. & Hsuanyu, Y. (1999). Kinetics of oxidation of serotonin by myeloperoxidase compounds I and II. *Biochem. Cell. Biol.* **77**, 449-457.

Eiglmeier, K., Fsihi, H., Heym, B. & Cole, S. T. (1997). On the catalase-peroxidase gene, *katG*, of *Mycobacterium leprae* and the implications for treatment of leprosy with isoniazid. *FEMS Microbiol. Lett.* **149**, 273-278.

Escolar, L., Perez-Martin, J. & de Lorenzo, V. (1999). Opening the iron box: transcriptional metalloregulation by the Fur protein. *J. Bacteriol.* **181**, 6223-6229.

Faguy, D. M. (2000). The controlled chaos of shifty pathogens. *Curr. Biol.* **10**, R498-501.

Faguy, D. M. & Doolittle, W. F. (2000). Horizontal transfer of catalase-peroxidase genes between archaea and pathogenic bacteria. *Trends. Genet.* **16**, 196-197.

Feldman, E. L., Stevens, M. J. & Greene, D. A. (1997). Pathogenesis of diabetic neuropathy. *Clin. Neurosci.***4**, 365-370.

Filizola, M., Laakkonen, L. & Loew, G. H. (1999). 3D modeling, ligand binding and activation studies of the cloned mouse delta, mu; and kappa opioid receptors. *Protein. Eng.* **12**, 927-942.

Fita, I. & Rossmann, M. G. (1985). The active center of catalase. *J. Mol. Biol.* **185**, 21-37.

Flohe, L., Gunzler, W. A. & Schock, H. H. (1973). Glutathione peroxidase: a selenoenzyme. *FEBS Lett.* **32**, 132-134.

Flohe, L. (1988). Glutathione peroxidase. *Basic Life Sci.* **49**, 663-668.

Forkl, H., Vandekerckhove, J., Drews, G. & Tadros, M. H. (1993). Molecular cloning, sequence analysis and expression of the gene for catalase-peroxidase (*cpeA*) from the photosynthetic bacterium *Rhodobacter capsulatus* B10. *Eur. J. Biochem.* **214**, 251-258.

Fridovich, I. (1975a). Superoxide dismutases. *Annu. Rev. Biochem.* . **44**, 147-159.

Fridovich, I. (1975b). Oxygen: boon and bane. *Am. Sci.* **63**, 54-59.

Fridovich, I. (1978). Superoxide dismutases: defence against endogenous superoxide radical. *Ciba. Found. Symp.*, 77-93.

Fridovich, I. (1995). Superoxide radical and superoxide dismutases. *Annu. Rev. Biochem.* . **64**, 97-112.

Fridovich, I. (1997). Superoxide anion radical ($O2^{-\cdot}$), superoxide dismutases, and related matters. *J. Biol. Chem.***272**, 18515-18517.

Fridovich, I. (1999). Fundamental aspects of reactive oxygen species, or what's the matter with oxygen? *Ann. N. Y. Acad. Sci.* **893**, 13-18.

Gardner, T. J. (1988). Oxygen radicals in cardiac surgery. *Free. Radic. Biol. Med.* **4**, 45-50.

Garnier, T., Eiglmeier, K., Camus, J. C. & other authors (2003). The complete genome sequence of *Mycobacterium bovis*. *Proc. Natl. Acad. Sci. U S A.* **100**, 7877-7882.

Ghiladi, R. A., Knudsen, G. M., Medzihradszky, K. F. & Ortiz de Montellano, P. R. (2005a). The Met-Tyr-Trp cross-link in *Mycobacterium tuberculosis* catalase-peroxidase (KatG): autocatalytic formation and effect on enzyme catalysis and spectroscopic properties. *J. Biol. Chem.***280**, 22651-22663.

Ghiladi, R. A., Medzihradszky, K. F. & Ortiz de Montellano, P. R. (2005b). Role of the Met-Tyr-Trp cross-link in *Mycobacterium tuberculosis* catalase-peroxidase (KatG) as revealed by KatG(M255I). *Biochemistry.* **44**, 15093-15105.

Ghiladi, R. A., Medzihradszky, K. F., Rusnak, F. M. & Ortiz de Montellano, P. R. (2005c). Correlation between isoniazid resistance and superoxide reactivity in *Mycobacterium tuberculosis* KatG. *J. Am. Chem. Soc.* **127**, 13428-13442.

Gouet, P., Jouve, H. M. & Dideberg, O. (1995). Crystal structure of *Proteus mirabilis* PR catalase with and without bound NADPH. *J. Mol. Biol.* **249**, 933-954.

Gray, H. B. & Winkler, J. R. (1996). Electron transfer in proteins. *Annu. Rev. Biochem.* **65**, 537-561.

Gray, H. B. & Winkler, J. R. (2003). Electron tunneling through proteins. *Q. Rev. Biophys.* **36**, 341-372.

Gregory, E. M. & Fridovich, I. (1974). Visualization of catalase on acrylamide gels. *Anal. Biochem.* **58**, 57-62.

Gutierrez, M. C., Brisse, S., Brosch, R., Fabre, M., Omais, B., Marmiesse, M., Supply, P. & Vincent, V. (2005). Ancient origin and gene mosaicism of the progenitor of *Mycobacterium tuberculosis*. *PLoS Pathog.* **1**, e5.

Gutteridge, J. M. & Mitchell, J. (1999). Redox imbalance in the critically ill. *Br. Med. Bull.* **55**, 49-75.

Harman, L. S., Carver, D. K., Schreiber, J. & Mason, R. P. (1986). One- and two-electron oxidation of reduced glutathione by peroxidases. *J. Biol. Chem.***261**, 1642-1648.

Hatchikian, E. C. & Henry, Y. A. (1977). An iron-containing superoxide dismutase from the strict anaerobe *Desulfovibrio desulfuricans* (Norway 4). *Biochimie.* **59**, 153-161.

Heering, H. A., Indiani, C., Regelsberger, G., Jakopitsch, C., Obinger, C. & Smulevich, G. (2002). New insights into the heme cavity structure of catalase-peroxidase: a spectroscopic approach to the recombinant *Synechocystis* enzyme and selected distal cavity mutants. *Biochemistry.* **41**, 9237-9247.

Heym, B., Alzari, P. M., Honore, N. & Cole, S. T. (1995). Missense mutations in the catalase-peroxidase gene, *kat*G, are associated with isoniazid resistance in *Mycobacterium tuberculosis*. *Mol. Microbiol.* **15**, 235-245.

Heym, B., Philipp, W. & Cole, S. T. (1996). Mechanisms of drug resistance in *Mycobacterium tuberculosis*. *Curr. Top. Microbiol. Immunol.* **215**, 49-69.

Hillar, A., Nicholls, P., Switala, J. & Loewen, P. C. (1994). NADPH binding and control of catalase compound II formation: comparison of bovine, yeast, and *Escherichia coli* enzymes. *Biochem. J.* **300 (Pt 2)**, 531-539.

Hillar, A. & Loewen, P. C. (1995). Comparison of isoniazid oxidation catalyzed by bacterial catalase-peroxidases and horseradish peroxidase. *Arch. Biochem. Biophys.* **323**, 438-446.

Hillar, A., Van Caeseele, L. & Loewen, P. C. (1999). Intracellular location of catalase-peroxidase hydroperoxidase I of *Escherichia coli*. *FEMS Microbiol. Lett.* **170**, 307-312.

Hillar, A., Peters, B., Pauls, R., Loboda, A., Zhang, H., Mauk, A. G. & Loewen, P. C. (2000). Modulation of the activities of catalase-peroxidase HPI of *Escherichia coli* by site-directed mutagenesis. *Biochemistry.* **39**, 5868-5875.

Hochman, A. & Goldberg, I. (1991). Purification and characterization of a catalase-peroxidase and a typical catalase from the bacterium *Klebsiella pneumoniae*. *Biochim. Biophys. Acta.* **1077**, 299-307.

Horsburgh, M. J., Clements, M. O., Crossley, H., Ingham, E. & Foster, S. J. (2001a). PerR controls oxidative stress resistance and iron storage proteins and is required for virulence in *Staphylococcus aureus*. *Infect. Immun.* **69**, 3744-3754.

Horsburgh, M. J., Ingham, E. & Foster, S. J. (2001b). In *Staphylococcus aureus*, fur is an interactive regulator with PerR, contributes to virulence, and is necessary for oxidative stress resistance through positive regulation of catalase and iron homeostasis. *J. Bacteriol.* **183**, 468-475.

Imlay, J. A. & Fridovich, I. (1991a). Assay of metabolic superoxide production in *Escherichia coli*. *J. Biol. Chem.***266**, 6957-6965.

Imlay, J. A. & Fridovich, I. (1991b). Superoxide production by respiring membranes of *Escherichia coli*. *Free. Radic. Res. Commun.* **12-13 Pt 1**, 59-66.

Imlay, K. R. & Imlay, J. A. (1996). Cloning and analysis of *sodC*, encoding the copper-zinc superoxide dismutase of *Escherichia coli*. *J. Bacteriol.* **178**, 2564-2571.

Ito, N., Phillips, S. E., Yadav, K. D. & Knowles, P. F. (1994). Crystal structure of a free radical enzyme, galactose oxidase. *J. Mol. Biol.* **238**, 794-814.

Itoh, S., Takayama, S., Arakawa, R., Furuta, A., Komatsu, M., Ishida, A., Takamuku, S. & Fukuzumi, S. (1997). Active site models for galactose oxidase. Electronic fffect of the thioether group in the novel organic cofactor. *Inorg. Chem.* **36**, 1407-1416.

Ivancich, A., Lutz, M. & Mattioli, T. A. (1997). Temperature-dependent behavior of bacteriochlorophyll and bacteriopheophytin in the photosynthetic reaction center from *Rhodobacter sphaeroides*. *Biochemistry.* **36**, 3242-3253.

Ivancich, A., Artz, K., Williams, J. C., Allen, J. P. & Mattioli, T. A. (1998). Effects of hydrogen bonds on the redox potential and electronic structure of the bacterial primary electron donor. *Biochemistry.* **37**, 11812-11820.

Ivancich, A., Mazza, G. & Desbois, A. (2001). Comparative electron paramagnetic resonance study of radical intermediates in turnip peroxidase isozymes. *Biochemistry.* **40**, 6860-6866.

Ivancich, A., Jakopitsch, C., Auer, M., Un, S. & Obinger, C. (2003). Protein-based radicals in the catalase-peroxidase of *Synechocystis* PCC6803: a multifrequency EPR investigation of wild-type and variants on the environment of the heme active site. *J. Am. Chem. Soc.* **125**, 14093-14102.

Jakopitsch, C., Ruker, F., Regelsberger, G., Dockal, M., Peschek, G. A. & Obinger, C. (1999). Catalase-peroxidase from the cyanobacterium *Synechocystis*

PCC 6803: cloning, overexpression in *Escherichia coli*, and kinetic characterization. *Biol. Chem.* **380**, 1087-1096.

Jakopitsch, C., Regelsberger, G., Furtmuller, P. G., Ruker, F., Peschek, G. A. & Obinger, C. (2001). Catalase-peroxidase from *Synechocystis* is capable of chlorination and bromination reactions. *Biochem. Biophys. Res. Commun.* **287**, 682-687.

Jakopitsch, C., Auer, M., Ivancich, A., Ruker, F., Furtmuller, P. G. & Obinger, C. (2003a). Total conversion of bifunctional catalase-peroxidase (KatG) to monofunctional peroxidase by exchange of a conserved distal side tyrosine. *J. Biol. Chem.***278**, 20185-20191.

Jakopitsch, C., Auer, M., Regelsberger, G., Jantschko, W., Furtmuller, P. G., Ruker, F. & Obinger, C. (2003b). The catalytic role of the distal site asparagine-histidine couple in catalase-peroxidases. *Eur. J. Biochem. / FEBS* **270**, 1006-1013.

Jakopitsch, C., Auer, M., Regelsberger, G., Jantschko, W., Furtmuller, P. G., Ruker, F. & Obinger, C. (2003c). Distal site aspartate is essential in the catalase activity of catalase-peroxidases. *Biochemistry.* **42**, 5292-5300.

Jakopitsch, C., Kolarich, D., Petutschnig, G., Furtmuller, P. G. & Obinger, C. (2003d). Distal side tryptophan, tyrosine and methionine in catalase-peroxidases are covalently linked in solution. *FEBS Lett.* **552**, 135-140.

Jakopitsch, C., Ivancich, A., Schmuckenschlager, F., Wanasinghe, A., Poltl, G., Furtmuller, P. G., Ruker, F. & Obinger, C. (2004). Influence of the unusual covalent adduct on the kinetics and formation of radical intermediates in *Synechocystis* catalase peroxidase: a stopped-flow and EPR characterization of the MET275, TYR249, and ARG439 variants. *J. Biol. Chem.***279**, 46082-46095.

Jakopitsch, C., Droghetti, E., Schmuckenschlager, F., Furtmuller, P. G., Smulevich, G. & Obinger, C. (2005a). Role of the main access channel of catalase-peroxidase in catalysis. *J. Biol. Chem.***280**, 42411-42422.

Jakopitsch, C., Wanasinghe, A., Jantschko, W., Furtmuller, P. G. & Obinger, C. (2005b). Kinetics of interconversion of ferrous enzymes, compound II and compound III, of wild-type *Synechocystis* catalase-peroxidase and Y249F: proposal for the catalatic mechanism. *J. Biol. Chem.***280**, 9037-9042.

Jenney, F. E., Jr., Verhagen, M. F., Cui, X. & Adams, M. W. (1999). Anaerobic microbes: oxygen detoxification without superoxide dismutase. *Science.* **286**, 306-309.

Johnsson, K., Froland, W. A. & Schultz, P. G. (1997). Overexpression, purification, and characterization of the catalase-peroxidase KatG from *Mycobacterium tuberculosis*. *J. Biol. Chem.***272**, 2834-2840.

Jovanovic, T., Ascenso, C., Hazlett, K. R. & other authors (2000). Neelaredoxin, an iron-binding protein from the syphilis spirochete, *Treponema pallidum*, is a superoxide reductase. *J. Biol. Chem.***275**, 28439-28448.

Jung, I. L. & Kim, I. G. (2003). Transcription of ahpC, katG, and katE genes in *Escherichia coli* is regulated by polyamines: polyamine-deficient mutant sensitive to H_2O_2 induced oxidative damage. *Biochem. Biophys. Res. Commun.* **301**, 915-922.

Kalko, S. G., Gelpi, J. L., Fita, I. & Orozco, M. (2001). Theoretical study of the mechanisms of substrate recognition by catalase. *J. Am. Chem. Soc.* **123**, 9665-9672.

Kao, S. M. & Hassan, H. M. (1985). Biochemical characterization of a paraquat-tolerant mutant of *Escherichia coli*. *J. Biol. Chem.***260**, 10478-10481.

Kapetanaki, S. M., Chouchane, S., Yu, S., Magliozzo, R. S. & Schelvis, J. P. (2005). Resonance Raman spectroscopy of Compound II and its decay in *Mycobacterium tuberculosis* catalase-peroxidase KatG and its isoniazid resistant mutant S315T. *Journal of inorganic Biochemistry.* **99**, 1401-1406.

Kapur, V., Li, L. L., Hamrick, M. R. & other authors (1995). Rapid Mycobacterium species assignment and unambiguous identification of mutations associated with antimicrobial resistance in *Mycobacterium tuberculosis* by automated DNA sequencing. *Arch Pathol Lab Med* **119**, 131-138.

Kelly, P. M. (1997). Wrong drug used for tuberculosis. *Int. J. Tuberc. Lung Dis.* **1**, 385.

Kengen, S. W., Bikker, F. J., Hagen, W. R., de Vos, W. M. & van der Oost, J. (2001). Characterization of a catalase-peroxidase from the hyperthermophilic archaeon *Archaeoglobus fulgidus*. *Extremophiles* **5**, 323-332.

Kengen, S. W., van der Oost, J. & de Vos, W. M. (2003). Molecular characterization of H_2O_2 forming NADH oxidases from *Archaeoglobus fulgidus*. *Eur. J. Biochem.* **270**, 2885-2894.

Kespichayawattana, W., Rattanachetkul, S., Wanun, T., Utaisincharoen, P. & Sirisinha, S. (2000). *Burkholderia pseudomallei* induces cell fusion and actin-associated membrane protrusion: a possible mechanism for cell-to-cell spreading. *Infect. Immun.* **68**, 5377-5384.

Klenk, H. P., Clayton, R. A., Tomb, J. F. & other authors (1997). The complete genome sequence of the hyperthermophilic, sulphate-reducing archaeon *Archaeoglobus fulgidus*. *Nature.* **390**, 364-370.

Klotz, M. G., Klassen, G. R. & Loewen, P. C. (1997). Phylogenetic relationships among prokaryotic and eukaryotic catalases. *Mol. Biol. Evol.* **14**, 951-958.

Klotz, M. G. & Loewen, P. C. (2003). The molecular evolution of catalatic hydroperoxidases: evidence for multiple lateral transfer of genes between prokaryota and from bacteria into eukaryota. *Mol. Biol. Evol.* **20**, 1098-1112.

Ko, T. P., Day, J., Malkin, A. J. & McPherson, A. (1999). Structure of orthorhombic crystals of beef liver catalase. *Acta. Crystallogr. D. Biol. Crystallogr.* **55**, 1383-1394.

Kono, Y. & Fridovich, I. (1983). Functional significance of manganese catalase in *Lactobacillus plantarum*. *J. Bacteriol.* **155**, 742-746.

Kunkel, T. A., Roberts, J. D. & Zakour, R. A. (1987). Rapid and efficient site-specific mutagenesis without phenotypic selection. *Methods Enzymol.* **154**, 367-382.

Larsen, M. H., Vilcheze, C., Kremer, L. & other authors (2002). Overexpression of *inhA*, but not *kasA*, confers resistance to isoniazid and ethionamide in *Mycobacterium smegmatis*, *M. bovis* BCG and *M. tuberculosis*. *Mol. Microbiol.* **46**, 453-466.

Layne, E. (1957). Spectrophotometric and turbidimetric methods for measuring proteins. *Methods Enzymol.* . **3,** 447-454

Lee, A. S., Tang, L. L., Lim, I. H., Ling, M. L., Tay, L. & Wong, S. Y. (1997). Lack of clinical significance for the common arginine-to-leucine substitution at codon 463 of the *katG* gene in isoniazid-resistant *Mycobacterium tuberculosis* in Singapore. *J. Infect. Dis* **176**, 1125-1127.

Leelarasamee, A. (2004). Recent development in melioidosis. *Curr. Opin. Infect. Dis.* **17**, 131-136.

Lei, B., Wei, C. J. & Tu, S. C. (2000). Action mechanism of antitubercular isoniazid. Activation by *Mycobacterium tuberculosis* KatG, isolation, and characterization of *inhA* inhibitor. *J. Biol. Chem.***275**, 2520-2526.

Li, L., Bannantine, J. P., Zhang, Q., Amonsin, A., May, B. J., Alt, D., Banerji, N., Kanjilal, S. & Kapur, V. (2005). The complete genome sequence of *Mycobacterium avium* subspecies paratuberculosis. *Proc. Natl. Acad. Sci. U S A.* **102**, 12344-12349.

Liochev, S. I. & Fridovich, I. (1992). Superoxide generated by glutathione reductase initiates a vanadate-dependent free radical chain oxidation of NADH. *Arch. Biochem. Biophys.* **294**, 403-406.

Liochev, S. I. & Fridovich, I. (1997). How does superoxide dismutase protect against tumor necrosis factor: a hypothesis informed by effect of superoxide on "free" iron. *Free. Radic. Biol. Med.* **23**, 668-671.

Loewen, P. (1996). Probing the structure of catalase HPII of *Escherichia coli*--a review. *Gene.* **179**, 39-44.

Loewen, P. C., Triggs, B. L., Klassen, G. R. & Weiner, J. H. (1983). Identification and physical characterization of a Col E1 hybrid plasmid containing a catalase gene of *Escherichia coli*. *Can. J. Biochem. Cell Biol.* **61**, 1315-1321.

Loewen, P. C. (1984). Isolation of catalase-deficient *Escherichia coli* mutants and genetic mapping of *katE*, a locus that affects catalase activity. *J. Bacteriol.* **157**, 622-626.

Loewen, P. C. & Triggs, B. L. (1984). Genetic mapping of *katF*, a locus that with *katE* affects the synthesis of a second catalase species in *Escherichia coli*. *J. Bacteriol.* **160**, 668-675.

Loewen, P. C., Switala, J. & Triggs-Raine, B. L. (1985a). Catalases HPI and HPII in *Escherichia coli* are induced independently. *Arch. Biochem. Biophys.* **243**, 144-149.

Loewen, P. C., Triggs, B. L., George, C. S. & Hrabarchuk, B. E. (1985b). Genetic mapping of *katG*, a locus that affects synthesis of the bifunctional catalase-peroxidase hydroperoxidase I in *Escherichia coli*. *J. Bacteriol.* **162**, 661-667.

Loewen, P. C. & Switala, J. (1986). Purification and characterization of catalase HPII from *Escherichia coli* K12. *Biochem. Cell Biol.* **64**, 638-646.

Loewen, P. C. & Switala, J. (1987a). genetic mapping of katA, a locus that affects catalase 1 level in *Bacillus subtilis*. *J. Bacteriol.* **169**, 5848-5851.

Loewen, P. C. & Switala, J. (1987b). Purification and characterization of catalase-1 from *Bacillus subtilis*. *Biochem. Cell Biol.* **65**, 939-947.

Loewen, P. C. & Switala, J. (1988). Purification and characterization of spore-specific catalase-2 from *Bacillus subtilis*. *Biochem. Cell Biol.* **66**, 707-714.

Loewen, P. C. (1989). genetic mapping of *katB*, a locus that affects catalase 2 levels in *Bacillus subtilis*. *Can. J. Microbiol.* **35**, 807-810.

Loewen, P. C., Switala, J., von Ossowski, I., Hillar, A., Christie, A., Tattrie, B. & Nicholls, P. (1993). Catalase HPII of *Escherichia coli* catalyzes the conversion of protoheme to cis-heme d. *Biochemistry.* **32**, 10159-10164.

Loewen, P. C., Carpena, X., Rovira, C., Ivancich, A., Perez-Luque, R., Haas, R., Odenbreit, S., Nicholls, P. & Fita, I. (2004). Structure of *Helicobacter pylori* catalase, with and without formic acid bound, at 1.6 Å resolution. *Biochemistry.* **43**, 3089-3103.

Lombard, M., Fontecave, M., Touati, D. & Niviere, V. (2000a). Reaction of the desulfoferrodoxin from *Desulfoarculus baarsii* with superoxide anion. Evidence for a superoxide reductase activity. *J. Biol. Chem.***275**, 115-121.

Lombard, M., Touati, D., Fontecave, M. & Niviere, V. (2000b). Superoxide reductase as a unique defense system against superoxide stress in the microaerophile *Treponema pallidum. J. Biol. Chem.***275**, 27021-27026.

Loprasert, S., Atichartpongkun, S., Whangsuk, W. & Mongkolsuk, S. (1997). Isolation and analysis of the *Xanthomonas* alkyl hydroperoxide reductase gene and the peroxide sensor regulator genes *ahpC* and *ahpF-oxyR-orfX. J. Bacteriol.* **179**, 3944-3949.

Loprasert, S., Sallabhan, R., Whangsuk, W. & Mongkolsuk, S. (2002). The *Burkholderia pseudomallei oxyR* gene: expression analysis and mutant characterization. *Gene.* **296**, 161-169.

Loprasert, S., Sallabhan, R., Whangsuk, W. & Mongkolsuk, S. (2003a). Compensatory increase in *ahpC* gene expression and its role in protecting *Burkholderia pseudomallei* against reactive nitrogen intermediates. *Arch. Microbiol.* **180**, 498-502.

Loprasert, S., Whangsuk, W., Sallabhan, R. & Mongkolsuk, S. (2003b). Regulation of the *katG*-dpsA operon and the importance of KatG in survival of *Burkholderia pseudomallei* exposed to oxidative stress. *FEBS Lett.* **542**, 17-21.

Loprasert, S., Whangsuk, W., Sallabhan, R. & Mongkolsuk, S. (2004). DpsA protects the human pathogen *Burkholderia pseudomallei* against organic hydroperoxide. *Arch. Microbiol.* **182**, 96-101.

Lundrigan, M. D., Arceneaux, J. E., Zhu, W. & Byers, B. R. (1997). Enhanced hydrogen peroxide sensitivity and altered stress protein expression in iron-starved *Mycobacterium smegmatis*. *Biometals* **10**, 215-225.

Magliozzo, R. S. & Marcinkeviciene, J. A. (1997). The role of Mn(II)-peroxidase activity of mycobacterial catalase-peroxidase in activation of the antibiotic isoniazid. *J. Biol. Chem.***272**, 8867-8870.

Maj, M., Nicholls, P., Obinger, C., Hillar, A. & Loewen, P. C. (1996). Reaction of *E. coli* catalase HPII with cyanide as ligand and as inhibitor. *Biochim. Biophys. Acta.* **1298**, 241-249.

Marcinkeviciene, J. A., Magliozzo, R. S. & Blanchard, J. S. (1995). Purification and characterization of the *Mycobacterium smegmatis* catalase-peroxidase involved in isoniazid activation. *J. Biol. Chem.***270**, 22290-22295.

Marttila, H. J., Soini, H., Huovinen, P. & Viljanen, M. K. (1996). *katG* mutations in isoniazid-resistant *Mycobacterium tuberculosis* isolates recovered from Finnish patients. *Antimicrob. Agents. Chemother.* **40**, 2187-2189.

Marttila, H. J., Soini, H., Eerola, E., Vyshnevskaya, E., Vyshnevskiy, B. I., Otten, T. F., Vasilyef, A. V. & Viljanen, M. K. (1998). A Ser315Thr substitution in KatG is predominant in genetically heterogeneous multidrug-resistant *Mycobacterium tuberculosis* isolates originating from the St. Petersburg area in Russia. *Antimicrob. Agents. Chemother.* **42**, 2443-2445.

McCord, J. M. & Fridovich, I. (1969a). The utility of superoxide dismutase in studying free radical reactions. I. Radicals generated by the interaction of sulfite, dimethyl sulfoxide, and oxygen. *J. Biol. Chem.***244**, 6056-6063.

McCord, J. M. & Fridovich, I. (1969b). Superoxide dismutase. An enzymic function for erythrocuprein (hemocuprein). *J. Biol. Chem.***244**, 6049-6055.

Mdluli, K., Slayden, R. A., Zhu, Y., Ramaswamy, S., Pan, X., Mead, D., Crane, D. D., Musser, J. M. & Barry, C. E., 3rd (1998a). Inhibition of a *Mycobacterium tuberculosis* beta-ketoacyl ACP synthase by isoniazid. *Science.* **280**, 1607-1610.

Mdluli, K., Swanson, J., Fischer, E., Lee, R. E. & Barry, C. E., 3rd (1998b). Mechanisms involved in the intrinsic isoniazid resistance of *Mycobacterium avium*. *Mol. Microbiol.* **27**, 1223-1233.

Menendez, M. C., Ainsa, J. A., Martin, C. & Garcia, M. J. (1997). *katG*I and *katG*II encode two different catalases-peroxidases in *Mycobacterium fortuitum*. *J. Bacteriol.* **179**, 6880-6886.

Messerschmidt, A. & Wever, R. (1996). X-ray structure of a vanadium-containing enzyme: chloroperoxidase from the fungus *Curvularia inaequalis*. *Proc. Natl. Acad. Sci. U S A.* **93**, 392-396.

Messner, K. R. & Imlay, J. A. (2002). In vitro quantitation of biological superoxide and hydrogen peroxide generation. *Methods Enzymol.* **349**, 354-361.

Middlebrook, G. (1952). Sterilization of tubercle bacilli by isonicotinic acid hydrazide and the incidence of variants resistant to the drug in vitro. *Am. Rev. Tuberc.* **65**, 765-767.

Middlebrook, G. (1954a). Techniques of drug-resistance tests. *Am. Rev. Tuberc.* **70**, 922-923.

Middlebrook, G. (1954b). Isoniazid-resistance and catalase activity of tubercle bacilli; a preliminary report. *Am. Rev. Tuberc.* **69**, 471-472.

Middlebrook, G., Cohn, M. L. & Schaefer, W. B. (1954a). Studies on isoniazid and tubercle bacilli. III. The isolation, drug-susceptibility, and catalase-testing of tubercle bacilli from isoniazid-treated patients. *Am. Rev. Tuberc.* **70**, 852-872.

Middlebrook, G., Cohn, M. L., Schaefer, W. B. & Kovitz, C. (1954b). Developments in the laboratory: the growth requirements and pathogenic properties of isoniazid-resistant tubercle bacilli. *Trans. Annu. Meet. Natl. Tuberc. Assoc.* **96**, 239-240.

Middlebrook, G. & Dressler, S. H. (1954). Clinical evaluation of isoniazid. *Am. Rev. Tuberc.* **70**, 1102-1103.

Millett, F., Miller, M. A., Geren, L. & Durham, B. (1995). Electron transfer between cytochrome *c* and cytochrome *c* peroxidase. *J. Bioenerg. Biomembr.* **27**, 341-351.

Mitchison, D. A. & Selkon, J. B. (1956). The bactericidal activities of antituberculous drugs. *Am. Rev. Tuberc.* **74**, 109-116; discussion, 116-123.

Morris, S., Bai, G. H., Suffys, P., Portillo-Gomez, L., Fairchok, M. & Rouse, D. (1995). Molecular mechanisms of multiple drug resistance in clinical isolates of *Mycobacterium tuberculosis*. *J. Infect. Dis. s* **171**, 954-960.

Morris, S. L., Nair, J. & Rouse, D. A. (1992). The catalase-peroxidase of *Mycobacterium intracellulare*: nucleotide sequence analysis and expression in *Escherichia coli*. *J. Gen. Microbiol.* **138**, 2363-2370.

Mukhopadhyay, S. & Schellhorn, H. E. (1994). Induction of *Escherichia coli* hydroperoxidase I by acetate and other weak acids. *J. Bacteriol.* **176**, 2300-2307.

Mulvey, M. R., Sorby, P. A., Triggs-Raine, B. L. & Loewen, P. C. (1988). Cloning and physical characterization of *katE* and *katF* required for catalase HPII expression in *Escherichia coli*. *Gene.* **73**, 337-345.

Mulvey, M. R., Switala, J., Borys, A. & Loewen, P. C. (1990). Regulation of transcription of *katE* and *katF* in *Escherichia coli*. *J. Bacteriol.* **172**, 6713-6720.

Murshudov, G. N., Melik-Adamyan, W. R., Grebenko, A. I., Barynin, V. V., Vagin, A. A., Vainshtein, B. K., Dauter, Z. & Wilson, K. S. (1992). Three-dimensional structure of catalase from *Micrococcus lysodeikticus* at 1.5 Å resolution. *FEBS Lett.* **312**, 127-131.

Murshudov, G. N., Grebenko, A. I., Barynin, V. & other authors (1996). Structure of the heme d of *Penicillium vitale* and *Escherichia coli* catalases. *J. Biol. Chem.***271**, 8863-8868.

Murthy, M. R., Reid, T. J., 3rd, Sicignano, A., Tanaka, N. & Rossmann, M. G. (1981). Structure of beef liver catalase. *J. Mol. Biol.* **152**, 465-499.

Musser, J. M. (1995). Antimicrobial agent resistance in mycobacteria: molecular genetic insights. *Clin. Microbiol. Rev.* **8**, 496-514.

Musser, J. M., Kapur, V., Williams, D. L., Kreiswirth, B. N., van Soolingen, D. & van Embden, J. D. (1996). Characterization of the catalase-peroxidase gene (*katG*) and *inhA* locus in isoniazid-resistant and -susceptible strains of *Mycobacterium tuberculosis* by automated DNA sequencing: restricted array of mutations associated with drug resistance. *J. Infect. Dis* **173**, 196-202.

Mutsuda, M., Ishikawa, T., Takeda, T. & Shigeoka, S. (1996). The catalase-peroxidase of *Synechococcus* PCC 7942: purification, nucleotide sequence analysis and expression in *Escherichia coli*. *Biochem. J.* **316 (Pt 1)**, 251-257.

Nagy, J. M., Cass, A. E. & Brown, K. A. (1995). Progress in the characterization of catalase-peroxidase from *Mycobacterium tuberculosis*. *Biochem. Soc. Trans.* **23**, 152S.

Nagy, J. M., Cass, A. E. & Brown, K. A. (1997). Purification and characterization of recombinant catalase-peroxidase, which confers isoniazid sensitivity in *Mycobacterium tuberculosis*. *J. Biol. Chem.***272**, 31265-31271.

Nagy, J. M., Jesmin, J., Servos, S., Cass, A. E. & Brown, K. A. (1998). Site-directed mutants of the catalase-peroxidase from *Mycobacterium tuberculosis*. *Biochem. Soc. Trans.* **26**, S281.

Nicholls, P. (1962). The role of the protein in haem enzymes. *Biochim. Biophys. Acta.* **60**, 217-225.

Obinger, C., Maj, M., Nicholls, P. & Loewen, P. (1997a). Activity, peroxide compound formation, and heme d synthesis in *Escherichia coli* HPII catalase. *Arch. Biochem. Biophys.* **342**, 58-67.

Obinger, C., Regelsberger, G., Strasser, G., Burner, U. & Peschek, G. A. (1997b). Purification and characterization of a homodimeric catalase-peroxidase from the cyanobacterium *Anacystis nidulans*. *Biochem. Biophys. Res. Commun.* **235**, 545-552.

Obinger, C., Regelsberger, G., Furtmuller, P. G., Jakopitsch, C., Ruker, F., Pircher, A. & Peschek, G. A. (1999). Catalase-peroxidases in cyanobacteria--similarities and differences to ascorbate peroxidases. *Free Radic. Res.* **31 Suppl**, S243-249.

Ostermeier, C., Harrenga, A., Ermler, U. & Michel, H. (1997). Structure at 2.7 A resolution of the *Paracoccus denitrificans* two-subunit cytochrome *c* oxidase complexed with an antibody FV fragment. *Proc. Natl. Acad. Sci. U S A.* **94**, 10547-10553.

Payton, M., Auty, R., Delgoda, R., Everett, M. & Sim, E. (1999). Cloning and characterization of arylamine N-acetyltransferase genes from *Mycobacterium smegmatis* and *Mycobacterium tuberculosis*: increased expression results in isoniazid resistance. *J. Bacteriol.* **181**, 1343-1347.

Pierattelli, R., Banci, L., Eady, N. A., Bodiguel, J., Jones, J. N., Moody, P. C., Raven, E. L., Jamart-Gregoire, B. & Brown, K. A. (2004). Enzyme-catalyzed mechanism of isoniazid activation in class I and class III peroxidases. *J. Biol. Chem.***279**, 39000-39009.

Preston, C. M. & Barrett, J. (1987). Heligmosomoides polygyrus: peroxidase activity. *Exp. Parasitol.* **64**, 24-28.

Pretorius, G. S., van Helden, P. D., Sirgel, F., Eisenach, K. D. & Victor, T. C. (1995). Mutations in *katG* gene sequences in isoniazid-resistant clinical isolates of *Mycobacterium tuberculosis* are rare. *Antimicrob. Agents. Chemother.* **39**, 2276-2281.

Ramaswamy, S. & Musser, J. M. (1998). Molecular genetic basis of antimicrobial agent resistance in *Mycobacterium tuberculosis*: 1998 update. *Tuber. Lung Dis.* **79**, 3-29.

Rawat, R., Whitty, A. & Tonge, P. J. (2003). The isoniazid-NAD adduct is a slow, tight-binding inhibitor of InhA, the *Mycobacterium tuberculosis* enoyl reductase: adduct affinity and drug resistance. *Proc. Natl. Acad. Sci. U S A.* **100**, 13881-13886.

Regelsberger, G., Jakopitsch, C., Engleder, M., Ruker, F., Peschek, G. A. & Obinger, C. (1999). Spectral and kinetic studies of the oxidation of monosubstituted phenols and anilines by recombinant *Synechocystis* catalase-peroxidase compound I. *Biochemistry.* **38**, 10480-10488.

Regelsberger, G., Jakopitsch, C., Ruker, F., Krois, D., Peschek, G. A. & Obinger, C. (2000). Effect of distal cavity mutations on the formation of compound I in catalase-peroxidases. *J. Biol. Chem.***275**, 22854-22861.

Regelsberger, G., Jakopitsch, C., Furtmuller, P. G., Rueker, F., Switala, J., Loewen, P. C. & Obinger, C. (2001). The role of distal tryptophan in the bifunctional activity of catalase-peroxidases. *Biochem. Soc. Trans.* **29**, 99-105.

Rice-Evans, C. & Baysal, E. (1987). Iron-mediated oxidative stress in erythrocytes. *Biochem. J.* **244**, 191-196.

Rice-Evans, P. & Rao, K. U. (1988). Evidence for positronium formation assisted by molecular recoil at a graphite surface covered with a semilayer of methane. *Physical Review Letters* **61**, 581-584.

Ristow, M., Mohlig, M., Rifai, M., Schatz, H., Feldmann, K. & Pfeiffer, A. (1995). New isoniazid/ethionamide resistance gene mutation and screening for multidrug-resistant *Mycobacterium tuberculosis* strains. *Lancet* **346**, 502-503.

Ro, Y. T., Lee, H. I., Kim, E. J., Koo, J. H., Kim, E. & Kim, Y. M. (2003). Purification, characterization, and physiological response of a catalase-peroxidase in *Mycobacterium* sp. strain JC1 DSM 3803 grown on methanol. *FEMS Microbiol. Lett.* **226**, 397-403.

Rocha, E. R., Owens, G., Jr. & Smith, C. J. (2000). The redox-sensitive transcriptional activator OxyR regulates the peroxide response regulon in the obligate anaerobe Bacteroides fragilis. *J. Bacteriol.* **182**, 5059-5069.

Rouse, D. A. & Morris, S. L. (1995). Molecular mechanisms of isoniazid resistance in *Mycobacterium tuberculosis* and *Mycobacterium bovis*. *Infect. Immun.* **63**, 1427-1433.

Rouse, D. A., DeVito, J. A., Li, Z., Byer, H. & Morris, S. L. (1996). Site-directed mutagenesis of the *katG* gene of *Mycobacterium tuberculosis*: effects on catalase-peroxidase activities and isoniazid resistance. *Mol. Microbiol.* **22**, 583-592.

Rozwarski, D. A., Grant, G. A., Barton, D. H., Jacobs, W. R., Jr. & Sacchettini, J. C. (1998). Modification of the NADH of the isoniazid target (InhA) from *Mycobacterium tuberculosis*. *Science.* **279**, 98-102.

Saint-Joanis, B., Souchon, H., Wilming, M., Johnsson, K., Alzari, P. M. & Cole, S. T. (1999). Use of site-directed mutagenesis to probe the structure, function and isoniazid activation of the catalase/peroxidase, KatG, from *Mycobacterium tuberculosis*. *Biochem. J.* **338 (Pt 3)**, 753-760.

Sambrook, J., Fritsch, E.F., and Maniatis, T. (1989) *Molecular Cloning : A Laboratory Manual.* Cold Spring Harbour Laboratory. Cold Spring Harbour Press. New York.

Sanger, F., Nicklen, S. & Coulson, A. R. (1977). DNA sequencing with chain-terminating inhibitors. *Proc. Natl. Acad. Sci. U S A.* **74**, 5463-5467.

Santoni, E., Jakopitsch, C., Obinger, C. & Smulevich, G. (2004a). Comparison between catalase-peroxidase and cytochrome *c* peroxidase. The role of the hydrogen-bond networks for protein stability and catalysis. *Biochemistry.* **43**, 5792-5802.

Santoni, E., Jakopitsch, C., Obinger, C. & Smulevich, G. (2004b). Manipulating the covalent link between distal side tryptophan, tyrosine, and methionine in catalase-peroxidases: an electronic absorption and resonance Raman study. *Biopolymers* **74**, 46-50.

Schellhorn, H. E. & Stones, V. L. (1992). Regulation of *katF* and *katE* in *Escherichia coli* K-12 by weak acids. *J. Bacteriol.* **174**, 4769-4776.

Schopf, J. W. (1993). Microfossils of the Early Archean Apex chert: new evidence of the antiquity of life. *Science.* **260**, 640-646.

Sevinc, M. S., Ens, W. & Loewen, P. C. (1995). The cysteines of catalase HPII of *Escherichia coli*, including Cys438 which is blocked, do not have a catalytic role. *Eur. J. Biochem. / FEBS* **230**, 127-132.

Sevinc, M. S., Switala, J., Bravo, J., Fita, I. & Loewen, P. C. (1998). Truncation and heme pocket mutations reduce production of functional catalase HPII in *Escherichia coli*. *Protein. Eng.* **11**, 549-555.

Sevinc, M. S., Mate, M. J., Switala, J., Fita, I. & Loewen, P. C. (1999). Role of the lateral channel in catalase HPII of *Escherichia coli*. *Protein Sci* **8**, 490-498.

Sharp, K. H., Moody, P. C., Brown, K. A. & Raven, E. L. (2004). Crystal structure of the ascorbate peroxidase-salicylhydroxamic acid complex. *Biochemistry.* **43**, 8644-8651.

Sherman, D. R., Sabo, P. J., Hickey, M. J., Arain, T. M., Mahairas, G. G., Yuan, Y., Barry, C. E., 3rd & Stover, C. K. (1995). Disparate responses to oxidative stress in saprophytic and pathogenic mycobacteria. *Proc. Natl. Acad. Sci. U S A.* **92**, 6625-6629.

Shi, W., Hoganson, C. W., Espe, M., Bender, C. J., Babcock, G. T., Palmer, G., Kulmacz, R. J. & Tsai, A. (2000). Electron paramagnetic resonance and electron nuclear double resonance spectroscopic identification and characterization of the tyrosyl radicals in prostaglandin H synthase 1. *Biochemistry.* **39**, 4112-4121.

Sies, H. (1991). Oxidative stress: from basic research to clinical application. *The American journal of medicine* **91**, 31S-38S.

Sies, H. (1993). Strategies of antioxidant defense. *Eur. J. Biochem. / FEBS* **215**, 213-219.

Singh, R., Wiseman, B., Deemagarn, T., Donald, L. J., Duckworth, H. W., Carpena, X., Fita, I. & Loewen, P. C. (2004). Catalase-peroxidases (KatG) exhibit NADH oxidase activity. *J. Biol. Chem.***279**, 43098-43106.

Sivaraja, M., Goodin, D. B., Smith, M. & Hoffman, B. M. (1989). Identification by ENDOR of Trp191 as the free-radical site in cytochrome *c* peroxidase compound ES. *Science.* **245**, 738-740.

Smirnoff, N. & Pallanca, J. E. (1996). Ascorbate metabolism in relation to oxidative stress. *Biochem. Soc. Trans.* **24**, 472-478.

Smith, A. T., Santama, N., Dacey, S., Edwards, M., Bray, R. C., Thorneley, R. N. & Burke, J. F. (1990). Expression of a synthetic gene for horseradish peroxidase C in *Escherichia coli* and folding and activation of the recombinant enzyme with Ca^{2+} and heme. *J. Biol. Chem.***265**, 13335-13343.

Smith, A. T. & Veitch, N. C. (1998). Substrate binding and catalysis in heme peroxidases. *Current opinion in chemical biology* **2**, 269-278.

Smulevich, G., Jakopitsch, C., Droghetti, E. & Obinger, C. (2006). Probing the structure and bifunctionality of catalase-peroxidase (KatG). *J. Inorg Biochem.* **100**, 568-585.

Stadtman, T. C. (1991). Biosynthesis and function of selenocysteine-containing enzymes. *J. Biol. Chem.***266**, 16257-16260.

Stehle, T., Ahmed, S. A., Claiborne, A. & Schulz, G. E. (1991). Structure of NADH peroxidase from *Streptococcus faecalis* 10C1 refined at 2.16 Å resolution. *J. Mol. Biol.* **221**, 1325-1344.

Stoeckle, M. Y., Guan, L., Riegler, N., Weitzman, I., Kreiswirth, B., Kornblum, J., Laraque, F. & Riley, L. W. (1993). Catalase-peroxidase gene sequences in isoniazid-sensitive and -resistant strains of *Mycobacterium tuberculosis* from New York City. *J. Infect. Dis. s* **168**, 1063-1065.

Su, W. J., Lee, P. Y., Yu, K. W. & Perng, R. P. (1997). Drug resistance of *Mycobacterium tuberculosis* isolated from patients at a medical center in Taiwan. *Chinese medical journal* **60**, 21-27.

Subsin, B., Thomas, M. S., Katzenmeier, G., Shaw, J. G., Tungpradabkul, S. & Kunakorn, M. (2003). Role of the stationary growth phase sigma factor RpoS of *Burkholderia pseudomallei* in response to physiological stress conditions. *J. Bacteriol.* **185**, 7008-7014.

Switala, J., Triggs-Raine, B. L. & Loewen, P. C. (1990). Homology among bacterial catalase genes. *Can. J. Microbiol.* **36**, 728-731.

Switala, J., O'Neil, J. O. & Loewen, P. C. (1999). Catalase HPII from *Escherichia coli* exhibits enhanced resistance to denaturation. *Biochemistry.* **38**, 3895-3901.

Switala, J. & Loewen, P. C. (2002). Diversity of properties among catalases. *Arch. Biochem. Biophys.* **401**, 145-154.

Touati, D., Jacques, M., Tardat, B., Bouchard, L. & Despied, S. (1995). Lethal oxidative damage and mutagenesis are generated by iron in delta fur mutants of *Escherichia coli*: protective role of superoxide dismutase. *J. Bacteriol.* **177**, 2305-2314.

Triggs-Raine, B. L. & Loewen, P. C. (1987). Physical characterization of *katG*, encoding catalase HPI of *Escherichia coli*. *Gene.* **52**, 121-128.

Triggs-Raine, B. L., Doble, B. W., Mulvey, M. R., Sorby, P. A. & Loewen, P. C. (1988). Nucleotide sequence of *katG*, encoding catalase HPI of *Escherichia coli*. *J. Bacteriol.* **170**, 4415-4419.

Tsai, A., Wu, G., Palmer, G., Bambai, B., Koehn, J. A., Marshall, P. J. & Kulmacz, R. J. (1999). Rapid kinetics of tyrosyl radical formation and heme redox state changes in prostaglandin H synthase-1 and -2. *J. Biol. Chem.***274**, 21695-21700.

Tsukamoto, K., Itakura, H., Sato, K., Fukuyama, K., Miura, S., Takahashi, S., Ikezawa, H. & Hosoya, T. (1999). Binding of salicylhydroxamic acid and several aromatic donor molecules to Arthromyces ramosus peroxidase, investigated by X-ray crystallography, optical difference spectroscopy, NMR relaxation, molecular dynamics, and kinetics. *Biochemistry.* **38**, 12558-12568.

Ursini, F., Maiorino, M., Brigelius-Flohe, R., Aumann, K. D., Roveri, A., Schomburg, D. & Flohe, L. (1995). Diversity of glutathione peroxidases. *Methods Enzymol.* **252**, 38-53.

Vainshtein, B. K., Melik-Adamyan, W. R., Barynin, V. V., Vagin, A. A. & Grebenko, A. I. (1981). Three-dimensional structure of the enzyme catalase. *Nature.* **293**, 411-412.

Vainshtein, B. K., Melik-Adamyan, W. R., Barynin, V. V., Vagin, A. A., Grebenko, A. I., Borisov, V. V., Bartels, K. S., Fita, I. & Rossmann, M. G.

(1986). Three-dimensional structure of catalase from *Penicillium vitale* at 2.0 Åresolution. *J. Mol. Biol.* **188**, 49-61.

Victor, T. C., Pretorius, G. S., Felix, J. V., Jordaan, A. M., van Helden, P. D. & Eisenach, K. D. (1996). *katG* mutations in isoniazid-resistant strains of *Mycobacterium tuberculosis* are not infrequent. *Antimicrob. Agents. Chemother.* **40**, 1572.

Visick, J. E. & Clarke, S. (1997). RpoS- and OxyR-independent induction of HPI catalase at stationary phase in *Escherichia coli* and identification of rpoS mutations in common laboratory strains. *J. Bacteriol.* **179**, 4158-4163.

Vojtechovsky, J., Chu, K., Berendzen, J., Sweet, R. M. & Schlichting, I. (1999). Crystal structures of myoglobin-ligand complexes at near-atomic resolution. *Biophys.***77**, 2153-2174.

von Ossowski, I., Mulvey, M. R., Leco, P. A., Borys, A. & Loewen, P. C. (1991). Nucleotide sequence of *Escherichia coli katE*, which encodes catalase HPII. *J. Bacteriol.* **173**, 514-520.

Wada, K., Tada, T., Nakamura, Y., Kinoshita, T., Tamoi, M., Shigeoka, S. & Nishimura, K. (2002). Crystallization and preliminary X-ray diffraction studies of catalase-peroxidase from *Synechococcus* PCC 7942. *Acta. Crystallogr. D. Biol. Crystallogr.* **58**, 157-159.

Wang, J. Y., Burger, R. M. & Drlica, K. (1998). Role of superoxide in catalase-peroxidase-mediated isoniazid action against mycobacteria. *Antimicrob. Agents. Chemother.* **42**, 709-711.

Weber, K., Pringle, J. R. & Osborn, M. (1972). Measurement of molecular weights by electrophoresis on SDS-acrylamide gel. *Methods Enzymol.* **26 PtC**, 3-27.

Welinder, K. G. (1991). Bacterial catalase-peroxidases are gene duplicated members of the plant peroxidase superfamily. *Biochim. Biophys. Acta.* **1080**, 215-220.

Welinder, K. G., Mauro, J. M. & Norskov-Lauritsen, L. (1992). Structure of plant and fungal peroxidases. *Biochem. Soc. Trans.* **20**, 337-340.

Wengenack, N. L., Uhl, J. R., St Amand, A. L., Tomlinson, A. J., Benson, L. M., Naylor, S., Kline, B. C., Cockerill, F. R., 3rd & Rusnak, F. (1997). Recombinant *Mycobacterium tuberculosis* KatG(S315T) is a competent catalase-peroxidase with reduced activity toward isoniazid. *J. Infect. Dis.* **176**, 722-727.

Wilming, M. & Johnsson, K. (1999). Spontaneous Formation of the Bioactive Form of the Tuberculosis Drug Isoniazid. *Angew. Chem. Int. Ed. Engl.* **38**, 2588-2590.

Wilming, M. & Johnsson, K. (2001). Inter- and intramolecular domain interactions of the catalase-peroxidase KatG from *M. tuberculosis*. *FEBS Lett.* **509**, 272-276.

Wood, P. M. (1988). The potential diagram for oxygen at pH 7. *Biochem. J.* **253**, 287-289.

Xia, R., Webb, J. A., Gnall, L. L., Cutler, K. & Abramson, J. J. (2003). Skeletal muscle sarcoplasmic reticulum contains a NADH-dependent oxidase that generates superoxide. *Am. J. Physiol. Cell. Physiol.* **285**, C215-221.

Yamada, Y., Saijo, S., Sato, T., Igarashi, N., Usui, H., Fujiwara, T. & Tanaka, N. (2001). Crystallization and preliminary X-ray analysis of catalase-peroxidase from the halophilic archaeon *Haloarcula marismortui*. *Acta. Crystallogr. D. Biol. Crystallogr.* **57**, 1157-1158.

Yokota, K. & Yamazaki, I. (1965). Reaction of peroxidase with reduced nicotinamide-adenine dinucleotide and reduced nicotinamide-adenine dinucleotide phosphate. *Biochim. Biophys. Acta.* **105**, 301-312.

Yokota, K. & Yamazaki, I. (1977). Analysis and computer simulation of aerobic oxidation of reduced nicotinamide adenine dinucleotide catalyzed by horseradish peroxidase. *Biochemistry.* **16**, 1913-1920.

Yoshikawa, S. (1997). Beef heart cytochrome *c* oxidase. *Current opinion in structural biology* **7**, 574-579.

Youatt, W. G. & Fay, L. D. (1959). Experimental brucellosis in whitetailed deer. *Am. J. Vet. Res.* **20**, 925-926.

Young, T. A., Delagoutte, B., Endrizzi, J. A., Falick, A. M. & Alber, T. (2003). Structure of *Mycobacterium tuberculosis* PknB supports a universal activation mechanism for Ser/Thr protein kinases. *Nat. Struct. Biol.* **10**, 168-174.

Yu, S., Girotto, S., Lee, C. & Magliozzo, R. S. (2003). Reduced affinity for Isoniazid in the S315T mutant of *Mycobacterium tuberculosis* KatG is a key factor in antibiotic resistance. *J. Biol. Chem.***278**, 14769-14775.

Zamocky, M., Janecek, S. & Koller, F. (2000). Common phylogeny of catalase-peroxidases and ascorbate peroxidases. *Gene.* **256**, 169-182.

Zamocky, M., Regelsberger, G., Jakopitsch, C. & Obinger, C. (2001). The molecular peculiarities of catalase-peroxidases. *FEBS Lett.* **492**, 177-182.

Zamocky, M. (2004). Phylogenetic relationships in class I of the superfamily of bacterial, fungal, and plant peroxidases. *Eur. J. Biochem.* **271**, 3297-3309.

Zhang, Y., Heym, B., Allen, B., Young, D. & Cole, S. (1992). The catalase-peroxidase gene and isoniazid resistance of *Mycobacterium tuberculosis*. *Nature.* **358**, 591-593.

Zhang, Y. & Young, D. B. (1993). Molecular mechanisms of isoniazid: a drug at the front line of tuberculosis control. *Trends. Microbiol.* **1**, 109-113.

Zhao, X., Girotto, S., Yu, S. & Magliozzo, R. S. (2004). Evidence for radical formation at Tyr-353 in *Mycobacterium tuberculosis* catalase-peroxidase (KatG). *J. Biol. Chem.***279**, 7606-7612.

Zhao, X., Yu, H., Yu, S., Wang, F., Sacchettini, J. C. & Magliozzo, R. S. (2006). Hydrogen peroxide-mediated isoniazid activation catalyzed by *Mycobacterium tuberculosis* catalase-peroxidase (KatG) and its S315T mutant. *Biochemistry.* **45**, 4131-4140.

Zheng, M., Aslund, F. & Storz, G. (1998). Activation of the OxyR transcription factor by reversible disulfide bond formation. *Science.* **279**, 1718-1721.

Zheng, M. & Storz, G. (2000). Redox sensing by prokaryotic transcription factors. *Biochem. Pharmacol.* **59**, 1-6.

Zoldak, G., Sut'ak, R., Antalik, M., Sprinzl, M. & Sedlak, E. (2003). Role of conformational flexibility for enzymatic activity in NADH oxidase from *Thermus thermophilus*. *Eur. J. Biochem. / FEBS* **270**, 4887-4897.

Zou, P., Borovok, I., Ortiz de Orue Lucana, D., Muller, D. & Schrempf, H. (1999). The mycelium-associated *Streptomyces reticuli* catalase-peroxidase, its gene and regulation by FurS. *Microbiology* **145 (Pt 3)**, 549-559.